Vol. 163, September 1, 1984
ISSN 0003-2670
Complete in one issue
ANABIOTEC '84 — International Symposium on Analytical Methods and Problems in Biotechnology, Noordwijkerhout, The Netherlands, April 17–19, 1984

ANALYTICA CHIMICA ACTA

International journal devoted to all branches of analytical chemistry

ELSEVIER

ANALYTICA CHIMICA ACTA

International journal devoted to all branches of analytical chemistry
Revue internationale consacrée à tous les domaines de la chimie analytique
Internationale Zeitschrift für alle Gebiete der analytischen Chemie

PUBLICATION SCHEDULE FOR 1984

	J	F	M	A	M	J	J	A	S	O	N	D
Analytica Chimica Acta	156	157/1	157/2	158/1 158/2	159	160	161	162	163	164	165	166

Scope. *Analytica Chimica Acta* publishes original papers, short communications, and reviews dealing with every aspect of modern chemical analysis, both fundamental and applied.

Submission of Papers. Manuscripts (three copies) should be submitted as designated below for rapid and efficient handling:

Papers from the Americas to: Professor Harry L. Pardue, Department of Chemistry, Purdue University, West Lafayette, IN 47907, U.S.A.

Papers from all other countries to: Dr. A. M. G. Macdonald, Department of Chemistry, The University, P.O. Box 363, Birmingham B15 2TT, England. Papers dealing particularly with computer techniques to: Professor J. T. Clerc, Universität Bern, Pharmazeutisches Institut, Baltzerstrasse 5, CH-3012 Bern, Switzerland.

Submission of an article is understood to imply that the article is original and unpublished and is not being considered for publication elsewhere. Upon acceptance of an article by the journal, authors will be asked to transfer the copyright of the article to the publisher. This transfer will ensure the widest possible dissemination of information.

Information for Authors. Papers in English, French and German are published. There are no page charges. Manuscripts should conform in layout and style to the papers published in this Volume. Authors should consult Vol. 160 for detailed information. Reprints of this information are available from the Editors or from: Elsevier Editorial Services Ltd., Mayfield House, 256 Banbury Road, Oxford OX2 7DH (Great Britain).

Reprints. Fifty reprints will be supplied free of charge. Additional reprints (minimum 100) can be ordered. An order form containing price quotations will be sent to the authors together with the proofs of their article.

Advertisements. Advertisement rates are available from the publisher.

Subscriptions. Subscriptions should be sent to: Elsevier Science Publishers B.V., Journals Department, P.O. Box 211, 1000 AE Amsterdam, The Netherlands. Tel: 5803 911, Telex: 18582.

Publication. *Analytica Chimica Acta* appears in 11 volumes in 1984. The subscription for 1984 (Vols. 156–166) is Dfl. 2145.00 plus Dfl. 231.00 (p.p.h.) (total approx. U.S. $914.00). All earlier volumes (Vols. 1–155) except Vols. 23 and 28 are available at Dfl. 215.00 (U.S. $82.70), plus Dfl. 15.00 (U.S. $6.00) p.p.h., per volume.

Our p.p.h. (postage, packing and handling) charge includes surface delivery of all issues, except to subscribers in Australia, Brazil, Canada, China, Hong Kong, India, Israel, Japan, Malaysia, New Zealand, Pakistan, Singapore, South Africa, South Korea, Taiwan and the U.S.A. who receive all issues by air delivery (S.A.L. — Surface Air Lifted) at no extra cost. For the rest of the world, airmail and S.A.L. charges are available upon request.

Claims for issues not received should be made within three months of publication of the issues. If not they cannot be honoured free of charge.

For further information, or a free sample copy of this or any other Elsevier Science Publishers journal, readers in the U.S.A. and Canada can contact the following address: Elsevier Science Publishing Co., Inc., Journal Information Center, 52 Vanderbilt Avenue, New York, NY 10017, U.S.A., Tel: (212) 370-5520.

INTRODUCING SYSTEM 1:

Now, a reliable, versatile DNA Synthesizer with extended-life reagents!

It's from Beckman, of course, with all the results, performance features, dependability and support you'd expect. And, you can get one without major capital expenditure.

The SYSTEM 1 DNA Synthesizer uses the licensed phosphoramidite chemistry. More reactive with shorter cycle time, it yields a better end product with less side reaction.

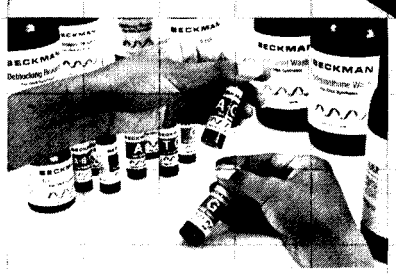

SYSTEM 1 gives you a choice of fully automatic programmed or manual operation. The microprocessor control panel keeps you informed every step of the way. Plus, you can program all or any part of a run and interrupt synthesis at will.

The reagents are an integral part of the system – products of uncompromising quality and purity. A unique packaging feature excludes moisture and oxygen, giving reagents extended life. All reagents and solvents come in convenient kits – enough to synthesize fully as many as 45 base additions with no concern about running out and ruining a synthesis-in-progress.

The SYSTEM 1 is economical to own and to operate. You can buy it outright or use our Base-Pak™ Plan to get one without major capital outlay.

Like our instruments for protein and peptide chemistries, the Beckman DNA Synthesizer is a *total system* with *total support* – applications, customer training, chemicals and service – worldwide. Unequalled.

The Beckman SYSTEM 1: Now, a DNA Synthesizer that combines quality results, easy, flexible operation and extended-life reagents.

For more information ask your Beckman Representative, or write: Beckman Instruments International S.A. 17, rue des Pierres-du-Niton, 1211 Geneva 6, Switzerland. Tel. (022) 36 20 70.

BECKMAN

applikon
Dependable instruments

DE BRAUWWEG 13
P.O. BOX 149
3100 AC SCHIEDAM, HOLLAND
PHONE 010 - 621855 TLX. 26302

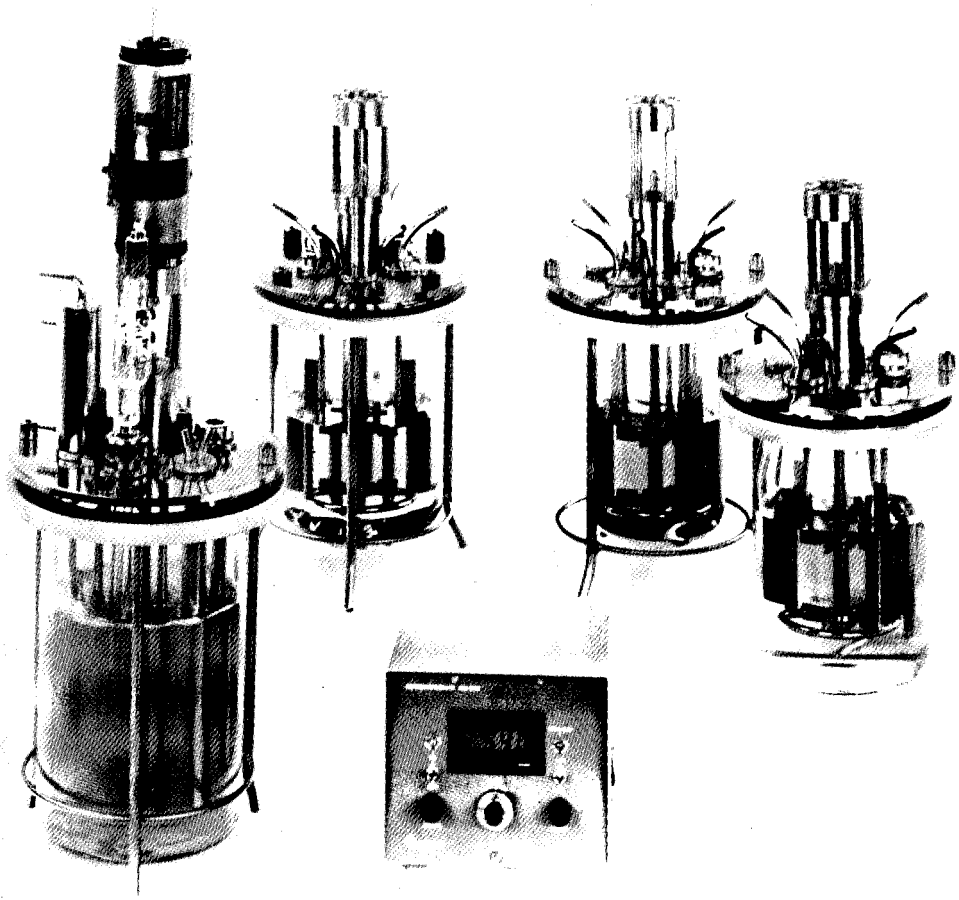

Applikon's small volume fermentor programme developed for "peace-of-mind" fermentations over a long, long period of time

The cultivation of micro organisms is as life itself, with usual and unusual problems. The Applikon fermentors are developed to meet both. More than 15 years of experience in the biotechnology is the solid basis for their DEPENDABILITY and FLEXIBILITY.

FLEXIBLE

- easy accessible topplate with up to 6 sensor ports for:
  - temperature
  - anti-foam
  - pH/redox
  - dissolved oxygen
  - turbidity
- quick connection of stirrer motor ensures easy mounting after autoclaving
- adjustable baffles (3 liter only)
- different types of vessels which fit to the same topplate

DEPENDABLE

- contamination free operation, thanks to the long term reliable non-graphit shaft sealing
- all removable parts are sealed by silicon O-rings
- the special design of the servo controlled stirrer ensures excellent reproducibility and stability of stirring speed, independent from changes in resistance and viscosity
- suitable for long term fermentation of pathogenic cultures, proven by specific tests
- no intensive maintenance required

Yes, I am interested in the biotechnology programme of Applikon Dependable Instruments.

☐ Please send me more information on your fermentation programme.

☐ I would like to make an appointment with one of your product-specialists.

Name . . . . . .

Title . . . . . .

Company . . . . . .

Address . . . . . .

City/State . . . . . .

Postal code . . . . . .

applikon

DEPENDABLE INSTRUMENTS
P.O. BOX 149
3100 AC SCHIEDAM, HOLLAND

FPLC means ...

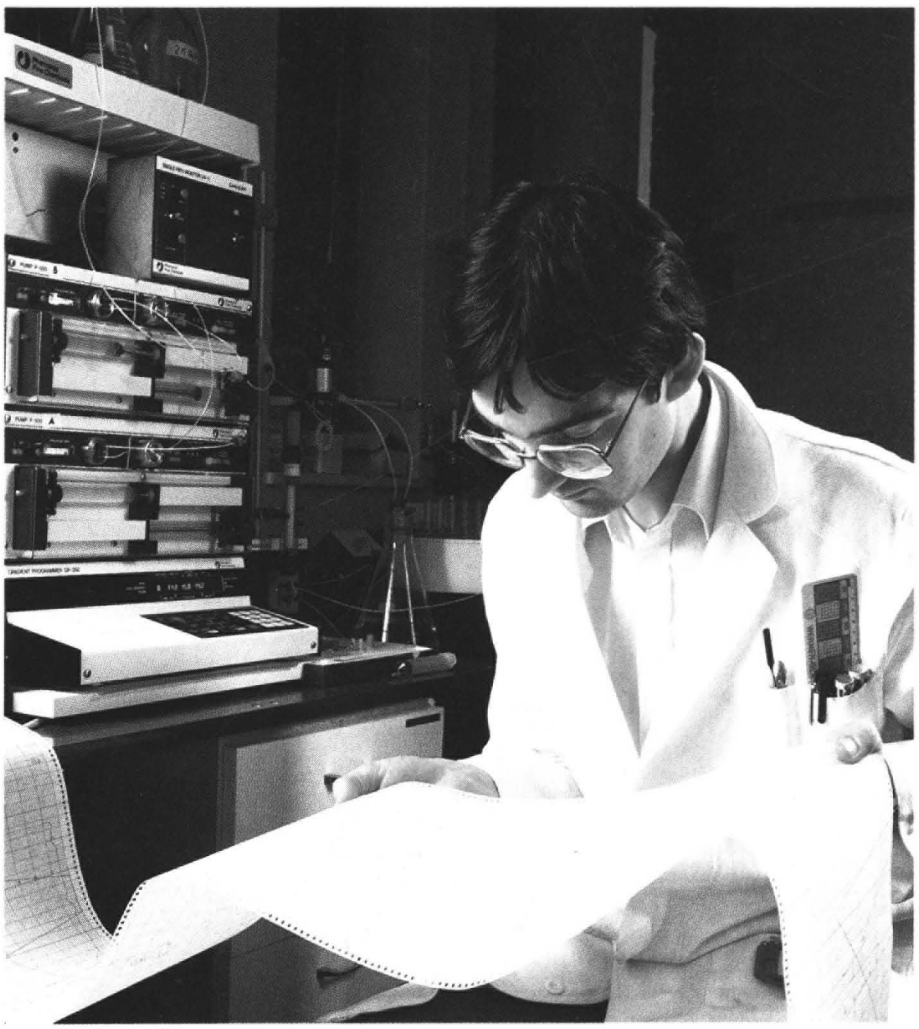

Separation power

Fast Protein/Peptide/Polynucleotide Liquid Chromatography – but speed is not its only virtue.

FPLC means new unique, hydrophilic, monodisperse media providing high performance resolution and high recovery of biological activity: and new silica based media providing high performance resolution, superior yields of proteins, peptides and polynucleotides – with sample sizes up to 100 mg.

FPLC means new instruments, new media and methods – the combination of which is a high performance liquid chromatography system providing a degree of resolution, capacity and speed previously unattainable for purifying proteins, peptides and polynucleotides.

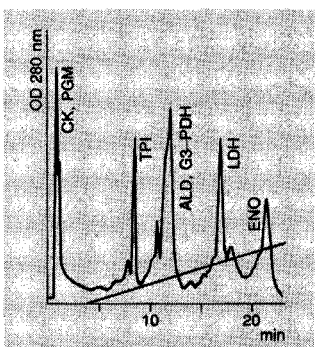

Enzyme purification with >90% recovery of activity.

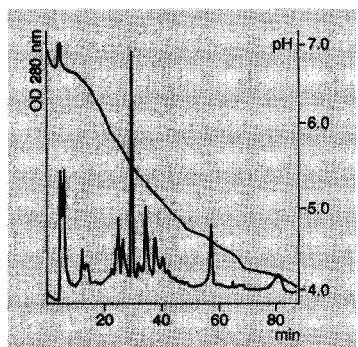

High resolution analysis of proteins (12 isoenzymes of L-aminoacid oxidase).

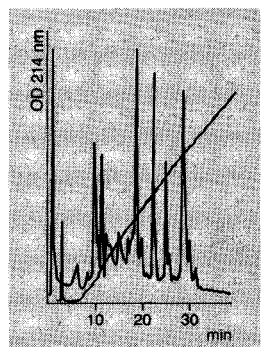

Peptide mapping and purification in 30 minutes (cellulase tryptic peptides).

For further information about the separation power of the FPLC System, please contact your local representative of Pharmacia Fine Chemicals.

Pharmacia Fine Chemicals AB
Box 175
S-751 04 Uppsala 1
Sweden

Pharmacia Fine Chemicals

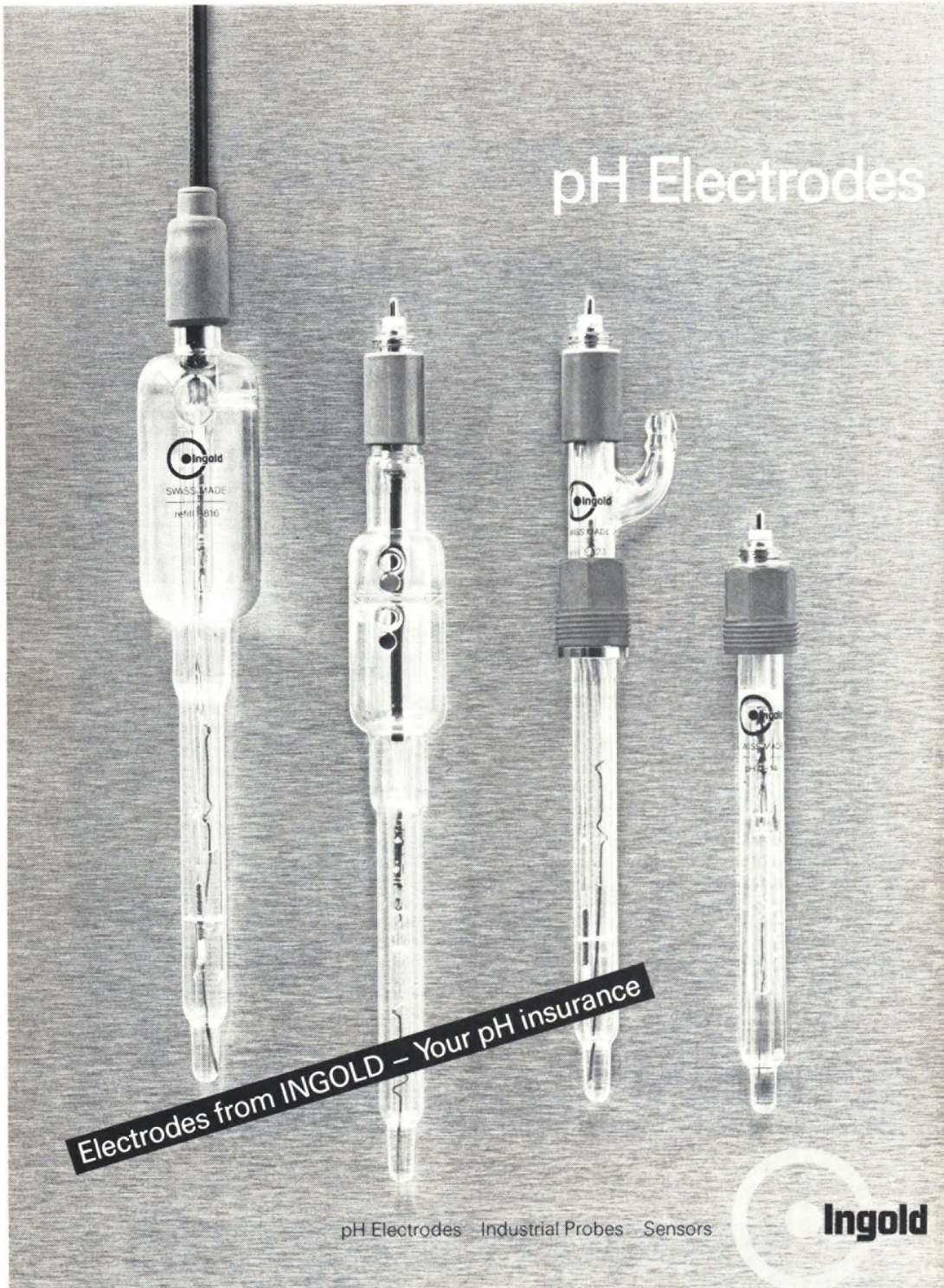

Dr. W. Ingold KG
Postfach 3308
D-6000 Frankfurt/Main 1
Germany
Tel. 0611-2 05 01
Telex 413 439 ionkg d

Ingold Electrodes Inc.
One Burtt Road
Andover, MA. 01810
USA
Phone 617-470-1102
Telex 9230-951096 ilinc andr

Ingold Technique
30, Bd. de Douaumont
F-75017 Paris
France
Tél. (1) 737 06 00
Télex 610 293 ingtech

Ingold Ind. e Com. Ltda.
Rua Francisco Tramontano 191
BR-05686 São Paulo
Brasil
Tel. 240-3924

Dr. W. Ingold AG
Industrie Nord
CH-8902 Urdorf
Switzerland
Tel. 01-734 38 00
Telex 52793 ionag ch

NEW BRUNSWICK SCIENTIFIC

GEN II

THE MICROPROCESSOR-CONTROLLED INSTRUMENT FOR FERMENTATION PROCESSES

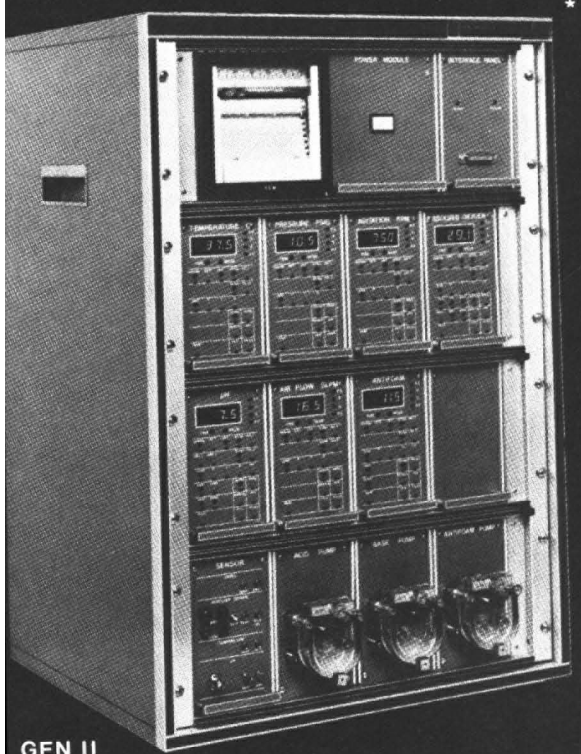

GEN II

* On line substrate/metabolite control
* Full PID or On-Off control, as well as monitoring of process variables
* Instrument-to-instrument communication for interactive control
* Control for temp., agit. speed, pH, DO, redox, etc.
* Working systems NOW available!

The GEN II shown here is integrated with the NBS fermentor MicroGen

FOR MORE INFORMATION AND ALSO FOR SHAKERS, INCUBATORS, CENTRIFUGES ETC., CALL US:

Netherlands — DUMEE b.v., p.o. box 71, 3760 AB Soest, 02155-16834

Germany — NBS GMBH, germaniastr 14-18, D 6050 Offenbach/Bieber, 0611-89 20 48

UK — NBS LTD, 6 Colonial way, Watford WD 24 PT Herts., 0923-23293

USA — NBS CO. INC, p.o. box 986, Edison N.J. 08818, 0201-287 1200

ANALYTICA CHIMICA ACTA
VOL. 163 (1984)

ANALYTICA CHIMICA ACTA

International journal devoted to all branches of analytical chemistry

ELSEVIER Amsterdam–Oxford–New York–Tokyo

Anal. Chim. Acta, Vol. 163 (1984)

0003-2670/84/$03.00

Printed in The Netherlands

SPECIAL ISSUE

ANABIOTEC '84

Proceedings of the International Symposium on Analytical Methods and Problems in Biotechnology, Noordwijkerhout, The Netherlands, April 17–19, 1984

Analytica Chimica Acta, 163 (1984) 1
Elsevier Science Publishers B.V., Amsterdam — Printed in The Netherlands

Foreword

The International Symposium on Analytical Methods and Problems in Biotechnology, held at Noordwijkerhout (The Netherlands) from 17 to 19 April, 1984, was intended to bridge the gap between experts in analytical methodology and experts in biotechnology. Indeed, the "Anabiotec" Symposium became a meeting ground for over 300 scientists, from both academic and industrial sides, interested in analytical aspects of biotechnology.

This special issue of *Analytica Chimica Acta* presents most of the papers submitted for publication by the authors of oral and poster contributions to the Symposium. Besides, a selection of the symposium papers, considered of interest to a wider audience, will be published in a special issue of Trends in Analytical Chemistry.

We are grateful to all who have contributed to the success of this "Anabiotec" Symposium 1984.

W. A. Scheffers
B. te Nijenhuis
J. Kragten

0003-2670/84/$03.00

Analytica Chimica Acta, 163 (1984) 3—15
Elsevier Science Publishers B.V., Amsterdam — Printed in The Netherlands

ON-LINE MEASUREMENT OF EXTRACELLULAR ENZYMES DURING FERMENTATION BY USING MEMBRANE TECHNIQUES

KARL HEINZ KRONER* and MARIA-REGINA KULA

Gesellschaft für Biotechnologische Forschung mbH., Mascheroder Weg 1, D-3300 Braunschweig (West Germany)

(Received 2nd April 1984)

SUMMARY

The measurement of enzymes during fermentation is of general interest for process control in industrial biotechnology. Studies are presented to develop an on-line measurement for extracellular hydrolases by using membrane separations as the main unit operation, first for achieving continuous sampling from the bioreactor prior to analysis, and secondly for measuring hydrolytic activities, by separating the cleavage products during reaction of enzymes with high-molecular-weight substrates by an ultrafiltration membrane. The evaluation of batchwise and continuous flow analysis for an alkaline protease and pullulanase are described, and the feasibility of on-line measurement during fermentation of *Bacillus licheniformis* and *Klebsiella pneumoniae* on a 30- and 70-l pilot scale is demonstrated, including aseptic continuous sampling.

The control and optimization of fermentations preferably needs on-line information about the biological processes involved. Beside the high standard reached in monitoring physical and physicochemical process parameters within the bioreactor [1], there is a need for on-line measurement of chemical process variables such as the concentration of substrates, ions and the product of interest, to establish more precise feedback for better control [2]. However, it is not possible to monitor many of these species within the bioreactor, because there is a lack of suitable sensors, and it cannot be hoped that sensors for all chemical and biochemical process variables will be available in the near future [2, 3].

One possibility for overcoming this problem is to run the desired analysis outside the fermenter, using automatic analyzers to give the necessary information relatively quickly. Sophisticated automatic analysis systems have been developed as well as various sampling devices. This technique has already been used to analyze some low-molecular-weight components, for example in yeast culture media [4, 5], and can be readily used for monitoring ammonia, phosphate, sugars, carbon dioxide, etc. [3]. However, there are some specific problems when such a system is coupled to a fermentor, such as clogging of the sampling device by microbial cells or solids from the broth, maintaining aseptic conditions at the sampling point, removal of the

0003-2670/84/$03.00

solids from the sample to be analyzed, and the time delay within the sampling device and analyzing system [2].

For monitoring high-molecular-weight components such as enzymes, the problems described are often severe, especially in separating enzymes continuously from the broth, and for adapting a given laboratory assay method to an automatic analyzer system [6]. At present, only a few data are available for on-line measurement of hydrolases, or for monitoring protease activity [7—9] and cellulase activity [10—12] using the classical Auto-Analyzer system. During our work with microbial proteases, it became desirable to measure these extracellular enzymes on-line during production, and thus replace the manual control probe from the bioreactor and the enzyme activity measurement using established assays, which are labor-intensive and time-consuming. The present paper demonstrates possibilities for solving the problems described by making use of membrane techniques. Specific examples are given and the potential of this method for on-line monitoring of hydrolases during a biochemical process is outlined.

EXPERIMENTAL

Continuous sampling device

For sampling a dynamic filtration device was used. A commercially available stirred ultrafiltration cell made of stainless steel (Berghof, Tübingen) was connected via a by-pass to the bioreactor (Fig. 1). The broth was pumped continuously through the filter by a peristaltic pump with a moderate feed-rate (0.5 l min^{-1}), and across a microporous or ultrafiltration membrane,

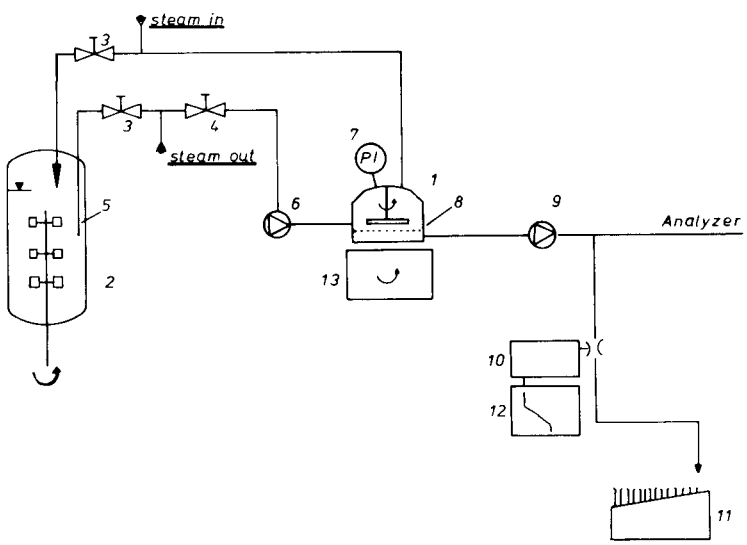

Fig. 1. Scheme for continuous sampling: (1) stirred cell, (2) fermenter, (3, 4) membrane valves, (5) sampling tube, (6) recirculating pump, (7) pressure indicator, (8) membrane, (9) filtrate pump, (10) detector (optional), (11) fraction collector (optional), (12) recorder (optional).

through which a continuous filtrate stream (0.2—1 ml min^{-1}) was produced, which could be connected directly to an analyzing system or a fraction collector. The pressure differential was set about 0.3—0.4 bar and the stirrer speed in the range of 200—500 rpm.

The membrane used had a diameter of 76 mm, and the filter area was about 45 cm^2. Any steam-sterilizable membrane (ultrafiltration or microfiltration) available could be used, the selection depending on the problem to be solved. The entire by-pass system could be steam-sterilized (20—30 min) separately, when connected to the bioreactor. This allows the system to be coupled or decoupled as required, for example, to change the membrane during cultivation, without risk.

Analytical methods

A new method has been introduced for the determination of extracellular hydrolases, e.g., proteases or glycosidases [13]. In principle, it is a kinetic assay based on the reaction of the enzymes with their natural high-molecular-weight substrates (or modified polymers). An ultrafiltration membrane was used to split the reaction volume continuously into two streams, which differ in the molecular size of the solutes (depending on the cut-off of the membrane). The change in the concentration of the solutes caused by the enzyme activity can be monitored, e.g., by a spectrophotometer, in the filtrate stream.

The general scheme for this procedure can be seen in Fig. 2. In this arrangement the pump (1) is connected to a reaction vessel (5) and the ultrafiltration cell (2); (6), (7) and (8) indicate devices for monitoring or regulating flow, pressure and temperature, respectively. The cell (2) is connected to the detector (3) and the latter is connected to the recorder (4) or

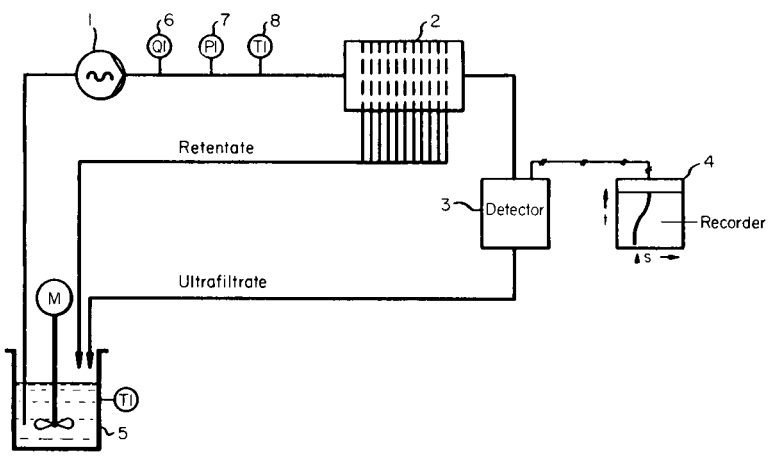

Fig. 2. General scheme for kinetic "membrane analysis", mode 1 (for description see text).

a computer. The process can be done either batchwise (in cycles for automated operation) or continuously; i.e., either the substrate or the enzyme is pumped continuously through the cell and the enzyme or substrate, respectively, is added intermittently, or both are continuously added and mixed. During detection it is possible to compare measurements with a reference cell, using an enzyme or substrate standard. Alternatively, the detection can be done in the retentate stream.

In general, standard analytical laboratory equipment was used, e.g., peristaltic pumps, nylon tubes (coils) and mixing and splitting devices known from the Auto-Analyzer system or in liquid chromatography equipment. The ultrafiltration cell was a small device with a spiral flow channel (Type CEC-1, Amicon Corp.), with a diameter of 90 mm. This cell has a low dead volume. Other ultrafiltration cells could also be used, but the ratio of dead volume to the effective membrane surface area (V_d/A_m) should be as small as possible. A ratio of $V_d/A_m \leqslant 1$ is best. The membranes used were commercially available ultrafiltration membranes of polysulphone or cellulose acetate, such as the PM, XM and YM types (Amicon Corp.), which were used throughout these experiments.

Procedure for determination of enzyme activity

Mode 1 operation. The whole apparatus was rinsed with buffer until a constant detector signal was obtained. Then an appropriate volume of the enzyme sample was added to the thermostatted reaction vessel, with stirring. This mixture was pumped through the ultrafiltration cell until a constant signal was reached again, which was set to zero. The reaction was started by adding an appropriate volume of substrate. After a brief delay, the reaction could be followed as a change in the detector signal with time (ΔS min^{-1}). After completion of the assay (5 min), the apparatus was rinsed with buffer (5 min) and was then ready for the next cycle. The enzyme activities were determined graphically from the steepest slope of the signal/time graph (ΔS min^{-1}). The corresponding value for the enzyme concentration was read from a calibration graph, or was calculated if the slope fell in the linear calibration range. If, for example, spectrophotometric measurements are used, S corresponds to the absorbance (A) at a given wavelength. Calibration can be done either with respect to the product or the substrate. In most cases, calibration was done with a defined enzyme standard.

Mode 2 operation. A continuous operation appeared preferable for the detection of enzyme activities on-line in the bioreactor. Therefore a flow-injection system without air-segmentation [14] was set up. A schematic diagram of the arrangement is presented in Fig. 3. Buffer solution and a stream of enzyme (from the sampling device) were pumped continuously through the thermostatted mixing and reaction coils, and the detector signal was set to zero. The reaction was started by injection of an appropriate volume of substrate into the continuous stream, employing a second pump operated in a pulsewise manner. The frequency of pulsing was chosen in rela-

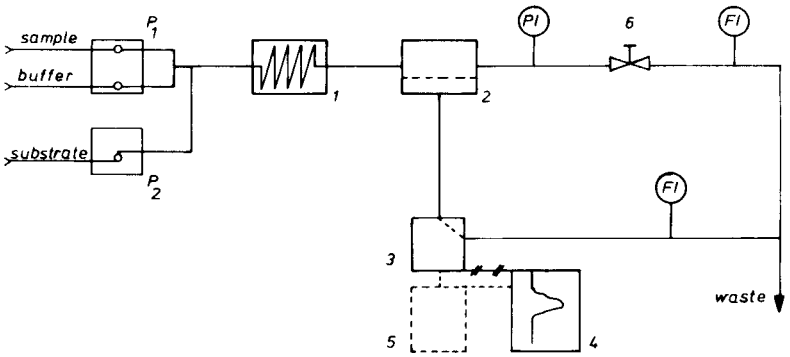

Fig. 3. General scheme for continuous flow "membrane analysis", mode 2: (1) residence and mixing coil, (2) membrane unit, (3) detector unit, (4) recorder, (5) computer (optional), (6) pressure regulating valve (pumps can be used instead); (P1, P2) peristaltic pumps, (PI, FI) pressure and flow indicators.

tion to the mean residence time in the coils and the ultrafiltration cell, either by a repeating timer or by initializing a switch connected to the analog output of the detector, after the zero signal had been reached again.

Enzyme activities could be determined graphically from a calibration graph obtained with an enzyme standard under identical conditions. For calculations, the evaluation of the area or the height of the resulting peaks was used. The calibration graphs produced were often not linear, but calculation of the data was improved by the use of a small computer. If needed, the enzyme sample with buffer was diluted by splitting the sample stream and diluting it in a further loop, prior to reaction.

Enzyme standards and standard assay procedures

In evaluation of the method, the following standard enzyme preparations were used for testing the analytical device and for calibration: bacterial alkaline protease (Maxatase; Gist Brocades Corp., Delft), and pullulanase (Pulluzym; ABM Chemicals, Stockport, England).

For comparing results and for checking the standards, the following enzyme assays were used. Alkaline protease activity was measured by a modified Anson method, with 1% casein (Hammarsten) as a substrate at pH 10 and 50°C, measuring the release of products at 290 nm; this was related to a standard (Henkel laboratory method) [15], and expressed in "Protease Units per ml" (PE ml^{-1}). Pullulanase activity was determined by the method of Nelson and Somogyi with 2% Pullulan (Serva, Heidelberg) as substrate at pH 5.0, 30°C, measuring the release of reducing sugars and comparing it with a calibration graph for maltotriose [16]. One unit of pullulanase is the amount of enzyme liberating 1 μmol of maltotriose per min.

In principle, the conditions and the substrates used for the standard assay procedures were also used to develop and evaluate the concept for contin-

uous assaying described above. In addition, alkaline proteases were monitored by using a water-soluble casein preparation coupled with remazol blue, which was a gift of Henkel, Düsseldorf [15].

Cultivation and enzyme production

For on-line tests during fermentation, a 30-l Dechema Normfermenter (Braun Melsungen, Melsungen) or a 70-l Chemap Fermenter (Chemap, Männedorf) was used. For these tests, an alkaline protease of a strain of *Bacillus licheniformis* was produced in a complex medium. For the production of an extracellular pullulanase, a strain of *Klebsiella pneumoniae* (*Aerobacter aerogenes*) was cultivated in a semisynthetic medium with maltose as the sole carbon source [16].

The membrane analysis system was coupled via the continuous sampling device directly to the bioreactor. The on-line measurements were done according to mode 2. For checking, individual samples were taken manually from the bioreactor at various times and analyzed separately by standard methods.

RESULTS

Evaluation of the membrane procedure in mode 1

The feasibility of the proposed method was examined by measuring the activity of an alkaline protease in the fermentation broth of *Bacillus licheniformis*. The concentration determined by the standard assay was 78 PE ml^{-1}. The conditions for operating were as follows: PM-30 membrane (cut-off 30 000 dalton); total flow 5.7 ml min^{-1}; filtrate stream 2.3 ml min^{-1}; temperature 50°C; reaction volume 5 ml; probe 1 ml; buffer 2.5 ml; casein substrate (1%) 1.5 ml; time delay 30 s; measuring time 3—5 min. The reaction was followed in the ultrafiltrate stream by detection at 280 nm.

The calibration graph obtained with the Maxtase standard is presented in Fig. 4. The graph was curved over the entire range 0—200 PE ml^{-1}, but up to 120 PE ml^{-1}, a linear correlation with a slope of 5.5×10^{-4} ΔA min^{-1}/PE ml^{-1} can be used for calculation. The intercept was 0.68×10^{-3} ΔA min^{-1}. The standard deviation was calculated to be ±8% and depended strongly on the concentration; its highest value was found at low concentrations, because of the high blank level. The enzyme activity was calculated from the equation $(\Delta A \times 10^3 - 0.68)/0.55$ = PE ml^{-1}. Six repeated analyses of a sample of fermentation broth gave a mean activity of 82.8 PE ml^{-1}, and a standard deviation of 7.9 PE ml^{-1}, compared with 78 PE ml^{-1} measured by the standard assay. There is no significant difference between the two values. The relative standard deviation, ca. 9%, is rather high, but may result from suboptimal handling as well as the high blank value (proteins, amino acids), as shown in Fig. 5, where the course of the detector signal with time is plotted. The main problems arise, however, from the graphical determination of the steepest slope of the sigmoidal curve.

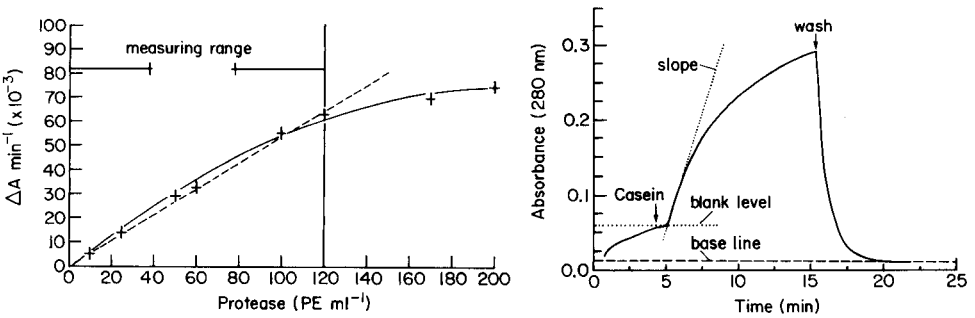

Fig. 4. Calibration graph for alkaline protease (Maxatase), mode 1 (1% casein as substrate, detection at 280 nm). (—) measured values; (---) calculated slope for the linear range.

Fig. 5. Change in detector signal with time during determination of alkaline protease, mode 1. The sample contained 120 PE ml^{-1}; arrows indicate points of casein injection and washing with buffer; recorder speed 500 mm h^{-1}; detection at 280 nm.

The determination of proteases in the presence of high concentrations of proteins, peptides and amino acids in the broth could be improved by using a modified casein. This was a water-soluble casein coupled with remazol blue. In this case, the reaction was followed by measuring the increase of absorbance at 660 nm, which was due to the formation of colored products only. The blank value was thus dramatically decreased. In a second experiment, alkaline protease in fermentation broth was measured under identical conditions as above, except that the concentration of the "blue casein", was increased to 2%. The calibration graph with maxatase was linear in the range 0—300 PE ml^{-1} with a slope of 1.4×10^{-4} ΔA min^{-1}/PE ml^{-1} and an intercept of 5×10^{-3} ΔA min^{-1}. Under these conditions, the sensitivity was decreased, compared to the unmodified substrate, but the standard deviation was decreased to ±3%. The assay was repeated eight times with a sample of 150 PE ml^{-1}, and the results were calculated from the equation (ΔA $min^{-1} \times 10^3 - 5)/0.14$ = PE ml^{-1}. The mean value obtained was 154 PE ml^{-1}, with a standard deviation of 6.5 PE ml^{-1} (<5%). Considering that during the production of alkaline protease, activity values as high as 2000—10 000 PE ml^{-1} are reached, the decrease in sensitivity was no problem and the improved dynamic range of the method with the modified substrate was suitable.

The next experiment was done with pullulanase, to demonstrate that not only proteases could be determined by the membrane procedure. The conditions for the pullulanase test were as follows: YM-5 membrane (5000 dalton cut-off); total flow 4 ml min^{-1}; filtrate stream 1.8 ml min^{-1}; reaction volume 6 ml; total loop volume 15.7 ml; temperature 35°C; enzyme (pulluzyme) probe 0.4 ml; buffer 5 ml; pullulan substrate 0.6 ml; time delay 1 min; measuring time 5 min. A pullulanase standard of 18 U ml^{-1} was used. Detection was done in the filtrate stream with a polarimeter set at 578 nm (Hg). For calculation, a calibration graph with maltotriose was produced

under the test conditions. The slope of the linear plot was 0.086 degrees μmol^{-1} ml^{-1} for $\leqslant 3$ mg ml^{-1} maltotriose.

The relation between enzyme concentration and signal output was also linear for $\leqslant 5$ U ml^{-1} pullulanase, with a standard deviation of around ±4%. Six determinations of the 18.0 U ml^{-1} standard gave a mean change in rotation of 0.045° min^{-1}, corresponding to a mean pullanase concentration of 20.7 U ml^{-1} and a standard deviation of 1.25 U min^{-1}, for a dilution factor of 39.3.

This example demonstrates well this new membrane procedure allows kinetic assays to be established for hydrolases acting on biopolymers using their natural substrates. In addition to the examples described here, amyloglucosidase, α-amylase and acid protease have been measured successfully by this method [13].

Continuous flow determination of alkaline protease with the membrane procedure in mode 2

Besides the possibility of automating mode 1 operation, e.g., by a repeated batch process, the on-line measurement of a hydrolase production in a bioreactor was investigated, with a continuous flow measurement (mode 2) based on flow-injection analysis [14]. The determination of alkaline proteases with "casein blue" by the membrane procedure as described for mode 1 was adapted for this method. The following conditions were used: YM-30 membrane (30 000 dalton cut-off), total flow 6.8 ml min^{-1}; filtrate stream 3.3 ml min^{-1}; buffer stream 6.6 ml min^{-1}; enzyme probe 0.2 ml min^{-1}; substrate injected (casein blue) 1 ml; absorbance measured at 660 nm (range 0.5 abs. ≈ 1 V ≈ 25 cm); reaction time 2 min; temperature 50°C; delay time 3 min; measuring time 5 min; maximal possible measuring frequency 4 h^{-1}.

For calibration, the maxatase standard was measured at different concentrations. The resulting graph was curved but with a good resolution up to 500 PE ml^{-1} (peak height), as shown in Fig. 6. The curve can be fitted simply

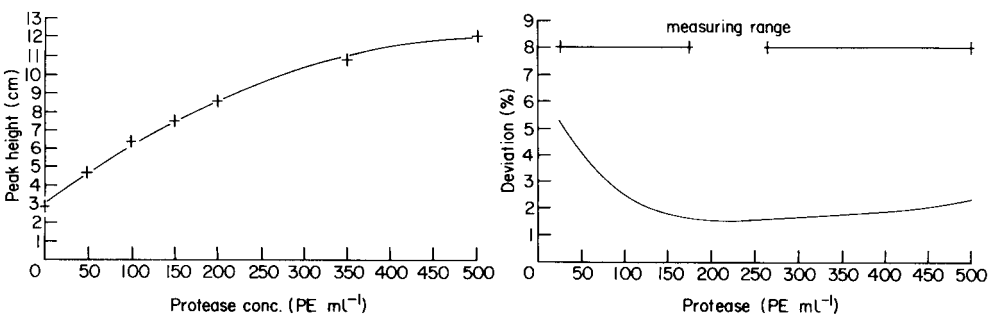

Fig. 6. Calibration graph for alkaline protease (Maxatase) in continuous flow analysis, mode 2. Substrate was casein blue; measurements at 660 nm, 1 cm = 0.02 absorbance.

Fig. 7. Average deviation of measured data points as a function of Maxatase concentration, mode 2. Values are given as % of the difference between measured and calculated points.

to a quadratic regression of the form $y = a + bx + cx^2$, where y is the peak height in cm, and x is the protease concentration (PE ml^{-1}), with $a = 3.06$, $b = 3.42 \times 10^{-2}$, $c = -3.27 \times 10^{-5}$. The relative standard deviation was about 2% and the correlation coefficient was 0.999. The calibration measurements were done in random order with 3 data points for each concentration. The deviations of the calibration points showed a minimum between 100 and 400 PE ml^{-1} (Fig. 7). The range of usefully reproducible measurement is 50—500 PE ml^{-1}. Determinations of protease in a culture broth containing 150 PE ml^{-1} were repeated nine times. The average value obtained was 150.9 with a standard deviation of 6.1 PE ml^{-1}, ca. ±4% (344 ± 8 mV peak height).

The major parameter influencing the sensitivity and reproducibility of the assay was the precise splitting of the streams. The influence of the flow ratio between retentate and filtrate on the signal response can be seen in Fig. 8. With increasing flow of the filtrate stream, the sensitivity increased, but so did the error probability. A decrease in the filtrate flow rate reduced the sensitivity, but the scale of operation could be extended to higher activities, because of the shorter residence time and increased dispersion of the sample [14]. This made it possible to expand the range of estimation without prior dilution.

To examine the feasibility of this method further, a production process was simulated by an enzyme gradient established with the maxatase standard, and the increase in enzyme activity was measured on-line in the mixing vessel. The gradient was formed by pumping 0.2 ml min^{-1} of a stock solution (1000 PE ml^{-1}) into a vessel containing a fixed volume of 100 ml of buffer with stirring, and withdrawing continuously 0.2 ml min^{-1} of the resulting mixture into the analytical system. Theoretically, the gradient can be calculated from the equation $C_t = C_A - C_A \exp(-V_t/V_0)$, where C_t is the concentration at time t, C_A is the concentration of the stock solution added, V_t is

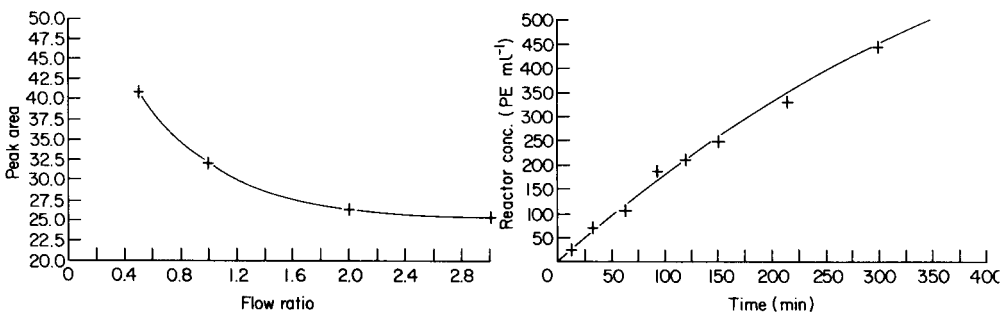

Fig. 8. Influence of the flow ratio between retentate and filtrate on the resolution of the continuous flow determination of Maxatase, mode 2. Peak area was measured graphically from the recorder chart.

Fig. 9. The increase of protease activity during reactor simulation. Maxatase determined with casein blue, mode 2. (—) Curve calculated from the equation for C_t; (+) activities measured.

the volume added at time t, and V_0 the volume of the mixed solution (constant).

The results of this test are presented in Fig. 9. As can be seen, the correlation between theory and practice is good, with a standard deviation of ±3% and a correlation coefficient of 0.994.

Performance of the continuous sampling device

The continuous sampling device was coupled to the 30-l bioreactor as described and the integrity and sterility of the complete system was proven with a standard glucose/yeast extract medium under aeration over a period of 100 h. A 0.22-μm sterile filter membrane (GVWP, Millipore) was used. The sampling stream was adjusted to 30 ml h^{-1}. The partial pressure of oxygen in the solution was monitored continuously; in addition, separate samples were taken from the bioreactor every 24 h and plated on glucose/yeast extract agar plates, to detect any infection. Initially, the oxygen partial pressure dropped slightly (<10%) and then remained constant for 100 h. The agar plates also showed that no infection of the fermenter was observed. The filtrate flow rate was constant over this time.

The delay time for total response to any change in concentration of a chemical parameter in the bioreactor was around 10 min for the sampling device, as was shown by monitoring the change in conductivity resulting from adding potassium chloride to produce a gradient inside the bioreactor. The steepest increase in the concentration gradient which could be handled within 95% response was around 4% min^{-1}, which should be adequate for fermentation control.

The continuous sampling device was next examined during cultivation of *B. licheniformis* in the 30-l bioreactor. A 0.45-μm microfiltration membrane (HVLP, Millipore) was used. The time course of protease production was followed by taking samples from the bioreactor and from the fraction collector connected to the sampling device. The assays were done by the standard method. Figure 10 shows the results. There was a good correlation between the two sets of results, and no infection of the bioreactor could be detected over the entire time of cultivation. The flow rate through the sampling device was constant at 30 ml h^{-1}.

Application of on-line measurement to fermentation

The continuous sampling device and the membrane analysis system were coupled to a 70-l Chemap bioreactor during production of an alkaline protease from *B. licheniformis*. The results are shown in Fig. 11. Samples taken separately from the broth were assayed by the standard method for comparison. The membrane analysis was operated in mode 2, as described above. The measuring frequency was 2 h^{-1}. There was good correlation between the two data sets. The deviation between the control samples and the on-line measurement was 5%. The total time delay was 15—20 min. The integrity of the process was checked by plating and a 70-l parallel cultivation without the modifications. No differences in productivity between the two bioreactors

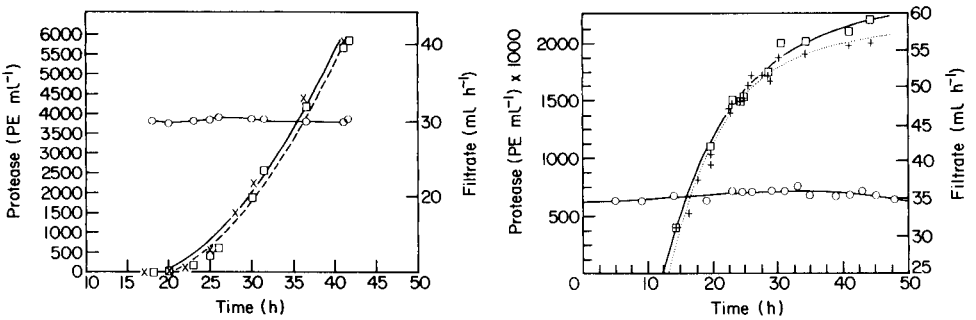

Fig. 10. Test run for the continuous sampling device coupled to a fermentation of *B. licheniformis*: (○) filtrate flow rate; (×) protease activity from broth samples; (□) protease activity in the filtrate.

Fig. 11. Continuous analysis of protease production during fermentation of *B. licheniformis*, mode 2: (○) filtrate flow rate; (□) protease activity from broth samples by standard assay; (+) protease activity by continuous analysis; (—) calculated productivity from control probes; (···) calculated productivity from continuous analysis.

could be observed. The sampling device and the membrane procedure worked well and without interference during a 48-h period.

As a second example of on-line measurement, pullulanase activity was determined during cultivation of *Klebsiella pneumonia* in a 30-l bioreactor. The following conditions for assaying the enzyme in mode 2 were chosen: YM-5 membrane; total flow 3.5 ml min^{-1}; filtrate flow 1.6 ml min^{-1}; buffer stream 3 ml min^{-1}; enzyme probe 0.5 ml min^{-1}; pullulan substrate (2%) 0.5 ml min^{-1} (in pulses); temperature 40°C; reaction time 2 min; delay time 5 min; measuring time 15 min; frequency 1 h^{-1}; detection with a polarimeter at 436 nm (Hg). Under these conditions the calibration graph for the pulluzyme enzyme standard was linear in the range 0–3 U ml^{-1}, with a slope of 9.4×10^{-3} degree min^{-1}/U ml^{-1} (peak height). The intercept was 0.43×10^{-3} degree min^{-1} and the correlation coefficient was 0.994.

Results for the on-line measurement of extracellular pullulanase compared to check samples from the centrifuged broth are compared in Fig. 12. A good correlation was observed but with a delay time of about 1 h. However, the time delay in this improvised case resulted from the fact that the length

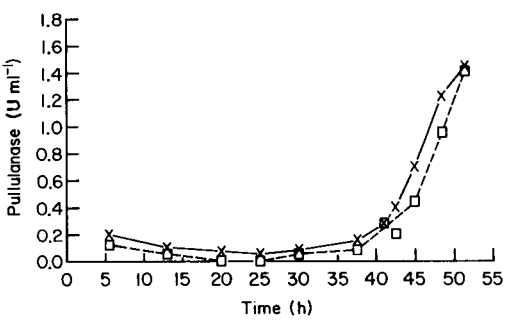

Fig. 12. Changes in pullulanase activity during fermentation of *Klebsiella pneumoniae*: (×) enzyme measured from centrifuged broth samples with the standard assay; (□) enzyme measured on-line, mode 2 (initial values arise from 3% inoculation).

of tube between the sampling device, the analytical system and the detector was too long. It should be noted that the concentration of the carbon source (maltose) could also be measured simultaneously in the analytical system because of a linear relationship between the detector signal (without substrate) and the concentration of maltose. Results will be reported separately.

CONCLUSIONS

The results demonstrate that the "membrane analysis" procedure could be well suited for measuring hydrolase activities during biochemical processes. Although in these studies the analytical set-up was improvised, using simple laboratory equipment, the data are highly significant when compared to those obtained by standard assay procedures. The method has potential not only for bioreactor monitoring but also for monitoring of enzyme reactors via enzyme activities and in the downstream processing of enzymes. Membrane analysis operating in the flow-injection mode is easier to achieve and cheaper than the standard AutoAnalyzer technique. The new method also offers the possibility of using the same set-up for different hydrolase assays by adapting the conditions of the standard laboratory methods based on high-molecular-weight (natural) substrates. The use of time-dependent data gives fast results and utilizes only one unit operation, namely membrane separation. So far, only one similar method has been described with preliminary results [17].

The service lifetime of modern ultrafiltration membranes should not present a problem, e.g., the YM-30 membrane could be used more than 200 times during 20 days. Cleaning with buffer solution containing a small amount of a laboratory nonionic detergent was done routinely after 20 test runs, with intermittent storage in 70% ethanol or 0.1% sodium azide solution. The method has not yet been fully optimized and should give more precise results when a microprocessor is used to control time functions and for integration and calculation of the data.

The feasibility of using dynamic filtration to obtain a continuous sampling stream, separating enzymes from the cell mass and particulate broth components continuously, prior to a measurement system for the enzyme, is reported here for the first time. Membrane filtration has been used so far only for determining low-molecular-weight components such as sugars, ions and metabolites in a culture broth. The system described here allows continuous operation under aseptic conditions with no serious retention of proteins owing to membrane polarization. Enzyme production in complex media, including those with high solid contents and some antifoams, could be followed successfully. The system is flexible and any suitable membrane available on the market can be incorporated, selecting a membrane "tailored" for each process.

We thank Mrs. S. Löslein, Mr. W. Stach, Mr. R. Reisner and Mr. A. Recktenwald for their skillful assistance in this work. We are obliged to

Dr. R. D. Schmid and Dr. W. Weiss, Henkel Corp., Düsseldorf, for the gifts of enzyme standard and "casein blue", and for their helpful and stimulating discussions.

REFERENCES

1 M. Meiners, in R. M. Lafferty (Ed.), Fermentation, Proc. II. Rothenburger Symp., Bad Karlshafen, Springer, Wien, 1981, p. 27.
2 L. Valentini and G. Razzano, in A. Halme (Ed.), Modelling and Control of Biotechnical Processes, Proc. of 1st IFAC-Workshop, Helsinki, Pergamon, Oxford, 1983, p. 253.
3 G. Imming, K. Schaller and M. Meiners, in A. Halme (Ed.), Modelling and Control of Biotechnical Processes, Proc. of 1st IFAC-Workshop, Helsinki, Pergamon, Oxford, 1983, p. 27.
4 J.-R. Mor, A. Zimmerly and A. Fiechter, Anal. Biochem., 52 (1973) 614.
5 D. W. Zabriskie and A. E. Humphrey, Biotechnol. Bioeng., 20 (1978) 1295.
6 G. Chotani and A. Constantinides, Biotechnol. Bioeng., 24 (1982) 2743.
7 M. K. Schwartz, Methods in Enzymology, Vol. 22, 1971, p. 5.
8 A. T. Tappel, Anal. Biochem., 23 (1968) 486.
9 M. Leisola, H. Ojama and V. Kauppinen, Enzyme Microb. Technol., 1 (1979) 51.
10 J. v. Lupin, D. Körner, A. Täufel and H. Ruttloff, Enzyme Microb. Technol., 4 (1982) 104.
11 M. Leisola and V. Kauppinen, Biotechnol. Bioeng., 20 (1978) 837.
12 M. Leisola, J. Virkkunen, E. Karvonen and A. Meskanen, Enzyme Microb. Technol., 1 (1979) 117.
13 K. H. Kroner, patent application: DOS 31 50 112, 1981.
14 J. Růžička and E. H. Hansen, Flow Injection Analysis, Wiley, New York, 1981.
15 R. D. Schmid and W. Weiss, Henkel Corp., Düsseldorf, personal communication.
16 K. Wallenfels, H. Bender and J. R. Rached, Biochem. Biophys. Res. Commun., 22 (1966) 254.
17 F. J. Stutzenberger and J. W. Lawson, Biotechnol. Bioeng., 24 (1982) 999.

Analytica Chimica Acta, 163 (1984) 17—24
Elsevier Science Publishers B.V., Amsterdam — Printed in The Netherlands

FRACTAL STRUCTURE OF GEL POROSITY

B. GELLERI and M. SERNETZ*

Institut für Biochemie und Endokrinologie, Justus Liebig-Universität Giessen, Frankfurter Str. 100, D-6300 Giessen (Federal Republic of Germany)

(Received 17th April 1984)

SUMMARY

The concept of fractals as a dimensional measure to describe random irregularity and fragmentation, applied to the structure of gels enables the distribution of pore sizes to be explained as a generalized log-logistic function. This is achieved by introducing upper and lower limits to the power function of self-similar structured organization. In contrast to previous empirical relations for gel-permeation techniques, this approach provides a theoretically based relation between the measured distribution coefficients and the size of the eluting molecules as a measure without undue assumptions. Linearization by transformation of the cumulative log-logistic distribution function is proposed for regression of experimental data. The validity of the theory is demonstrated with size-exclusion data for different gel matrices. Other systems with properties based on irregularity and fragmentation of their heterogeneous structure could be described and analyzed by the same theory.

Knowledge of the porosity of a gel, defined as the differential or cumulative frequency distribution of pore sizes or of the inner volume or surface, as a function of the size of permeating or interacting sample molecules is of special importance for the analytical description of gels. Such knowledge is also valuable in making the best practical use of inert permeation gel matrices (e.g., in gel chromatography) or of activated carrier matrices (e.g., for the immobilization of enzymes and the development of enzyme reactors).

Some methods for the determination of porosity, such as mercury porosimetry, nitrogen capillary condensation or scanning-electron microscopy, are restricted to porous materials in the dry state. Therefore, they can give only indirect information on the supramolecular organization which is responsible for the peculiar properties of the swollen gel. Gel-permeation (size-exclusion) chromatography provides the actual pore-size distribution, because it enables the relative accessible volume of the gel to sample molecules of known size to be evaluated from their elution volumes.

The regression of experimental data within a given range of validity has previously been based either on empirical relations such as proportionality between distribution coefficient and molecular weight or on the assumption of postulated formal distributions. Usually, normal distributions [1, 2] or

0003-2670/84/$03.00

log-normal distributions [3] of pore sizes have been assumed. Both these distributions have been adopted merely for convenience and from lack of logical arguments, but both include wrong assumptions. Thus, the normal distribution with a range from $-\infty$ to $+\infty$ includes pores with negative diameter, whereas the log-normal distribution with range from 0 to $+\infty$ allows pores of unlimited size. This is also unrealistic because the radius of the biggest pores cannot surpass, indeed cannot even reach, the size of the gel particles, and at least an upper limit of pore sizes is logically essential.

A theoretical approach is described here for the general analysis of gel structure. The approach needs no prior assumptions on the kind of pore-size distribution; instead, the distribution function is derived rationally as a consequence of the nature of the gel. No statement on the gel is used other than that the irregular, fragmented and isotropic structure of the network of polymer chains is fractal, and in particular self-similar within a range sufficiently far from upper and lower limits.

THEORY

Fractal and self-similar structure

The theoretical approach, here applied to gel porosity, starts from the interpretation of pore porosity as a cumulative pore-volume distribution. It is based on the general observation that the measurable inner volume (i.e., the dependent, measured property) increases with reduction of the size of the sample molecules (the measure) or, in other words, with the scale of resolution. The fractal concept is now widely used to describe a shape or structure as a function of the scale of resolution; for example, if the description of a fractal structure at the macroscopic level will remain valid at the microscopic level and even for large molecular aggregates, it becomes self-similar within that range.

When a measurable property of a system is not independent, but remains a function of the measure used, or of the scale of resolution, the system under observation is considered to be of fractal structure [4]. For any scale, the dependence of the measured function y on the size of the measure x can be described by a power function

$$y = a\, x^{[D_T - D_F(x)]} \tag{1}$$

in which D_T denotes the expected topological integer dimension and D_F the so-called fractal dimension at the range x of the measure. By generalization, the term dimension includes non-integer values. It becomes a measure of the gradation (degree, excess or intensity) by which a real property of a structure evades the measuring procedure with a topologically defined measure within a certain range of scale. The structured system deviates into a dimension alien to the dimension of the topological measure.

The value of the fractal exponent $D_T - D_F$, the dimensional excess, may change in different ranges of scale, according to the changing degree of irregularity observed. Thus the fractal exponent defines a measure of the

degree of structured organization, given by a certain geometrical or statistical rule of substructure formation. In ranges where there is no dependence on the measure or scale, D_F becomes D_T. If, however, the extent of gradation remains identical over a wide range of scales, and therefore the fractal exponent remains constant, i.e., $(D_T - D_F)$ = constant = b, then the fractal system becomes self-similar. In a self-similar structure, the scale of resolution can no longer be perceived from the extent of structured organization in any partial frame. In the self-similar case, the fractal dependence becomes a power function with constant exponent b

$$y = a\,x^b \tag{2}$$

which in a double logarithmic plot, log y vs. log x, is a straight line with the slope $b = D_T - D_F$. The derivative of the power function, without limits, describes the hyperbolic density distribution (Pareto distribution) of the structural components [4].

Limited self-similarity

In contrast to the unlimited mathematical case, natural systems are self-similar only within certain limits and are bounded by upper and lower limits, namely physical constraints of the structural elements. Starting from the self-similar domain, these borders may be reached asymptotically with decreasing frequencies of the typical structures.

This fractal mode of interpretation can easily be used to describe the porosity of gels and carrier matrices, as measured by gel-permeation techniques. The dependence of the inner volume y on the molecular size x can be presented in a logarithmic plot with linear approximation in the central part. With the smallest molecules, accessible to the entire inner volume and thus yielding constant elution volume $V_{e,max}$, the upper limit O_y of structured organization is reached asymptotically; likewise, with molecules too big for permeation, the smallest elution volume $V_{e,min}$ is reached as lower limit U_y. Beyond these limits, the gel structure is scale-independent with respect to porosity. The difference $O_y - U_y$ is the maximum volume range available for gel permeation and exclusion by molecular size.

Without any limiting constraints, the gel structure would be described as self-similar, and the pore volume distribution would follow the self-similar power function (Eqn. 2). Into this power function, the upper limit O_y and lower limit U_y are introduced as properties of the real natural system in such a way that the derivative of the power function, $dy/dx = y\,b/x$, becomes zero on approaching these limits [5], i.e.,

$$dy/dx = [(O_y - y)(y - U_y)/(O_y - U_y)]\,[b/x] \tag{3}$$

Thus the unlimited self-similar relation of the power function (Eqn. 2) becomes a fractal relationship within the range $O_y - U_y$ (Eqn. 3). The solution of this differential equation [6] yields the function

$$y = (O_y P x^b + U_y)/(1 + P x^b) \tag{4}$$

which is called log-logistic here, because of its relationship to the logistic function. By rearrangement, the parameter of position, P, is

$$P = [(y_0 - U_y)/(O_y - y_0)]\,[1/x_0]^b \tag{5}$$

defined by the limits of integration x_0 and y_0 and by the exponent b. Whereas in the self-similar power function (Eqn. 2), the exponent b characterizes the dimensional excess (i.e., the extent to which the structure deviates from the dimension of the topological, unstructured measure), in the log-logistic function (Eqn. 4) the exponent becomes the parameter of dispersion of a distribution function.

In a double logarithmic plot, the power function of self-similarity is a straight line with slope b as dimensional excess. The corresponding log-logistic function is sigmoidal with a wide, quasilinear central range. The scale-dependent dimensional excess m, i.e., the slope for any scale, can be found from the logarithmic derivative

$$m = \mathrm{d}\log y/\mathrm{d}\log x = b(O_y - U_y)Px^b/(1 + Px^b)(O_yPx^b + U_y) \tag{6}$$

The broader the quasi-linear fitted range of the log-logistic function, the smaller the difference between the maximum slope m_i at the inflexion point i of the log-logistic function and the exponent b of the self-similar case.

The log-logistic function (Eqn. 4) results from the kind of approach towards the borders chosen, i.e., equal weighting of the distances. It yields symmetry in logarithmic coordinates. In differently defined structural systems, other asymptotic transitions may be possible. Here, linear transformation of the log-logistic function (Eqn. 4) by a logit transformation [7]

$$\mathrm{logit} = \log[(y - U_y)/(O_y - y)] = \log P + b\log x \tag{7}$$

is proposed for graphical regression of experimental data in a logit-log plot. If the upper and lower limits O_y and U_y are known from experiments (i.e., $V_{e,\max}$ and $V_{e,\min}$ in gel permeation), then the transformation provides P as parameters of position and b as dispersion.

EXPERIMENTAL

Experimental results on Eupergit C (Röhm-Pharma, Darmstadt) and literature data on size exclusion for Sephadex G-100 (Pharmacia, Uppsala) [8] and Merckogel SI-100 (Merck, Darmstadt) [3] were used to prove the validity of the proposed fractal concept and to demonstrate the suitability of the log-logistic function to describe gel porosity.

Experiments on Eupergit C were done with glass chromatographic columns (60 cm long, 1.6 cm i.d.) with a bed volume of about 85 ml. The oxirane groups of the gel matrix were deactivated by 2-mercaptoethanol. Adsorption was prevented by 1% sodium dodecyl sulphate (SDS). Details of the procedures are available elsewhere [6]. The substances used for size-exclusion chromatography and their molecular data are listed in Table 1.

TABLE 1

Molecular data of test substances used for gel permeation on deactivated Eupergit C, and experimental elution volumes V_e, distribution coefficients K_d and increments of difference distribution p

Substance tested	Mol. wt. (10^{-3} Dalton)	Radius (nm)	f/f_0	Runs n	V_e (ml)[a]		K_d	p
1 Dextran blue	2000	37.4	—	25	41.7	2.2	0.0	
2 Thyreoglobulin	660	8.2	—	11	41.4	2.8	0.0	0.03
3 Ferritin	340	5.2	—	8	42.4	3.5	0.004	0.22
4 BSA	68	3.5	1.34	16	48.3	3.1	0.239	1.14
5 Ovalbumin	43.5	2.7	1.18	10	52.6	2.8	0.384	1.27
6 Chymotrypsinogen	22.8	2.1	1.12	5	55.6	2.8	0.485	0.92
7 Myoglobin	17	1.8	1.11	7	62.0	3.1	0.7	3.18
8 Cytochrome C	12.3	1.7	1.11	6	64.1	3.0	0.771	2.8
9 Insulin A-chain	2.5	1.0	—	8	65.7	3.1	0.825	0.24
10 Lactose	0.36	0.44	—	7	67.4	2.2	0.882	0.16
11 Glucose	0.18	0.36	—	7	69.3	3.9	0.963	0.72
12 D_2O	0.020	0.1	—	5	70.9	2.1	1.0	0.1
13 Latex 0.22 μm	—	110.0	—	2	40.7	—	—	—

[a]Mean and standard deviation.

RESULTS AND DISCUSSION

The results of size-exclusion chromatography on deactivated Eupergit C are presented in Table 1. The elution volumes, V_e, were normalized to a 100-ml column and conventional K_d values were derived. In Table 1, p denotes the difference distribution of pore radii, defined as

$$p = \Delta V_e / V_i \Delta \log r \tag{8}$$

which is the relative increment of pore size as a function of the molecular size.

Figure 1 shows the elution volumes of Eupergit C, Sephadex G-100 and Merckogel SI-100 in a double logarithmic plot. These volumes correspond to discrete points of the actually continuous cumulative distribution of the inner volume of the gel. They can be fitted by the log-logistic function. The excellent agreement of the experimental data of three independent gels, covering the entire measuring range, demonstrates the validity of the theoretical approach based on the fractal concept. This fractal concept is characterized by the acceptance of limits to the self-similarity of gel structure. The specific access to the limits results in the log-logistic function of pore-size distribution.

This seems to be the first theoretically justified approach on the description and analysis of the structure of porous gels, which avoids undue preliminary conditions. The description of gel structure becomes independent of the assumption of formal mathematical distributions, such as the Gaussian

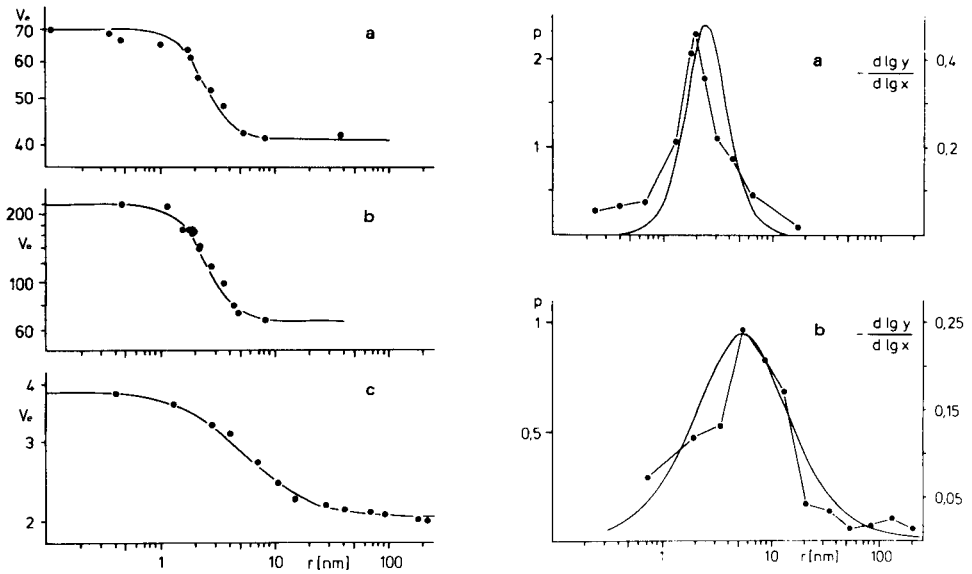

Fig. 1. Elution volume V_e as a function of molecular radius r with logarithmic coordinates. Experimental results for (a) Eupergit C, (b) Sephadex G-100 and (c) Merckogel SI-100 were fitted by the log-logistic function.

Fig. 2. Difference distribution p of pore radii for (a) Eupergit C and (b) Merckogel SI-100 in comparison with the pore-size distribution d log y/d log x, calculated from the logarithmic derivative of the log-logistic function.

[2] or log-Gaussian distribution [3] as approximations. It is well known that the conventional distribution coefficients K_d can be used only in a limited range, usually $0.2 < K_d < 0.8$ for approximation of Gaussian distributions, because of systematic deviations outside that range. In the present case, e.g., with Eupergit C, only five K_d values (Table 1, compounds 4—8) could have been used for linearization, whereas with the log-logistic function the entire range of molecular data shown in Table 1 can be utilized.

Figure 2 shows the difference distributions p (Eqn. 8) of the pore sizes for Eupergit C and Merckogel SI-100 in comparison with the differential pore-size distributions d log y/d log x, calculated from the logarithmic derivative of the log-logistic function. These plots represent the portion of pores of a certain size over the entire pore size distribution. Compared to the smooth course of the differential distribution, a plot of the difference distribution p is of course highly sensitive to experimental noise, both with respect to elution differences ΔV_e and with the molecular data Δ log r. Nevertheless, the fit of the distributions is very satisfactory. The fit to the log-logistic function seems distinctly more appropriate than the formal approximation to a log-Gaussian distribution [3].

With the distinct experimental limiting conditions O_y and U_y, the log-logistic distribution provides by the parameter $P = x_w^b U_y/O_y$, the mode x_w and by the parameter b the dispersion of the pore sizes of the gel.

Figure 3 shows the linearization of experimental data in a logit-log plot and the estimation of the parameters. Because of its theoretical justification, this is more powerful than empirical relations like K_d vs. log (m.w.), which exhibit only restricted ranges with approximately linear dependence.

Thus the log-logistic distribution describes the structure of the gel by the dispersion of porosity within the natural borders O_y and U_y. Shifting of these borders to infinity, namely $O_y \rightarrow \infty$ and $U_y \rightarrow 0$, re-establishes the unlimited self-similar case, described by the power function in Eqn. 2. In doing so, the parameter b of the log-logistic function as a measure of dispersion again becomes the exponent b of the power function and thus the fractal dimension as the measure of gradation and structured organization. This is a new, unconstrained and meaningful characterization of a peculiar structural property, here of a gel, which previously has been considered only by operational correction terms such as tortuosity or a labyrinth factor.

The relation between the log-logistic dependence in a limited system and the power function in the unlimited case for self-similar structure can be transferred to a series of analogous relationships and processes. Introducing fractal or self-similar concepts into descriptions of log-logistic phenomena

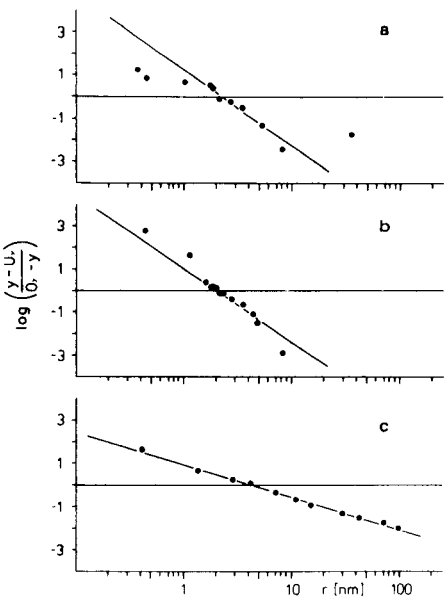

Fig. 3. Linearization of the cumulative log-logistic pore-size distribution by logit transformation (logit-log plot) for (a) Eupergit C, (b) Sephadex G-100 and (c) Merckogel SI-100.

should allow better understanding of these systems on the basis of heterogeneity of molecular states or irregularity and fragmentation of their structure. This applies especially for all functions that can be described by the general equation $y = (Ax^b + C)/(B + x^b)$. Examples are the heterogeneity of the Freundlich isotherm, the cooperativity of oligomeric enzymes, the generalized antigen-antibody interaction, or the dose-response relation in pharmacology, where the exponent b of interaction represents (as dispersion) the heterogeneity of molecular states.

This investigation was supported by Grant Se 315/11-6 of the Deutsche Forschungsgemeinschaft.

REFERENCES

1 G. K. Ackers, J. Biol. Chem., 242 (1967) 3026.
2 W. Boguth, R. Repges and M. Sernetz, Z. Anal. Chem., 243 (1968) 464.
3 J. Halasz and K. Martin, Angew. Chem., 90 (1978) 954.
4 B. B. Mandelbrot, Fractals: Form, Chance, Dimension, W. H. Freeman, San Francisco, 1977.
5 J. Petroll, Staub-Reinhalt. Luft, 34 (1974) 445.
6 B. Gelleri, Thesis, Giessen, 1982.
7 W. D. Ashton, The Logit Transformation, Griffin, London, 1972.
8 P. Andrews, Biochem. J., 91 (1964) 222.

Analytica Chimica Acta, 163 (1984) 25—33
Elsevier Science Publishers B.V., Amsterdam — Printed in The Netherlands

HIGH-PERFORMANCE LIQUID CHROMATOGRAPHY OF CARBAPENEM ANTIBIOTICS IN COMPLEX BIOLOGICAL SAMPLES WITH COLUMN SWITCHING AND SIMULTANEOUS MULTICHANNEL ULTRAVIOLET MONITORING

GEORG DECRISTOFORO

Biochemie GmbH, Research and Development Department, A-6250 Kundl (Austria)

(Received 16th April 1984)

SUMMARY

During fermentative production of new carbapenem compounds of the OA-6129 type, many interfering by-products, exhibiting physicochemical properties very similar to the main components, are produced. The compounds of interest, especially OA-6129 A, B1, B2 and C, are difficult to quantify because of the complex biological matrix and the broad spectrum of by-products. High-performance liquid chromatography (h.p.l.c.) is used to quantify OA-6129 B2. In order to assign the chromatographic peaks clearly to the wanted substances, h.p.l.c., t.l.c. and a selective chemical degradation method proved to be necessary. This procedure was considerably simplified by combined use of a column-switching technique and a diode-array detector. The polar by-products and much of the interfering matrix were eliminated by column switching. Positive identification of OA-6129 B2 was feasible by monitoring chromatograms simultaneously at different wavelengths and by use of the diode-array detector. Additional information on uniformity and purity of the peaks was obtained by u.v.-absorbance ratio recording.

A relatively new group of carbapenem β-lactam antibiotics, which were isolated from a culture broth of *Streptomyces* sp. OA-6129, was described recently [1, 2]. These substances differ from previously known 7-oxo-1-azabicyclo[3.2.0]hept-2-ene (carbapenem) derivatives mainly by the pantothenic acid moiety on the substituent in the 3-position of the molecule. The chemical structures of these new carbapenem substances OA-6129 A, B1, B2 and C were elucidated by spectroscopic investigations and by chemical reactions [3]

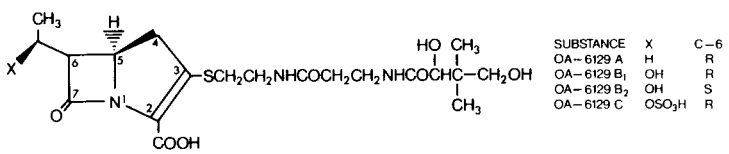

Carbapenem antibiotics from fermentation solutions have already been determined by various methods, e.g., paper- and thin-layer chromatography (t.l.c.) and electrophoresis, mostly in combination with bioautography

0003-2670/84/$03.00

[4, 5]. Determinations of this class of substances in samples of fermentation broth are hindered by two main problems. Carbapenem-producing organisms also generate many by-products which can have chemical and physical properties very similar to those of the required main metabolites and therefore are difficult to separate. Also, an interfering biological matrix is produced which cannot be eliminated by conventional methods of sample preparation. These problems make it necessary not only to apply separations with high resolution, but also to identify sample components during the analysis.

Initially, these complex problems were solved by application of several methods, such as high-performance liquid chromatography (h.p.l.c.), t.l.c. [6] and a chemical degradation method selective for OA-6129 carbapenems. Although unambiguous assignment was thus feasible, the procedure was very time-consuming and laborious. Therefore, the work described here was undertaken to achieve an on-line sample clean-up by a column-switching technique [7, 8], and to obtain positive substance identification by multichannel monitoring with a diode-array detector [9—13].

EXPERIMENTAL

Apparatus

For h.p.l.c., a modular system was used consisting of a SP-8700 high-pressure pump (Spectra Physics), a HP-1040A diode-array detector with a 9133V mass storage unit (3.5 in. floppy disk drive combined with 5.25 in. Winchester drive, 270 kB + 4.8 MB; Hewlett-Packard) and a cooled automatic sampler ISS-100 (Perkin-Elmer). Cooling was done with a Haake D3G constant-temperature circulator. The column switching valve, which was a pneumatic 6-port valve (Valco Instruments, Houston, TX) was controlled by an event-control module (HP-18653B; Hewlett-Packard). Quantitative evaluation was done via an analog/digital converter (HP-18652A). The event control and converter were connected to a HP-3357 data-processing system. The second pump used in the column-switching method was an Altex 110-A (Beckman/Altex).

Standards and reagents

A standard sample of OA-6129 B2 (Sanraku Company, Fujisawa, Japan) was used as the primary standard. A reference sample, which was found to have 34.9% of B2 compared to the primary standard, was isolated in this Department and was used for further investigations. A sample of OA-6129 C with a content of 70.0% was a gift from Sandoz (Basle, Switzerland). A sample of OA-6129 A was available only as a lyophilised form with a content of approximately 1%; this was used for comparison purposes. 4-Dimethylaminobenzaldehyde was of analytical grade (Fluka). The other solvents and reagents used were all of analytical grade (Merck) unless stated otherwise.

Sample preparation

Culture broth samples for qualitative t.l.c. were vigorously shaken and centrifuged at 13 000 rpm for 5 min; 200 μl of the supernatant solution was transferred to a reaction vial and 50 μl of saturated sodium chloride solution was added. For h.p.l.c., the fermentation samples were diluted (1 + 4, v/v) with phosphate buffer (pH 7.5) and centrifuged at 13 000 rpm, and an aliquot of supernatant solution was injected onto the h.p.l.c. column after filtration through a 0.5-μm Millex HA filter (Millipore).

Chromatographic procedures

H.p.l.c. — 1 (isocratic method). The eluent was an ammonium formate buffer (0.25 M formic acid adjusted to pH 8.5 with ammonia) with methanol in the ratio 4:1 (i.e., 20% methanol). Nucleosil C_{18} (Macherey & Nagel) with a particle size of 10 μm served as the stationary phase in a stainless steel 316 column 250 mm long, 6.35 mm o.d., 4.7 mm i.d.) The flow rate was 2.0 ml min^{-1}, a back-pressure of 100—140 bar (10.0—14.0 MPa) developed in the system. The column was kept at ambient temperature. The volume of the injected sample is 30 μl. The effluent was monitored with a u.v. detector at 300 nm. Evaluation was done by peak-area measurement against an external standard.

H.p.l.c. — 2 (gradient elution). The conditions were the same as in the h.p.l.c. 1 method, except that gradient elution was used. Initially, only the aqueous ammonium formate buffer at pH 8.5 was pumped through the column. During 10 min, the methanol content was raised to 35%, and then the composition was maintained, isocratically, for a further 3 min. During 2 min, the eluent composition was returned to its initial condition, which was maintained for 5 min. The total gradient time was 20 min.

H.p.l.c. — 3 (column switching). Both the above gradient method and the isocratic method were combined when the column-switching technique was used, in order to achieve pre-separation and clean-up of the sample on the first column and separation of the products of interest on the second column [10]. A 10-cm column served as the pre-column and the separating column was 21 cm long. The other conditions were as mentioned above.

The biological sample was injected onto the pre-column (column 1) and the eluent gradient was used to elute the polar matrix. The column-switching valve was set to position A (Fig. 1) at this time and the eluate was run to waste. The largest possible part of the matrix was eluted and, immediately before the elution of the substances to be determined, the valve was switched to position B. The compounds of interest were then loaded on the top of column 2, where the chromatographic separation was conducted isocratically after switching back the valve into position A. Column 1 was flushed in the meantime by finishing the gradient elution. The whole cycle was started again in position A of the column-switching valve, when the next sample was injected. The gradient and valve-control times are listed in Table 1.

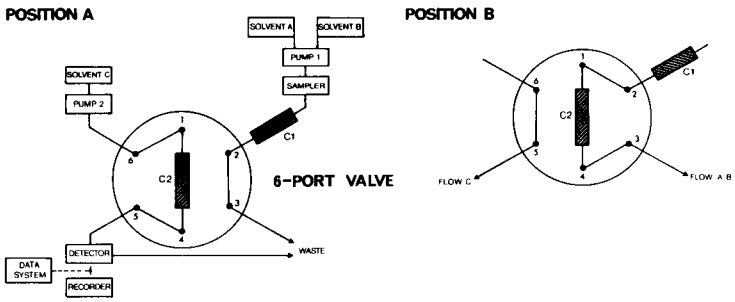

Fig. 1. Column-switching scheme. C indicates column.

Thin-layer chromatography. A t.l.c. method was used for qualitative confirmation of h.p.l.c. results. The eluent was chloroform, methanol and phosphate buffer pH 7.5 (0.015 M) in the ratio 8:6:1 (v/v). Saturated (26.4% w/v) sodium chloride solution was added to the sample and standard solutions, to give a final sodium chloride concentration 5—6% (w/v). Interfering effects of the biological matrix were thus suppressed; otherwise, the matrix caused high and very variable R_f values. The addition of sodium chloride also produced more compact spots. Aliquots (2 μl) of the prepared sample solution were spotted on a pre-coated silica gel h.p.t.l.c. plate (Merck) which was then dried in a desiccator under vacuum for 5—10 min. The t.l.c. plate was then developed with the above mixture (without chamber saturation) at 4°C for 45 min. The solvent front migrated 7 cm under these conditions. After drying under vacuum again, the plate was sprayed with a solution of Ehrlich reagent (300 mg of 4-dimethylaminobenzaldehyde in 54 ml of n-butanol, 9 ml of concentrated hydrochloric acid and 9 ml of ethanol) and was dried at 105°C for 5 min. The carbapenems appeared as violet-red spots. The R_f values of carbapenems OA-6129 A, B2 and C were 0.46, 0.29 and 0.19, respectively.

TABLE 1

Times for gradient and column switching for the h.p.l.c. — 3 method

Time	Switching valve position	Column	Eluent composition		Function
			Aq. (%)	MeOH (%)	
0	A	1	100	0	Start, sample inject
5.5	B	1 + 2	81	19	Loading step on column 2
10.0	A	1	65	35	Separation on column 2, gradient stop
13.0	A	1	65	35	Flushing of column 1, end of separation on column 2
15.0	A	1	100	0	Reset to initial conditions
20.0	A	1	100	0	Equilibration, end

RESULTS AND DISCUSSION

The carbapenem compounds OA-6129 A, B1, B2 and C can be quantified with the isocratic h.p.l.c. method, if the analytes are pre-cleaned culture broth filtrates or isolated products, where the biological matrix is largely removed. Figure 2(a) shows the isocratic chromatogram from an isolated raw product containing the OA-6129 A, B1, B2 and C. When a fermentation broth sample was analysed by the same method, the substances to be determined (primarily B2) were detected at the tail of a broad matrix peak (Fig. 2b). Chromatograms of this type can be evaluated quantitatively by means of a suitable integration method (tangent skimming). The dotted line in Fig. 2(b) is a simultaneously recorded chromatogram at 270 nm, in order to detect metabolites that are not seen at 300 nm. When the isocratic method is used routinely for carbapenems in fermentation broths, the main problem is that the biological matrix is only partly eluted from the column; thus the separation efficiency is significantly decreased after several sample injections, and the column pressure rises steadily.

This problem can be overcome by column flushing or by application of a gradient h.p.l.c. method. Figure 3 shows a chromatogram of a culture-broth sample developed by gradient elution. Under these conditions, many substances, including impurities from the biological matrix which had been retained on the sorbent formerly, were eluted from the separation column. Positive identification of the carbapenem compounds to be quantified, and quantitative evaluation by peak area integration is obviously difficult from such a chromatogram. To identify the carbapenems OA-6129 A, B1, B2 and C, a chemical degradation method with trichloroacetic acid (TCA) was used;

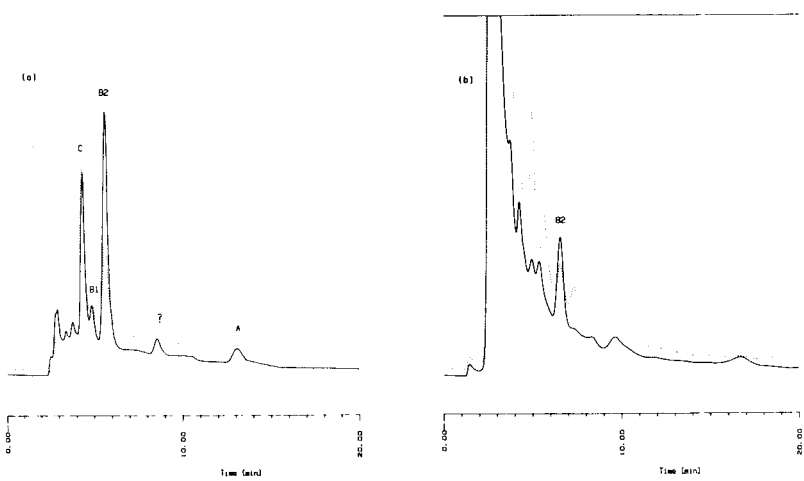

Fig. 2. Chromatograms from isocratic h.p.l.c.: (a) a crude mixture of the carbapenems OA-6129 A, B1, B2 and C; (b) a carbapenem fermentation sample. Conditions: column, Nucleosil C_{18}; eluent ammonium formate buffer pH 8.5/methanol (4:1); flow rate, 2.0 ml min^{-1}; (—) detection at 300 nm; (···) detection at 270 nm.

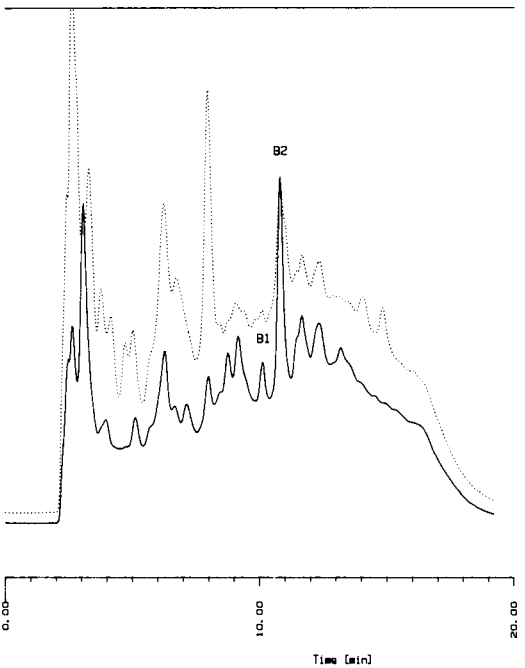

Fig. 3. Chromatogram from h.p.l.c. with gradient elution for a carbapenem fermentation sample. Conditions as for Fig. 2, except that the eluent was ammonium formate buffer pH 8.5/methanol with a gradient from 0% to 35% methanol in 10 min.

this destroyed all the carbapenem compounds selectively in contrast to the interfering substances. Usually 750 μl of sample solution was mixed with 100 μl of aqueous 50% (v/v) TCA solution to achieve the needed concentration of 6—7% (w/w) TCA. After reaction for 1 min, the filtered solution was injected into the h.p.l.c. system. The disappearance of the carbapenem peaks was followed by h.p.l.c. and by t.l.c.; a TCA degradation in a fermentation sample is shown in Fig. 4.

Definite identification of carbapenem peaks in a gradient chromatogram was attempted by multichannel u.v.-detection and on-line spectroscopy. However, the spectra of peaks sitting on a co-eluted matrix background, do not provide information about identity and purity, as only mixed spectra can be obtained. This problem can be solved directly only by a computer program that can subtract a whole gradient or matrix background from the sample data set.

For optimal utilization of the diode-array detector, it was therefore necessary to combine an on-line sample clean-up procedure with isocratic h.p.l.c. by a column-switching technique. Figure 5 shows the chromatograms obtained for a standard sample and a fermentation sample by the column switching method. The concentration of the B2 standard determined by the gradient elution method was 59.1 μg ml^{-1}, and by the column-switching

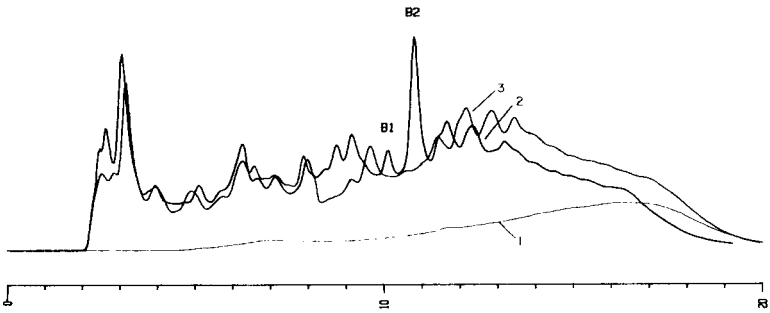

Fig. 4. Carbapenem degradation with trichloroacetic acid (TCA). Chromatograms: (1) blank gradient; (2) fermentation sample; (3) TCA-treated fermentation sample. Chromatographic conditions as given in Fig. 3.

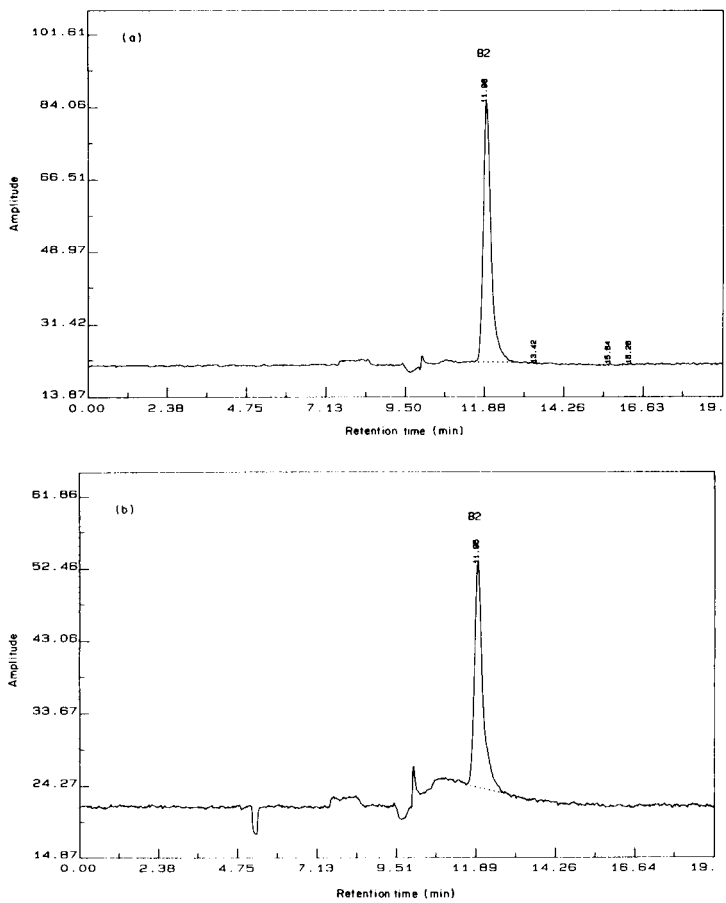

Fig.5. Chromatograms from h.p.l.c. with column switching (see text): (a) an OA-6129 B2 standard solution; (b) a carbapenem fermentation sample.

TABLE 2

OA-6129 from fermentation broth

B2 added[a] (μg ml^{-1})	41.7	67.3	122.0	178.6	230.6
B2 found (μg ml^{-1})	59.0	81.6	139.1	188.5	252.9
Recovery (%)	101.9	97.7	100.7	96.8	102.5

[a]The amount originally present was 16.2 μg ml^{-1}.

method it was 60.7 μg ml^{-1}, which is very good agreement. The linearity of the response of the column-switching method was checked in the range 10—500 μg ml^{-1} by injecting different concentrations of solutions of B2. The calibration function followed a linear equation ($y = kx + d$; $k = 250.5$, $d = 284.3$, $r = 0.99998$). To establish the percentage recovery of B2 from fermentation broths, different amounts of B2 were added to the sample; the results (Table 2) are very satisfactory.

Despite the limitations caused by gradient and background effects, multichannel u.v. detection can be a valuable tool for unambiguous assignment of

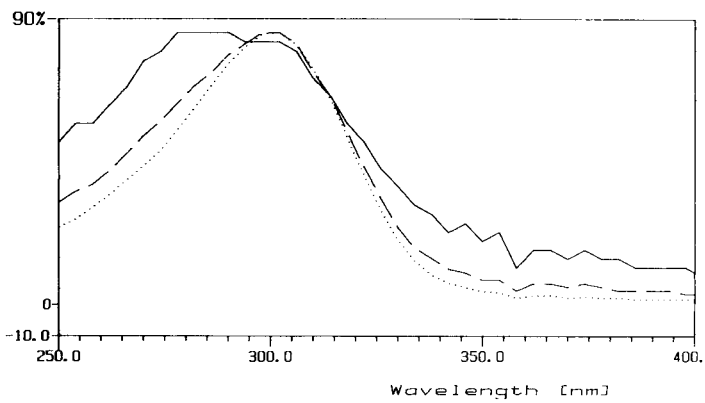

Fig. 6. Examination of B2 peak homogeneity by an overlay of the upslope (—), apex (···) and downslope (— — —) spectra. An impurity is indicated in the upslope region. Conditions and sample as in Fig. 2(a).

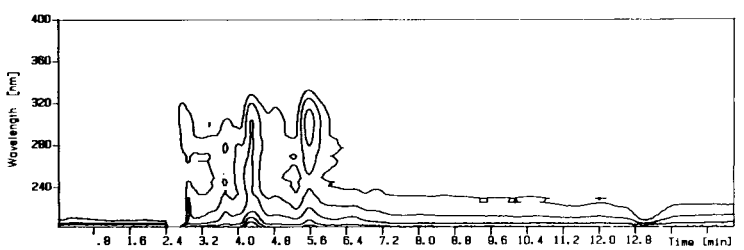

Fig. 7. Plot of isoabsorbance lines for the separation of the crude carbapenem mixture. Chromatographic conditions and sample as in Fig. 2(a).

chromatographic peaks to compounds sought, even in the presence of many by-products and interfering substances. A simple and rapid examination concerning uniformity of obviously separated peaks and the purity of isolated substances is feasible by diode-array detection. The u.v. spectra are recorded and stored within very short times (0.010 s). Except for the two wavelength channels that produce data available in "real time" during a chromatographic run, further evaluation is done from the stored data set after the run ends.

A raw product containing a mixture of different carbapenems was examined for B2 peak purity and for the presence of further by-products. The chromatograms at 300 nm and 270 nm are displayed in Fig. 2(a). The calculation of the absorbance ratio at the two wavelengths over the whole B2 peak did not indicate any inhomogeneity of the B2 substance; the ratio appeared to be constant over the whole peak. But when u.v. spectra were recorded in the upslope, apex and downslope of the B2 peak, there was a significant shift of the absorption maximum from 300 nm to 278 nm in the upslope region. The spectra taken at apex and downslope correspond to the B2 standard spectrum (Fig. 6). Additionally, in a two-dimensional projection (Fig. 7) of a three-dimensional chromatogram for this raw product, where all points with the same absorbance are connected (isoabsorbance lines), an otherwise invisible impurity at the upslope of the B2 peak could be detected.

The author expresses his gratitude to his coworkers F. M. Bogner and A. Rupprechter for excellent technical assistance.

REFERENCES

1 M. Okabe, S. Azuma, I. Kojima, K. Kouno, R. Okamoto, Y. Fukagawa and T. Ishikura, J. Antibiot., 35 (1982) 1255.
2 M. Sakamoto, I. Kojima, M. Okabe, Y. Fukagawa and T. Ishikura, J. Antibiot., 35 (1982) 1264.
3 T. Yoshioka, I. Kojima, K. Isshiki, A. Watanabe, Y. Shimauchi, M. Okabe, Y. Fukagawa and T. Ishikura, J. Antibiot., 36 (1983) 1473.
4 M. Okabe, K. Kiyoshima, I. Kojima, R. Okamoto, Y. Fukagawa and T. Ishikura, J. Chromatogr., 256 (1983) 447.
5 K. Okamura, S. Hirata, Y. Okumura, Y. Fukagawa, Y. Shimauchi, K. Kouno and T. Ishikura, J. Antibiot., 31 (1978) 480.
6 M. Okabe, private communication.
7 C. J. Little, D. J. Tompkins, O. Stahel, R. W. Frei and C. E. Werkhoven-Goewie, J. Chromatogr., 264 (1983) 183.
8 F. Erni, H. P. Keller, C. Morin and M. Schmitt, J. Chromatogr., 204 (1981) 65.
9 S. A. Borman, Anal. Chem., 55 (1983) 836A.
10 K. Zech, R. Huber and H. Elgass, J. Chromatogr., 282 (1983) 161.
11 A. M. Krstulović and H. Colin, TrAC, 3 (1984) 43.
12 K. Hostettmann, B. Domon, D. Schaufelberger and M. Hostettmann, J. Chromatogr., 283 (1984) 137.
13 F. Overzet, A. Rurak, H. v. d. Voet, B. F. H. Drenth, R. T. Ghijsen and R. A. De Zeeuw, J. Chromatogr., 267 (1983) 329.

Analytica Chimica Acta, 163 (1984) 35—42
Elsevier Science Publishers B.V., Amsterdam — Printed in The Netherlands

MOLECULAR WEIGHT FRACTIONATION FOR THE STUDY OF COMPLEX BIODEGRADATION PROCESSES

H. A. LEIDNER*, TH. FLEISCHMANN and G. HAMER

Swiss Federal Institute for Water Resources and Water Pollution Control, Swiss Federal Institutes of Technology, CH-8600 Dübendorf (Switzerland)

(Received 30th March 1984)

SUMMARY

Simulated synthetic sewage was treated in a laboratory-scale, completely mixed, activated sludge plant. Careful control of flow, loading and sludge recycle allowed the plant to be maintained in an essentially steady-state condition for extended periods. "Lumped parameter" determinations were done to assess the plant operating performance in conventional terms. For comparison, more sophisticated determinations were also applied: molecular weight fractionation, amino acids, ammonium-, nitrate- and nitrite-nitrogen, and carbon and nitrogen in the biomass (sludge). Molecular weight fractionation allowed a better characterization of dissolved carbonaceous pollutants. Samples were initially concentrated by low-temperature vacuum evaporation, followed by fractionation by low-pressure gel chromatography. The results demonstrate the value of this method in establishing the fate of complex carbonaceous pollutants present in the feed to bio-treaters and in indicating the residual carbonaceous pollutants in the discharge.

Secondary aerobic biotreatment processes for the purification of municipal sewage and/or industrial waste-waters are highly complex in their nature and account for a significant portion of the capital and operating costs of overall treatment technology. In many European countries, legislation designed to combat water pollution demands ever more strict discharge standards; as a result, it is becoming increasingly important to understand the detailed operation of the processes employed for treatment. Traditional "lumped parameters" for describing sewage and waste-water, such as, BOD_5, COD, DOC, TOC, etc., will require supplementation by more selective analytical techniques.

Bio-oxidation processes utilize and produce organic matter [1, 2]. Utilization and production depend on both the microbes employed and the operating conditions used. In biotreatment processes, the aim is to convert soluble, particulate and immiscible organic pollutants into a minimum quantity of microbial biomass (sludge) and a maximum quantity of carbon dioxide as a result of microbial growth and oxidation, but inevitably some extracellular metabolic products and lysis products will be produced simultaneously. Several workers [3—5] have described, on the basis of group analysis, the residual soluble organic matter in the discharge from bio-

treatment processes. Some of the residual components that are present at very low concentrations have been identified [2] and are clearly compounds that were present in the process feed and known to be recalcitrant to biodegradation. However, for the most part, the bulk of the residual soluble organic matter in biotreater discharges is of microbial origin. Other workers, including Chudoba et al. [6], Grady and Williams [7], Kim et al. [8] and Daigger and Grady [1], have suggested that residual organic matter in biotreatment process discharges are either primary or secondary metabolites, but it would seem an equally plausible hypothesis to suggest that such residual matter results from microbial cell death and lysis in the biotreatment system.

The above-mentioned idea provides the basis for the experimental work, with a laboratory-scale activated sludge plant, that is discussed here. The research program was divided into several stages, involving a gradation with respect to the complexity of the synthetic sewage that was subjected to treatment in the laboratory-scale plant. During each operational stage, lasting ca. 50 days, the object was to maintain steady-state conditions in both the bioreactor and in its associated settling tank, from which microbial biomass was recycled to the bioreactor. Operating parameters in the bioreactor that were measured and controlled included air flow rate, pH, dissolved oxygen concentration, temperature, and both inlet and outlet liquid flow rates. In order to obtain more detailed knowledge of the residual organic components present in the bioreactor discharge, molecular weight distribution (MWD) analysis by gel chromatography [9—11] was used.

In a recent study, Grady et al. [12], working with a laboratory-scale activated sludge plant fed with either simple or complex synthetic sewage, found that the MWD in the plant effluent, determined by membrane fractionation, was primarily influenced by the operating pH and dissolved oxygen concentration in the bioreactor, rather than by the components present in the feed to the bioreactor. A high-molecular-weight fraction was found irrespective of the complexity of the feed utilized, but in the case of simple feeds, greater variations occurred in the MWD as a result of changes in operating parameters.

EXPERIMENTAL

Construction and operation of laboratory-scale plant

The laboratory-scale activated sludge plant (Schmizo AG, CH-4800 Zofingen) used is shown diagrammatically in Fig. 1. It comprises an aeration tank (A, 3 l), a settling tank (B) fitted with a pneumatic, time-controlled sludge recycle system (D), and a final clarifier (C, settling tank). The aeration tank (A) is provided with a lid (E) in which there are seven ports for a thermostat finger, an air outlet fitted with a condenser, a control thermometer, a pO_2 electrode, a pH electrode, an acid/alkali addition tube and a medium feed tube. Aeration is provided through a sintered glass plate in

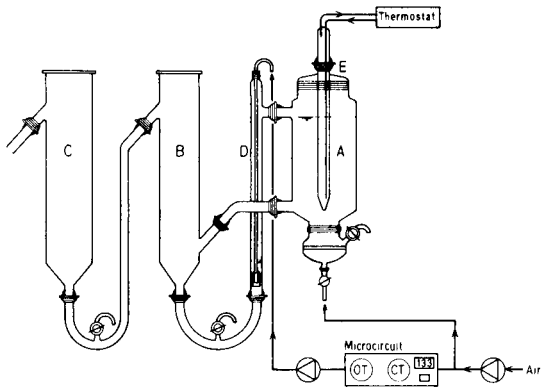

Fig. 1. Model activated sludge plant. For details, see text.

the base of the aeration tank supplied with metered, pressure controlled air from the laboratory compressed-air system. The medium composition used was 250 mg l^{-1} each of glutamic acid and D-glucose, 0.022 mg l^{-1} KH_2PO_4, 0.6 mg l^{-1} NH_4NO_3 and 0.1 mg l^{-1} $MgSO_4 \cdot 7\,H_2O$. The medium was mixed, by using two MP-3 peristaltic tube pumps (Rikakikai, Tokyo), with tap water in the ratio 1:2.75, to give a feed DOC concentration of ca. 53 mg l^{-1}.

The inoculum for the laboratory-scale plant was taken directly from the aeration tank of a municipal activated sludge plant. The hydraulic residence time in the aeration tank of the laboratory-scale plant was maintained constant at 10 h and the system was operated without sludge wastage. A thermostat maintained the aeration tank temperature at 20°C, and the pH was measured and automatically controlled (pH-controller Type 505-D, L. H. Fermentation, Bucks., England) at pH 7.0; the dissolved oxygen concentration was monitored (pO_2 monitor, Type 507, L. H. Fermentation) and was, under the operating conditions used, essentially constant at 7 mg l^{-1}. The pO_2 monitor was calibrated by using the manual Winkler method [13].

Analytical procedures

Routine methods. Daily liquid samples taken from the bioreactor inlet and outlet were analyzed for dissolved organic carbon, nitrate-N, nitrite-N and ammonium-N. The sample was first filtered through a 0.4-μm membrane filter (Nuclepore). The dissolved organic carbon (DOC) was measured after acidification with hydrochloric acid and purging the inorganic carbon with nitrogen using a Type Tocor 2 DOC analyzer (Maihak, D-Hamburg). The NO_3^--N, NO_2^--N and NH_4^+-N were determined by using an automatic spectrophotometric analyzer (Skalar Analytical, Breda, The Netherlands); proprietary method no. 21527 was used for NO_3^--N and NO_2^--N and no. 22125 for NH_4^+-N.

The concentration of sludge (on a dry weight basis) was determined by filtering a 100-ml sample through a 0.4-μm membrane filter and drying at

100°C for 16 h. The carbon and nitrogen contents of the dry sludge were determined with a model 185 CHN analyzer (F & M Scientific). D-Glucose was determined spectrophotometrically by the enzymatic Peridochrom-Glucose method (Boehringer, D-Mannheim) and glutamic acid by first concentrating the sample with a rotary evaporator at 40°C, and subsequent processing in an amino-acid analyzer (model BC-200; Biocal, D-München).

Preparation of cell extracts. A 100-ml sample of sludge from the aeration tank was centrifuged at 5000 rpm for 10 min and washed with physiological saline. The sludge was then resuspended in distilled water and the cells that comprised the sludge were disrupted in a French Press (Aminco, Silver Spring, MD). To separate the cell debris, samples were centrifuged at 20 000 rpm for 10 min and the supernatant liquid was filtered through a 0.2-μm membrane filter. Prior to molecular weight fractionation, the cell extract was diluted with carbon-free distilled water to give a DOC value of ca. 200 mg l^{-1}.

Preparation of liquid-phase samples. In order to prepare dissolved material from the aeration tank effluent for molecular weight fractionation, an appropriately sized aliquot was filtered through a 0.4-μm membrane filter and evaporated to dryness in a rotary vacuum evaporator, so that on redissolving in 10 ml of acidic carbon-free distilled water (pH 3), the DOC concentration was ca. 200 mg l^{-1}. Prior to fractionation, inorganic carbon was purged from the sample and the sample pH was adjusted to pH 7 by addition of phosphate (Na_2HPO_4/KH_2PO_4) buffer. Samples were then stored in Sovirel tubes fitted with rubber septa to prevent any contamination of the sample with carbon dioxide.

Molecular weight fractionation. For molecular weight fractionation, a K 15/90 chromatographic column (Pharmacia) was used. The column packing was pre-swelled Sephadex gel G-25 (fine), with a fractionation range of 100—5000 daltons on the basis of dextran calibration. Because both the ionic strength and the pH can influence the fractionation [14], the eluent used was a 10^{-2} M phosphate (1.37 g l^{-1} $Na_2HPO_4 \cdot 2H_2O$ and 0.75 g l^{-1} KH_2PO_4) buffer (pH 7). The eluent flow, delivered by a type 110 pump (Altex), was 1 cm^3 min^{-1}. The column effluent was split and one part was transferred to an on-line DOC detector [15, 16], so as to allow direct comparison of chromatograms on an identical DOC basis. Because present interest concerns molecular weight distribution rather than actual molecular weights of the components present, the column was calibrated with a mixture of dextran-4 (m.w. 4000—6000), dextrin-20 (m.w. 3200) (Serva Feinbiochemica, D-Heidelberg) and fructose (m.w. 180) (Fig. 2). The exclusion limit of the column packing was for components with m.w. >5000. Samples were applied with a syringe to a loop-injector (1 cm^3) which was protected by a 0.45 μm membrane filter.

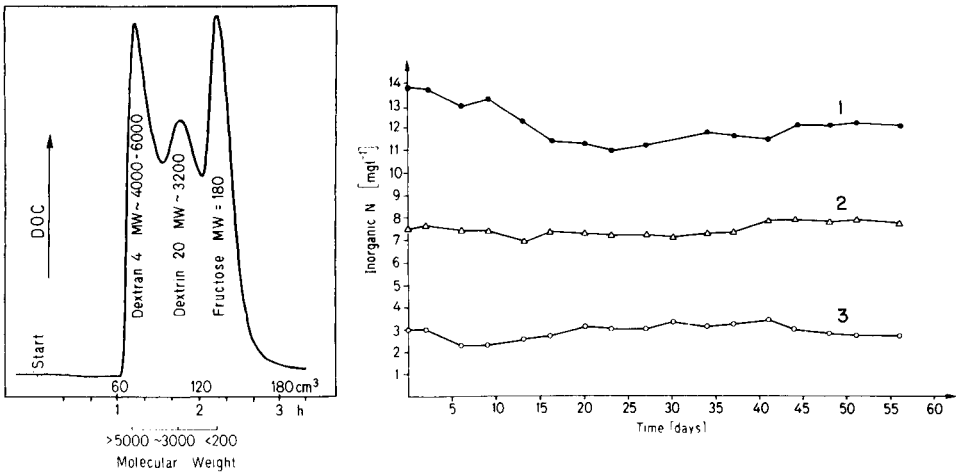

Fig. 2. Calibration of Sephadex G-25 column. Conditions: 1 cm^3 (loop injection) of standard containing 1.3 mg each of Dextran-4, Dextrin-20 and fructose; eluent 10^{-2} M phosphate buffer ($Na_2H\ PO_4/KH_2\ PO_4$), pH 7.0; flow rate 1 $cm^3\ min^{-1}$; DOC detector; carrier gas CO_2 free air at 9 l h^{-1}; range 2, span 10; recorder at 3 cm h^{-1}.

Fig. 3. Inorganic nitrogen components in mg l^{-1} nitrogen in the inflow and outflow of the plant. Curves: (1) NO_3^--N effluent, $\bar{x}$ = 12.1, s = 0.9; (2) NO_3^--N feed, $\bar{x}$ = 7.4, s = 0.4; (3) NH_4^+-N feed $\bar{x}$ = 2.8, s = 0.6.

RESULTS AND DISCUSSION

After an adaptation and stabilization period of 30 days under the operating conditions described earlier, sampling and quantitative work were commenced. The experimental period lasted 56 days. The concentration of nitrogenous compounds, as mg l^{-1} nitrogen, in both the inlet and outlet flows of the aeration tank are shown in Fig. 3. The actual points shown are mean values for two or three successive daily samples. The overall mean values and the standard deviations are given in the legend. The NO_3^--N concentration in the inlet flow comprises the sum of the nitrate in the medium and that in the diluting (tap) water. The higher concentration of NO_3^--N in the outlet flow indicates that all the NH_4^+-N that was not assimilated by the microbes was nitrified to produce NO_3^--N. Neither NH_4^+-N nor NO_2^--N could be detected in the outlet flow of the aeration tank.

The dry weight of sludge remained essentially constant at 2.1 (s = 0.2) g l^{-1} during the experimental period. Because no sludge wastage occurred, this suggests that the microbial growth and death/lysis rates balanced each other. The mean carbon and nitrogen contents of the dried sludge, measured 16 times over 56 days, were 39.1% (s = 1.10) and 8.75% (s = 0.26), respectively. The results indicate that the sludge was essentially homogeneous and of constant composition throughout the experimental period.

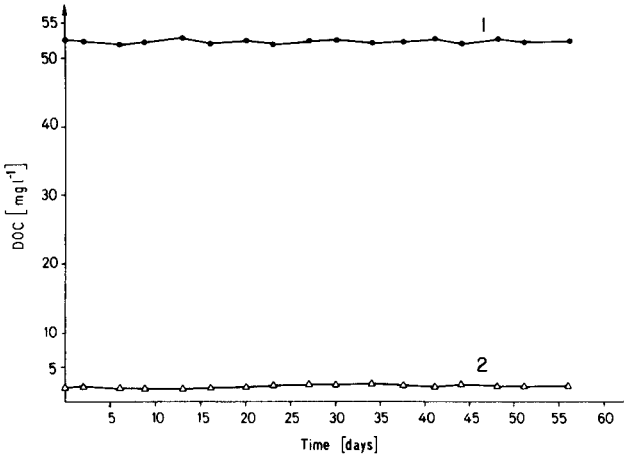

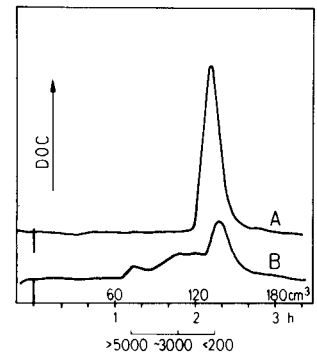

Fig. 4. Dissolved organic carbon (DOC) in mg l^{-1} in the inflow (line 1) and outflow (line 2) of the plant.

Fig. 5. Molecular weight distribution of the DOC in the inflow (curve A) and outflow (curve B) of the plant fractionated with a Sephadex G-25 column. Conditions: 1 cm^3 injection (sample adjusted to 200 mg C l^{-1}); otherwise as in Fig. 2.

Figure 4 shows the DOC values for the inflow and outflow of the model treatment plant. The points represent mean values obtained on the same basis as before. The overall mean values for DOC in the feed and effluent were 52.7 mg l^{-1} (s = 0.4) and 2.4 mg l^{-1} (s = 0.2), respectively. The DOC oxidation was 95.5% (s = 0.4) complete at a mean hydraulic residence time of 10 h, but the key question of what comprises the residual carbon in the plant effluent remains. Potentially, the residual carbon could include the complete range of microbial metabolites that can be produced from glucose and/or glutamic acid at concentrations below the limits of detection of established, straightforward, analytical methods. Analysis of occasional samples of the plant effluent for glucose and glutamic acid indicated a probable absence of both, i.e., <280 nmol l^{-1} glucose (<20 μg l^{-1} DOC) and <20 nmol l^{-1} glutamic acid (<1.2 μg l^{-1} DOC). Hence, their potential DOC contribution would not be detectable.

However, by examining the molecular weight distribution (MWD), it was possible to compare the inlet and outlet compositions of the plant, thereby gaining valuable insight into the character of the compounds present. The MWD pattern of the inlet-flow DOC is shown in Fig. 5. As would be expected, only low-molecular-weight compounds were detected in the inlet flow, but in the outlet flow the DOC present comprized two distinct fractions at the extremes of the fractionation range of the gel and an indistinct distribution of compounds between the two extremes. These findings are partially consistent with those recently reported by Grady et al. [12] for activated

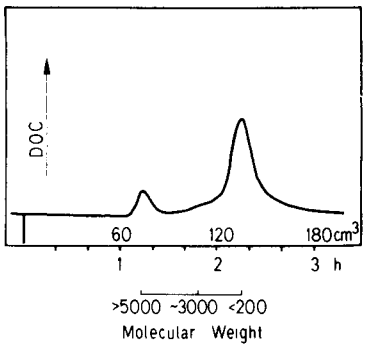

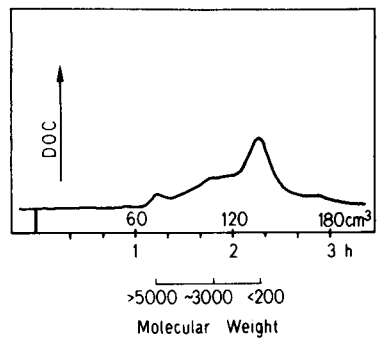

Fig. 6. Molecular weight distribution of the DOC of the biomass (sludge) cell-free extract fractionated with a Sephadex G-25 column. Conditions as in Fig. 5.

Fig. 7. Molecular weight distribution of the DOC in the plant effluent after percolation through a cation ion-exchange column, pH 2, fractionated with a Sephadex G-25 column. Conditions as in Fig. 5.

sludge processes where the DOC in the feed comprised low-molecular-weight substances, but their results, obtained by applying a membrane filtration technique, indicated inverse fractions of compounds of low and high molecular weight when compared with the results reported here. Under the experimental conditions employed, no contribution by substrates to the molecular weight fractions present in the outlet flow could be detected by component-selective procedures, and so the fractions detectable in the outlet flow can only be of microbial origin. In order to confirm this hypothesis, a comparative study with a cell-free extract of activated sludge from the model plant was undertaken. As can be seen from Fig. 6, the fractionation of the cell-free extract only showed compounds at the two extremes; no compounds between the extremes, were evident. This result suggests that both lysis products and cell debris produced during operation of activated sludge processes, are subject to some degree of degradation during process operation.

Both proteinaceous matter and free amino acids that can result from cell lysis and/or excretion during microbial growth are probably easily degraded. When a sample was percolated through a cation-exchange column at pH 2, there was no change in its MWD compared with the normal effluent sample, as can be seen when Figs. 5 and 7 are compared. Hydrolysis of the residual organic matter present in the effluent resulted in a high concentration of NH_4^+-N, which suggests the presence, amongst the residual organic compounds, of nucleic acids and bases and/or related compounds [17], and this is presently under investigation.

Conclusions

Molecular weight fractionation of residual organic matter present in effluents discharged from sewage and waste-water biotreatment processes offers

a technique which, when used in association with traditional analytical techniques, allows an increased understanding of the functioning of the treatment process to be developed. Further, it provides a basis for the initiation of additional research that could result in improved biotreatment processes. In addition to its application for biotreatment processes, the technique will undoubtedly find application in studies of both aerobic and anaerobic sludge digestion (stabilization) processes.

Thanks are due to Dr. G. Frank for some initial amino acid analyses and for advice concerning such analyses, to Ms. Ch. Schenk for typing the manuscript, to Ms. H. Bolliger for art work and to Mr. P. Schlup for photographic work. This research forms an initial part of EAWAG Research Project No. 20-832.

REFERENCES

1 G. T. Daigger and C. P. L. Grady, Jr., Water Res., 11 (1977) 1049.
2 H. A. Painter, Chem. Ind., (1973) 818.
3 J. Manka and M. Rebhun, Water Res., 16 (1982) 399.
4 H. A. Painter, M. Viney and A. Bywaters, J. Proc. Inst. Sewage Purif., 60 (1961) 302.
5 M. Rebhun and J. Manka, Environ. Sci. Technol., 5 (1971) 606.
6 J. Chudoba, J. Cervenka and M. Zima, Technol. Water, 14 (1969) 5.
7 C. P. L. Grady, Jr. and D. R. Williams, Water Res., 9 (1975) 171.
8 B. R. Kim, V. L. Snoeyink and F. M. Saunders, J. Water Pollut. Control. Fed., 48 (1976) 120.
9 H. Determann, Gelchromatographie, Springer Verlag, Berlin, 1967.
10 O. O. Hart, Prog. Water Technol., 12 (1980) 525.
11 F. Fuchs and B. Raue, Vom Wasser, 57 (1981) 95.
12 C. P. L. Grady, Jr., E. J. Kirsch, M. K. Koczwara, B. Trgovich and R. D. Watt, Water Res., 18 (1984) 239.
13 Deutsche Einheitsverfahren zur Wasser-, Abwasser- und Schlammuntersuchung, Verlag Chemie, Weinheim, 1983.
14 R. S. Swift and A. M. Posner, J. Soil. Sci., 22 (1971) 237.
15 R. Gloor and H. Leidner, Anal. Chem., 51 (1979) 645.
16 R. Gloor, H. Leidner, K. Wuhrmann and Th. Fleischmann, Water Res., 15 (1981) 457.
17 G. F. Parkin and P. L. McCarty, Water Res., 15 (1981) 139.

Analytica Chimica Acta, 163 (1984) 43—54
Elsevier Science Publishers B.V., Amsterdam — Printed in The Netherlands

IDENTIFICATION AND DETERMINATION OF METABOLITES IN PLANT CELL BIOTECHNOLOGY BY GAS CHROMATOGRAPHY AND GAS CHROMATOGRAPHY/MASS SPECTROMETRY

Application to Nonpolar Products of *Chrysanthemum cinerariaefolium* and *Tagetes* Species

A. F. GRONEMAN*

Research Institute ITAL, P.O. Box 48, 6700 AA Wageningen (The Netherlands)

M. A. POSTHUMUS

Laboratory of Organic Chemistry, Agricultural University Wageningen, P.O. Box 8026, 6700 EG Wageningen (The Netherlands)

L. G. M. TH. TUINSTRA and W. A. TRAAG

State Institute for Quality Control of Agricultural Products, P.O. Box 230, 6700 AE Wageningen (The Netherlands)

(Received 17th April 1984)

SUMMARY

Gas-liquid chromatography (g.l.c.) and gas-liquid chromatography/mass spectrometry (g.c./m.s.) were used for profile analysis and for identification, confirmation and determination of traces of nonpolar metabolites synthesized in plant tissue, calli and in suspension-cultured cells of *Chrysanthemum cinerariaefolium* (pyrethrum) or *Tagetes* species (marigold). When dried leaf samples (1—20 mg) were tested, six pyrethrins were detected simultaneously at the picogram level with an electron capture detector. This method permits the early selection of high yielding tissues and calli for the development of plant cell cultures. α-Terthienyl was quantified at the nanogram level with the electron capture detector; calibration graphs were linear between 0.2 and 20 ng and the minimum detectable quantity was about 0.1 ng. The concentration of α-terthienyl in air-dried roots of *T. erecta* was 140 $\mu g\ g^{-1}$. However, this procedure used alone is not reliable, because α-terthienyl and the pyrethrin Cinerin I have the same retention time. Mass spectrometry is needed for identification and confirmation. Profile analysis of a leaf extract of *T. minuta* by high-resolution g.c./m.s. and accurate mass measurements showed 13 nonpolar compounds, of which 9 were tentatively identified; they include 2 sesquiterpenoids, 3 thiophenes, 2 sterols with a precursor and ethyl linolenate. Analyses of *T. minuta* indicated that in calli and cell suspensions, plant sterols are synthesized but sesquiterpenoids or thiophenes are not produced.

Research in plant cell cultures has progressed to such a point that biotechnological applications are considered [1] and one application on a commercial basis has started [2]. The main interest is focussed on the production of valuable secondary metabolites. In early work [3], it was found that various interesting compounds synthesized by intact plants are also formed in calli and in cell suspension cultures. In a few selected cases, the production of

0003-2670/84/$03.00

specific metabolites in plant cell cultures exceeds that of differentiated tissue in the parent plant [1, 4].

In this investigation, the plant species chosen for studies with plant tissues, calli, and cell suspensions all belong to the Compositae family. The first species chosen was *Chrysanthemum cinerariaefolium* (pyrethrum), which is of commercial interest because it produces natural insecticides known as pyrethrins. The other species selected were three *Tagetes* species (marigold): *T. minuta*, *T. patula* and *T. erecta*. These were used as models for studies with suspended plant cells because they produce thiophenes, which have strong nematocidal properties.

Metabolites in plant tissue and in plant cell cultures are intermediates or end-products of a number of metabolic pathways. Because the absence or presence of metabolites may reflect physiological situations and aberrations of the plant tissue and cells, the identification of metabolites, and possibly their determination, is essential to obtain more insight into the biosynthesis of metabolic products and their pathways. It is therefore necessary to develop adequate analytical methods to measure profiles of compounds in samples and to identify traces of metabolites.

This paper deals with the potentials of gas-liquid chromatography (g.l.c.) and gas-liquid chromatography/mass spectrometry (g.c./m.s.) for profile analysis and the identification, confirmation and determination of traces of nonpolar metabolites synthesized in plant tissues, calli or in suspension-cultured cells of *Chrysanthemum cinerariaefolium* or of *Tagetes* species.

EXPERIMENTAL

Reference compounds and plant materials

The World Standard Pyrethrum Extract was kindly provided by the Pyrethrum Board of Kenya. Synthetic α-terthienyl was generously supplied by Prof. H. Wijnberg, State University of Groningen.

Seeds of pyrethrum, originating in Dalmatia, were supplied by Lyon Botanical Garden "Tête d'Or", France. Marigold seeds (*Tagetes erecta* and *T. minuta*) were purchased (Tubergen Seed Co., The Netherlands). Pyrethrum and marigold seeds were germinated in potting soil in the glasshouse. *Tagetes* species grew much more quickly than pyrethrum. Young leaves of one month old *T. minuta* plants and of approximately six months old pyrethrum plants were randomly sampled, dried at 40°C and stored over silica gel until use. Roots of one month old *T. erecta* plants were harvested, washed with tap water, and treated as described for the leaves.

Callus was obtained from hypocotyls of germinated sterilized seeds of *T. minuta* on semisolid Murashige and Skoog (MS) medium [5] supplemented with 2% sucrose, vitamins and growth regulators. The developing calli, consisting of highly vacuolated unorganized cells, were subcultured regularly to maintain good growth in darkness.

Cell suspension cultures were obtained from calli of *T. minuta*. Suspension cultures of cells and small aggregates were formed by shaking (120 rpm) in liquid MS medium after initial manual disintegration of the calli.

The cells analysed were subcultured batchwise at regular intervals and grown in liquid MS medium (2% sucrose and 1% polyvinylpyrrolidone, PVP-40) at 2800 lux (Philips TL 40W/33) and 24° C. Detailed descriptions of the growing conditions of calli and cell suspensions are available from the authors on request.

Harvested calli and cells of suspension cultures were lyophilized prior to extraction and analysis.

Extraction. Samples (1.0—100 mg) of dried and ground leaves, roots, calli or cells were extracted with n-hexane for at least 48 h at 35° C. Portions of the clear supernatant solutions were filtered through 45-μm filters and analysed directly after appropriate dilution with n-hexane.

Qualitative and quantitative procedures

The primary method was g.l.c. of the extracts on a Pye-Unicam GCV gas chromatograph fitted with a 90 cm × 2 mm i.d. glass column packed with 1.5% OV-17 and 1.95% OV-202 (isotherm at 190° C). A 1.5 m × 2 mm i.d. glass column packed with 3% OV-17 was used for preparative work in conjunction with the g.c./m.s. investigation. The Pye-Unicam instrument was equipped with electron capture (ECD) and flame ionization (FID) detectors, that could be used alternatively. Accurate injections of 5-μl samples were done with a Pye S8 Autojector, that also electronically started a HP-3390 plotting/reporting integrator for an accurate measurement of retention times and for integration of detector signals.

High-resolution gas chromatography was done with a Carlo Erba HRGC instrument. A 25 m × 0.3 mm i.d. open duran glass column coated with SE-52 was used with a Grob on-column injector. The initial oven temperature was 80° C; one minute after injection, the temperature was raised at 25° C min^{-1} to 200° C. The ECD and FID were mounted in series (300° C) and their signals were integrated by two HP-3390 plotting/reporting integrators. For confirmation and identification of compounds, g.c./m.s. was used. For accurate mass measurements, a VG MM-7070-F mass spectrometer was attached to a Pye-Unicam 204 gas chromatograph fitted with a 1.5 m × 2 mm i.d. glass column packed with 3% OV-17. In conjunction with high-resolution gas chromatography, a Finnigan 4000 mass spectrometer with an INCOS system was used. With the Finnigan 9610 gas chromatograph, a 25 m CP-Sil 19 CB fused silica capillary (0.22 mm i.d.) column was connected to the mass spectrometer. A volume of 5 μl was injected splitless at an injection port temperature of 260° C while the oven temperature was adjusted at 80° C; after 4 min, the oven temperature was raised to 260° C at 10° C min^{-1}.

RESULTS AND DISCUSSION

Analysis of pyrethrins

The problems associated with qualitative and quantitative analyses of pyrethrins have been extensively studied because of industrial, scientific, toxicological, pharmacological and environmental interests. The commercial method adopted in the United States in 1940 was the Association of Official Agricultural Chemists (AOAC) method [6]. Methods adopted in Europe include the Pyrethrum Board of Kenya (PBK) method [7] and the Tanganyika Extract Co. (TECO) method [8]. These methods are unsuitable for this research because they need relatively large amounts of pyrethrins with a detection limit of 40 mg of total pyrethrins. The amounts of pyrethrins I and II are determined colorimetrically, neglecting the fact that each consists of three natural esters (Table 1).

Thin-layer chromatography (t.l.c.) is valuable for the detection of pyrethrins [9], but a disadvantage is the occurrence of pyrethrin photolysis. High-performance liquid chromatography (h.p.l.c.) with a u.v. detector (254 nm) has also been proposed for pyrethrins [10]; this method can separate the six esters in a refined standard solution but a more sophisticated detector would be needed to avoid interferences.

TABLE 1

Names and molecular characteristics of pyrethrins and the thiophene α-terthienyl, and ratio of the sensitivity of an electron capture detector to a flame ionization detector

Name	Molecular weight	Formula	Chemical structure		Concentration in n-hexane ($\mu g\ \mu l^{-1}$)	Response ratio ECD/FID
Pyrethrins			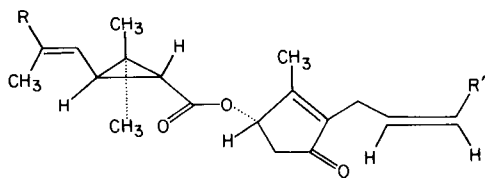			
Pyrethrins I			R	R'		
Cinerin I	316	$C_{20}H_{28}O_3$	CH_3	CH_3	1.33	119
Jasmolin I	330	$C_{21}H_{30}O_3$	CH_3	C_2H_5	0.58	209
Pyrethrin I	328	$C_{21}H_{28}O_3$	CH_3	$CH{=}CH_2$	5.02	83
Pyrethrins II						
Cinerin II	360	$C_{21}H_{28}O_5$	$COOCH_3$	CH_3	1.78	316
Jasmolin II	374	$C_{22}H_{30}O_5$	$COOCH_3$	C_2H_5	0.61	514
Pyrethrin II	372	$C_{22}H_{28}O_5$	$COOCH_3$	$CH{=}CH_2$	4.14	234
Thiophene						
α-terthienyl	248	$C_{12}H_8S_3$	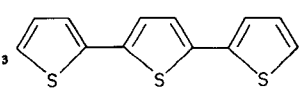		0.002	9.4

Gas—liquid chromatography (g.l.c.) is relatively sensitive and is less affected by interfering substances, because only about 20% of all known organic compounds can be treated by g.c. without prior chemical modification [11]. The six pyrethrins can be detected by a flame ionization detector; the response/concentration plots are linear for each ester between 5 and 20 μg of total pyrethrins. The minimum detectable quantity is about 1 μg of total pyrethrins [12]. However, other volatile compounds, such as certain alkanes, can interfere with the FID response to pyrethrins [12]. The most sensitive, well-documented method takes advantage of the electron-capturing properties of pyrethrins [13]. Table 1 gives information about the sensitivity of the ECD for six pyrethrins in the sample of World Standard Pyrethrum Extract (WSPE) 1977. The ratios of the two integrated signal responses of the ECD and FID connected in series indicate that the ECD is 80—500 times more sensitive than the FID. These ratios depend on both the concentration and the compound of interest. The electron affinity of a compound, which governs the ECD response, varies greatly from one component to another.

The molecular weights and the structures of the six insecticidal constituents present in pyrethrum are shown in Table 1. Cinerin I, Jasmolin I and Pyrethrin I are all esters of chrysanthemic acid formed with the alcohols cinerolone, jasmololone and pyrethrolone, respectively [14]. Cinerin II, Jasmolin II and Pyrethrin II are similarly related, but are esters of pyrethric acid formed with the three mentioned alcohols. The ECD/FID response ratios in Table 1 suggest that the alcoholic constituent jasmololone causes the highest electron affinity when esterified with both acids.

Pyrethrins can be detected at the picogram level in pesticide residues by g.l.c. with the electron capture detector [15]. An application of trace analyses of plant tissue is presented in Fig. 1. A chromatogram of a diluted sample of the WPSE 1977 is shown in Fig. 1A and a chromatogram of traces of pyrethrins extracted from 21.3 mg of tissue from a section of the top part of a young pyrethrum leaf in Fig. 1B. Another section of the same leaf was used to generate callus. The g.c. separation of the six esters in the WPSE is good and there is no indication of sample decomposition. It is interesting

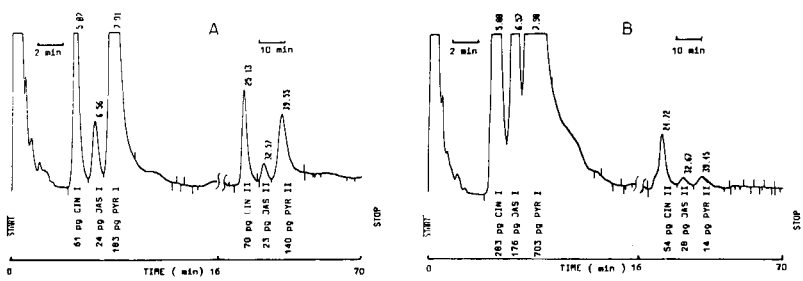

Fig. 1. Isothermal packed-column chromatograms (190° C, 1.5% OV-17 + 1.95% OV-202) with the ECD: (A) pyrethrins is a sample of the World Standard Pyrethrum Extract; (B) pyrethrins in a sample of an extract of a young pyrethrum leaf.

that the profile of the pyrethrins from the standard, which is obtained by extracting dried flowers, differs significantly from that obtained from the leaves. The profile of hexane-extractable pyrethrins in the sample of the pyrethrum leaf is typical for the available pyrethrum plants. It indicates that of the six pyrethrins, three esters of chrysanthemic acid are mainly present at the following concentrations (in $\mu g\ g^{-1}$): Cinerin I, 319; Jasmolin I, 199; Pyrethrin I, 794; total pyrethrins I, 1312. The esters of pyrethric acid occur at much lower concentrations (in $\mu g\ g^{-1}$): Cinerin II, 61; Jasmolin II, 32; Pyrethrin II, 16; total Pyrethrins II, 109.

Gas-liquid chromatography with the ECD makes it possible to find small parts of plant tissue where biosynthetic activities are most explicit. In this way, it is feasible to select the highest yielding plant tissues for the development of calli and cell suspensions for biotechnological purposes. An ECD has the disadvantage that noise and contamination problems can easily arise. To avoid detector disturbances and excessive down-time, considerable care must be taken in conditioning the detector and in preparing the samples.

Confirmation of pyrethrins and iso-pyrethrins by g.c./m.s.

In order to check the results obtained by g.l.c. with the electron capture detector, a few key samples of extracts of pyrethrum leaves and flowers were subjected to g.c./m.s. The mass spectra of the pyrethrins in the extracts were compared with the corresponding spectra from a sample of the WSPE 1977. The presence of the six pyrethrins in the extracts of pyrethrum leaves and flowers was qualitatively confirmed by g.c./m.s.

It has been reported that iso-pyrethrins are produced in calli of *Tagetes minuta* [16]. Because natural iso-pyrethrins have not been detected in pyrethrum but are only found after thermal isomerization at 200° C [17], there was a need to determine relative retention times and to confirm the presence of iso-pyrethrins. Figure 2 shows the reconstructed ion-current chromatogram of pyrethrins separated on a packed column. Iso-pyrethrins were also identified by this procedure by using a temperature high enough to isomerize a fraction of Pyrethrin I and Pyrethrin II into Iso-pyrethrin I and Iso-pyrethrin II, respectively. The relative retention times of the two iso-pyrethrins are in fair agreement with reported results found in investigations in which g.l.c. was combined with chemical ionization mass spectrometry with isobutane as the reagent gas [18].

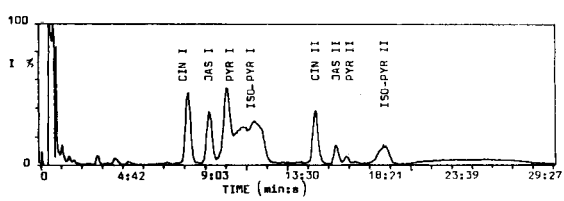

Fig. 2. Reconstructed ion-current chromatogram of pyrethrins and iso-pyrethrins. Conditions: 3% OV 17, temperature programmed from 180° C to 250° C at 4° C min^{-1}.

Analysis for α-terthienyl

Qualitative and quantitative analyses for α-terthienyl in plant tissues have received relatively little attention. No generally adopted method was found in the literature. The reported analyses were mainly done in organic chemistry departments in universities [19, 20]; there was only one research effort in industry [21]. The methods required the collection and extraction of several kilograms of plant material; the extracts were concentrated and separated by preparative chromatography. Repeated chromatography on columns of aluminium oxide yielded the pure compound, which was identified and determined by i.r. or u.v. spectrophotometry, or both. Recently, two methods based on h.p.l.c. have been published; these methods need 0.5—2 g of fresh plant tissue [22] or 1—5 g of dry plant material [23].

Because most of the published methods are relatively material- and time-consuming and no information could be found on the degree of electron-capturing properties of α-terthienyl, similar experiments were done as described above for the pyrethrins. The results (Table 1) indicate that α-terthienyl has electron-capturing properties and that the sensitivity of an ECD to 2 ng of α-terthienyl in n-hexane is about 10 times higher than the sensitivity of the FID.

This higher sensitivity with the ECD was used to quantify α-terthienyl with a high-resolution g.l.c. system. When diluted standard solutions of α-terthienyl were examined, the calibration graphs were linear between 0.2 and 20 ng of α-terthienyl in n-hexane with correlation coefficients $r \geqslant 0.99$. The minimum detectable quantity was approximately 0.1 ng of α-terthienyl for this system.

Separation of pyrethrins and α-terthienyl

It has been reported that iso-pyrethrins and pyrethrins are produced in calli [16, 24] and cells [25] of *Tagetes* species. The analytical methods applied in those investigations included g.l.c. with a flame-ionization detector; the responses were compared with those of standard solutions prepared from a WSPE sample.

However, comparison of the chromatograms of α-terthienyl (Fig. 3A) and pyrethrins (Fig. 3B) shows that the retention times of α-terthienyl and Cinerin I are almost the same. A Grob on-column co-injection of α-terthienyl with pyrethrins confirmed that the peaks of α-terthienyl and Cinerin I practically coincided (Fig. 3C). Gas-liquid chromatography with the ECD of an extract of *T. erecta* roots showed a peak which coincided with the retention times of Cinerin I and α-terthienyl, and other peaks corresponding to unidentified components. To identify the Cinerin I or the α-terthienyl or both compounds and the other components, it was decided to use high-resolution g.c./m.s. with the Finnigan 4000.

Figure 4 shows the reconstructed ion-current chromatogram of a sample of the root extract of *T. erecta* together with the chromatogram of synthetic standard α-terthienyl. The mass spectrum of the compound of interest (scan

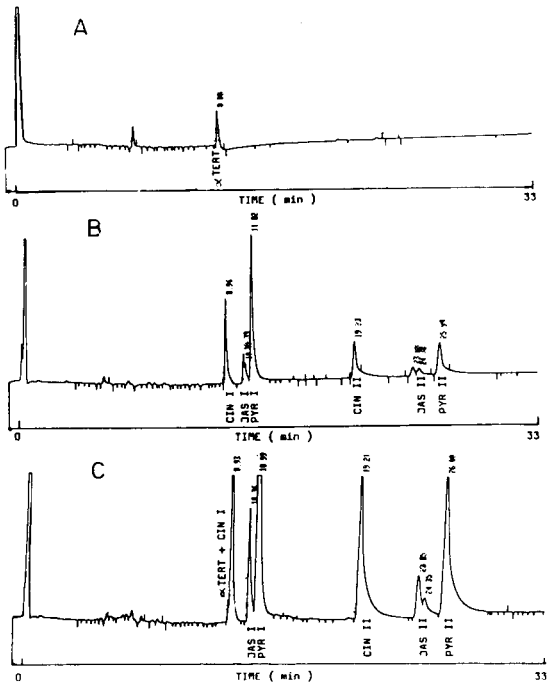

Fig. 3. Chromatograms: (A) α-terthienyl; (B) pyrethrins of the WSPE; (C) a co-injection of α-terthienyl and pyrethrins using on-column injection. Conditions: 25 m capillary glass column SE-52; ECD. Temperature programmed: 80°C for 1 min, then 25°C min^{-1} to 200°C. Injected volume 1 μl.

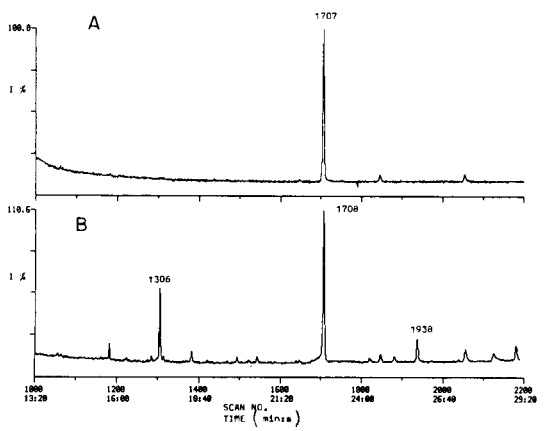

Fig. 4. Reconstructed ion-current chromatograms: (A) the synthetic standard α-terthienyl; (B) a root extract of *T. erecta*.

1708 in Fig. 4B) corresponds excellently with that of authentic α-terthienyl (Fig. 4A) and not with that of Cinerin I. The other peaks present in the chromatogram of the root extract of *T. erecta* (scans 1306 and 1938 in Fig. 4B) also seem to be due to sulfur compounds, as readily recognized from the prominent appearance of ^{34}S-isotopic satellite peaks (Fig. 5A, B and C).

Accurate mass measurements indicated that the molecular formulae were $C_{12}H_8S_2$ and $C_{14}H_{12}O_2S_2$, respectively. Furthermore, the mass spectrum of the compound $C_{14}H_{12}O_2S_2$ showed intense mass peaks at 43 (Ac^+) and at 216 [$(M - 60)^+$], indicating an acetate (Fig. 5C). The compounds are tentatively identified as 5-(but-3-en-1-ynyl)-2,2′-bithiophene, and aceto-(but-3-en-1-ynyl)-2,2′-bithiophene. These compounds were also identified in earlier reports on *T. patula* [22, 23].

Quantitative work indicated that the concentration of α-terthienyl in the dried roots was about 140 $\mu g\ g^{-1}$. This is in fair agreement with an earlier estimate of 100 $\mu g\ g^{-1}$ α-terthienyl in air-dried roots [21] obtained by analysis of 24 kg of clean, freshly harvested roots of *T. erecta*.

Profile analysis

Extracts of plant tissues, calli or cells suspension culture are often multicomponent. The use of high-resolution g.l.c. can provide a detailed profile of a given sample. The profiling approach is valuable in disclosing biosynthetic pathways or metabolic aberrations of plant cells.

Preliminary results for a sample of leaf extract of *T. minuta* obtained by high-resolution g.l.c. showed more unidentified peaks than identified compounds such as terthienyl and bithiophenes. Again, high-resolution g.l.c. combined with mass spectrometry was used in order to obtain definite information about extractable nonpolar metabolites present in samples of leaves, calli and cell suspensions of available *T. minuta*. Figure 6 shows the reconstructed ion-current chromatograms obtained, one with 11 major peaks for a sample of leaf extract (Fig. 6A) and one for a sample of an extract of cells of a suspension culture of *T. minuta* (Fig. 6B). For seven compounds, the corresponding elemental compositions were determined by accurate mass measurements in a companion run with the VG-MM 7070 mass spectrometer. These spectra also indicated the presence of sterols in leaves and calli. The results of the profile analyses with the tentative identification of nine compounds are summarized in Table 2. Caryophyllene and elemene are sesquiterpenoids, which occur in nature in many essential oils.

Four different sulfur compounds were found in the leaf of *T. minuta*. They are identified as 2,2′:5′,2″-terthiophene (scan 1824) and 5-(but-3-en-1-ynyl)-2,2′-bithiophene (scan 1557), 5-(but-3-en-1-ynyl)-5′-methyl-2,2′-bithiophene (scan 1651) and a substituted bithiophene (scan 1956). Three of these four compounds have been reported to occur in *T. patula* [22, 23, 26] and *T. minuta* [23]. It is speculated that compounds 1557 and 1651 are precursors of compound 1824 [26], but confirmation is still needed. The last group of metabolites found in the leaves are plant sterols. β-Sitosterol is also very

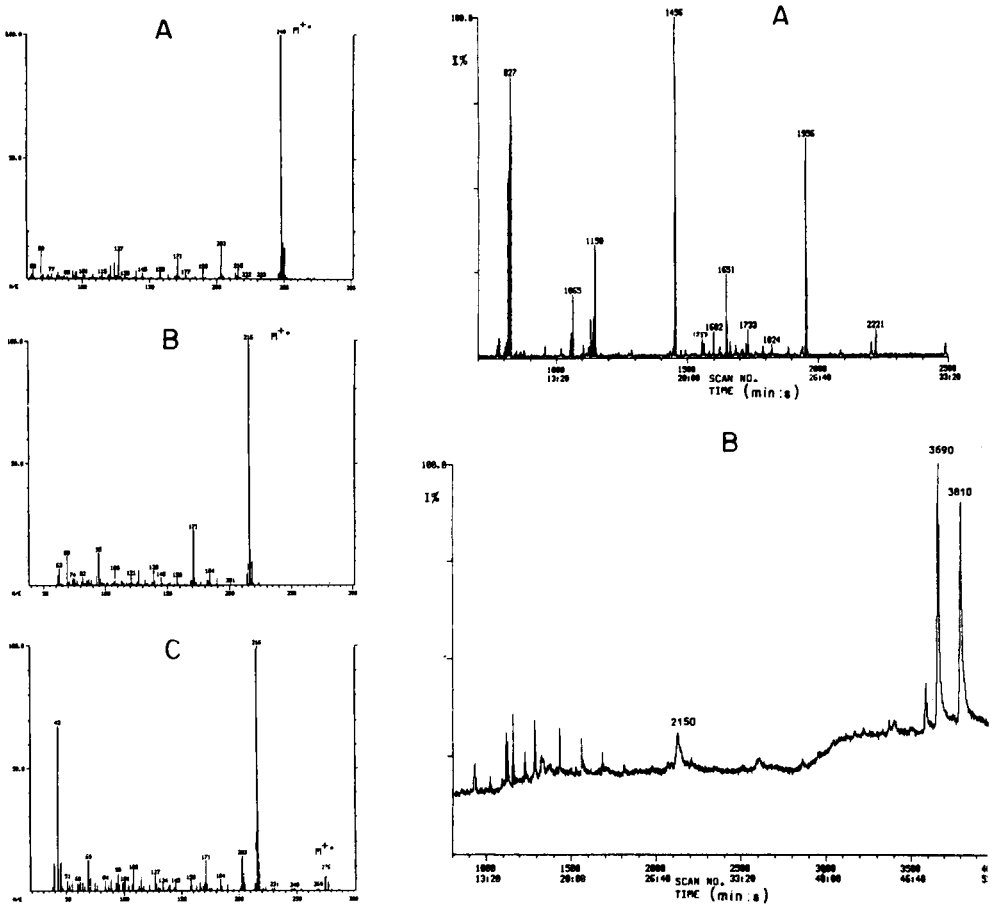

Fig. 5. Mass spectra of compounds in a root extract of *T. erecta* in Fig. 4: (A) compound 1708; (B) compound 1306; (C) compound 1938.

Fig. 6. Reconstructed ion-current chromatograms: (A) a sample of leaf extract; (B) a sample of cell suspension extract of *T. minuta*.

common in other plants. Squalene is an intermediate in the biosynthesis of sterols.

The profile of compounds in the sample of the cell extract (Fig. 6B) indicates that no sesquiterpenoids or bi- and ter-thiophenes were detected in extracts from green cells of *T. minuta*, grown batchwise in suspension cultures. This investigation also provides no evidence for the presence of pyrethrins or iso-pyrethrins in leaves or cells of *T. minuta*. However, the biosynthesis of squalene, stigmasterol and β-sitosterol that occurs in the leaves also appeared to take place in cell suspension cultures. Results from the analysis of calli from *T. minuta* were very similar to those of the suspended

TABLE 2

List of tentatively identified compounds in extracts of leaves and of cells of suspension culture of *Tagetes minuta*

Scan number	Name of compound	Molecular weight	Formula
Leaves			
827	Unidentified	150	$C_{10}H_{14}O$[a]
1065	β-Caryophyllene	204	$C_{15}H_{24}$[a]
1150	γ-Elemene	204	$C_{15}H_{24}$[a]
1456	Unidentified	278	$C_{20}H_{38}$[a]
1557	5-(But-3-en-1-ynyl)-2,2′-bithiophene	216	$C_{12}H_8S_2$[a]
1602	Unidentified	—	—
1651	5-(But-3-en-1-ynyl)-5′-methyl-2,2′-bithiophene	230	$C_{13}H_{10}S_2$[a]
1733	Linolenic acid, ethyl ester	360	$C_{20}H_{34}O_2$
1824	2,2′:5′,2″-Terthiophene	248	$C_{12}H_8S_3$
1956	Substituted bithiophene	262	$C_{13}H_{10}S_3$[a]
2221	Squalene	410	$C_{30}H_{50}$
	Stigmasterol	412	$C_{29}H_{48}O$
	β-Sitosterol	414	$C_{29}H_{50}O$
Cells			
2150	Squalene	410	$C_{30}H_{50}$
3690	Stigmasterol	412	$C_{29}H_{48}O$
3810	β-Sitosterol	414	$C_{29}H_{50}O$

[a]Determined by accurate mass measurements.

cells and not presented here. They indicate that the biosynthesis of sesquiterpenoids and thiophenes was already suppressed at the level of calli but that the biosynthesis of squalene, stigmasterol and β-sitosterol continues at the callus and cell suspension level.

We thank M. Jansen and P. Pikaar for culturing and providing the calli and cell cultures of marigold. This research was supported jointly by the Ministries of Agriculture and Fisheries, and Education and Science (Directorate-General for Science Policy), The Netherlands. Thanks are extended to Dr. H. Breteler for critical reading of the manuscript and to Miss S. Bakker for the typing.

REFERENCES

1 M. W. Fowler, Chem. Ind. (London), 7 (1981) 229.
2 C. Tudge, New Sci., 12 January (1984) 25.
3 Z. Puhan and S. M. Martin, Prog. Ind. Microbiol., 9 (1971) 14.
4 M. H. Zenk, in T. A. Thorpe (Ed.), Frontiers of Plant Tissue Culture 1978, University of Calgary, Canada, 1978, p. 1.
5 T. Murashige and F. Skoog, Physiol. Plant., 15 (1962) 473.
6 Official Methods of Analysis of the A.O.A.C., 10th edn., Association of Official Agricultural Chemists, Washington DC, 1965, p. 50.

7 Official Method of Analysis of Pyrethrum Board of Kenya, Pyrethrum Board of Kenya, Nakuru, Kenya, 1954.
8 Method for the determination of Pyrethrins, Tanganyika Extract Co. Ltd. (TECO), 1954.
9 E. Stahl and J. Pfeifle, Pyrethrum Post, 8 (1966) 8.
10 D. Mourot, J. Boisseau and G. Gayot, Anal. Chim. Acta, 97 (1978) 191.
11 L. R. Snyder and J. J. Kirkland, Introduction to Modern Liquid Chromatography, Interscience-Wiley, New York, 1979, p. 2.
12 S. W. Head, Pyrethrum Post, 9 (1967) 12.
13 S. W. Head, Pyrethrum Post, 8 (1966) 3.
14 M. Elliott, Chem. Ind. (London), (1969) 776.
15 K. R. Hill, Pure Appl. Chem., 51 (1979) 1615.
16 S. C. Jain, Planta Med., 31 (1977) 68.
17 M. Elliott, J. Chem. Soc. (London), (1964) 882.
18 R. L. Holmstead and D. M. Soderlund, Pyrethrum Post, 14 (1978) 79.
19 F. Bohlmann, T. Burkhardt and C. Zdero, Naturally Occurring Acetylenes, Academic Press, London, 1973, p. 3.
20 F. J. Gommers, Meded. Landbouwhogesch. Wageningen 73-17 (1973) 44.
21 J. H. Uhlenbroek and J. D. Bijloo, Rec. Trav. Chim., 77 (1958) 1004; 78 (1959) 382.
22 R. Sütfeld, Planta, 156 (1982) 536.
23 K. R. Downum and G. H. N. Towers, J. Nat. Prod., 46 (1983) 98.
24 P. Khanna and R. Khanna, Indian J. Exp. Biol., 14 (1976) 630.
25 P. Khanna, R. Sharna and R. Khanna, Indian J. Exp. Biol., 13 (1975) 508.
26 R. Jente, G. A. Olatunji and F. Bosold, Phytochemistry, 20 (1981) 2169.

Analytica Chimica Acta, 163 (1984) 55—66
Elsevier Science Publishers B.V., Amsterdam — Printed in The Netherlands

THE DEGRADATION PATTERN OF OLIGOMERS AND POLYMERS FROM LIGNOCELLULOSES

HANS-ULRICH KÖRNER, DIETER GOTTSCHALK, JÜRGEN WIEGEL[a] and JÜRGEN PULS*

Institute of Wood Chemistry and Chemical Technology of Wood, Federal Research Centre of Forestry and Forest Products, Leuschnerstr. 91, D-2050 Hamburg 80 (Federal Republic of Germany)

(Received 3rd April 1984)

SUMMARY

Only the carbohydrate portion in lignocelluloses can become a source of food, feed, and chemicals. At different stages of the biological conversion processes, carbohydrates are present as polymers, oligomers or monomers. Carbohydrate samples from lignocelluloses contain many by-products originating from the material (lignin, extracted substances, silica) or from the conversion processes (enzyme proteins, acids, fermentation by-products). Liquid-chromatography is used with emphasis on performance rather than pressure for highly contaminated samples. Most of the systems used here have an integrated post-column reaction system for the detection of carbohydrates. Monomeric and some oligomeric sugars are analyzed by borate ion-exchange chromatography. As an example of application of the system, the products of the stepwise enzymatic degradation of 4-*O*-methylglucuronoxylan are identified. Oligomeric sugars are separated by polyacrylamide gel chromatography. This system is used to optimize a pentose-to-ethanol process by thermophilic anaerobic bacteria. Polymers such as cellulose can only be analyzed by liquid chromatography after derivatization. The molecular-weight distribution of carbanilated birchwood celluloses after pretreatment and different stages of enzymatic attack is described. The large through-put of the automated units justifies their high cost.

Lignocellulose materials such as low-grade wood and agricultural residues are of economic interest as easily renewable resources for the production of food, feed, and chemicals. At present, only the carbohydrates can be converted to such products by biotechnical processes. A wide range of chromatographic methods is available for the determination of monomeric sugars. The only viable methods for the present purpose are those which provide separation of all neutral wood sugars and also of distinctly acidic sugars. During pretreatment processes of lignocelluloses, as well as in hydrolysis processes with strong acids, water-soluble oligomers are formed. Sometimes the oligomers derived from hemicelluloses and cellulose are further hydrolyzed by enzymatic or acidic hydrolysis; in other cases, the oligomers are fermented

---

[a]Present address: Department of Microbiology, The University of Georgia, Athens, GA 30602, U.S.A.

0003-2670/84/$03.00

as such to valuable products. Characterization of their nature is always a prerequisite for optimal utilization.

In the course of pretreatment processes and in pulping processes, the degree of polymerization of cellulose is decreased. A change in the molecular-weight distribution is expected. Visualization of the molecular-weight distribution of cellulose would give valuable hints for its optimal use as paper pulp or chemical pulp or as a substrate for enzymatic hydrolysis. Such a method would also help to elucidate the role of the different enzymes involved in the enzymatic breakdown of cellulose.

EXPERIMENTAL

Monomeric sugars

A schematic diagram of the sugar analysis system is given in Fig. 1. The mobile phase is pumped by means of a piston pump through a precolumn (10 × 0.6 cm) filled with Dowex 1-X4 to the thermostated separation column (30 × 0.32 cm, 60°C) filled with Durrum DA-X4 (20 μm). For the separation of neutral sugars, the mobile phase is 0.475 M potassium tetraborate buffer pH 9.2 (40 ml h^{-1}). In this case, the anion-exchange resin is in the borate form. Acidic sugars like galacturonic acid and glucuronic acid are eluted with 1 M potassium tetraborate buffer. Therefore the separation of mixtures of neutral and acidic sugars requires a stepwise gradient from 0.36 M to 1 M borate buffer over a period of 1.4 h. When only acidic sugars are present, they can be separated with the same resin but in the acetate form; in this case the mobile phase is 0.1 M sodium acetate buffer pH 5.9 (30 ml h^{-1}). The sugars are detected by post-column derivatization in a teflon coil (30 m × 0.5 mm) at 110°C. If reducing sugars are to be detected, the reagent is the copper(I) complex of disodium 2,2'-bicinchoninate (BCA) with detection at 546 nm [1] at a flow rate of 20 ml min^{-1}. When non-reducing sugars like saccharose are present, the non-corrosive bicinchoninate reagent is replaced by 0.1% (w/v) 3,5-dihydroxytoluene in concentrated

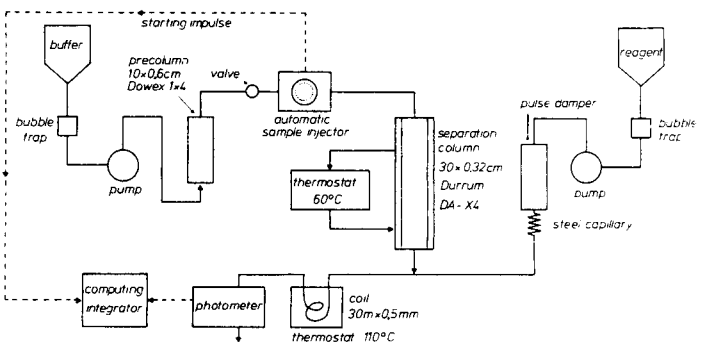

Fig. 1. Schematic diagram of the carbohydrate analytical system for monomers. For details of mobile phases and reagents, see text.

sulfuric acid with detection at 420 nm. This reagent is also added to the column eluate by means of a piston pump as in Fig. 1 [2]. Aliquots of 10 μl containing 0.1—3 μg of sugar (Cu-bicinchoninate) or 3—10 μg of sugar (sulfuric acid) are applied to the column by means of an automatic sample injector.

Oligomeric sugars

The analytical system for oligomeric sugars is outlined in Fig. 2. The stationary phase is Biogel P4 (—400 mesh; BioRad Laboratories). Fractionation of the gel by repeated settling and decanting the fines leads to an improved resolution of the peaks [3]. The gel bed is 100 × 2.5 cm. The column is operated at 40°C with 0.05 M Tris/HCl buffer pH 7.8. The flow rate is 30 ml h^{-1}. The oligomeric sugars are detected by post-column derivatization with 0.1% (w/v) 3,5-dihydroxytoluene in 65% sulfuric acid in an Auto-Analyzer system (Technicon), absorbance being measured at 420 nm. Aliquots (0.5 ml) of 0.1—0.4% (w/v) aqueous solutions are applied to the column via a sample loop.

The size-exclusion chromatographic system consists of 2 BioRad HPX 42A columns (300 × 7.8 mm) coupled in sequence and heated to 60°C in an oven. The mobile phase is degassed water (80°C), which is pumped at a flow rate of 0.6 ml min^{-1} through the columns by an extremely pulse-free h.p.l.c. pump. The detector is an Optilab Multiref 902 differential refractometer.

Water-insoluble carbohydrates

Figure 3 outlines the whole size-exclusion chromatographic system. The column set consists of three columns with upper permeability ranges of 5 × 10^6 daltons (Showa Denko Shodex A-805, 8 × 500 mm), 8 × 10^7 daltons (Showa Denko Shodex A-806, 8 × 500 mm), and 4 × 10^7 daltons

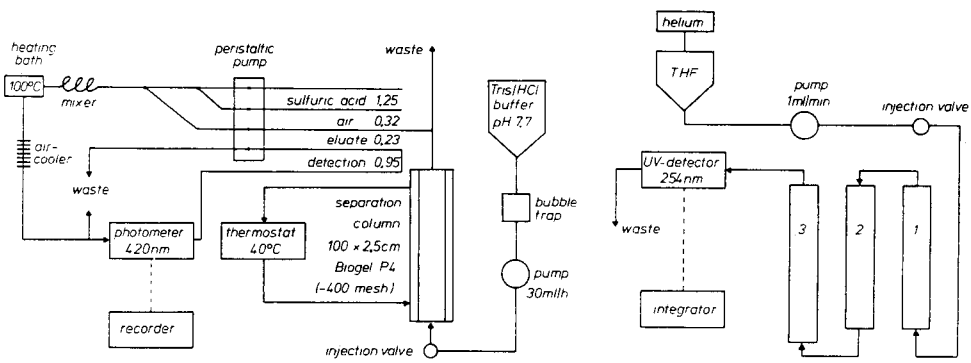

Fig. 2. Schematic diagram of the carbohydrate analytical system for oligomers.

Fig. 3. Schematic of the analytical system for water-insoluble carbohydrates. For details, see text.

(Polymer Laboratories PL 10 μm, 7.7 × 600 mm) for columns 1, 2 and 3, respectively. All the stationary phases are macroporous resins consisting of styrene/divinylbenzene copolymers. Tetrahydrofuran (THF) is used as the solvent at a flow rate of 1 ml min^{-1}. The concentration of the sample ranges from 0.5 to 0.9% with an injection volume of 100 μl. Data recording and evaluation are done by a computing integrator (Spectra Physics SP-4100) by employing the programs MWDCAL and MWDADP (Spectra Physics). A Waters Model 440 u.v. detector, operating at 254 nm, is connected to the third column. The preparation of cellulose tricarbanilates (CTC; phenyl isocyanates) has been described by Schroeder and Haigh [4]. The basic procedure used for the preparation of CTC is as follows: 0.1 g of absolutely dry cellulose is treated with 7.2 ml of phenyl isocyanate in 100 ml of anhydrous pyridine at 80° C, the reaction time being 24—72 h. After cooling, 4 ml of methanol is added to remove unreacted phenyl isocyanate. The solution is filtered through a sintered frit and methanol is added to precipitate the CTC, which is then washed by methanol and water and finally freeze-dried.

In order to calibrate the size-exclusion system, a set of four CTC standards, each with small molecular-weight distribution [5], is used. The molecular weights of these CTC standards were determined by a low-angle laser light-scattering photometer [6]. The calibration data were plotted on semilog paper.

Carbohydrates

The neutral sugars used as standards were Baker Ultrex Grade. Glucuronic acid and galacturonic acid were from Fluka. The preparation of the neutral xylo-oligomers, the acidic xylo-oligomers, and 4-*O*-methylglucuronic acid will be described elsewhere. The crude enzyme preparations were gifts of Röhm Chemische Fabrik, Darmstadt.

The separated carbohydrates are listed in Table 1. The numbers correspond to the peak numbering in the chromatograms.

TABLE 1

Carbohydrates used as standards

1. Xylobiose	10. 4-*O*-methyl-D-glucuronic acid
2. Cellobiose	11. Glucose
3. Xylotriose	12. Galacturonic acid
4. Sucrose	13. Glucuronic acid
5. Rhamnose	14. 2-*O*-(4-*O*-methyl-α-D-glucuronic acid)-D-xylopentaose
6. Mannose	15. 2-*O*-(4-*O*-methyl-α-D-glucuronic acid)-D-xylotetraose
7. Arabinose	16. 2-*O*-(4-*O*-methyl-α-D-glucuronic acid)-D-xylotriose
8. Galactose	17. 2-*O*-(4-*O*-methyl-α-D-glucuronic acid)-D-xylobiose
9. Xylose	18. 2-*O*-(4-*O*-methyl-α-D-glucuronic acid)-D-xylose
	19. Mixture of xylo-oligouronic acids

RESULTS AND DISCUSSION

Mixtures of monomeric, dimeric or trimeric sugars from lignocelluloses are mostly obtained after enzymatic or acidic hydrolysis processes. Often these hydrolysates are contaminated by acids, enzyme proteins and water-soluble lignin. After fermentation, a couple of by-products in addition to the desired end-product may disturb a qualitative and quantitative sugar analysis. In order to evaluate unused residues of the initial substrates, the sensitivity of the detection system has to be appropriate. In recent years, there has been great progress in the separation of carbohydrates by liquid chromatography. Three types of liquid chromatography are mostly used: partition chromatography on chemically bonded phases, partition chromatography on ion-exchange resins, and ion-exchange chromatography of carbohydrate complexes. The choice of the chromatographic system obviously depends on the samples. Separation systems with bonded phases are easiest to bring into operation. The elution times of sugars (i.e., the time required for one chromatographic run) are short. Nevertheless, the injection of many dirty samples of low pH may decrease the resolution, because the bonded phase (e.g., amino groups) is sensitive to repeated acidic contacts. Therefore, in addition to a filtering step, a time-consuming cleaning procedure including treatment with ion exchangers is needed.

Partition chromatography on ion-exchange resins is usually done with cation exchangers and water as mobile phase; this gives good separations of monosaccharides and shorter oligosaccharides. Again, acidic samples may cause an exchange of the cations (mainly lead, silver and calcium) against hydrogen, which produces a dramatic decrease in resolution. Therefore, most manufacturers of these columns recommend the use of small precolumns for protection. With dirty samples, the precolumns have to be exchanged quite often.

The extent to which borate ions react with carbohydrates to form negatively charged carbohydrate/borate complexes on the anion-exchange resin depends on the concentration of the borate ions and the pH of the mobile phase. The borate concentration and pH parameters are used for optimization of the separation. With a 0.475 M borate buffer pH 9.2, separation of all neutral sugars derived from lignocelluloses including 4-*O*-methylglucuronic acid can be achieved within 70 min (Fig. 4). If glucuronic acid and galacturonic acid are present, they are eluted with 1 M borate buffer. Figure 5 shows the separation of neutral sugars and uronic acids, with a stepwise gradient from 0.36 M to 1 M potassium borate buffer pH 9.2. The use of this gradient, however, prolongs the separation time to 110 min. As an alternative, anion-exchange separations of uronic acids in acetate medium may be accomplished more quickly (see below).

An application of the borate system is shown in Fig. 6. This system is used for monitoring the mode of action of the enzymatic degradation of hardwood xylans. With a purified xylanase, the 4-*O*-methyl-D-glucuronosyl-

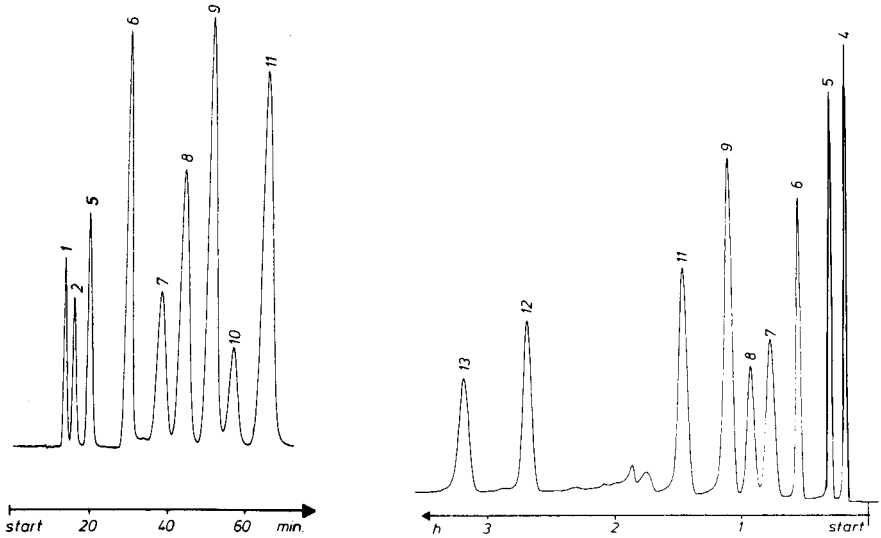

Fig. 4. Separation of neutral sugars including 4-*O*-methylglucuronic acid. Column: Durrum DA-X4 (20 μm; 0.32 × 30 cm). Mobile phase: 0.475 M potassium tetraborate buffer pH 9.2, 40 ml h^{-1}. Detection: BCA reagent at 20 ml h^{-1}, reaction coil 30 m × 0.5 mm i.d. at 110°C. Photometer: 546 nm, AFS = 0.2. Recorder: 10 mV, 0.125 cm min^{-1}.

Fig. 5. Separation of neutral sugars and uronic acids with a stepwise gradient. Column as for Fig. 4. Mobile phase: 0.36 M potassium tetraborate buffer pH 9.2, 1 M potassium tetraborate buffer after 1.4 h, 40 ml h^{-1}. Detection 0.1% 3,5-dihydroxytoluene in concentrated sulfuric acid (40 ml h^{-1}), reaction coil 10 m × 0.7 mm i.d. at 100°C. Photometer: 420 nm, AFS = 2. Recorder: 50 mV, 0.1 cm min^{-1}.

substituted xylan is split to neutral xylo-oligomers (mainly xylobiose and xylotriose) and the corresponding 4-*O*-methyl-D-glucuronosyl-substituted xylo-oligomers. Only traces of free 4-*O*-methyl-α-D-glucuronic acid can be detected in the first step. In the second step, an α-D-glucuronidase is added to the hydrolysate. This enzyme selectively detaches the acidic side chains and leads to an increase of free 4-*O*-methyl-α-D-glucuronic acid. The enzyme preparation used here had also some β-xylosidase activity. Therefore, an increase in xylose concentration was also found. In the third step, β-xylosidase activity hydrolyses the neutral xylo-oligomers to xylose. As can be seen from the chromatogram, only small amounts of xylobiose and acidic xylo-oligomers are left.

A disadvantage of the borate system is that it is not capable of separating xylose and 2-*O*-(4-*O*-methyl-α-D-glucuronic acid)-D-xylose. However, this separation is possible by anion-exchange chromatography in sodium acetate medium [7] (see Fig. 7). The general set-up is the same as the borate system, but the resin must be converted to the acetate form and the mobile phase has to be changed. With these modifications, it was verified that the end-products of the three-step hydrolysis of hardwood xylans were xylose and 4-*O*-methylglucuronic acid.

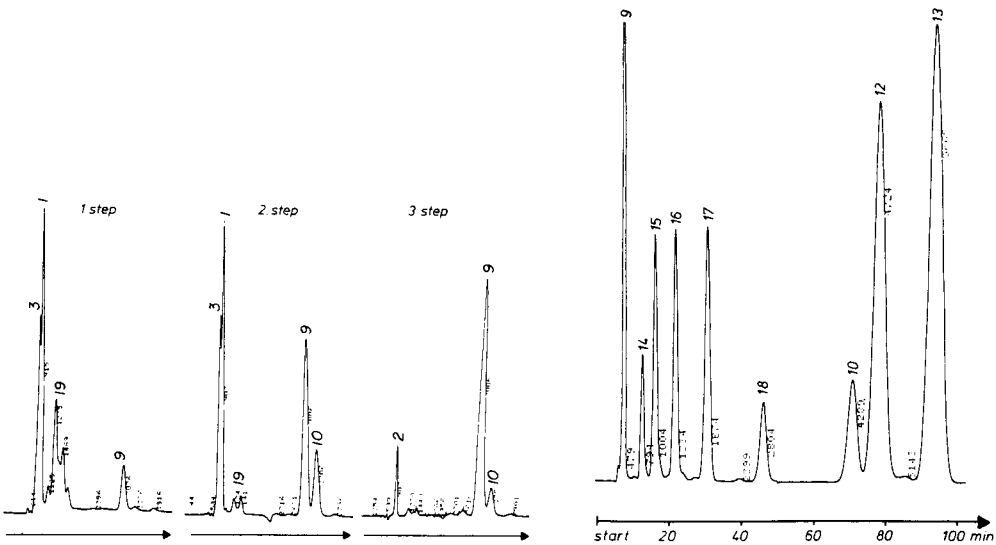

Fig. 6. Stepwise enzymatic hydrolysis of 4-*O*-methylglucuronoxylan by (1) xylanase, (2) α-glucuronidase, (3) β-xylosidase. For identification of sugars, see Table 1. Separation and detection conditions as in Fig. 4.

Fig. 7. Separation of uronic acids with the acetate system. For identification of sugars, see Table 1. Column: see Fig. 4. Mobile phase: 0.1 M sodium acetate buffer pH 5.9 (30 ml h^{-1}). Detection: see Fig. 4.

The acetate system conforms to the above statements about partition chromatography on chemically bonded phases or on ion-exchange resins. Thus, if more strongly acidic anions (e.g., sulfate, chloride or phosphate) are present, acetate ions are exchanged if the samples are not deionized. This exchange leads to a rapid loss in separation power after a certain time. In contrast, because of the high borate molarity, the borate columns regenerate themselves continuously, and contaminants are tolerated to a high degree. Aqueous solutions can be analyzed without any prior manipulation such as deionization or deproteinization. In this way, reactions of enzymes and acids can be studied by analyzing series of samples without interfering treatments. This is especially valuable for samples with uronic acids present. In the case of deionization of such samples, the uronic acids would also be removed.

The borate system is capable of achieving separation of oligomeric sugars even when the buffer molarity is drastically reduced to 0.1 M or less. Better separations of oligosaccharides, however, were obtained with other techniques. Separations of oligosaccharides up to a polymerization degree of 35 can be achieved by reverse-phase chromatography on bonded-phase silica with an aqueous acetonitrile gradient as mobile phase [8]. The samples, however, have to be acetylated, and so considerable sample clean-up is

required. Size-exclusion chromatography with water as mobile phase on cation-exchange resins in the silver or calcium form was used for the separation of oligomeric sugars. Figure 8 shows the separation of cello-oligomers on HP-X42A (2X). The oligomers were obtained after hydrolysis of cellulose with 42% hydrochloric acid.

For many purposes, this set-up offers a fast and efficient separation, especially when the inselective refractive index detector can be applied. Such a system was installed here in order to obtain deeper insight into the conversion of xylo-oligomers to ethanol by anaerobic thermophilic bacteria [9]. The by-products of the fermentation (mainly acetic acid), however, were eluted from the column together with the unseparated higher oligomers in the void volume. Without a selective post-column reaction system for carbohydrates, it became impossible to distinguish organic acids from higher oligomers. Consequently, a post-column system with 3,5-dihydroxytoluene/sulfuric acid was installed. This arrangement caused such peak broadening that the higher oligomers were not separated from each other. Accordingly, the slower, but far more powerful, separation on polyacrylamide gels was preferred. Figure 9 shows the separation on Biogel P4 of the

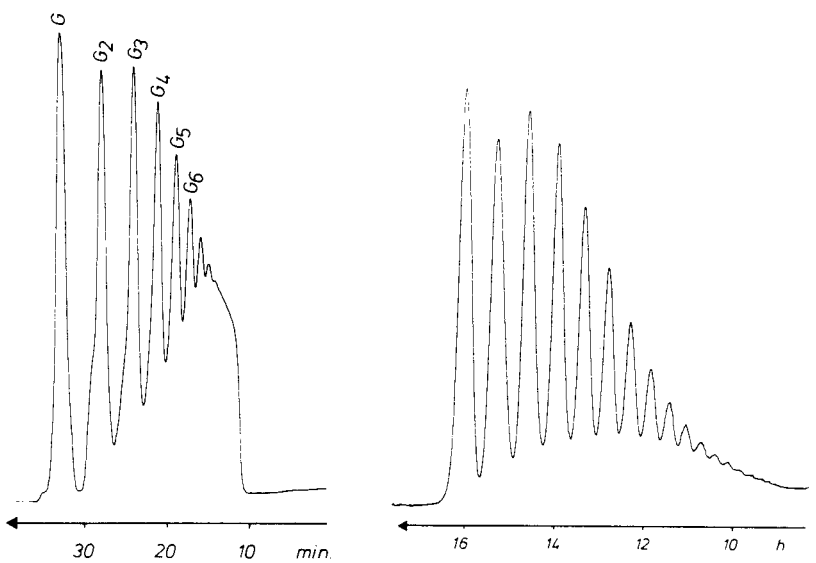

Fig. 8. Separation of cello-oligomers by size-exclusion chromatography. Column: 2 × Bio-Rad HP-X42A (300 × 7.8 mm), 60°C. Mobile phase: deionized water, 0.6 ml min^{-1}. Detection: Optilab Multiref 902 differential refractometer, sensitivity ×100. Recorder: 10 V, 0.3 cm min^{-1}.

Fig. 9. Separation of cello-oligomers by polyacrylamide gel chromatography. Column: Biogel P4 (—400 mesh), 100 × 2.5 cm. Mobile phase: 0.05 M Tris/HCl buffer pH 7.8, 30 ml h^{-1}. Detection: 0.1% 3,5-dihydroxytoluene in 65% sulfuric acid in the system shown in Fig. 2. Photometer: 420 nm, E = 2, Recorder: 20 mV, 2 cm h^{-1}.

same mixture of cello-oligomers that was analyzed before by size-exclusion chromatography. The increase in resolution for the higher oligomers is clearly seen. The efficiency of polyacrylamide gel chromatography for the separation of oligosaccharides up to DP60 has been demonstrated before with water as mobile phase [3]. However, a gel bed height of 200 cm and a run time of 20 h were necessary. Impurities of water-soluble lignin, tannins, and coloured by-products from the fermentation tend to adsorb on the column in this system.

For the present application, the bed height of the gel was reduced to 100 cm and the water was replaced by 0.05 M Tris/HCl buffer pH 7.8; this had the positive effect that no adsorption occurred. The reduced separation time allowed two separations per day. Figure 10 shows an application of the system (cf. Fig. 2), the utilization of prehydrolyzed beechwood xylan by *Thermoanaerobacter ethanolicus* JW200 L-large [10]. The prehydrolysis step with 100 mM phosphoric acid under sterile conditions liberates 2 series of xylo-oligomers from xylan: a neutral series consisting of xylose, xylobiose, xylotriose, up to DP7, and an acidic series consisting of 2-*O*(4-*O*-methyl-α-D-glucopyranosyluronic-acid)-D-xylo-oligomers. The separation parameters were selected so that the neutral oligomers were eluted according to size-exclusion principles, whereas the acidic oligomers were separated by partition principles. Although different in molecular weight, 2-*O*(4-*O*-methyl-α-D-glucopyranosyluronic-acid)-D-xylose was eluted at the same time as xyloheptose. After a fermentation time of 47 h, most of the neutral xylo-oligomers had been fermented. Most of the α-1,2-substituted xylo-oligomers, however, withstood the enzymatic attack, even after 139.5 h of fermentation. The carbohydrates marking the void volume were also resistant to enzymatic attack.

Liquid chromatography of water-insoluble carbohydrates such as cellulose and native hemicelluloses requires a derivatization step in order to make the compounds soluble in a common chromatographic solvent. Tricarbanilated cellulose (CTC) with tetrahydrofuran (THF) as mobile phase has shown promise for evaluating the molecular-weight distribution of cellulose [11]. The suitability of this method is based on the non-degradative nature of derivatization at 80°C, the complete tri-substitution and the long-term stability of the product. However, the derivatization procedure takes 24—72 h. The carbanilation of normal pulps including all artificial substrates used as model compounds for enzymatic hydrolysis of cellulose is no problem. Complete derivatization of pretreated lignocelluloses, however, requires extensive breaking up of the structure of the cell wall.

Apart from the derivatization, calibration of the gel-chromatographic system is another barrier to exact molecular-weight determination and to correct interpretation of the molecular-weight distribution of cellulose. These systems are usually calibrated with polystyrene standards. However, polystyrene has a different hydrodynamic volume from carbanilated cellulose on the separation columns, so that the polystyrene calibration leads only

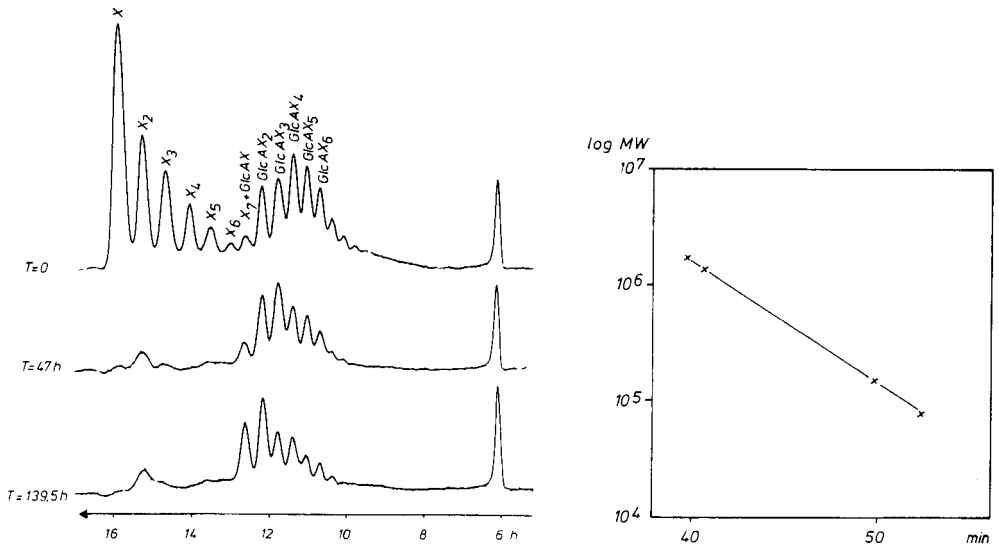

Fig. 10. Utilization of prehydrolyzed 4-*O*-methylglucuronoxylan by *Thermoanaerobacter ethanolicus* for ethanol production. The oligosaccharides were obtained by partial hydrolysis with 100 mM phosphoric acid for 30 min at 120°C. Separation and detection conditions as in Fig. 9.

Fig. 11. Typical calibration graph for the system. Columns: Shodex A-805 (8 × 500 mm), Shodex A-806 (8 × 500 mm), and Polymer Laboratories PL 10 μm (7.7 × 600 mm). Mobile phase: Tetrahydrofuran, 1 ml min^{-1}. Detection: Waters 440 u.v. detector, 254 nm, AFS = 0.5. Calibration graph plotted by means of the programs MWDCAL and MWDADP (Spectra Physics). The standards were cellulose tricarbanilates of m.w. 1 685 700, 947 500, 98 500, and 50 600.

to relative values. The most elegant, but costly method of obtaining absolute molecular-weight distribution figures is to integrate a low-angle laser light-scattering detector into the liquid chromatograph. The third possibility is to use carbanilated cellulose preparations, each with a small range of molecular weights and to determine the mean molecular weights previously with the light-scattering detector specified. This is our standard procedure for the characterization of the chain-length distribution of cellulose. Figure 11 shows a calibration graph for four carbanilated celluloses of mean m.w. 1 685 700, 947 500, 98 500, and 50 600 for the three separation columns with an upper exclusion limit of m.w. 5×10^6 daltons, 8×10^7 daltons, and 4×10^7 daltons.

One application of the system (Fig. 3) is given in Fig. 12(a—d). The system is useful for visualization of the degradation pattern of pretreated wood cellulose by cellulases. The four graphs show not only the respective differential molecular-weight distribution curves but also the integral curves. Figure 12(a) shows the plots for the starting material consisting of birchwood after pretreatment by the steaming-extraction process [12]. The

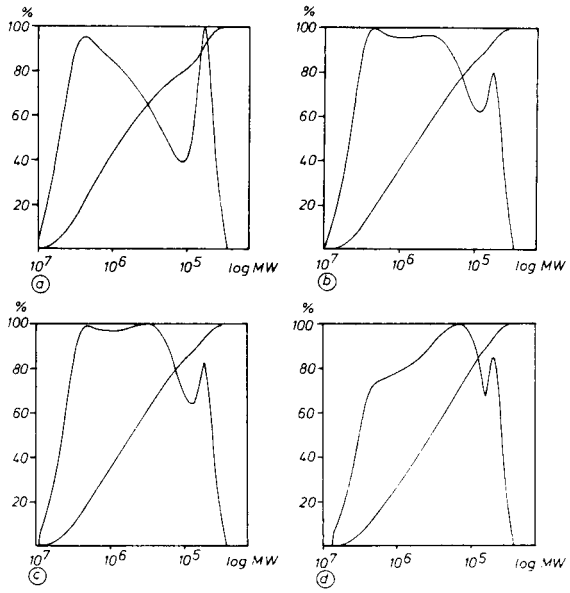

Fig. 12. Development of the molecular-weight distributions of steam-pretreated birchwood during enzymatic attack by Trichoderma reesei cellulases. Separation and detection conditions as in Fig. 11. (a) Steam-treated birchwood (190°C, 15 min); (b) substrate after 1-h enzymatic degradation with 9 FPU g^{-1} fibre; (c) substrate after 4 h enzymatic degradation; (d) substrate after 24 h enzymatic degradation. See text for details.

high-molecular-weight part marks the cellulose portion, whereas the peak in the lower-molecular-weight range is identical with the xylan residue in the steamed and water-extracted material. The other plots (b—d) show the shift of the molecular-weight distribution of cellulose to smaller units under the action of 9 FPU (Filter Paper Unit) g^{-1} fibre of a cell-free commercially available cellulase preparation of *T. reesei* after 1, 4 and 24 h. Figure 12(d) shows very clearly the preferential attack of this enzyme preparation at the high-molecular-weight side. This method can also be used to characterize substrates obtained under different pretreatment conditions [13].

Detection of carbohydrates

A broad range of detection systems for carbohydrates was used in this work. The simplest is the u.v. detector at 254 nm for carbanilated celluloses (Fig. 12). For monomeric and oligomeric sugars, u.v. detection at 190 nm or refractive index detection (Fig. 8) are too susceptible to trouble or too inselective. In ion-exchange chromatography of sugars as borate complexes, the eluates should be treated colorimetrically. Anthrone or phenol/sulfuric acid reagents have been used for colour development. More frequently, 3,5-dihydroxytoluene/sulfuric acid, better known as orcinol-sulfuric acid, proved to have the broadest application for the detection of all monomeric

(Fig. 5) and oligomeric sugars (Fig. 10). As little as 0.5 μg of an individual sugar can be quantified. This reagent also involves some disadvantages; because of its high reactivity, it has to be handled with care, and the detection system must be well maintained. Piston pumps normally used for h.p.l.c. need minor modifications, and peristaltic pumps need special tubing for adding the reagent to the column eluate.

The application of 3,5-dihydroxytoluene/sulfuric acid can be restricted to occasions when non-reducing sugars like sucrose or higher oligomers have to be detected. Reducing sugars can advantageously be detected with the non-corrosive copper(I) complex of 2,2'-bicinchoninate [1, 14] (Figs. 4, 6, 7). The minimal detectable quantity of carbohydrates is in the range 0.1—0.2 μg. Other detection systems, including the cuprammonium-reagent [15], were tested in order to find a non-corrosive reagent sensitive for non-reducing sugars. However, no system has so far been found with the same sensitivity and accuracy as the bicinchoninate system.

As can be estimated from Figs. 1—3, the equipment required for the identification and determination of monomeric, oligomeric, and polymeric carbohydrates, partly with post-column reaction systems, is quite high. Although the separation systems presented need a comparatively long time per run, their performance is excellent, which is usually necessary for the separation of complex sugar mixtures. All the systems have the advantage of being relatively trouble-free, and they can be run continuously and automatically, so that sample throughput is comparatively good.

We thank A. Borchmann for preparation of the xylo-oligomers. This work was supported by BMFT project 521-729-RN8202 and EC contract BOS-012-D (B).

REFERENCES

1 M. Sinner and J. Puls, J. Chromatogr., 156 (1978) 197.
2 M. Sinner, M. H. Simatupang and H. H. Dietrichs, Wood Sci. Technol., 9 (1975) 307.
3 M. John, J. Schmidt, Ch. Wandrey and H. Sahm, J. Chromatogr., 247 (1982) 281.
4 L. R. Schroeder and F. C. Haigh, TAPPI, 62/10 (1979) 103.
5 H.-U. Körner, D. Gottschalk and J. Puls, Das Papier, 38 (1984) 255.
6 J. J. Cael, D. J. Cietek and F. J. Kolpak, Proc. 5th International Dissolving Pulp Conference/TAPPI Conference papers, (1980) 216.
7 S. Johnson and O. Samuelson, Anal. Chim. Acta, 36 (1966) 1.
8 G. B. Wells and R. L. Lester, Anal. Biochem., 97 (1979) 184.
9 J. Wiegel and J. Puls, in A. Strub, P. Chartier and G. Schleser (Eds.), Energy from Biomass, Applied Science Publishers, London, 1983, p. 994.
10 J. Wiegel, L. H. Carreira, Ch. P. Mothershed and J. Puls, Biotechnol. Bioeng. Symp., 13 (1983) 193.
11 J. Danhelka, I. Kössler and V. Bohachova, J. Polym. Sci., Polym. Chem. Ed., 14 (1976) 287.
12 J. Puls, C. Ayla and H. H. Dietrichs, J. Appl. Polym. Sci. Appl. Polym. Symp., 37 (1983) 685.
13 J. Puls, D. Gast and H. U. Körner, in L. Munck and R. Hill (Eds.), Proc. Int. Conf. New Approaches Res. Cereal Carbohydrates, Copenhagen, June 24—29, 1984, Elsevier, Amsterdam, in press.
14 K. Mopper and E. M. Gindler, Anal. Biochem., 56 (1973) 440.
15 G. K. Grimble, H. M. Barker and R. H. Taylor, Anal. Biochem., 128 (1983) 422.

Analytica Chimica Acta, 163 (1984) 67—72
Elsevier Science Publishers B.V., Amsterdam — Printed in The Netherlands

IMMOBILIZED ENZYME KINETICS ANALYZED BY FLOW-THROUGH MICROFLUORIMETRY

Resorufin-β-D-galactopyranoside as a New Fluorogenic Substrate for β-Galactosidase

J. HOFMANN and M. SERNETZ*

Institut für Biochemie und Endokrinologie, Justus Liebig-Universität Giessen, Frankfurter Str. 100, D-6300 Giessen (West Germany)

(Received 17th April 1984)

SUMMARY

Bioreactor kinetics depend on the dispersion of catalytic parameters within the catalyst particle population. In the conventional determination, reactor performance is assessed from the total turnover rate. In the proposed method the dispersion of turnover rates in reacting immobilized enzyme gel spheres of a continuously stirred tank reactor is evaluated. This more informative method is based on flow-through microfluorimetry and is exemplified with β-galactosidase immobilized on Sepharose 4B, with resorufin-β-D-galactopyranoside as a new fluorogenic substrate. By use of sieved gel fractions, effectiveness factors and Damköhler numbers determined in individual beads can be correlated with integral turnover rates of the reactor.

Activity measurements of enzymes immobilized on gel spheres are conventionally made in continuously stirred tank reactors (CSTR) by determining the total turnover, for instance of chromogenic substrates in a separate photometer unit. The total turnover, however, represents only the mean, resulting from a possibly broad and unknown dispersion of catalytic activities within the enzyme—gel suspension. Better knowledge of this dispersion could be of great interest, because kinetic calculations are usually derived from theoretical assumptions on the processes of diffusion and reaction postulated within and around the microscopic gel beads. This could not previously be proved directly. Evaluation of the dispersion of kinetic parameters could also be important for many practical applications like optimization of efficiencies and flow rates.

This paper describes a new method for simultaneous, integral and dispersive analysis of immobilized enzyme activities from CSTR experiments. It combines a conventional, continuous flow fluorimetric technique for measurement of total turnover rates of the reactor with a special version of continuous, dispersive flow-through microfluorimetry, modified and adapted to the needs of activity determination in gel particles (Fig. 1). The high sensitivity necessary for measuring turnover in single particles is achieved by using fluorogenic substrates.

0003-2670/84/$03.00

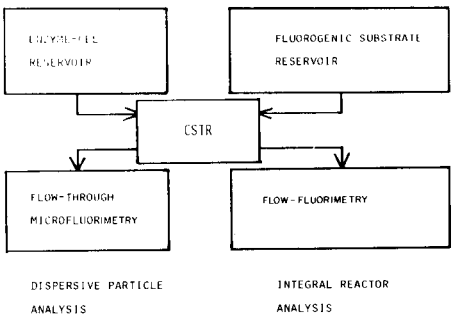

Fig. 1. Schematic diagram of CSTR arrangement with simultaneous dispersive particle analysis by flow-through microfluorimetry and integral reactor analysis by flow fluorimetry.

In this paper results are presented for β-galactosidase immobilized to Sepharose 4B, using a newly developed fluorogenic substrate, resorufin-β-D-galactopyranoside [1]. Compared to previously used di-substituted fluorescein derivatives [2—5] this substrate has the advantage of a one-step hydrolysis following Michaelis-Menten kinetics in addition to its red fluorescence emission.

EXPERIMENTAL

Reactor

The system is outlined in Fig. 1. A continuously stirred tank reactor (CSTR) with a capacity of 15 ml, filled with the β-galactosidase/Sepharose suspension, was supplied with the fluorogenic substrate from a reservoir by peristaltic pumps. An equivalent amount of the reaction solution containing the product was released via a filter into the cuvette of a flow fluorimeter for integral analysis. From a second reservoir, enzyme/gel bead suspension is fed into the CSTR independently to compensate for the withdrawal of gel beads for the dispersive analysis. This arrangement provides the possibility of independent variation of substrate and enzyme gel concentration, flow rates, stirring and residence times as well as reactor performance under steady-state conditions.

Flow-through microfluorimetry

The suspension of reacting particles in the CSTR is released through a capillary into a glass tube with a conical bore where a second, particle-free water stream envelopes and hydrodynamically focusses the particle flow. The single particles pass through the broadened beam of a laser. During this passage, the fluorescence of the product which has accumulated in the beads by diffusion, is excited, and the fluorescence pulses, together with scattered light pulses, are recorded by photomultiplier tube, elec-

tronically processed and stored in a computer. The information can be displayed as pulse-height frequency distributions. Details have been given elsewhere [5].

Immobilized β-galactosidase

β-Galactosidase (Boehringer, Mannheim) was immobilized on Sepharose 4B (Pharmacia, Uppsala) by the cyanogen bromide method [6], and sieve fractions with a narrow distribution of radii (Δr = 2.5 μm) were obtained by ultrasonic wet sieving (Retsch, Haan) [1]. Three samples different in radius and activity were used in the experiments (Table 1).

Fluorogenic substrate: resorufin-β-D-galactopyranoside (RG)

In search of suitable fluorophores, the red fluorescent resorufin with excitation maximum at 570 nm and emission maximum at 580 nm (Fig. 2), was chosen for investigation. Acyl derivatives of this fluorophor have been used as a fluorogenic substrate for acylases [7]. Synthesis of RG [1] was done by first reducing resazurin (Fluka) to resorufin with ammonium hydrogensulfite solution. Resorufin was condensed with acetobromo-α-D-galactose (Sigma) in the conventional way [8], yielding the tetraacetylated intermediate (RGA). This was deacetylated with sodium methoxide to give RG, which can be distinguished from starting material and intermediates by thin-layer chromatography. On kieselgel plates (Merck) with dichloromethane/methanol (9:1) as solvent, the R_f values were 0.1 for RG, 0.4 for resorufin and 0.9 for RGA.

Resorufin-β-D-galactopyranoside is an essentially non-fluorescent com-

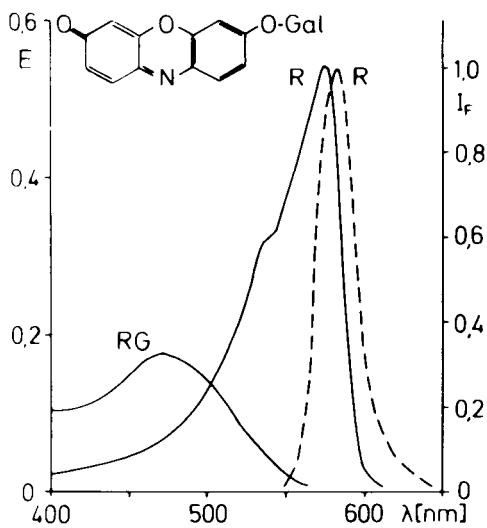

Fig. 2. (—) Absorption spectra: (RG) resorufin-β-D-galactopyranoside; (R) resorufin. (— —) Emission spectrum of resorufin.

pound giving an orange-yellow aqueous solution. The enzymatic hydrolysis by soluble β-galactosidase yields fluorescent resorufin in a single step following Michaelis—Menten kinetics. The kinetic constants were found to be K_M = 0.38 mM and K_{cat} = 730 s^{-1} (in 0.1 M potassium phosphate buffer, pH 7.0, containing 1 mM magnesium chloride, at 22°C). Lactose, as a competitive substrate, inhibits the reaction, with a measured K_I = 2.1 mM. The stability of the substrate is high and its solubility and that of resorufin is sufficient for most kinetic purposes.

The absorption spectra of resorufin and RG are given in Fig. 2. It should be emphasized that the excitation spectrum of resorufin allows the use of visible light sources such as argon ion lasers. Moreover, RG can be used as a chromogenic substrate.

RESULTS AND DISCUSSION

Figure 3 shows an example of experimental results with simultaneous integral and dispersive measurements obtained with the arrangement in Fig. 1, during the reaction of RG in the CSTR, using a sieve fraction (95—100 μm diameter) of Sepharose 4B with β-galactosidase (preparation II). Figure 3B shows the change in product concentration with time in the effluent of the CSTR, measured by conventional flow fluorimetry as a direct measure of the integral turnover. Figure 3A shows the pulse-height frequency distributions of product fluorescence in the gel particles, measured with the disper-

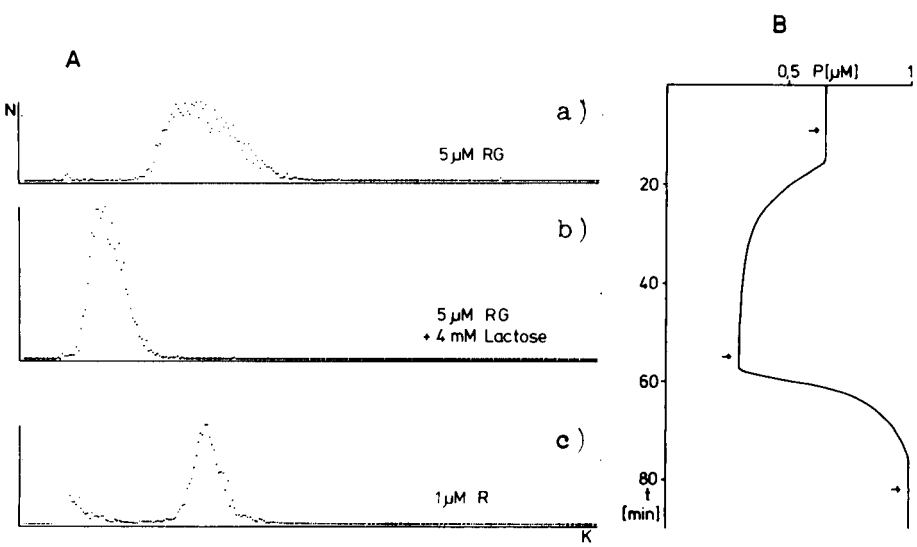

Fig. 3. Corresponding data for dispersive analysis (A) and integral analysis (B). Pulse-height frequency distributions of particle fluorescence are compared with product concentration in the effluent from the reactor. For details, see text.

sive method at the positions marked by the arrows. Three different experimental conditions are presented: (a) steady-state turnover of 5 μM RG; (b) steady-state turnover of 5 μM RG in the presence of 4 mM lactose as a competitive substrate for variation of K_M; (c) calibration with 1 μM resorufin alone. Stirrer speeds were kept sufficiently high to minimize external diffusional resistances.

The addition of lactose as a competitive substrate leads to a significant drop in the integral turnover. The theory of heterogeneous catalysis predicts that a decreased enzymatic turnover also leads to lower concentrations of the fluorescent product in the beads. This is consistently reflected by a shift of the frequency distribution towards lower energies, proportional to the channel number K.

The positions of the pulse-height frequency distributions do not simply follow the exterior product concentration in the reactor. The existence of real diffusional product accumulation in the beads can easily be derived from the greater ratio of reaction to calibration fluorescence in the frequency distributions compared to the corresponding values measured in the bulk solution. A representative bead fluorescence intensity of product accumulation in a sieve fraction can then be approximated by using the medians of the frequency distributions. This representative bead fluorescence I_{rel} is given by

$$I_{rel} = (I_t - I_p)/I_s D_s'/D_p' \tag{1}$$

where I_t is the observed total intensity from the reacting sphere, I_s is the calculated fluorescence of a bead in pure product solution equivalent to the substrate concentration used in the experiment, and I_p is the calculated fluorescence of the bead in pure product solution equivalent to the steady-state concentration in the experiment. I_s and I_p can easily be calculated from the calibration distribution. The ratio of the effective diffusion coefficients of substrate and product in the gel, D_s'/D_p', was estimated to be 0.75.

For this representative bead fluorescence I_{rel}, the Damköhler number σ can be determined from numerically calculated graphs [9]. Damköhler number σ and efficiency η are strictly correlated for a given substrate concentration S. If the effective diffusion coefficient for RG is taken as $D_s' = 3.6 \times 10^{-6}$ cm^2 s^{-1}, and if the parameters σ, η, S are known, together with the particle radius r, or here the mean radius $\bar{r}$ of a sieve fraction, the total reactor turnover can be calculated from the dispersive data of flow-through microfluorimetry. The data were normalized on the gel volume G and the substrate concentration S to yield the rate constant k^* of the reactor. The rate constant k^*, calculated from the dispersive measurements, is given by $\sigma\eta D_s' r^{-2}$, whereas the integral determination of k^* requires the measurement of the flow rate F and product concentration P in the CSTR; here $k^* = PF/GS$.

Table 1 compares the rate constants k^* from integral measurements with the values calculated from the dispersive microfluorimetric data. The agree-

TABLE 1

Reactor conditions and rate constants, k^*, calculated from dispersive particle data and measured by integral analysis

Preparation	Particle diameter (μM)	Stirrer rps (s^{-1})	S (μM)	J (mM)	Dispersive method			Integral method k^* (s^{-1})
					σ	η	k^* (s^{-1})	
I	65—70	12	4.1	—	7	0.72	1.61	1.64
			4.35	3.7	3.1	0.86	0.85	0.84
II	95—100	12	4.1	—	3.3	0.85	0.42	0.64
			4.4	3.7	1.8	0.92	0.25	0.23
			4.5	—	3.1	0.86	0.39	0.44
			4.5	1.9	2.4	0.89	0.33	0.34
			4.6	3.7	1.8	0.92	0.26	0.28
III	95—100	24	3.9	—	500	0.13	9.7	5.1
			4.0	1.9	104	0.27	4.2	4.5
			4.1	3.8	68	0.32	3.3	4.0

ment between these entirely different experimental approaches is remarkably good, considering the large number of experimental parameters in the calculations.

Flow-through microfluorimetry provides a powerful tool for the dispersive analysis of immobilized enzyme activity. The results of this study suggest that important experimental material may also be obtained by this method in other fields, e.g., in the characterization of complex kinetics of immobilized enzymes, preferably in sieved gel fractions, or in the dispersive analysis of the usually broad dispersion of commercial enzyme catalysts used for industrial purposes, including static parameters like protein binding. Moreover, resorufin-β-D-galactopyranoside has been shown to be a suitable new substrate for immobilized β-galactosidase. This compound and corresponding glycosides are expected to open up a new range of fluorogenic substrates for many analytical applications.

This investigation was supported by grant Se 315/11-6 of the Deutsche Forschungsgemeinschaft.

REFERENCES

1 J. Hofmann, Diss. Marburg, 1984.
2 B. Rotman, J. A. Zderic and M. Edelstein, Proc. Natl. Acad. Sci., 50 (1963) 1.
3 J. Hofmann and M. Sernetz, Fresenius Z. Anal. Chem., 311 (1982) 368.
4 J. Hofmann and M. Sernetz, Anal. Biochem., 131 (1983) 180.
5 J. Hofmann and M. Sernetz, Trends Anal. Chem., 2 (1983) 172.
6 J. Porath and R. Axén, in K. Mosbach (Ed.), Methods in Enzymology, Vol. 44, Academic Press, New York, 1976, p. 19.
7 G. G. Guilbault, Anal. Chem., 37 (1967) 120.
8 W. Pigman (Ed.), The Carbohydrates, Vol. 7, Academic Press, New York, 1957.
9 O. Hannibal-Friedrich and M. Sernetz, J. Solid Phase Biochem., 3 (1978) 301.

Analytica Chimica Acta, 163 (1984) 73—84
Elsevier Science Publishers B.V., Amsterdam — Printed in The Netherlands

RAPID DETERMINATION OF CEPHALOSPORINS WITH AN IMMOBILIZED ENZYME REACTOR AND SEQUENTIAL SUBTRACTIVE SPECTROPHOTOMETRIC DETECTION IN AN AUTOMATED FLOW-INJECTION SYSTEM

GEORG DECRISTOFORO* and FRANZ KNAUSEDER
Biochemie Ges.m.b.H., Research and Development Department, A-6250 Kundl (Austria)
(Received 16th April 1984)

SUMMARY

A flow-injection system is described for the rapid automated determination of different cephalosporins in aqueous solution. Measurement is based on a selective enzymatic cleavage of the cephalosporin-β-lactam ring in a small immobilized enzyme reactor, which contains highly purified cephalosporinase covalently bound to activated glass beads. Samples are injected into a phosphate buffer stream. The opening of the β-lactam ring is accompanied by a significant decrease in the ultraviolet (u.v.) absorbance. The difference between the absorbances of untreated and degraded cephalosporin is measured at 254 nm and is related linearly to cephalosporin concentration over the range 10—800 $\mu g\ ml^{-1}$. Several commercially available cephalosporins including some β-lactamase-resistant types were examined. The accuracy of the enzyme reactor/flow injection system was evaluated by comparison with h.p.l.c. results; the correlation was good. The relative standard deviation, evaluated from 15 consecutive injections of the same sample, was 0.7%; 2 $\mu g\ ml^{-1}$ cephalosporin C was the minimal detectable concentration. A single determination took about 2 min; sample throughput is 30 h^{-1}. Different β-lactamases were examined for enhancement of substrate selectivity.

Immobilized enzymes have found widespread application in flow-injection analysis (f.i.a.) [1]. Solid-bed reactors containing enzymes can be used for the determination of different substrates in connection with most detectors for liquid chromatography (e.g., ultraviolet, infrared, fluorimetric, refractometric, mass spectrometric, electrochemical, enthalpimetric) [2]. Although much work has been done with enzyme reactor/flow-injection systems in the inorganic [3—7] and organic [8—14] fields, only one such method has been reported for β-lactams. An enthalpimetric f.i.a. method for determination of penicillins and cephalosporins with an enzyme thermistor was described recently [15]. In the present paper, the automated determination of different cephalosporins at low concentrations by f.i.a. with ultraviolet measurements is described.

THEORY

The cleavage of the β-lactam ring of Δ3-cephalosporins by nucleophilic agents such as water, hydroxide, amines and enzymes has a different mechanism from the hydrolysis of penicillins, which leads to relatively stable penicilloic acid derivatives [16, 17]. The special behaviour of cephalosporins (I) is primarily due to their Δ3-double bond; the enamine resonance thus possible weakens the β-lactam amide bond for nucleophilic attacks. If there is a substituent at the C-3 position of the molecule which can act as a suitable leaving group (L), intermediate compounds with an exomethylene moiety (II) are formed; these intermediates exhibit an absorption maximum at 230 nm. If no suitable C-3 substituents are present, cephalosporoic acid derivatives ($\lambda_{max} \approx 260$ nm; **III**) are formed, most of which are unstable and undergo further degradation to various fragments absorbing at other wavelengths. In all these cases, degradation of the cephalosporin molecule is followed by destruction of the u.v. chromophore with, typically, an absorption maximum at 260 nm, i.e., the absorbance at 260 nm decreases significantly and sometimes new chromophores can be formed. An exception is the desacetylcephalosporin C-lactone, an α,β-unsaturated γ-lactone, where enamine resonance cannot develop; after hydrolytic cleavage of the β-lactam ring, the cephalosporoic acid structure ($\lambda_{max} = 265$ nm; **IV**) is stabilized, and the absorbance at 260 nm is largely maintained [18]. Extensive n.m.r. investigations [19] have shown that the cephalosporoic acid derivative is the cause for the maintenance of absorbance at 265 nm and not the α,β-unsaturated γ-lactone ring. Substituted α,β-unsaturated γ-lactones, e.g., 2-oxo-3,4-dimethyl-2,5-dihydrofuran (V), exhibit absorption maxima between 210 nm and 220 nm [20].

To utilize these observations, appropriately prepared sample solutions are injected into the enzyme reactor/flow system. An immobilized β-lactamase degrades the cephalosporins selectively, so that the u.v.-chromophore ($\lambda_{max} = 260$ nm) is destroyed. Each sample is injected twice and passes through a dummy column of exactly the same geometric dimensions as the

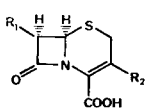

(I)

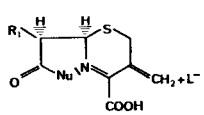

(II)

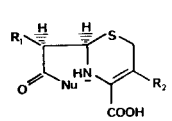

(III)

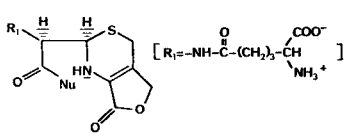

(IV)

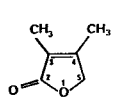

(V)

enzyme reactor, filled with inert glass carrier material during the first run. In this run, the total absorbance of the sample and sample matrix is measured at 260 nm. Before the second injection of the sample, the enzyme reactor is switched into the flow line; only the cephalosporins in the sample lose their chromophore. The difference of the A_{260} values between untreated and enzymatically degraded sample is proportional to the concentration of cephalosporins. Peak areas are measured, in order to overcome the differences in sample dispersion caused by varying kinetics.

EXPERIMENTAL

Apparatus

The flow system is outlined in Fig. 1. Absorbances were measured with a fixed wavelength detector (254 nm; model 1036 A, Hewlett-Packard). The flow stream was maintained at 3.0 ml min^{-1} with a h.p.l.c. Altex 110 pump (Altex/Beckman). Sampling was done by a cooled ISS-100 automatic sampler (Perkin-Elmer); cooling was done with a Haake D3G constant-temperature circulator. An interface for control of the whole system and for synchronization of the sampler and the data system was designed and built by the Electronic Department of this company. A Servogor 210 pen recorder was used for immediate visualization. Digitizing was done by a Hewlett-Packard HP-18652 A/D-converter (ADC) and the data were evaluated by a HP-3357 data system. For method comparison, a h.p.l.c. apparatus (HP-1084-B) with variable-wavelength detector and automatic sampler was used.

Connecting tubing was of stainless steel (0.2 mm i.d.) with Swagelok joints. The total length of tubing from the injection valve to the detector was $\geq$70 cm. The reactor columns were of stainless steel tubing (0.64 cm o.d., 0.47 cm i.d., 5.0 cm long) fixed at both ends with Swagelok reductions to 1.6 mm and sealed with 2-μm stainless steel frits.

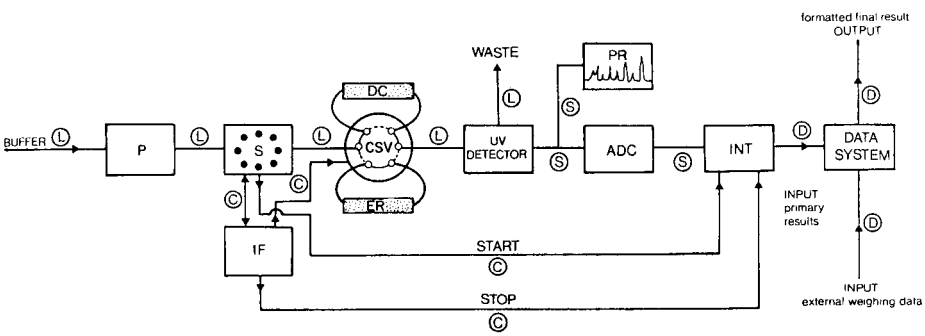

Fig. 1. The automated enzyme reactor/flow injection system. P, Pump; S, sampler; IF, interface; CSV, column switching valve; DC, dummy column; ER, immobilized enzyme reactor; PR, pen recorder; ADC, analog-digital converter; INT, integrator; L, liquid line; C, control line; S, signal line. For details, see text.

Reagents and chemicals

The controlled-pore glass (CPG) beads used for enzyme immobilization (Pierce Chemical Co., Rockford, IL) had a pore diameter of 50 nm and a particle size of 125—175 μm. Different enzymes were bound covalently to this glass: cephalosporinase from *Enterobacter cloacae* (P-99) with 66 IU mg^{-1} (Miles Laboratories, Elkhart, IN) and penicillinase P-6018 (type II) from *Bacillus cereus* with 70 IU mg^{-1}, against benzylpenicillin as substrate (Sigma Chem. Corp.). For activation of the CPG, 3-(triethoxysilyl)-propylamine (Merck) was used as received. Cephalosporin C (sodium salt, dihydrate, 97.5% pure) and desacetylcephalosporin C (sodium salt, dihydrate, 94.0% compared with the cephalosporin C salt) were produced by Biochemie GmbH (Kundl, Austria). Desacetoxycephalosporin C (sodium salt, dihydrate, 92.9% pure) was made by Proter (Milano, Italy). Other compounds used were ceftriaxone-disodium salt (Rocephin) and cefalexin (both Biochemie GmbH), cefazolin, cefamandole, cefachlor and cefalotin (all sodium salts; Eli Lilly, Indianapolis, IN), cefoxitin-Na (Merck, Sharp & Dohme, Rockway, NY), cefaloridine (Sigma Chem. Corp.) and cephaloglycine (a gift from Sandoz Research Institute, Vienna, Austria).

Methanol (p.a. quality; Riedel de Haen) and tetrabutylammonium bromide (Fluka) were used for h.p.l.c. The stationary phase for h.p.l.c. was Nucleosil C_{18} reverse-phase material (5 μm; Macherey & Nagel, Düren, FRG). The other chemicals and reagents were p.a. grade (Merck).

Procedures

Enzyme immobilization. The enzymes used were bound covalently to the activated porous glass. The glass was washed in boiling 5% nitric acid, silanized with 3-(triethoxysilyl)propylamine to give the alkylamino glass, and treated with 2.5% glutaraldehyde in an aqueous system [21]. The cephalosporinases were bound to the pretreated glass by gentle shaking at +4°C. Concentrations of 5—15 mg protein/g derivatized glass yielded sufficient enzyme concentrations. Stirring of the carrier material in the enzyme solution should be avoided, because it tends to break up the porous glass beads, with later clogging of the reactor.

Sample preparation. Sample preparation of biological material caused few problems, because the sensitivity of the method allows high dilutions to be used. Interfering effects by the biological matrix and particle contaminations are thus kept very low. Samples from fermentation process were diluted by a factor of 100, centrifuged and pipetted into glass sample vials. Standard solutions were prepared with twice-distilled water in the concentration range 100—500 μg ml^{-1}.

Flow-injection method. In the system shown in Fig. 1, the eluent is a 0.15 M phosphate buffer (pH 7) containing sodium azide (0.065 g l^{-1}; 0.001 M) which is pumped continuously at 3.0 ml min^{-1}. Sample volumes (100 μl) are injected into the buffer stream by an automatic sampler, which holds up to 100 samples and is cooled to +4°C. With the packed

reactor columns in position, the back-pressure for the system is 6—8 bar (0.6—0.8 MPa). The enzyme reactions are done at ambient temperature. The switching between the enzyme reactor and the dummy column is done with a pneumatic 6-port valve. The special interface for communication between sampler, ADC and data system counts the sample injections, controls the column-switching valve, starts and stops both sampler and ADC and synchronizes the whole procedure. The interface timing diagram is shown in Fig. 2. Before the first sample is injected, the column-switching valve is automatically set to a position such that the buffer solution flows through the dummy column and that the absorbance of the whole untreated sample is measured. Before the second injection of the same sample, the enzyme reactor is switched into the flow stream and the residual absorbance of the reacted sample is recorded. Before each further injection, the pneumatic valve is switched to the other position. A preset number of single injections (2 per sample) is used (40 injections, see below) and then the sampler is stopped after a delay of 10 s. Then a second delay time of 1.5 min is allowed in order to obtain the last peak and to regain the integration baseline. Then the ADC is stopped for result output and a third delay is started in order to finish the data evaluation. A new start command by the interface activates the cycle again for the next sample set. The detector sensitivity was set to 1.024 AFS; the recorder scale was 10 mV and the chart speed was 0.5 cm min^{-1}.

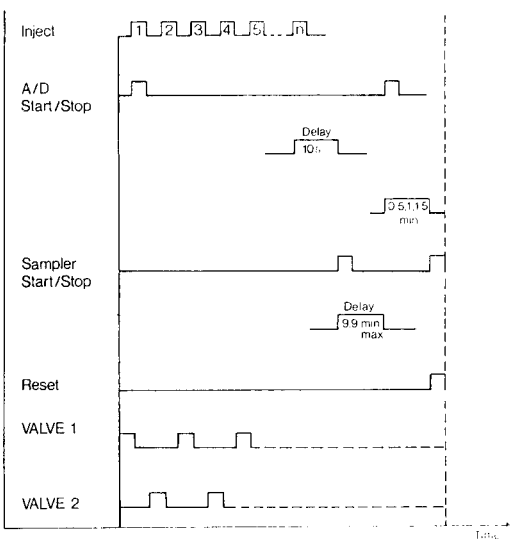

Fig. 2. Interface timing diagram, showing the cycles for injection, integrator start/stop, sampler start/stop and column-switching valve.

RESULTS AND DISCUSSION

Evaluation of data

The curve shape of the signals generated corresponds approximately to a normal distribution, similarly to chromatographic peaks. The peaks are evaluated by area rather than height because of different sample dispersion within the dummy and enzyme reactors, probably because of kinetic effects.

The sample concentrations are calculated by means of a multiple internal-standard method. A large number of samples can be handled in a minimal overall time by collecting the data for 3 standards and 17 samples in one group. The results of the 20 runs (40 single injections) are then evaluated by the data system, analogously to a single chromatogram with 40 peaks. A typical recorder output for a run is shown in Fig. 3. The size of the sample groups and the number, concentrations and positions of the standard solutions in the sampler can be freely chosen during method development. The sample concentrations are calculated on the basis of a corrected calibration curve, which is derived from the standards contained in every particular group of samples. A statistical test is applied to all internal calibration functions automatically by application of curve-fitting by the least-squares method. As a measure of the quality of the results, the correlation coefficient (r) is displayed in each final report; the value of r must be $\geqslant 0.999$ for three internal standards, otherwise the results for the block of sample runs are discarded because of statistical unreliability.

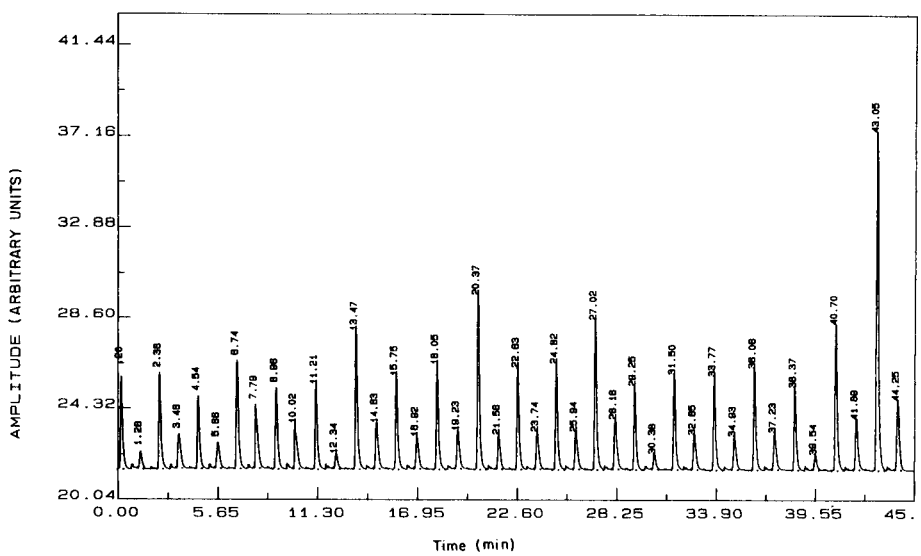

Fig. 3. An example of the recording for a run of cephalosporin C samples (17 samples and 3 standards).

Determination of cephalosporin C

Different cephalosporins can be determined with the proposed system rapidly and selectively. The extent of substrate conversion in the enzyme reactors was tested under the conditions described above. Highly concentrated cephalosporin C (CC) solutions (1 mg CC ml^{-1} and 5 mg CC ml^{-1}) were injected into the system, the eluting liquid was collected and the amount of unreacted CC was determined by h.p.l.c.; <0.1% of the injected amount of CC could be recovered, thus the rate of conversion was >99.9% even for the most concentrated solution.

In biological samples, which contained both desacetylcephalosporin C (DA-CC) and cephalosporin C, both substances were detected together. The response time of the system taken from injection of the sample is only 10 s and a peak is complete after 30 s. Nevertheless, the time for one sample is approximately 2 min, because each sample is injected twice and the automatic sampler used is limited in cycle time by its rinsing and sample uptake processes. The long-term stability of the enzyme reactor is excellent because of the high sensitivity of the method and the high dilutions. Several thousand samples can be processed without any remarkable decrease in signal yield with one reactor (Fig. 4). The minimal detectable amount of CC is 2×10^{-7} g. The response was measured in the range 10—1000 $\mu g\ ml^{-1}$; the calibration graph became nonlinear above 800 $\mu g\ ml^{-1}$ as shown in Fig. 5 ($N = 16$, $k = 193.85$, $d = 2357$, $r = 0.998$). Precision of the method was determined by 15-fold injection of an identical sample. The relative standard deviation was 0.7% ($N = 15$, $\bar{x} = 207.23\ \mu g\ ml^{-1}$, SD = $\pm 1.368\ \mu g\ ml^{-1}$).

Comparison of results for cephalosporin C

The accuracy of the proposed method was assessed by comparison with a h.p.l.c. method: 44 samples from a fermentation process, which contained

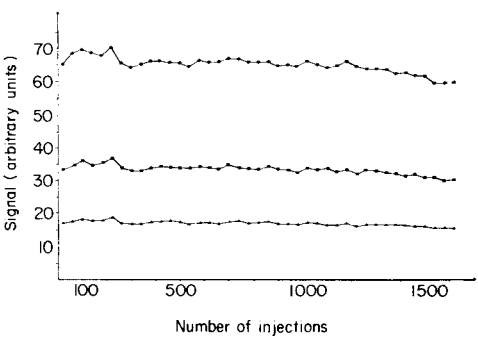

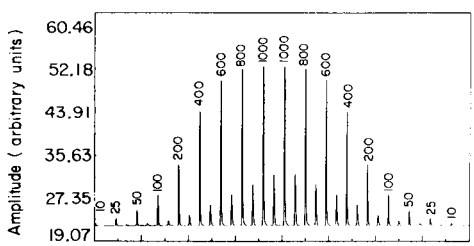

Fig. 4. Long-term stability of a P-99 β-lactamase reactor. Cephalosporin C concentration: (•) 400; (▪) 200; (▲) 100 $\mu g\ ml^{-1}$.

Fig. 5. Calibration curve from 16 cephalosporin C standard solutions in the range 10—1000 $\mu g\ ml^{-1}$.

cephalosporin C in concentrations of 0.1—13.0 mg g^{-1} of culture broth, were analyzed simultaneously by the two methods. For h.p.l.c., an octadecylsilica reverse-phase column (Nucleosil C_{18}; 5 μm) was used with an eluent consisting of a 0.01 M tetrabutylammonium bromide in water/methanol (3 + 1). The chromatographic column was 10 cm long (0.64 cm o.d., 0.47 cm i.d.) thermostatted at 40°C; the flow rate was 2.0 ml min^{-1} and the back-pressure was ca. 230 bar (23.0 MPa). The detector wavelength was 260 nm and the injection volume was 30 μl. The correlation plot between the two methods was linear ($y = kx + d$; $N = 44$, $k = 0.9805$, $d = 0.192$). The correlation coefficient ($r = 0.993$) proved good correspondence between the flow-injection and h.p.l.c. methods.

Additionally, a double-sided data paired t-test was applied to a further 40 samples analyzed by both methods. There was no difference between the results of the two methods at a 95% significance level [22] ($N = 40$, $t_{39,\alpha(2P=0.05)} = 1.33 < 2.023$). The results from 15 parallel determinations of fermentation samples are collected in Table 1.

Enhancement of selectivity for cephalosporin C in the presence of other cephalosporin derivatives

When the β-lactamase from *Enterobacter cloacae* P-99 was used, only the determination of cephalosporin C (CC) and desacetylcephalosporin C (DACC) together was possible from fermentation samples. Attempts to enhance selectivity for CC were therefore made. A β-lactamase of type II from *Bacillus cereus* has been reported, which is reactive towards CC (80% compared with benzylpenicillin as substrate), but does not affect DACC (0.02%) or desacetoxycephalosporin C (DAOCC) (0.4%) [23]. Immobilization on the CPG carrier was done as described under Experimental. A series of CC sample solutions containing different amounts of DACC was investigated by the flow-injection method. Significantly enhanced

TABLE 1

Results from 15 parallel determinations of cephalosporin C (plus desacetylcephalosporin C) in fermentation samples by h.p.l.c. and the proposed method

Sample	Concentration found (mg g^{-1})		Error (%)	Sample	Concentration found (mg g^{-1})		Error (%)
	H.p.l.c.	F.i.a.			H.p.l.c.	F.i.a.	
1	3.41	3.32	−2.64	9	7.63	7.78	+1.97
2	3.71	3.77	+1.62	10	8.36	8.26	−1.20
3	4.24	4.40	+3.77	11	9.63	9.13	−5.19
4	4.59	4.39	−4.36	12	9.84	9.39	−4.57
5	5.24	5.75	+9.73	13	10.64	10.67	+0.28
6	6.23	6.28	+0.8	14	10.77	10.51	−2.41
7	6.65	6.61	−0.6	15	10.96	11.25	+2.65
8	7.03	7.28	+3.56				

selectivity for CC is illustrated in Fig. 6. Although the results obtained for CC in the presence of fermentation by-products such as DACC and DAOCC were improved by the use of the type II β-lactamase, these enzyme reactors turned out to be far less stable than the original reactors with β-lactamase from *Enterobacter cloacae*. The decrease of enzyme activity in continuous use is shown in Fig. 7. The loss in activity was ca. 20% after 380 injections on the *Bacillus cereus* 569/H β-lactamase reactor, but was scarcely detectable when the *Enterobacter* P-99 β-lactamase reactor was used for the same number of samples.

Application to commercially available cephalosporin derivatives

Twelve commercially available cephalosporins were investigated on the flow-injection apparatus for their relative susceptibility to the *Enterobacter cloacae* enzyme reactor. Table 2 lists the chemical structures and the absorption maxima of the investigated cephalosporins [24] in the order of their reactivities. Solutions of these compounds (ca. 100 μg ml^{-1}) were processed through the system, with measurement at 254 nm, and the percentage differences in the absorbances between the treated and degraded cephalosporins were related to their reactivity with the immobilized enzyme. Cephalosporin C exhibited the highest relative reactivity and was taken as reference with 100%. The results are listed in Table 3. It was found the nature of the leaving group in the 3-position has the most important effect on the enzymatic cleavage of cephalosporins, but that substituents in the 7-position also play an important role in the mechanism of further degradation of the molecule.

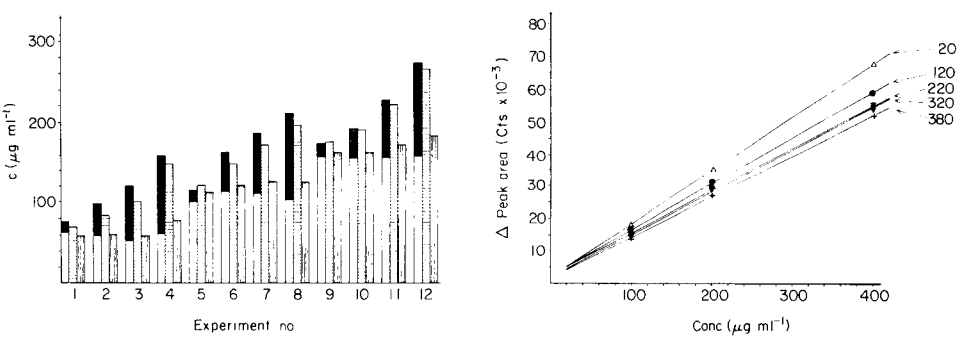

Fig. 6. Diagram showing the selective determination of cephalosporin C in presence of desacetylcephalosporin C in standard solutions by means of cephalosporinase from *Bacillus cereus* 569/H. Horizontally dashed columns correspond to β-lactamase from *Enterobacter cloacae*; vertically dashed columns correspond to β-lactamase from *Bacillus cereus*. Open and filled columns correspond to the concentrations of CC and DACC, respectively.

Fig. 7. Decrease in column efficiency of a *Bacillus cereus* 569/H β-lactamase reactor in dependence of the number of samples processed (indicated on the plots).

TABLE 2

Chemical structure and absorption maxima of the cephalosporins investigated

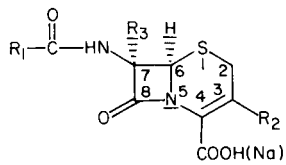

Substance	R_1	R_2	R_3	λ_{max} (nm)
Cephalosporin C	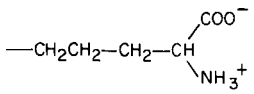	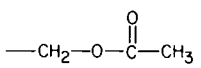	—H	260
Cefalotin	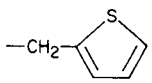	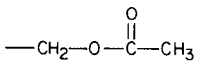	—H	260
Cefaloglycine	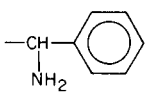	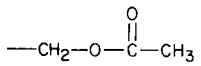	—H	260
Cefaloridine	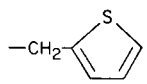	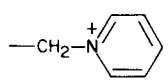	—H	255
Cefaclor	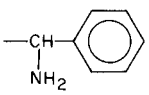	—Cl	—H	262
Cefalexin	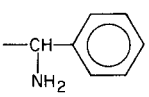	$-CH_3$	—H	260
DAOCC	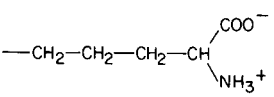	$-CH_3$	—H	260
Cefazolin	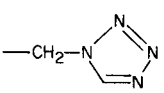	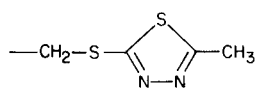	—H	271
DACC	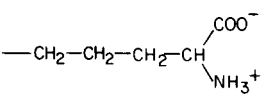	$-CH_2-OH$	—H	260
Cefamandole	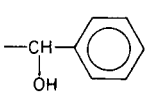	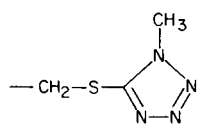	—H	265
Ceftriaxone (Rocephin)	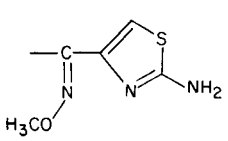	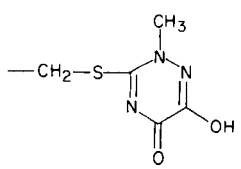	—H	242 272
Cefoxitin	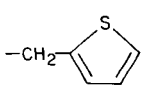	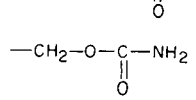	$-OCH_3$	262.5

TABLE 3

Relative reactivity of different cephalosporins with β-lactamase from *Enterobacter cloacae* P-99, measured with the flow-injection system at 254 nm

Substance	Peak areas (arbitrary units)		Reactivity[a] (%)	Substance	Peak areas (arbitrary units)		Reactivity[a] (%)
	Untreated	Treated[b]			Untreated	Treated[b]	
Cephalosporin C	23500	18200	100.0	DAOCC	19200	11900	80.0
Cefalotin	33600	23900	91.7	Cefazolin	29500	18150	79.4
Cefaloglycine	25000	17450	90.1	DACC	26950	16100	77.0
Cefaloridine	52900	33900	82.7	Cefamandole	26300	10300	50.6
Cefaclor	24300	15450	82.1	Ceftriaxone	26300	9200	19.1
Cefalexin	27800	17300	80.3	Cefoxitin	28300	3100	14.2

[a]Compared with CC—$Na \cdot 2H_2O$ = 100%. [b] Difference after treatment.

As an example, cefoxitin differs from cefalotin only in the 7-α-methoxy moiety and the carbamoyl instead of the acetyl function in the 3-position, but its reactivity against P-99 β-lactamase is only 13% compared with cefalotin. The acetoxy moiety seems to be the most effective leaving group, followed by the pyridine molecule in cefaloridine. The heterocyclic substituents of the cefazolin, cefamandole and ceftriaxone molecules do not show leaving-group properties to the same extent. The influence of the leaving group in the 3-position is also clearly demonstrated in the series CC, DACC and DAOCC. A special case is DACC lactone, which shows only a small difference in its u.v. absorbance; it is affected by P-99 β-lactamase, but the product is a relatively stable cephalosporoic acid derivative which has much the same u.v. absorption as the original compound.

Conclusion

The applications of the enzyme reactor/flow-injection system are not limited to the determination of cephalosporins. In principle, it is possible to determine any substance that undergoes a sufficiently selective enzyme reaction to form a product with a significantly different u.v. absorption spectrum. In such cases, the stability of chemical compounds to different enzymes can also be investigated. Enhancement of sample capacity is the aim of future work either by changes in the dimensions or by use of other types of reactor.

The authors express their gratitude to R. Leutgeb for the construction of the electronic interface, to J. Patka for developing the computer software, and to B. Helm and I. Röck for excellent technical assistance.

REFERENCES

1 J. Růžička and E. H. Hansen, Flow Injection Analysis, Interscience-Wiley, New York, 1981, Chs. 2, 4, 5, 6.
2 P. W. Carr and L. D. Bowers, Immobilized Enzymes in Analytical and Clinical Chemistry, Interscience-Wiley, New York, 1980, Chs. 4, 8.
3 B. Mattiasson, K. Mosbach and Å. Svensson, Biotechnol. Bioeng., 19 (1977) 1556.
4 L. Ogren and G. Johansson, Anal. Chim. Acta, 96 (1978) 1.
5 D. R. Senn, P. W. Carr and L. N. Klatt, Anal. Chem., 48 (1976) 954.
6 L. J. Forrester, D. M. Yourtee and H. D. Brown, Anal. Lett., 7 (1974) 599.
7 H. H. Weetall and M. A. Jacobson, Proc. IV IFS Ferment. Technol. Today, 361 (1972) 361.
8 G. Johansson, K. Edstrom and L. Ögren, Anal. Chim. Acta, 85 (1976) 55.
9 B. Mattiasson, B. Danielsson and K. Mosbach, Anal. Lett., 9 (1976) 217.
10 D. C. Williams, G. F. Huff and W. R. Seitz, Clin. Chem., 22 (1976) 372.
11 L. P. Leon, M. Sansur, L. R. Snyder and C. Horvath, Clin. Chem., 24 (1977) 1556.
12 D. J. Inman and E. W. Hornby, Biochem. J., 137 (1974) 25.
13 B. Danielsson, K. Gadd, B. Mattiasson and K. Mosbach, Anal. Lett., 9 (1976) 987.
14 C. W. Bradberry and R. N. Adams, Anal. Chem., 55 (1983) 2439.
15 G. Decristoforo and B. Danielsson, Anal. Chem., 56 (1984) 263.
16 G. G. F. Newton, E. P. Abraham and S. Kuwabara, Antimicrob. Agents Chemother., (1967) 449.
17 M. A. Schwartz, in J. M. T. Hamilton-Miller and J. T. Smith (Eds.), β-Lactamases, Academic Press, London, 1979, p. 51.
18 J. M. T. Hamilton-Miller, G. G. F. Newton and E. P. Abraham, Biochem. J., 116 (1970) 371.
19 J. M. T. Hamilton-Miller, E. Richards and E. P. Abraham, Biochem. J., 116 (1970) 385.
20 D. E. Ames, R. E. Bowman and T. F. Grey, J. Chem. Soc., (1954) 375.
21 H. H. Weetall, in K. Mosbach (Ed.), Methods in Enzymology, Vol. 44, Academic Press, New York, 1976, p. 134.
22 R. Kaiser and G. Gottschalk, Elementare Tests zur Beurteilung von Meßdaten, Bibliographisches Institut, Mannheim, 1972, Ch. 9.
23 E. P. Abraham and S. G. Waley, in J. M. T. Hamilton-Miller and J. T. Smith (Eds.), Academic Press, London, 1979, p. 324.
24 E. E. Roets, J. H. Hoogmartens and H. J. Vanderhaeghe, J. Assoc. Off. Anal. Chem., 64 (1981) 166.

Analytica Chimica Acta, 163 (1984) 85—90
Elsevier Science Publishers B.V., Amsterdam — Printed in The Netherlands

AN AUTOMATED NEPHELOMETRIC SYSTEM FOR EVALUATION OF THE GROWTH OF BACTERIAL CULTURES

KL. MECHSNER

Swiss Federal Institute for Water Resources and Water Pollution Control, Swiss Federal Institutes of Technology, CH-8600 Dübendorf (Switzerland)

(Received 14th May 1984)

SUMMARY

An automated system comprising sixteen similar, independently controlled bioreactors is described. The operating parameters that can be varied in each bioreactor include pH, aeration, agitation and inlet and outlet liquid flow rates. Automatic turbidity measurements in each bioreactor are possible by employment of a nephelometer mounted on a track such that it aligns with the side arm of each bioreactor. Measurements are plotted automatically on either a linear or a semilogarithmic basis with respect to time. The response of the nephelometer is linear with respect to bacterial concentration throughout its operating range. Results that demonstrate the suitability of the system for studying bacterial oxidation processes where substrate concentrations are very low and where substrate affinity is important are presented.

Both the design and operation of bioreactors used for bacterial bio-oxidation processes require detailed knowledge of the characteristics of the bacteria employed. To describe the growth of bacterial cultures, Monod [1, 2] and Herbert et al. [3] developed the widely used theoretical equations that link the specific growth rate constant (μ), the bacterial biomass concentration on a dry weight basis (x), the limiting substrate concentration (s), the saturation constant (K_s) and, in the case of completely mixed continuous flow cultures, the dilution rate (D). The generation of data for inclusion in their equations normally requires extensive, labour-intensive and time-consuming experiments, so that automated data collection systems have an obvious rôle. For many years, turbidity measurements have been widely used for the evaluation of bacterial concentrations in growing cultures, and instruments for the automatic measurement of the turbidity of growing bacterial cultures in single bioreactors have been described by Ševčík et al. [4] and by Szcepula et al. [5]. Few techniques for following bacterial growth, other than turbidity measurements, are readily suited for automation, particularly when extremely dilute substrate concentrations, which are frequently encountered in wastewater treatment research, are considered. For example, production of carbon dioxide [6] can be used only when dense cell suspensions are encountered.

0003-2670/84/$03.00

In order to accelerate the collection of data on growth of bacteria on dilute substrates, particularly when the main interest lies in the effect of a range of additive concentrations, a system that automatically measures the turbidity of growing bacterial suspension in sixteen, independently controlled, laboratory-scale bioreactors was developed. The system is described and its capability demonstrated by the inclusion of some results that have been obtained with it.

EXPERIMENTAL

Equipment

The system comprises a nephelometer (see below) mounted on a sliding carriage that traverses a track placed behind a 2.65-m long bench on which sixteen bioreactors are mounted. The arrangement is such that the nephelometer stops and aligns with the side-arm on each bioreactor in turn. The interval for each turbidity measurement and the number of vessels surveyed can be selected. At the termination of each measurement cycle, the nephelometer returns to its starting point on the sliding carriage. The turbidity measurements are recorded with a 24-channel recorder on either a linear or a semi-logarithmic basis as required. The eight additional channels of the recorder are used for recording the pH in selected bioreactors during the return of the nephelometer to its starting point. The minimum time interval for each turbidity measurement is 30 s, giving a minimum overall cycle time of 12 min.

Bioreactor. Each bioreactor is a cylindrical glass vessel (75 mm in diameter and 170 mm high) fitted with a flanged glass lid which has a central ground-glass port and six peripheral screw-threaded ports. The vessel is connected, at two levels below the surface of the broth, to a vertical glass side-arm (17 mm in diameter) which serves as a cuvette for turbidity measurements, and which reaches above the top of the bioreactor. During operation, each bioreactor contains 500 ml of medium and rapid cycling between the cylindrical vessel and the side-arm is ensured by the mixing action of a magnetically-driven stirrer bar. The drive for the stirrer is mounted directly under each bioreactor and the rotational speed of each stirrer can be varied independently. Bacterial film formation on the wall of the side-arm (cuvette) is removed by a plunger fitted with O-rings which is automatically activated at the end of each operating cycle. For aerobic growth, air enters the bioreactor through a cotton-wool plugged port, and is distributed throughout the medium by vortex aeration. The central port in the lid is used to hold a pH electrode. When the bioreactor is operated in the continuous flow mode, addition and removal of medium is achieved by tubes that are introduced through the screw-threaded ports. The lid of the bioreactor is clamped to the body and sealed with an O-ring set into the flange. The bioreactors are sterilized prior to use, with medium in situ, by autoclaving at 121°C for 20 min.

Control unit and pH meter. The electronic control unit is placed beneath

the bank of bioreactors and coordinates the steps necessary for the sequence of operations and measurements and allows selection of the number of bioreactors surveyed during each operational cycle.

The pH meter, also placed beneath the bank of reactors, is an eight-channel instrument with a pH range of 4—11. Sterilizable combined pH electrodes are used.

Nephelometer and recorder. A Sigrist photometer type UP51-T65 fitted with a type 5T65-HWF3 high-sensitivity measuring system was adapted for use as a nephelometer in the automatic equipment. This photometer operates on the nephelometric two-beam/swinging-mirror principle; in addition to high sensitivity, it has no dependence on the colour of the growth medium. It is provided with automatic zero compensation. The original cuvette housing of the photometer was replaced by an inverted U-shaped bracket, arranged so that the mirror is attached to the outer limb of the bracket, whilst the side-arm cuvette of each bioreactor replaces the original flow cell of the photometer. The mirror reflects the light beam into the cuvette where the scattered light is generated.

The signal produced by the nephelometer is recorded on a 24-channel Linseis LC24 recorder, which has a range on each channel of 0—200 mV. The printing interval is variable between 30 and 100 s and any one of sixteen chart speeds between 1 mm h^{-1} and 100 mm min^{-1} can be selected. A linear-logarithmic converter is fitted between the photometer and the recorder so that the results obtained can be directly plotted in a semilogarithmic form on either a one- or two-cycle basis.

The correlation between turbidity and bacterial numbers is linear from 0 to 370 units of turbidity. By linear regression, the relationship obtained was Bacterial number ml^{-1} = 2.66 turbidity unit $\times$ 10^4 with a correlation coefficient (r) of 0.998, when simultaneous turbidity measurements and bacterial cell counts were done for a growing culture of an *Achromobacter* species.

Bacteria and medium

Two bacteria were used: an *Achromobacter* sp., isolated from settled municipal sewage, and *Pseudomonas denitrificans* ATCC 13867.

The mineral base medium used contained, per litre of 2 mM phosphate buffer (pH 7.5), 2.5 mg of magnesium sulfate heptahydrate, 1.5 mg of calcium chloride, 12.0 mg of ammonium chloride and 0.01 ml of trace element solution. The buffering capacity of the medium was sufficient to maintain the pH above 7.4 during bacterial growth. The carbon-energy substrates used were either glucose or sodium lactate.

Bioreactor operation

After sterilization, the bioreactors were positioned on the fitted bench and appropriate connections were made. The rotational speed on the magnetic stirrers was set at the required value by measurement with a stroboscope.

The nephelometer was compensated for original turbidity in the medium. After one hour of initial operation, the bioreactors were inoculated with washed cells of the bacterium under study; subsequently, the growth process was monitored by the automatic system. A typical print-out, on a semi-logarithmic basis, for a series of growth experiments employing a range of carbon-energy substrate concentrations is shown in Fig. 1.

RESULTS

In order to demonstrate the types of data that can be generated and the performance of the automatic growth-following system, two experiments concerning growth at low initial carbon-energy substrate concentrations are presented below.

An *Achromobacter* sp., grown batchwise on a series of concentrations of glucose as carbon-energy substrate at 15 and 25°C, exhibited different specific growth rate constants, depending on the initial glucose concentration. The effects of initial glucose concentration (C_s) on the specific growth rate constant (μ) for the two temperatures are shown in Fig. 2(a); these curves assume the hyperbolic shape typical of the Monod relationship, i.e., $\mu = \mu_m C_s/(K_s + C_s)$, where μ_m is the maximum value of the specific growth rate constant, even though this relationship is based on actual, rather than initial substrate concentrations. Double reciprocal (Lineweaver—Burk) plots of the data (Fig. 2b) allowed evaluation, by linear regression, of the constants μ_m and K_s. At 25°C, μ_m was 0.095 h^{-1} and K_s was 0.48 μmol l^{-1} glucose; at 15°C, the values were 0.046 h^{-1} and 0.49 μmol l^{-1} glucose, respectively. Although these results are clearly out of line with established bacterial growth theory, similar findings have been reported by Gaudy et al. [7].

In the second experiment, *Ps. denitrificans* was grown with sodium lactate as the carbon-energy substrate at 25°C. Three growth curves (turbidity vs.

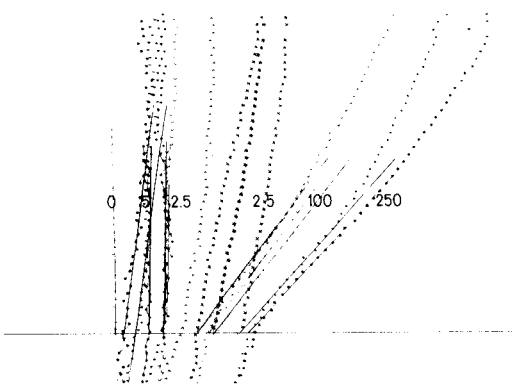

Fig. 1. Recorder chart indicating batch growth curves for *Ps. denitrificans* at 25°C at a series of glucose concentrations (0—250 μmol l^{-1}) after logarithmic conversion. The horizontal axis is logarithmic; the chart speed was 10 mm h^{-1}.

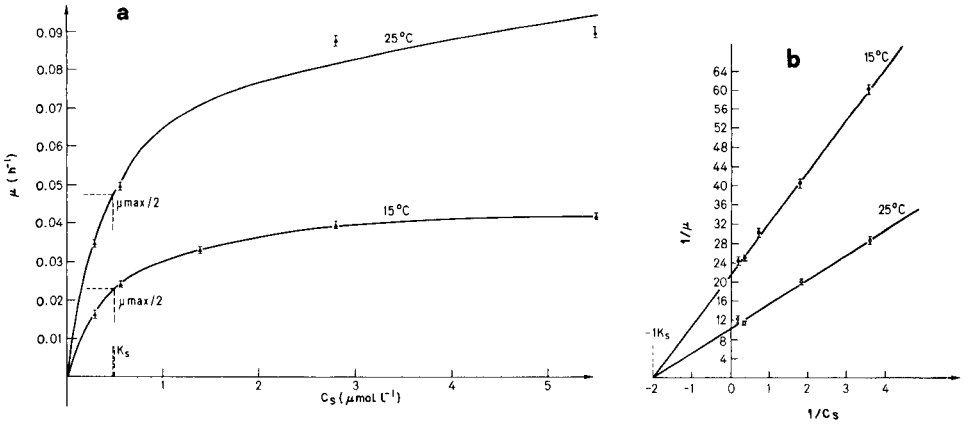

Fig. 2(a). The rate constant/substrate concentration diagrams for an *Achromobacter* sp. grown on glucose at 15° and 25°C. (b) The Lineweaver—Burk plots for the data given in (a).

time) for each of three bioreactors operated batchwise were obtained at a series of different initial sodium lactate concentrations. The results obtained at one such concentration are shown in Fig. 3. The parallel nature of the set of growth curves is clearly evident.

Conclusions

The automated nephelometric system described can generate growth curves even when very dilute substrates are used. Thus, growth experiments under conditions where affinity becomes relevant can be undertaken. The monitoring of long-term processes is facilitated by the fully automatic operation of the instrument, avoiding the need for continuous observations and manipula-

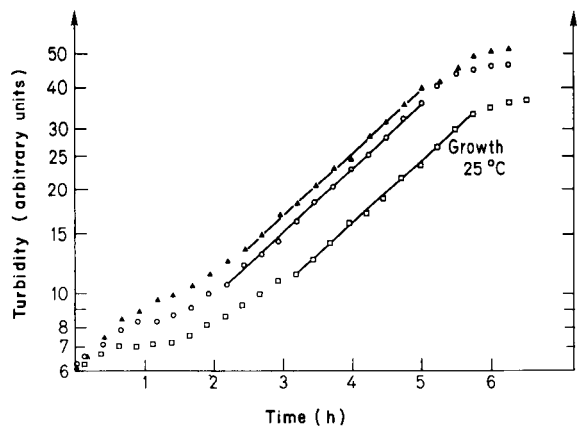

Fig. 3. A series of growth curves for *Ps. denitrificans* at 25°C and an initial sodium lactate concentration of 57 μmol l^{-1}.

tions during an experimental run. The logarithmic conversion of turbidity measurements allows easy interpretation of the plotted growth curves. Interesting effects of initial substrate concentration in batch cultures have been clearly demonstrated using the system.

I thank Prof. Dr. K. Wuhrmann for urging the design and construction of the apparatus, L. Kalman and H. Suter for their skilled construction work and P. Egli for assistance with the experiments. I also thank Prof. Dr. G. Hamer for revision of the manuscript.

REFERENCES

1 J. Monod, Recherches sur la croissance des cultures bactériennes, Hermann & Cie., Paris, 1942.
2 J. Monod, Ann. Inst. Pasteur, 79 (1950) 390.
3 D. Herbert, R. Elsworth and R. C. Telling, J. Gen. Microbiol., 14 (1956) 601.
4 F. Ševčíc, B. Liska and B. Hošek, Folia Microbiol., 8 (1964) 125.
5 W. Szcepula, J. Kalinowski and J. Bodziński, Acta Microbiol. Pol., 16 (1967) 189.
6 D. T. Boyle, Biotechnol. Bioeng., 19 (1977) 297.
7 A. F. Gaudy, Jr., A. Obayashi and E. T. Gaudy, Appl. Microbiol., 22 (1971) 1041.

Analytica Chimica Acta, 163 (1984) 91—100
Elsevier Science Publishers B.V., Amsterdam — Printed in The Netherlands

ISOLATION OF 3,4-DIHYDROXYPHENYLACETIC ACID PRODUCED FROM *p*-HYDROXYPHENYLACETIC ACID BY IMMOBILIZED PLANT CELLS OF *MUCUNA PRURIENS* AND ITS IDENTIFICATION BY LIQUID CHROMATOGRAPHY/MASS SPECTROMETRY

A. P. BRUINS*

State University, Department of Pharmacy, A. Deusinglaan 2, 9713 AW Groningen (The Netherlands)

N. PRAS

State University, Pharmaceutical Biotechnology Research Group, A. Deusinglaan 2, 9713 AW Groningen (The Netherlands)

(Received 17th April 1984)

SUMMARY

A cell suspension culture originating from a *Mucuna pruriens* (L.) DC f. *utilis* (Wall ex Wight) Back cultivar was immobilized in calcium alginate. Biotransformation of *p*-hydroxyphenylacetic acid to 3,4-dihydroxyphenylacetic acid was done in a bubble-jar containing a suitable incubation medium. To obtain a sample suitable for combined liquid chromatography/mass spectrometry (l.c./m.s.), electrolytes, proteins and carbohydrates were removed from the medium by chromatography on Sephadex G-10 and Affigel-601 columns. Product formation and isolation were followed by high-performance liquid chromatography with electrochemical and u.v. detection, and by continuous u.v. detection. The identity of 3,4-dihydroxyphenylacetic acid was confirmed by l.c./m.s., which also detected an impurity or by-product not observed by electrochemical or u.v. detection.

Mucuna pruriens grown in vitro and immobilized in calcium alginate beads can transform L-tyrosine (β-*p*-hydroxyphenylalanine) to dihydroxyphenyl-L-alanine (L-DOPA) [1]. This biotransformation appears to be achieved by a tyrosinase present in cells of *Mucuna pruriens* [2] grown in-vitro. Analogously, the addition of the substrate *p*-hydroxyphenylacetic acid to the immobilized cells would be expected to produce 3,4-dihydroxyphenylacetic acid (DOPAA). The identity of the product can be confirmed by a suitable work-up procedure, followed by comparison of infrared, nuclear magnetic resonance and mass spectra with spectra of a reference compound. Product identification is also possible by extraction and derivatization, followed by gas chromatography/mass spectrometry (g.c./m.s.). Highly sensitive g.c./m.s. procedures have been reported for catecholamines and their metabolites [3, 4]; co-extracted by-products are detected if they contain functional groups that can be derivatized by the reagents used. Polar components in a

0003-2670/84/$03.00

mixture can conveniently be identified by liquid chromatography/mass spectrometry (l.c./m.s.). Derivatization is avoided, but sample work-up cannot be omitted, as it is doubtful if any l.c./m.s. system will tolerate the repeated injection of raw samples of a biotransformation medium. Reviews giving the principles and status of l.c./m.s. techniques have appeared [5].

For the work described here, a micro liquid chromatograph was combined with a chemical-ionization quadrupole mass spectrometer [6]. A simple capillary interface can couple the micro l.c. and the m.s., allowing introduction of the total l.c. effluent into the ion source [7—9]. The sensitivity is sufficient for taking full mass spectra of 10—50-ng samples injected onto the column. The capillary interface is simple and inexpensive, but has one serious disadvantage: experiments and calculations [10] have shown that eluent and sample are evaporated together inside the heated capillary so that non-volatile matter eluting from the column will block the interface. Phosphate buffers cannot be applied. A buffer solution made up of volatile components such as ammonium acetate, acetic acid and ammonia has to be used instead. The sample injected into the l.c./m.s. must also be free of salts, carbohydrates, proteins, etc. The present paper describes the necessary purification steps. This l.c./m.s. procedure not only offers convenient identification of compounds that have been observed by high-performance liquid chromatography (h.p.l.c.) with electrochemical and ultraviolet detection, but also establishes the presence or absence of impurities or products not observable by the other methods of detection mentioned.

EXPERIMENTAL

Plant cell culture and biotransformation of p*-hydroxyphenylacetic acid*

Cell suspension cultures originating from a *Mucuna pruriens* (L.) DC f. *utilis* (Wall ex. Wight) Back cultivar were grown as described by Huizing and Wichers [1]. After 7 days of subculturing, the cells were immobilized in calcium alginate, as described by Wichers et al. [11]; biocatalyst beads with a diameter of 3—4 mm were produced. These beads were washed twice for 10 min with the incubation medium omitting *p*-hydroxyphenylacetic acid. The final incubation medium consisted of an aqueous solution containing 25 mM barbital (sodium), 25 mM sodium acetate, 0.5% (w/v) calcium chloride dihydrate, 154 mM sodium chloride, and 2 mM *p*-hydroxyphenylacetic acid (Janssen Chimica, Beerse, Belgium) as substrate. The pH was adjusted to 6.00 with concentrated hydrochloric acid. After autoclaving for 20 min at 121°C, sodium ascorbate was added as an antioxidant at a final concentration of 5 mM.

In a bubble-jar with a working volume of 125 ml, 300 beads were incubated in 100 ml of incubation medium at 28°C at an air flow of 16 l h^{-1}, until the sodium ascorbate was oxidized as judged from the h.p.l.c. profiles obtained with the electrochemical detector (see below).

Routine determination of p-*hydroxyphenylacetic acid and its product during the biotransformation process*

Samples of the incubation medium from the bubble-jar were analyzed by h.p.l.c. on a 15 cm × 4.6 mm i.d. Nucleosil-5 C_{18} column (Macherey-Nagel, Düren, F.R.G.). The eluent consisted of McIlvaine buffer/methanol (90:10) adjusted to pH 4.70. The product (i.e., the expected DOPAA) and sodium ascorbate were determined with a graphite electrode detector [12]. *p*-Hydroxyphenylacetic acid was determined with a SF-770 Spectroflow monitor (Schoeffel Instrument, U.S.A.) at 280 nm in the absorption mode. The DOPAA used as reference compound was from Fluka (Buchs, Switzerland).

Product isolation by means of column chromatography

Preliminary purification on a Sephadex G-10 column. A 2-ml sample of the incubation medium was centrifuged for 8 min at 10 000 *g* in an Eppendorf-5415 centrifuge (Eppendorf Gerätebau, F.R.G.) and the clear supernatant liquid was applied to a Sephadex G-10 column (Pharmacia Fine Chemicals, Sweden) prepared in a long Pasteur pipette (bed volume 1.5 ml). Prior to use, the column was washed with 3.0 ml of 0.02 M ammonia and 3.0 ml of 0.01 M formic acid as described by Westerink and Mulder [13]. After the sample had passed through the column, the column was washed with 1.5 ml of 0.01 M formic acid. The expected DOPAA was collected by successive elution with 1.5 ml of 0.01 M formic acid and 2.5 ml of 0.005 M sodium dihydrogenphosphate.

Further purification by means of affinity chromatography on an Affigel-601 column [14]. The pH of the combined formic acid-phosphate fraction that eluted from the Sephadex G-10 column was adjusted to 6.00 with 0.7 M ammonia. The column for affinity chromatography was prepared by packing Affigel-601 (Bio-Rad) into a long Pasteur pipette (bed volume 1.5 ml). The column was equilibrated with water. The elution behaviour of electrolytes and carbohydrates, initially present in the sample, was monitored during flushing of the column with six 1.0-ml portions of water with the aid of a conductivity meter (Konduktometer CG 857, measuring cell with K = 1.04 cm^{-1}; Schott Geräte, F.R.G.), and with a routine sucrose/glucose/fructose assay (UV-tests 139106 and 15824; Boehringer Mannheim, F.R.G.). Barbital sodium was detected by means of the Parri reaction as described in the Dutch Pharmacopoeia (VI^2 edition). The product was eluted from the column with twelve 0.5-ml portions of 1 M acetic acid.

Elution was also monitored with a single-path UV-1 monitor (Pharmacia Fine Chemicals, Sweden). Substrate and product were quantified with the h.p.l.c. method described above. The most concentrated fraction of the product usually eluted after application of two 0.5 ml portions of 1 M acetic acid. This fraction was lyophilized and the product was redissolved in 1 M acetic acid to give a final concentration of approximately 250 $\mu g\ ml^{-1}$.

Liquid chromatography and mass spectrometry

The Jasco Familic 100-N micro l.c. system (Jasco, Japan) consisted of a micro feeder, a 0.5-ml glass syringe pump, a variable-wavelength u.v. detector equipped with a 0.3-μl micro cell and a 0.3-μl loop injector. The 20-cm long column was made of teflon tubing (2.0 mm o.d. × 0.5 mm i.d.) [15] packed at a pressure of 70 bar with Nucleosil-5 C_{18} reversed-phase material. The eluent system was 80% water, containing 0.1 M ammonium acetate and 0.1 M acetic acid, and 20% acetonitrile. The mixture was acidified to pH 4.70 with acetic acid. The flow rate was 5 μl min^{-1} during all experiments.

The mass spectrometer was a Finnigan 3300/6110 g.c./m.s./computer system, equipped with the standard chemical-ionization source and modified for negative ion operation [16]. The total effluent from the u.v. detector of the chromatograph was fed into the chemical-ionization source via a fused silica capillary tube (50 μm i.d.). The design and operation of the interface probe in which the capillary tube is contained have been described earlier [6, 10]. In its present version, the 6.4 mm o.d. stainless steel tube is water-cooled to prevent premature evaporation. The capillary is slid through the cooled probe shaft and protrudes so far through the heated copper block that it is just visible under a magnifying glass. The length of the copper block was increased from 5 mm in the original version [6, 10] to 20 mm in the present interface, because difficulties were expected in sustaining stable vaporization of the polar buffer system, which contains a high percentage of water.

The ion source pressure was measured with an MKS Baratron capacitance manometer (type 222 BHS; MKS Instruments, U.S.A.) capable of measurements between 0.001 and 10.000 mbar. It was mounted on a hollow direct insertion probe, slid into the mass spectrometer via an additional vacuum lock mounted on the source pumping line [17]. The original ion repeller plate was replaced by a plate equipped with a hole. The hollow probe shaft, which has an isolated tip, was slid against the modified repeller, making a gas-tight seal, and allowing pressure measurement independent of gas composition during l.c./m.s. experiments. An eluent flow of 5 μl min^{-1} gave a source pressure of 0.200 to 0.210 mbar. In the case of positive-ion chemical ionization, methane was introduced into the source via the solid probe solenoid valve up to a total pressure (l.c. + methane) of 0.35 mbar. Ammonia was then added up to a final pressure of 0.40 mbar.

In the case of negative-ion chemical ionization, methane was introduced up to a pressure reading of 0.385 mbar, followed by Freon-12 (difluorodichloromethane) up to a final pressure of 0.395 mbar. No corrections were made for the difference in temperature between the ion source (240°C) and the capacitance manometer (30°C).

The ion-source temperature is of decisive importance in l.c./m.s. with a vaporizing capillary interface. The source temperature was kept constant by means of a CRL-405 digital temperature controller (CRL, England) using the original Finnigan thermocouple as sensor. The sensor was removed from the

top of the ion source and clamped inside a hole drilled in the source block 4 mm away from the solid probe inlet port, into which the heat transferring copper block of the interface is inserted. The temperature read-out was calibrated against a platinum resistance thermometer inserted into the ion source via the solid probe inlet port. Positive-ion spectra were recorded from m/z 110 to 250, and negative-ion spectra from m/z 121 to 270. Spectra were taken by repetitive scanning at 6-s cycle time and 32-ms integration time. All spectra were stored on disk and retrieved for reconstruction of total ion current and extracted ion-current profiles [18].

RESULTS AND DISCUSSION

Isolation procedure

An example of a routine determination of substrate and product in a raw sample taken from the biotransformation medium is shown in Fig. 1. To obtain a sample suitable for introduction into the l.c./m.s., electrolytes and carbohydrates have to be removed. Samples from the biotransformation medium were subjected to two types of column chromatographic clean-up procedures. Prepurification was done on a Sephadex G-10 column; compounds with a molecular weight higher than 700 dalton are excluded from this gel. After the column had been washed with one volume of 1.5 ml of 0.01 M formic acid, any proteins present in the sample were found in the void volume, while low-molecular-weight compounds (including the expected DOPAA) were retained by the Sephadex G-10 gel. These compounds were eluted with 1.5 ml of 0.01 M formic acid followed by a 2.5 ml of 0.005 M sodium dihydrogenphosphate. The eluate contained the expected

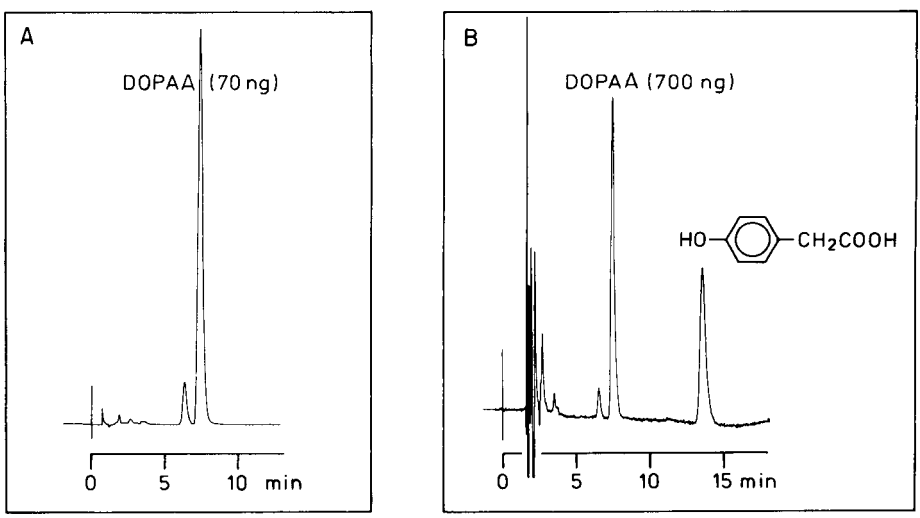

Fig. 1. Elution of *p*-hydroxyphenylacetic acid and DOPAA from a 15 cm × 4.6 mm i.d. reversed-phase h.p.l.c. column at a flow rate of 1 ml min^{-1}. (A) Electrochemical detection; (B) detection at 280 nm.

DOPAA, unreacted *p*-hydroxyphenylacetic acid and components from the incubation medium with a low-molecular-weight as judged from h.p.l.c. with the electrochemical and u.v. detector and from conductivity measurements.

For the isolation of a catechol compound, the eluate was passed through an Affigel-601 column. Affigel 601 is a cross-linked, beaded polyacrylamide gel with phenylboronic acid as the ligand. It displays a high capacity for binding low-molecular-weight compounds with coplanar *cis*-diol groups, including catechol compounds and certain carbohydrates. During these experiments, it became evident that sodium ascorbate competitively interfered with the binding of the expected DOPAA on Affigel 601. Catechol-type compounds are readily oxidized and an anti-oxidant such as sodium ascorbate had to be added to the biotransformation medium in order to prevent atmospheric and enzymatic oxidation. To avoid the interference of ascorbate on Affigel-601, the biotransformation process was continued until ascorbate was no longer detectable by h.p.l.c. with the electrochemical detector, because of its oxidation to dehydroascorbate in the bubble-jar. It was also very important that the highly acidic Sephadex G-10 eluate was adjusted to pH 6.00 before application to the affinity chromatographic column. After this eluate had been drained into the Affigel-601 bed, carbohydrates, electrolytes and unreacted *p*-hydroxyphenylacetic acid were removed from the column by washing with water.

During elution with 1 M acetic acid, the expected DOPAA was released from the column. The elution profile is shown in Fig. 2. According to the results obtained by h.p.l.c. with the electrochemical and u.v. detectors, and from the carbohydrate assay, the Parri reaction for barbital sodium and the conductivity measurements, which indicated the absence of these compounds, the expected DOPAA fraction appeared to be suitable for l.c./m.s.

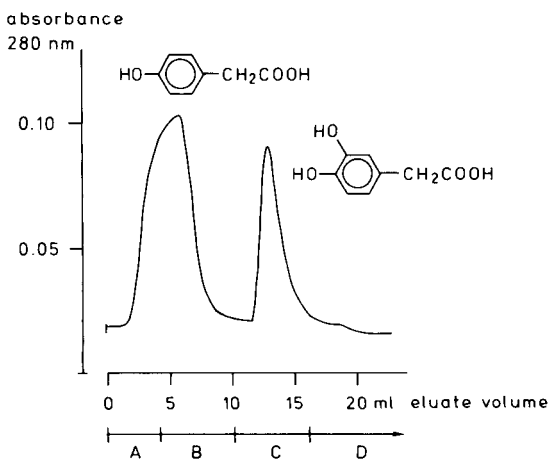

Fig. 2. Separation of *p*-hydroxyphenylacetic acid from DOPAA by affinity chromatography on Affigel-601. Eluate volumes: (A) sample, pH 6.0, 4.2 ml; (B) water, 6 ml; (C) 1 M acetic acid pH 2.4, 6 ml; (D) water.

Liquid chromatography/mass spectrometry

When the total effluent from the micro liquid chromatograph is introduced into the ion source, the evaporated solvents (ammonium acetate and acetic acid) can be used as the reactant gas mixture for chemical ionization. Clusters between ions and polar neutral molecules create a fairly strong background spectrum extending to m/z 143 in the positive-ion mode and up to m/z 148 in the negative-ion mode. In order to reduce the background level and make recording of full spectra below m/z 150 feasible, the reactant ion spectrum was modified by the addition of other reactant gases (methane, ammonia or Freon). The ion source of the Finnigan 3300 is designed for direct connection of a packed gas-chromatographic column to the ion source, allowing for the use of methane as the carrier gas at 20—30 ml min^{-1}. The source and its oil diffusion pump can therefore accept the effluent from the micro l.c. at 5 μl min^{-1}, which gives a source pressure of 0.20 mbar, together with additional reagent gases. Methane is supplied to provide a reducing agent, compensating for the oxidizing action of water on the rhenium electron emitting filament of the ion source, but does not contribute to the reactant ion spectra. In the positive-ion mode, NH_3 produced NH_4^+ ions and a cluster with acetonitrile. In the negative-ion mode, the addition of 2—3% difluorodichloromethane produced abundant chloride ions, partially clustered with acetic acid. Positive and negative reactant ion spectra are given in Fig. 3.

Ammonia is a stronger base than methane, water, acetonitrile and acetic acid [19] and finally accepts the proton transferred in ion-molecule reactions between the reactant gas components. Chloride ion is formed from difluorodichloromethane by dissociative electron capture. Its production apparently removes near-thermal electrons so efficiently from the source that water, acetonitrile and acetic acid are not ionized by electron-capture processes. Furthermore, chloride is such a weak base [20] that it will not abstract a proton from water, acetonitrile or acetic acid. The lowest background level in the mass region of interest was observed under negative-ion

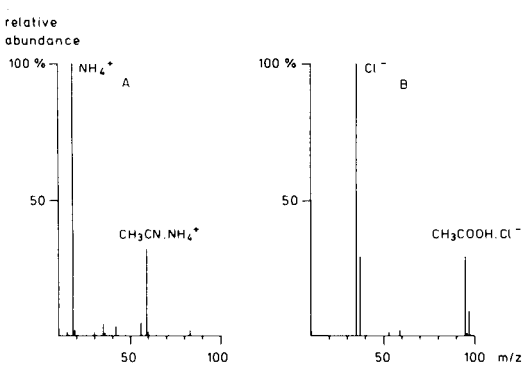

Fig. 3. Reactant ion spectra: (A) positive ions generated from l.c. eluate + CH_4 + NH_3; (B) negative ions generated from l.c. eluate + CH_4 + CF_2Cl_2.

chemical ionization conditions, resulting in a less noisy baseline in the total negative ion-current profile than in the liquid chromatogram recorded in the positive-ion mode.

Sample molecules containing hydroxyl groups and the carboxylic acid function are ionized by the following proton-transfer and clustering reactions [21, 22].

$$M + NH_4^+ \rightleftharpoons \begin{matrix} \rightarrow MH^+ + NH_3 \\ \rightsquigarrow M \cdot NH_4^+ \ (M + 18) \end{matrix}$$

$$M + Cl^- \rightleftharpoons \begin{matrix} \rightarrow [M{-}H]^- \\ \rightsquigarrow M \cdot Cl^- \ (M + 35/37) \end{matrix}$$

Stable and smooth evaporation of the l.c. effluent in a vaporizing interface becomes increasingly difficult at high water concentrations [9].

The proportion of 20% acetonitrile present in the l.c. eluent provided a chromatographic resolution which was far from optimal. The present study was aimed at an exploratory investigation of how l.c./m.s. can support biotechnology, rather than optimization of the techniques. Pushing the interface and mass spectrometer to the limits of performance by the use of more than 80% water was avoided.

The u.v. detector trace in Fig. 4 indicates the presence of minor contaminants eluting closely before and after the main component. The total ion-current profile in Fig. 4 reveals the presence of a sample component not observed by u.v. detection at 240, 260, 280 or 300 nm. The extracted ion-current profiles in Fig. 4 and the negative-ion mass spectrum in Fig. 5 present strong evidence that the major component isolated from the incubation medium is indeed DOPAA; this is further supported by the positive-ion spectrum in Fig. 5 and by comparison with data from authentic DOPAA. Ions observed in the negative- and positive-ion spectra of the unknown component were *m/z* 183/185 and *m/z* 166, respectively, corresponding to $M \cdot Cl^-$

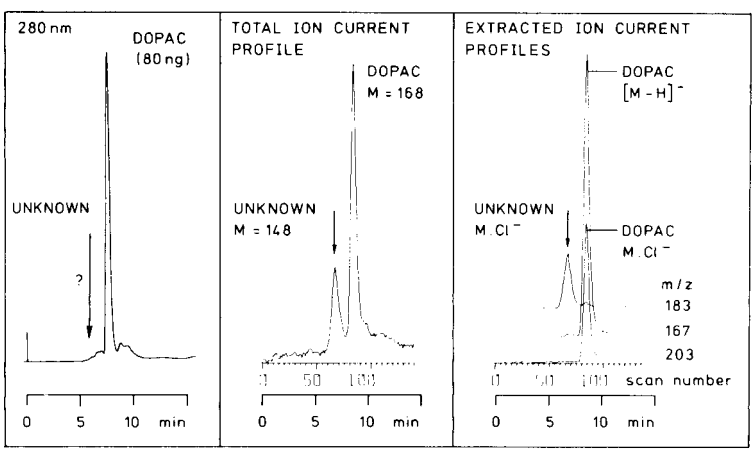

Fig. 4. Liquid chromatography/mass spectrometry of purified biotransformation product with the u.v. detector and mass spectrometer connected in series. Mass spectra recorded by negative-ion chemical ionization. Flow rate 5 μl min^{-1}.

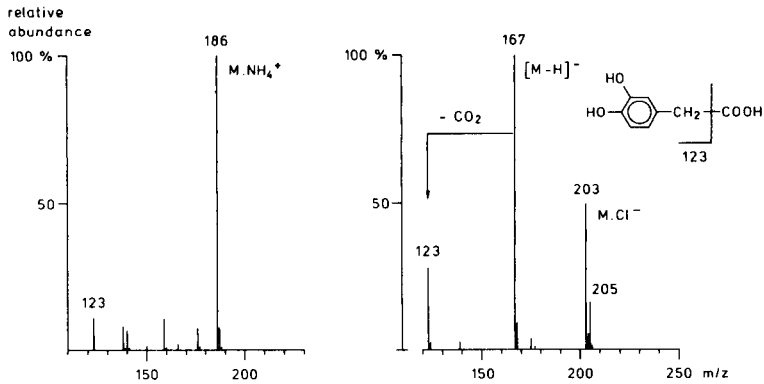

Fig. 5. Mass spectra of the major component in the liquid chromatogram of Fig. 4.

and $M \cdot NH_4^+$ of a compound with molecular weight 148, which has functional groups capable of clustering with NH_4^+ and Cl^-, but does not absorb u.v. light between 240 and 300 nm. At present, there is no clear relationship between this molecular weight and the components present in the incubation medium, based on simple oxidation and/or hydrolysis reactions. The compound might be an artifact introduced during the isolation procedure, or a substance excreted by the entrapped plant cells during the biotransformation process. The unknown compound is expected to be well separated from DOPAA under standard l.c. conditions, and to elute between 2 and 6 min. The chromatograms obtained after sample work-up did not reveal a component eluting within this period (Fig. 6). The minor impurity observed in Fig. 6 coeluted with DOPAA under the micro l.c. conditions used above; the mass spectrometer detected at least 3 contaminants at low percentage levels coeluting with DOPAA.

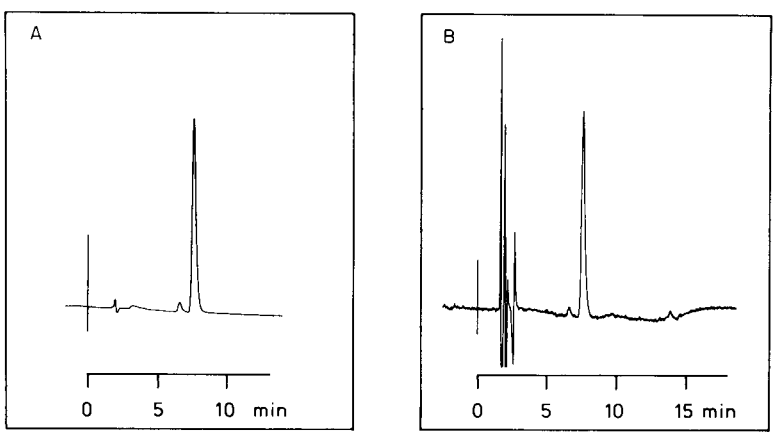

Fig. 6. Liquid chromatograms of the purified biotransformation product (DOPAA). Standard 15 cm × 4.6 mm column at a flow rate of 1 ml min^{-1}. (A) Electrochemical detection; (B) detection at 280 nm.

The authors thank H. J. Huizing and H. J. Wichers for advice on biotechnology, J. de Jonge for the construction of the l.c./m.s. interface and J. Duitsch for photography. Financial support from the "Van Leersumfonds" is gratefully acknowledged.

REFERENCES

1 H. J. Huizing and H. J. Wichers, in H. H. Houwink and R. R. van der Meer (Eds.), Biotechnological research in the Netherlands, Progress in Industrial Microbiology Series, Elsevier, Amsterdam, 20 (1984) 217.
2 H. J. Wichers, G. J. Peetsma, Th. M. Malingré and H. J. Huizing, Planta, in press.
3 F. A. J. Muskiet, C. G. Thomasson, A. M. Gerding, D. C. Fremouw-Ottevangers, G. T. Nagel and B. G. Wolthers, Clin. Chem., 25 (1979) 453.
4 J. T. Martin, J. D. Barchas and K. F. Faull, Anal. Chem., 54 (1982) 1806.
5 See, e.g., C. G. Edmonds, J. A. McCloskey and V. A. Edmonds, Biomed. Mass Spectrom., 10 (1983) 237.
6 A. P. Bruins and B. F. H. Drenth, Int. J. Mass Spectrom. Ion Phys., 46 (1983) 213.
7 S. Rottschaefer, L. B. Killmer, G. D. Roberts, R. J. Warren and J. E. Zarembo, 30th Pittsburg Conf. Anal. Chem. Appl. Spectrosc., Cleveland, OH, 1979, paper 019.
8 J. D. Henion and G. A. Maylin, Biomed. Mass Spectrom., 7 (1980) 115.
9 K. H. Schäfer and K. Levsen, J. Chromatogr., 206 (1981) 245.
10 A. P. Bruins and B. F. H. Drenth, J. Chromatogr., 271 (1983) 71.
11 H. J. Wichers, Th. M. Malingré and H. J. Huizing, Planta, 158 (1983) 482.
12 B. Oosterhuis, K. Brunt, B. H. C. Westerink and D. A. Doornbos, Anal. Chem., 52 (1982) 203.
13 B. H. C. Westerink and T. B. A. Mulder, J. Neurochem., 36 (1981) 1449.
14 S. Higa, T. Suzuki, A. Hayoshi, I. Tsuge and Y. Yamammura, Anal. Biochem., 77 (1977) 18.
15 D. Ishii, K. Asai, K. Hibi, T. Jonokuchi and M. Nagaya, J. Chromatogr., 144 (1977) 157.
16 A. P. Bruins, Biomed. Mass Spectrom., 10 (1983) 46.
17 J. A. G. Roach, A. J. Malatesta, J. A. Sphon, W. C. Brumley, D. Andrzejewski and P. A. Dreifuss, Int. J. Mass Spectrom. Ion Phys., 39 (1981) 151.
18 W. L. Budde and J. W. Eichelberger, J. Chromatogr., 134 (1977) 147.
19 R. Walder and J. L. Franklin, Int. J. Mass Spectrom. Ion Phys., 36 (1980) 85.
20 J. E. Bartmess, J. A. Scott and R. T. McIver, J. Am. Chem. Soc., 101 (1979) 6046.
21 T. Keough and A. J. DeStefano, Org. Mass Spectrom., 16 (1981) 527.
22 H. P. Tannenbaum, J. D. Roberts and R. C. Dougherty, Anal. Chem., 47 (1975) 49.

Analytica Chimica Acta, 163 (1984) 101—109
Elsevier Science Publishers B.V., Amsterdam — Printed in The Netherlands

ON-LINE ANALYSIS OF FERMENTATION MEDIA

W. J. SCHMIDT, H.-D. MEYER and K. SCHÜGERL*

Institut für Technische Chemie, Universität Hannover, D-3000 Hannover 1 (Federal Republic of Germany)

W. KUHLMANN

B. Braun Melsungen, D-3508 Melsungen (Federal Republic of Germany)

K.-H. BELLGARDT

Gesellschaft für Biotechnologische Forschung mbH, D-3300 Braunschweig (Federal Republic of Germany)

(Received 6th April 1984)

SUMMARY

A continuous on-line analysis system for components of the medium during the anaerobic and aerobic fermentation of glucose by *Saccharomyces cerevisiae* is described. The procedures used include: analysis of the outlet gas by conventional analyzers (CO_2, O_2) and a mass spectrometer; continuous sampling of the liquid phase with microfiltration and subsequent determination of phosphate and glucose (spectrophotometer), glucose (polarimeter) and ammonium ion (ion-sensitive sensor); and continuous separation of volatile components and dissolved gases with diffusion through a silicone rubber membrane in high vacuum and determination of mass (m/z = 18, 28, 31, 32, 40, 44) by means of a mass spectrometer. The system was tested on a batch reactor and a continuously operated three-stage cascade consisting of stirred tank reactors. This equipment was connected to a process computer. Glucose was quantified either polarimetrically or spectrophotometrically with *p*-hydroxybenzoic acid hydrazide; the latter was far more sensitive and was preferred to enzymatic methods, with which correlation was good. Only acetoin was found to interfere. Problems with operating a mass spectrometer for fermentation control in the exit stream and with membrane sampling are discussed.

In general, fermentation media are three-phase systems which are difficult to analyze. They are complex solutions of inorganic and organic substrates, physically dissolved gases and dispersed solids of different sizes, such as microorganisms or particles of cellulose. It is impossible to identify and determine all components; therefore measurements must be confined to the most important process variables. Continuous on-line determination of these components of the medium during fermentation is a prerequisite for effective process control. For this purpose, a computer-coupled real-time analytical system was developed and applied to the anaerobic and aerobic fermentation of glucose by *Saccharomyces cerevisiae*.

0003-2670/84/$03.00

ON-LINE ANALYZING SYSTEMS

It is important to prevent the culture medium from being contaminated, either by using sterilizable sensors or by applying membrane separation techniques for sterile sampling. Figure 1 shows a batch reactor (B. Braun Melsungen) and a cascade of three stirred-tank reactors for continuous operation (Institut für Technische Chemie). Sensors and instruments are implemented for measurement and control of the following parameters: temperature (Pt 100, Jones/Analogic AN 2576, measuring bridge); stirrer speed (agitation rate control, TRB 107, Stephan Werke); pH value (electrode 465, Ingold/pH control RV-PP, Bruetsch AG); aeration rate (mass flow meter, 5811/4250, Brooks); pressure (DMS pressure sensor G-F-9.53/ measuring bridge 9193, Burster); acid/base consumption (B. Braun Melsungen); antifoam agent consumption (B. Braun Melsungen); media feed rates (pumps FE 211, B. Braun Melsungen); and dissolved oxygen concentration (Clark electrode, Institut für Technische Chemie). Automatic analyzing systems were also included in the system.

This equipment was coupled to a Digital Equipment PDP 11/34 computer. The computer controls 12 magnetic valves, 2 motor valves and 2 relays for connecting the sampling lines from the four fermenters to the analyzing

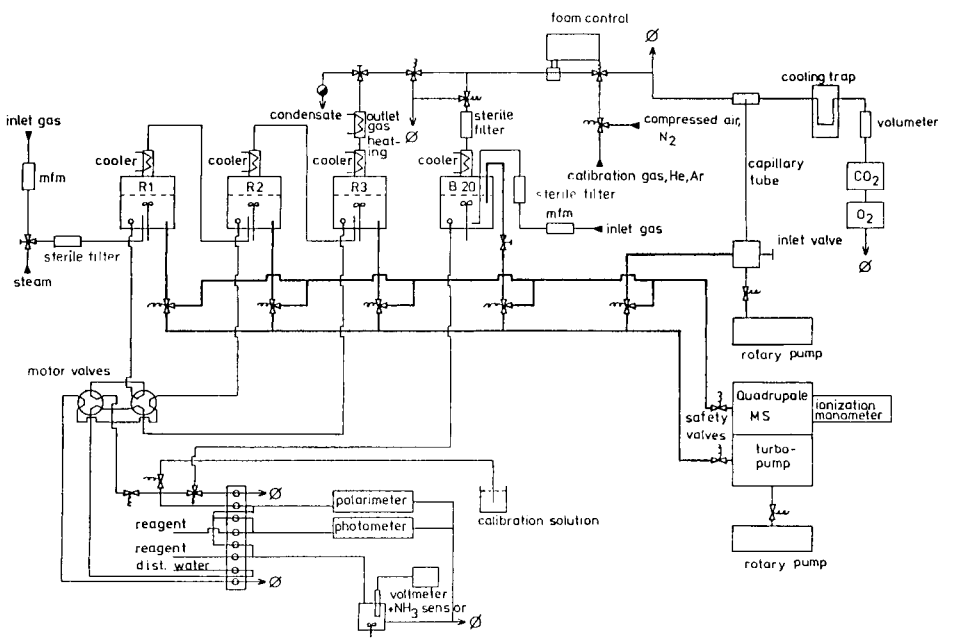

Fig. 1. Coupling of automatic analyzer, mass spectrometer and exhaust gas measurement to a batch fermenter and a 3-stage cascade.

systems. The response times (needed for reaching 98% of the equilibrium) for step input functions in concentration were: 5 min for the exhaust gas analyzers (air → nitrogen); maximally 13 min for the measurement of the liquid phase with the automatic analyzing system ($C_{PO_4^{3-}}$ = 0.72 g l^{-1} to 1.44 g l^{-1}; and 6 min for the measurement of volatile components and dissolved gases with the mass spectrometer (QMG 311, Balzers) ($C_{ethanol}$ = 0 to 6.3 g l^{-1}).

Analysis of exhaust gas

Carbon dioxide and oxygen concentrations in the exhaust gas were measured with an infrared analyzer (Unor 6, Maihak) and a paramagnetic analyzer (Oxygor 3, Maihak), respectively. Alternatively, the outlet gas was analyzed with a mass spectrometer equipped with a capillary inlet system. The instruments were protected by a glass fibre filter and an electrical conductivity foam detector in the exhaust gas line. For reliable measurements, residual water was removed from the sampling gas by cooling with a dry ice/methanol mixture.

Continuous aseptic sampling

Sampling of volatile components from the reactors for mass spectrometry was done with probes covered with silicone-rubber membranes. All the vacuum pipes connecting the probes to the mass spectrometer were evacuated simultaneously by the pumping system of the spectrometer. The pressure in the vacuum system was estimated with an ionization manometer (IMG 070, Balzers). Automatic closing of two safety valves at 10^{-5} mbar protected the cathode and the secondary electron multiplier from an increase in pressure by any chance leakage.

For continuous sampling of the liquid medium, a sterilizable filtration unit with a flat microfiltration membrane was developed. This unit was positioned close to the stirrer inside the fermenter to avoid mechanical fouling of the membrane. The filters were back-flushed periodically by a switching operation of two motor valves (Latec) which made long-term measurements in continuous fermentations possible. Nylon membranes with a pore diameter of 0.2 μm were found to be more suitable for this purpose, in terms of durability and flow rate of filtrate, than cellulose derivatives.

Determination of ammonium, glucose and phosphate

Continuous determination of ammonium, phosphate and glucose in the filtrate was done with automatic analyzer systems. For the measurement of ammonium ion with an ammonia-sensitive electrode (Philips IS-570), the medium was diluted with water and mixed with 1 M NaOH/0.025 EDTA as reagent. The calibration plots were linear over the range 20—2000 mg l^{-1} NH_3—N. The slope of the plots showed long-term stability. However, the lines drifted with time towards more positive potentials because of the

aging of the hydrophobic microporous teflon membrane. The regular recalibration of this unit was controlled by the process computer.

For glucose concentrations higher than 2 g l^{-1}, a 1-ml flow-through polarimeter cuvette (Perkin-Elmer 241) was used to measure the polarization angle at 365 nm. Below this concentration, the relative error was too high and the presence of other optically active compounds had a greater influence. Calibration lines are shown in Fig. 2. For the determination of orthophosphate, the medium was diluted with sulphuric acid, and the modified vanadomolybdate reagent of Gohla et al. [1] was added. The absorbance of the yellow vanadomolybdophosphoric acid was measured at 450 nm with a spectrophotometer (Beckman 24). The calibration plot was linear up to 1.5 g l^{-1} phosphate ($C = 1.404A - 0.0646$, where A is absorbance).

Determination of glucose with p-*hydroxybenzoic acid hydrazide*

Lower concentrations of sugars were determined by chemical reaction of glucose with *p*-hydroxybenzoic acid hydrazide (*p*-HBAH) as described by Lever [2] in slightly alkaline solution. The calibration line for the determination of glucose in the medium without a dilution step was linear up to 0.6 g l^{-1} glucose ($C = 0.369A - 0.011$). The measurement was carried out at 410 nm. The appropriate wavelength for the glucose or phosphate in the flow-through cuvette was set by a microprocessor. *p*-Hydroxybenzoic acid hydrazide is a selective reagent for reducing sugars with a sensitivity comparable to enzymatic methods. The *p*-HBAH method is cheaper than the

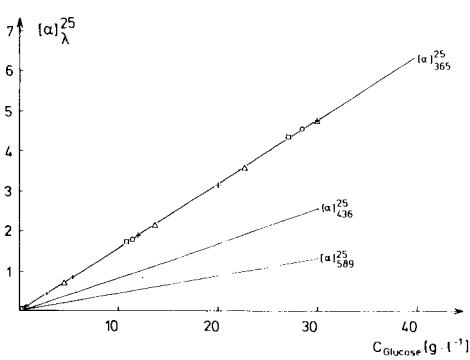

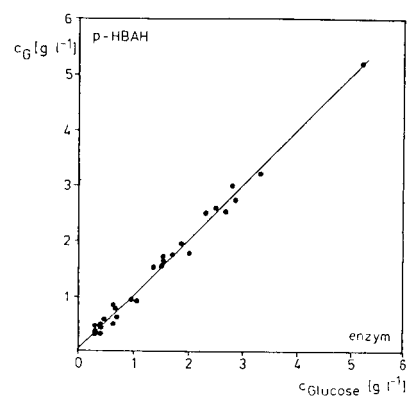

Fig. 2. Polarimetric calibration lines for D-glucose. Angle of rotation α^{25} at 25°C as a function of glucose concentration at different wavelengths: (△) pure glucose solution; (+) glucose in nutrient salt medium; (○) glucose in nutrient salt medium + 5% ethanol; (□) glucose in nutrient salt medium + 10% ethanol. For the $[\alpha]^{25}_{365}$ measurements, $C_{glucose} = 6.277\alpha$.

Fig. 3. Correlation of the glucose concentration measured enzymatically and with *p*-hydroxybenzoic acid hydrazide during the anaerobic fermentation of *Saccharomyces cerevisiae*.

enzymatic methods and is easier to handle. The influence of the matrix and of microbial products was determined. Several cross-sensitivities were eliminated by suitable adaptation of the method. Figure 3 shows the correlation between the glucose concentrations determined by the *p*-HBAH and enzymatic procedures during anaerobic fermentation of *Saccharomyces cerevisiae*. The most important co-reacting component was acetoin. In aerobic fermentations with *S. cerevisiae*, acetoin is produced in concentrations up to 1 g l^{-1}. In this case, an independent acetoin determination would be advantageous, e.g., determination with *p*-HBAH after enzymatic conversion of glucose with an immobilized glucose oxidase/catalase reactor.

MASS SPECTROMETRY

Various problems arise when a mass spectrometer is used for analyzing the outlet gas as well as dissolved gases and volatiles in the liquid phase. These problems include peak interference, nonlinearity of the measuring range, sensitivity changes of the secondary electron multiplier, and measurement of background signals during a fermentation. The tightness of the vacuum system is vital, especially for the measurement of small oxygen concentrations, and condensation effects in the vacuum tubings can influence the response time. Changes of the flow resistance in the capillary inlet and pressure fluctuations in the mass spectrometer also cause difficulties. Finally, alterations of the process variables in the fermenters cause changes in the ion currents.

Sampling in the reactors was done with the probe outlined in Fig. 4. A thin (100-μm) silicone rubber film (dipropylpolysiloxane) was prepared by spreading a silicone paste (Silopren paste E/AC-VP 3011, transparent, Bayer AG) over the metal support around a ceramic frit.

A quadruple mass spectrometer with a secondary electron multiplier was controlled by a data processor (QDP 101, Balzers). Thus, the measurement of the masses 18 (water), 28 (nitrogen), 31 (ethanol), 32 (oxygen), 40 (argon) and 44 (carbon dioxide) was possible at a frequency up to 1000 Hz. After subtraction of the background currents, the contribution of the fragments of ethanol and carbon dioxide to the representative signals of other components was taken into account. Figure 5 shows the linear relation between the ion currents and the pressure in the mass spectrometer for the pressure range between 10^{-7} and 10^{-6} mbar. Correction for the sensitivity of the secondary electron multiplier was possible by measuring a defined gas mixture in any opening position of the capillary inlet system. The background currents for every sampling membrane and the capillary inlet were measured by analyzing helium or argon as well as nitrogen of very high purity (99.999%). During continuous fermentation, the background currents were estimated in the same way, but for carbon dioxide it was necessary to stop feeding the medium into the reactors.

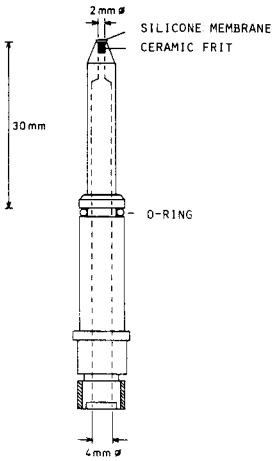

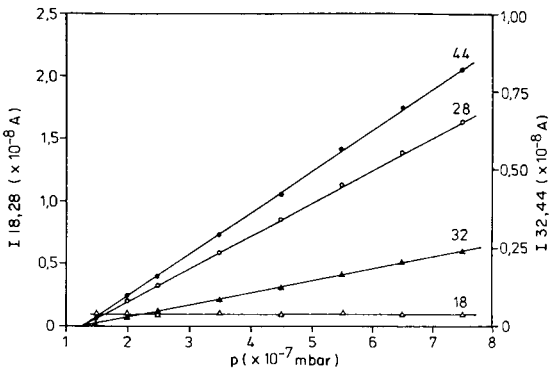

Fig. 4. Aseptic mass spectrometer sampling probe for dissolved gas and volatile components based on pervaporation.

Fig. 5. Dependence of the signals on the pressure in the mass spectrometer, measured by means of the capillary inlet system, from a gas mixture (78% N_2, 5% CO_2, 17% O_2).

A pressure less than 10^{-7} mbar could be obtained by using just one small turbomolecular pump rated at 100 l s^{-1} for the entire vacuum system. 10 KF flanges and valves (Herion) with viton gaskets instead of CF flanges and special vacuum valves were used for cheapness, the contribution of the background noise to the measured signal was about 90% in detecting an oxygen concentration of 0.1 mg l^{-1} for a membrane-covered probe. Condensation effects in the vacuum tubings increased the response time of the signals, especially for ethanol and water. Heating of the analyzer, the capillary and the membrane inlet tubing to a constant temperature of 105° C helped to avoid these effects to a large extent.

Quantifying the composition of the outlet gas with a mass spectrometer and capillary inlet system is widely used in monitoring fermentation processes. The major advantages of this system are that its response is very fast and there is no alteration in gas composition in the pressure-reducing system. Direct measurement of the total pressure is not possible because of the dependence of the pressure reading of the ionization manometer on the gas composition. In this way, changes of the ion currents caused by pressure fluctuations in the vacuum system were corrected by using nitrogen as an internal standard. Figure 6 shows the calibration lines for carbon dioxide and oxygen. The relation of the ion current of a gas to the ion current of nitrogen is proportional to the concentration of the component measured if the partial pressure of nitrogen is constant. In aerobic fermentations with $RQ \neq 1$, and especially in anaerobic fermentations, the altered partial pressure

of nitrogen must be taken into account. This is possible because the slopes of the calibration lines yield the relative sensitivities of the gases.

Application of the membrane-covered probe caused a change in gas composition. The permeability of the silicone-rubber membrane depends on the solubility and diffusivity of the volatiles in the silicone polymer. Mass transport in the evacuated tubings occurred in the molecular flow range. Therefore, calibration of every membrane-covered probe is necessary for every component.

Alterations of numerous process variables in the fermenters could change the signals measured with the mass spectrometer. Such variables include aeration rate, stirrer speed, pressure, temperature, pH value, glucose concentration, ethanol concentration, concentration of salts, concentration of cell mass, concentration of complex substrates like yeast extract, and concentration of antifoam agents.

Some results of investigations on the influence of process variables on ion currents as measuring signals for the partial pressures of volatiles can be summarized as follows. The stirrer speed influenced the measured signals; above 500 rpm, the peaks remained nearly constant but were decreased below 500 rpm for oxygen and carbon dioxide; the signals for ethanol and water were not affected down to 300 rpm. Obviously, the thickness of the liquid film is increased by less effective mixing. There was no influence of the aeration rate in the range of 0.1—1.0 $l\,l^{-1}\,h^{-1}$. Fluctuations of the signals caused by gas bubbles were observed only at agitation speeds less than 200 rpm and high aeration rates.

Figure 7 shows the signals of dissolved gases which increase with overpressure in the fermenter because of their solubilities. The overpressure is caused by the flow resistance of the exhaust gas sterile filter and can change

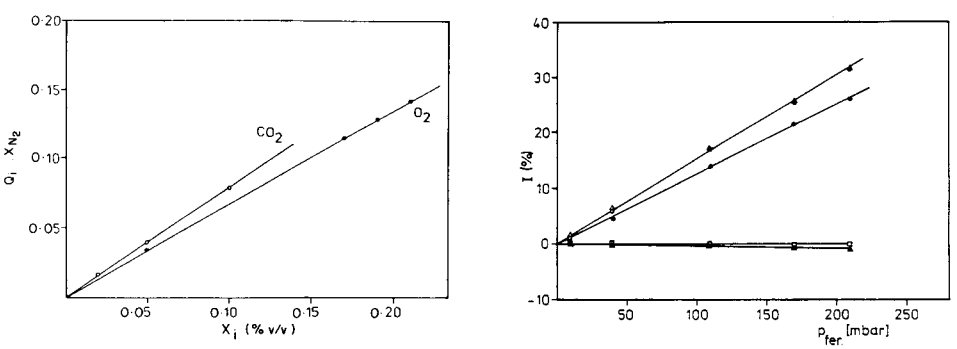

Fig. 6. Calibration lines for the measurement of the exhaust gas: signals of O_2 and CO_2 in relation to nitrogen, measured by means of calibration gases with different nitrogen concentrations. $Q_i = I_i/I_{N_2}$. $X_{N_2} = (1 + \Sigma Q_i/f_i)^{-1}$, where f_i is the slope.

Fig. 7. Dependence of the signals on the pressure in the fermenter, measured by means of the membrane probe. Gas mixture: 78% N_2, 5% CO_2, 17% O_2 with 4 g l^{-1} ethanol. Lines (△) O_2; (○) N_2; (●) CO_2; (□) ethanol; (▲) water.

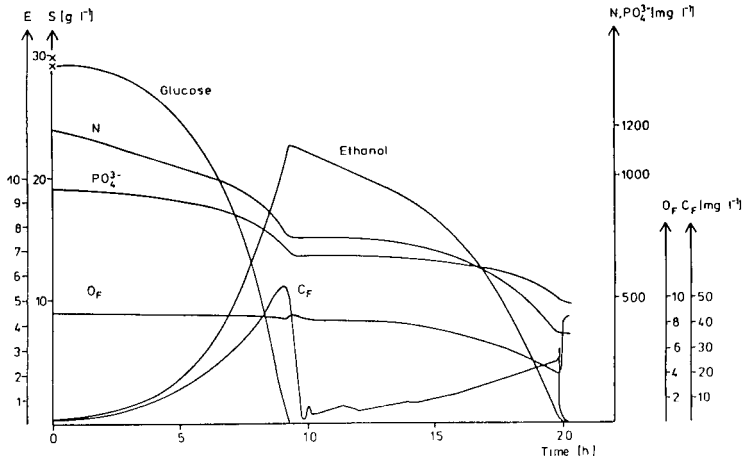

Fig. 8. Concentrations measured on-line during the growth of *Saccharomyces cerevisiae* on nutrient medium in batch operation: E, ethanol; S, glucose (g l^{-1}); N, nitrogen; PO_4^{3-}, orthophosphate; O_F, dissolved oxygen; C_F, dissolved CO_2 (mg l^{-1}).

during a fermentation. Altering the temperature in the reactor influences all measured signals, especially that of water and ethanol because their vapor pressure is strongly temperature-dependent. Any change in the partial pressure of a gas caused by an altered medium composition is mainly caused by gas solubility.

The influence on the signals of oxygen, nitrogen and carbon dioxide caused by different concentrations of glucose (measured in the range 0—470 g l^{-1}), some salts (0—0.4 mol l^{-1}), yeast extract (0—20 g l^{-1}) and ethanol (0—50 g l^{-1}) was investigated and compared with calculated gas solubilities [3, 4]. There was very good agreement between the measured signals and the solubility of oxygen changed by the glucose concentration [5]. Antifoam agent (Desmophen) at a concentration of about 0.01%, cell mass (dry weight 0—10 g l^{-1}) and pH values in the range 3—7 had no significant influence on the signals. The salting out of ethanol caused by salts and glucose, however, has a considerable influence. For fermentations of a 30 g l^{-1} glucose concentration, the changes in the concentrations of the gas solubilities were small. Hence, a mean value of the oxygen and carbon dioxide concentrations, estimated by Schumpe et al. [3] during a fermentation of this yeast, was used. The increase in the ethanol signal of about 3% through the nutrient medium Table 1 [6—8] was taken into account [6].

To give an impression of the efficiency of this analytical system, Fig. 8 shows on-line measured concentrations of process variables of a batch fermentation without monitored outlet gas.

TABLE 1

3% D-glucose nutrient medium for aerobic growth

Glucose · H_2O	33 g l^{-1}	$MnSO_4 \cdot H_2O$	10.5 mg l^{-1}
$(NH_4)_2SO_4$	4.5 g l^{-1}	$CuSO_4 \cdot 5H_2O$	2.4 mg l^{-1}
$(NH_4)_2HPO_4$	1.44 g l^{-1}	*m*-Inositol	60 mg l^{-1}
KCl	0.9 g l^{-1}	Ca-pantothenate	30 mg l^{-1}
$MgSO_4 \cdot 7H_2O$	0.339 g l^{-1}	Thiamine · HCl	6 mg l^{-1}
$CaCl_2 \cdot 2H_2O$	0.42 g l^{-1}	Pyridoxol · HCl	1.5 mg l^{-1}
$FeCl_3 \cdot 6H_2O$	15 mg l^{-1}	Biotine	0.03 mg l^{-1}
$ZnSO_4 \cdot 7H_2O$	9 mg l^{-1}		

REFERENCES

1 W. Gohla, H. D. Nielen and G. Sorbe, GIT Fachz. Lab., 23, 2 (1979) 89.
2 M. Lever, Anal. Biochem., 47 (1972) 273.
3 A. Schumpe, G. Quicker and W.-D. Deckwer, Adv. Biochem. Eng., 24 (1982) 1.
4 Solubility Data Series, Vols. 7 (1981), 10 (1982), Pergamon Press, Oxford.
5 M. Popović, H. Niebelschütz and U. Reuß, Eur. J. Appl. Microbiol. Biotechnol., 8 (1979) 1.
6 W. Kuhlmann, Diss. Universität Hannover, 1983.
7 H. P. Knoepfel, Diss. Nr. 4906, ETH Zürich, 1972.
8 H. Schatzmann, Diss. Nr. 5504, ETH Zürich, 1975.

Analytica Chimica Acta, 163 (1984) 111—118
Elsevier Science Publishers B.V., Amsterdam — Printed in The Netherlands

MEASUREMENT OF BIOLOGICAL PARAMETERS DURING FERMENTATION PROCESSES

T. SCHEPER, A. GEBAUER, A. SAUERBREI, A. NIEHOFF and K. SCHÜGERL*
Institut für Technische Chemie, Universität Hannover, Callinstr. 3, 3000 Hannover (Federal Republic of Germany)

(Received 6th April 1984)

SUMMARY

Efficient fermentation control requires the measurement of biological parameters. Three techniques were tested for monitoring. In the first, the NADH-fluorescence of micro-organisms was measured in batch and in continuous cultures under aerobic and anaerobic conditions, providing information on the metabolic status of the cells. The effects of cell concentration and of different substrates (glucose, ethanol and oxygen) were studied. The second technique is the calorimetric determination of various substrates, such as penicillin or enzymes, by an enzyme/thermistor device. With immobilized penicillin acylase (E.C. 3.5.1.11) or penicillinase (E.C. 3.5.2.6), penicillin was determined selectively in a fermentation broth. The thermistor was also used to measure penicillin acylase activity. The third technique is laser flow cytometry. A commercial double-beam flow cytometry system was used to determine cell size, light scattering and the protein, DNA and RNA contents of single cells. Flow cytometry allows rapid and sensitive control of fermentation processes with genetically modified *E. coli* 5K (pHM12) cells. The results of monitoring the cell size, light scattering, and protein and DNA contents of different micro-organisms during fermentation are outlined.

The measurement of biological parameters that describe the actual situation in the fermentor is important for effective and efficient fermentation control. Three different methods of getting additional biological information for more extensive research on such control are discussed here.

MONITORING OF CULTURE FLUORESCENCE

Monitoring of the fluorescence of micro-organisms, especially NADH-dependent fluorescence, can be very useful. A suitable fluorimetric probe was developed by Beyeler et al. [1]: a low-pressure mercury lamp serves as u.v. source and a special system of filters and lenses focuses the excitation wavelength of 365 nm for NADH fluorescence on quartz fibers, which guide the excitation light into the bioreactor. The emission at 460 nm passes normal glass fibers, which are mixed with the quartz fibers. The fluorescent light is filtered for 460 nm and detected by a photodiode. The intensity of the u.v. source is controlled by a second photodiode directly in front of the source. The fibre optics are valuable for reaching and monitoring all parts of

0003-2670/84/$03.00

the fermenter without problems of radiation intensity. This probe was tested for quinine, which has nearly the same fluorescence properties as NADH; the response was linear up to concentrations of about 500 $\mu g\ l^{-1}$. The response of open-ended detectors to the quinine concentration is always hyperbolic [2].

Fluorescence monitoring of aerobic fermentations of *Saccharomyces cerevisiae* and *E. coli* was studied. During the growth of *S. cerevisiae* on glucose the fluorescence signal increased steadily; when the glucose was consumed completely, the yeast started to grow on ethanol, and the culture fluorescence changed in a typical way. Later, the signal increased again until all substrate had been consumed, at which point the fluorescence decreased instantly. A single addition of glucose during the growth on ethanol was accompanied by increased fluorescence. A typical fluorescence output from an *E. coli* batch fermentation is shown in Fig. 1. Again, it is obvious that the fluorescence is a function of biomass concentration. When the oxygen supply is turned off, the aerobic—anaerobic transition is indicated by increased fluorescence below 3.5% dissolved oxygen. When aeration is turned on again, the signal decreases instantly.

Some effects of culture fluorescence in continuous fermentation of *S. cerevisiae* with cross-flow microfiltration may be used for reactor control. For example, an increase in glucose concentration is followed by a decrease in NADH fluorescence; this suggests that NADH-consuming steps (e.g., respiration or ethanol production) are proceeding more quickly than NADH-producing glucose degradation. The signal will also show a short period of

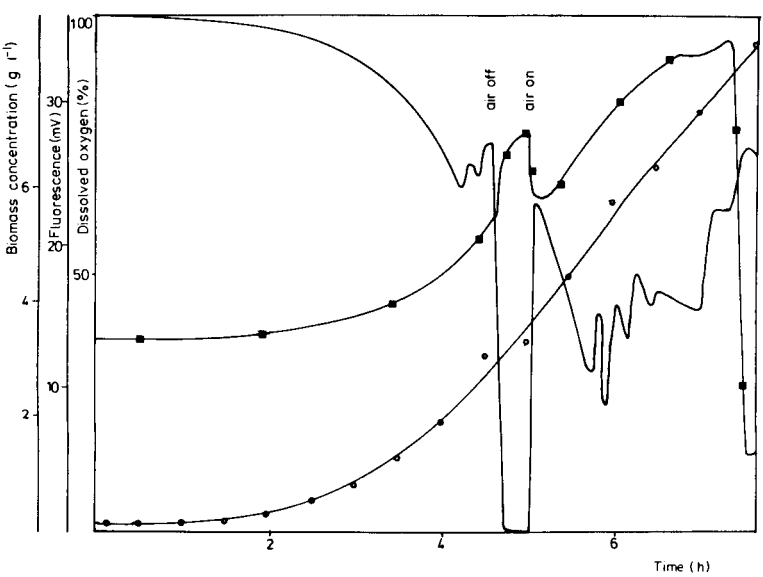

Fig. 1. Culture fluorescence during an aerobic batch fermentation of *E. coli* (complex medium). (—) Dissolved oxygen; (■) fluorescence; (●) biomass.

overoxidation of NADH; a brief interruption in the glucose feed is accompanied by an abrupt increase in the fluorescence signal. As there is no time lag with this sensor, any defects in the substrate feed can be detected very quickly and corrected. The fluorescence signal can also be used to monitor the dilution rate.

Biomass concentration (X) can be calculated from culture fluorescence data by means of the equation $X = [\exp(-b)I_{net}]^{1/a}$ [3], where I is the net fluorescence intensity and a and b are obtained from a fermentation by plotting ln X vs. ln I_{net}. These parameters of all organisms were used to calculate the biomass concentrations for the other fermentations. Calculated and measured data of several fermentations showed good agreement during the first exponential growth; deviations up to 15% occur during the change of the metabolism from the growth on glucose to the growth on ethanol, or when glucose is added to starved cells. However, the parameters a and b are only valid for one type of reactor; the parameters obtained for a stirred tank reactor cannot be used for biomass calculation in a bubble column. Obviously, a biomass estimation from the fluorescence is suitable only for routine fermentation, i.e., when all conditions are the same as during the calibration fermentation.

Not only NADH-dependent fluorescence is of interest, but also the fluorescence of other metabolites, and the mixing time behavior in the reactor. A fluorescence probe for simultaneous monitoring of NADH and tetracycline fluorescence with one excitation wavelength is under development. It is useful for mixing-time experiments in a bubble column with an external loop; increasing flow in the loop changes the mixing behavior and, if the flow rates are high, up to four recirculations of quinine tracer can be observed.

The monitoring of culture fluorescence is useful for obtaining information on the metabolic status of the cells. The effect of different substrates (e.g., glucose, ethanol and oxygen) and the influence of cell concentration on the redox status of the microorganisms can be studied [4, 5]. A fluorimeter can also be used for the detection of other fluorophores, such as tetracycline, and for studying the mixing behavior in reactors [6].

THE ENZYME THERMISTOR

The second method for the measurement of biological parameters is the calorimetric detection of various substrates or enzymes by an enzyme thermistor. A suitable design has been described by Danielsson et al. [7]. Two small plastic columns are used, one containing the immobilized enzyme and the other (reference) containing the support material; these columns are surrounded by a thermostated aluminium block. Small thermistors are placed on top of the columns. Buffer solution is pumped through each column separately after passing a heat-exchange coil and the sample is injected into each stream. The differential temperature signal represents

the calorimetric effect of the enzymatic reaction. Many substances can be determined in this way [8].

This thermistor device was recently modified for the determination of penicillin in fermentation broth and for the detection of penicillin-G-acylase (E.C. 3.5.1.11) in bacterial cells. Calibration graphs for penicillin-G with immobilized penicillinase (E.C. 3.5.2.6) in 0.05 M phosphate buffer, pH 7.5, and with the more selective penicillin-G-acylase in 0.1 M Tris buffer, pH 8.0, were linear up to 450 and 100 mmol l^{-1} penicillin-G, respectively, when peak areas were plotted. The enzymes were immobilized with glutaraldehyde on controlled pore glass beads.

Simple modifications make the thermistor device useful for the detection of enzyme activity. Substrate and buffer solutions are pumped continuously through a nylon tube located inside the column; 0.5 ml of the enzyme solution is injected into the buffer stream, where it reacts with the substrate inside the tube. The thermal effects are monitored. Different modifications of the column with regard to mixing behavior and residence time were tested; the use of nylon tube gave the best results, i.e., the highest thermal effects and the best reproducibility. The calibration curve of penicillin-G-acylase from *E. coli* 5K (pHM12) [9] was linear over the range 10–60 U ml^{-1}. No reference column was used in these tests, hence the curve did not terminate at the origin. The substrate solution was 0.1 M penicillin in 0.2 M phosphate buffer pH 7.5. A sample was injected every 10 min. The method is suitable for following the pH dependence of enzyme activity.

These methods could be improved by better arrangement of the thermistor device for faster throughput, and by using a reference column. However, the enzyme/thermistor devices are valuable for biotechnological analysis: several substrates can be determined with immobilized enzymes and the enzyme activity of bacterial penicillin-G-acylase can be measured. The latter method might be used for the control and monitoring of fermentations of *E. coli* cells producing this acylase.

LASER FLOW CYTOMETRY

The laser flow cytometry system was developed by the Gesellschaft für Strahlenund Umweltforschung, and the cytometer is commercially available (Parthograph FMP; Kratel, Germany). The system allows the simultaneous optical measurement of cell size, light scattering of particles, absorption and two-wavelength fluorescence. Figure 2 shows the principles of the flow cytometer. The cells are orientated and aligned in the laminar flow stream by hydrodynamic focussing. Sheath 1 surrounds the sample stream and is focussed by a capillary. One cell after another leaves the capillary orientated with its longest axis in the direction of the flow. An outer sheath is added to match the optical conditions of the plane observation windows. The laser beam is perpendicular to the flow and is focussed to a spot of some micrometers. The diameter of the focus can be varied by changing the optical

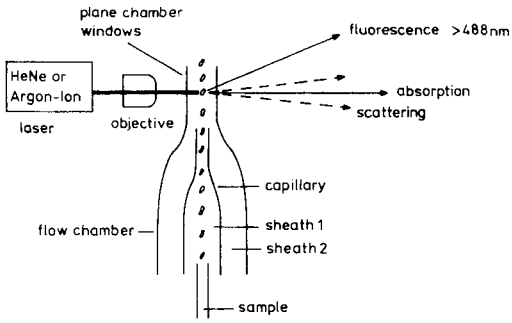

Fig. 2. Principles of laser flow cytometry.

arrangement. For cell-size measurements, the beam diameter should always be smaller than the cells; cells can be measured in the size range 2—200 μm, and processing rates up to 100 000 cells per second are possible. To extend the size range to below 2 μm, scattered light is a parameter, and smaller particles like *E. coli* can be measured. The absorption and the light-scattering are detected by photodiodes. Stained cells are stimulated for fluorescence by the 30-mW argon ion laser. The resulting fluorescence signal is split by a dichroic mirror and red and green fluorescence is detected by two photomultiplier tubes. Before the cytometry, the cells are stained with fluorochromes which bind to or associate with specific components in the cells, e.g., protein, DNA or RNA. The signals, derived from the photodiodes and the photomultiplier tubes, are evaluated for pulse width, pulse height and pulse integral. These data are converted to signals, the pulse heights being proportional to the measured value. The signals are converted, stored, displayed and processed by a microcomputer system.

Figure 3 presents some results from the size-measurements of different micro-organisms. Figure 3(a) shows the size distribution of a mixture of different latex beads 1.28, 2.02 and 4.18 μm in diameter; the particles were measured individually by the absorption signals and every peak corresponds to particles of a certain size. The latex beads can be used for the calibration of the system. Figure 3(b—d) shows the plots of cell size distributions of an established cell line of lepidoptera (*Spodoptera frugiperda*) at times of 0, 24 and 72 h. At the beginning of the fermentation, few cells and much cell debris are in the broth, but after 24 h the cell peak increases and broadens; during the next 72 h, the peak becomes smaller. The standard deviation is about 9% at that point. Only a little cell debris is left in the fermentation broth. Figure 3(e—g) shows some size measurements of yeast cells at the start of fermentation (e) and during batch growth on glucose (f) and ethanol (g). The cells seem to become larger during fermentation. While the ethanol is consumed, the cells decrease again slowly (the right-hand peak becomes lower).

The size analysis of plasmid-containing cells is interesting. The above-

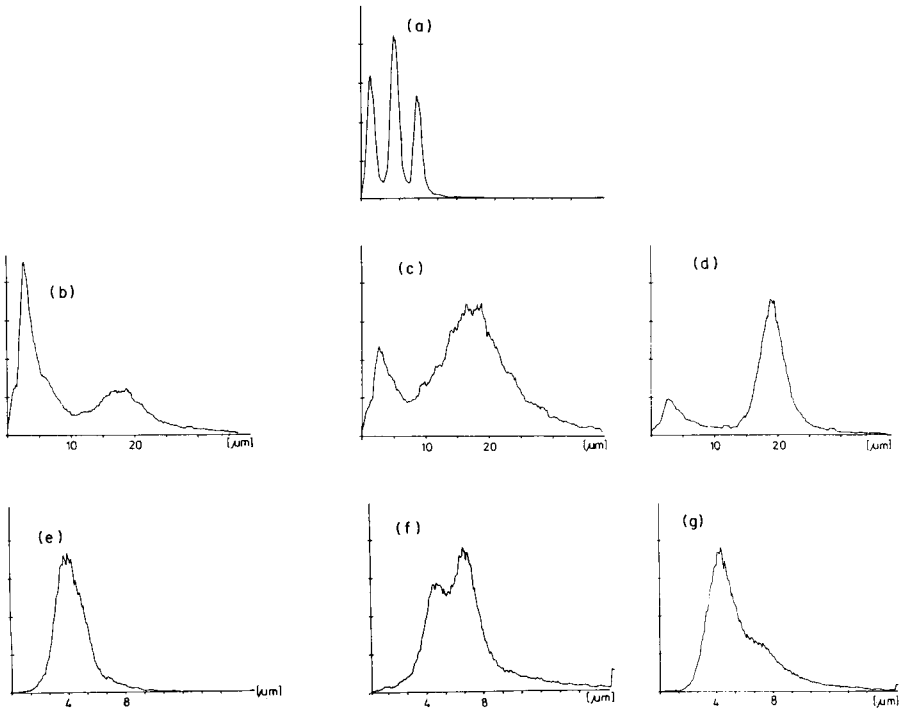

Fig. 3. Cell size measurements. For detail, see text.

mentioned strain of *E. coli* produces large amounts of penicillin-G-acylase. By the addition of β-lactam antibiotics (e.g., penicillin-G) to *E. coli*, cells elongate because the antibiotics interfere with the cell wall septum formation [10]. Plasmid-containing cells will not elongate in media containing penicillin-G because the enzyme hydrolyzes the antibiotic. Figure 4 (upper part) shows the results of adding penicillin-G to the fermentation medium at the beginning of exponential growth; the left-hand peak represents plasmid-carrying cells, and the right-hand peak plasmid-free cells 90 min after the penicillin addition. The light-scattering measurements indicate the elongation of the cells. This may be a method for fermentation control of plamid-containing cells, because information on the distribution of plasmid-containing and plasmid-free cells can be obtained [11].

Dual-parameter plots are shown in the lower part of Fig. 4. Plasmid-containing *E. coli* cells were withdrawn from the culture during exponential growth and were stained with fluorecein isothiocyanate (FITC), a protein-specific dye, after fixation in ethanol [12]. Protein-associated fluorescence and scattered light were measured simultaneously. The scattered light and the FITC fluorescence are nearly proportional. Considering that scattered light is a function of cell size, these results suggest that cell size and the protein content of *E. coli* cells are proportional.

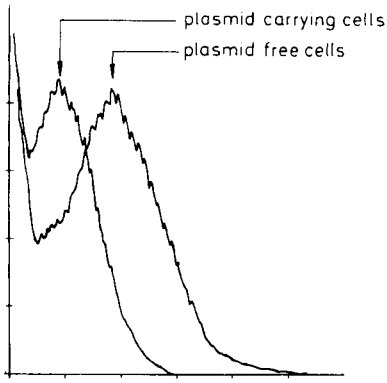

Light scattering measurement of plasmid free and plasmid containing cells (90 min after penicillin addition to the medium)

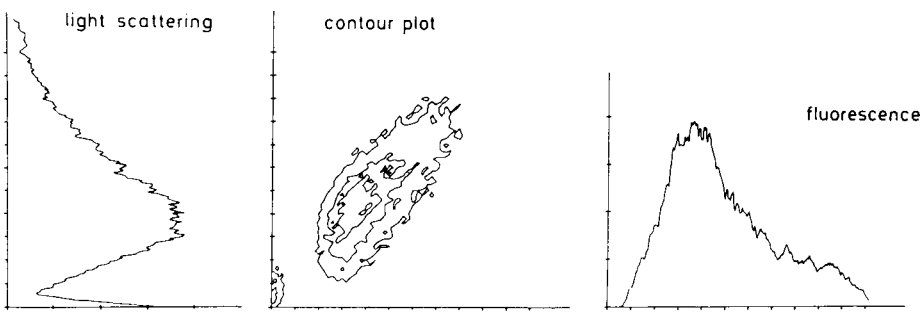

Fig. 4. Light scattering and fluorescence measurements of plasmid-carrying *E. coli* cells. The upper part shows light-scattering measurements 90 min after addition of penicillin-G. For further detail, see text.

The DNA and protein contents are useful parameters for studying the characteristics of cells during fermentation. Some work was done on a batch fermentation of *S. cerevisiae*. During growth of the cells on glucose, the protein content increased, but when the second growth phase on ethanol began, the protein content decreased. These data correspond to other FMF studies on the protein content of *S. cerevisiae* [13]. For the DNA measurements the cells were stained with propidium iodide, which stains double-stranded nucleic acid, i.e., all RNA (60—70% of the rRNA in *S. cerevisiae* is double-stranded [14]) has to be destroyed by RNAse. Apart from the background fluorescence, two peaks were observed after 4 h of growth on glucose, but after 10 h, only a single large peak represented the DNA content of the cells, even during the second growth phase on ethanol. No significantly different cell cycle features were observed, as reported by Agar and Bailey for *S. pombe* [15]. Optimization of this method is now in progress, but the results outlined here indicate the wide range of possibilities of cytometry for biotechnology research.

The authors gratefully acknowledge the assistance of M. Weiß, Dr. H. Mayer and Dipl.-Chem. U. Eberhard.

REFERENCES

1 W. Beyeler, A. Einsele and A. Fiechter, J. Appl. Microbiol. Biotechnol., 13 (1981) 10.
2 S. Udenfried, Fluorescence Assay in Biology and Medicine, Academic Press, New York, 1962.
3 D. W. Zabrisky, Biotechnology and Bioengineering (Symp. No. 9), (1979) 117.
4 D. L. Ristroph, C. M. Watteew, W. B. Armigo and A. E. Humphrey, J. Ferm. Technol., 55 (1977) 599.
5 A. Einsele, D. L. Ristroph and A. F. Humphrey, Eur. J. Appl. Microbiol. Biotechnol., 6 (1979) 335.
6 W. Beyeler, K. Geschwend and A. Fiechter, Chem. Ing. Tech., 55 (1983) Nr. 5, 869.
7 B. Danielsson, L. Buelow, C. R. Lowe, J. Satoh and K. Mosbach, Anal. Biochem., 117 (1981) 84.
8 K. Mosbach and B. Danielsson, Anal. Chem., 53 (1981) 83A.
9 H. Mayer, J. Collins and F. Wagner, Enzyme Engineering, Vol. 5, Plenum Press, New York, 1980, p. 61.
10 D. Greenwood and F. O'Grady, J. Infect. Dis., 128 (1973) 791.
11 K. Dennis, F. Srienc and J. E. Bailey, Biotechnol. Bioeng., 25 (1983) 2485.
12 E. Boyce, M. B. Steen and K. Skarstad, J. Microbiol., 129 (1983) 973.
13 M. F. Gilbert, D. N. McQuitty and J. E. Bailey, App. Env. Microbiol., (1978) 615.
14 C. Gatti and E. Fredericq, Arch. Int. Physiol. Biochem., 83 (1974) 772.
15 D. W. Agar and J. E. Bailey, Cytometry, Vol. 3, No. 2 (1982) 123.

Analytica Chimica Acta, 163 (1984) 119—125
Elsevier Science Publishers B.V., Amsterdam — Printed in The Netherlands

MONITORING THE PRODUCTION OF BIOSYNTHETIC HUMAN GROWTH HORMONE BY MICRO ENZYME-LINKED IMMUNOSORBENT ASSAY

BO DINESEN* and HENRIK DALBØGE ANDERSEN
Nordisk Gentofte, Niels Steensensvej 1, DK-2820 Gentofte (Denmark)
(Received 2nd April 1984)

SUMMARY

A micro enzyme-linked immunosorbent assay (e.l.i.s.a.) has been developed for monitoring the production of human growth hormone (hGH) in *E. coli*. The method is unusually flexible, as it is possible to modify its conditions to give a sensitive (detection limit 4 ng l^{-1}) or a fast (6 h) version. The assay is reproducible; the between-assay relative standard deviation is 6%. The effects of temperature, incubation time and the concentrations of protein and the most important reagents (the solid-phase antibody and the labelled antibody) are described. The utility of the method is demonstrated in experiments optimizing the conditions for production of hGH in *E. coli*.

The development of a method for production of human growth hormone (hGH) from genetically engineered *E. coli* requires flexible monitoring of products. In some experiments, there is a demand for a quick analysis; in others, the demand is for screening hundreds of clones for hGH production. Because the medium for growing micro-organisms may not always be suitable for immunoassay, sensitivity is needed so that the samples can be diluted. Micro enzyme-linked immunosorbent assay (micro-e.l.i.s.a.) meets these demands. A micro-test plate is used as the solid phase; 96 samples are kept in an area 9 × 13 cm, which gives high capacity and makes the method appropriate for screening purposes. Speed and sensitivity result from using high-affinity antibodies in the stable reagents, which are the solid-phase antibody and the peroxidase-labelled $F_{ab'}$-fragment of anti-hGH.

The e.l.i.s.a. method consists of four steps: coating the micro-test plate with anti-hGH, antigen incubation, incubation with peroxidase-labelled antibody, and enzyme activity measurement. The individual steps are separated by washing steps.

EXPERIMENTAL

Materials

The lysozyme buffer is 50 mmol l^{-1} Tris—HCl buffer containing 50 mmol l^{-1} EDTA, 15% sucrose, 0.03% sarcosyl and 1 mg ml^{-1} lysozyme, pH 8.0. The DNase buffer is 150 mmol l^{-1} Tris—HCl buffer containing 280 mmol l^{-1} mag-

0003-2670/84/$03.00

nesium chloride, 4 mmol l^{-1} calcium chloride and 66 μg ml^{-1} DNase-I, pH 8.0. The coating buffer is sodium carbonate buffer (100 mmol l^{-1}, pH 9.8). The antigen incubation buffer is sodium phosphate buffer (40 mmol l^{-1}) containing 0.1 M sodium chloride, 0.5% human serum albumin (Hoechst, "Trocken, reinst"), 0.05% Tween-20 and 0.024% thiomersal, pH 7.4. The labelled antibody incubation buffer is the same as for the antigen incubation buffer but without thiomersal. The washing solution is 0.9% sodium chloride, 0.05% Tween-20. The substrate buffer is 34 mmol l^{-1} citric acid, 66 mmol l^{-1} disodium hydrogenphosphate, pH 5.0 (all % values are w/v).

Peroxidase was ex horseradish (Worthington, code 6498). Sarcosyl, DNase-I, isopropyl-β-D-thiogalactoside (IPTG) and *o*-phenylenediamine (OPD) were from Sigma. Ultrogel ACA-34 and -44 were from LKB. All other chemicals were of analytical grade.

For the enzyme substrate, 40 mg of OPD was dissolved in 25 ml of substrate buffer and kept in the dark until the addition of 15 μl of 30% hydrogen peroxide immediately before use. Anti-hGH were raised in guinea pigs against pituitary hGH by Henny Bang Jakobsen (Nordisk Gentofte). The standard used was Nanormon, batch 0617, Nordisk Gentofte (pituitary hGH). Methionine-hGH in *E. coli* lysate was used as the control material, and Nunc Immunoplate-I (code 239454; Nunc, Denmark) was used as the solid phase.

The washing equipment and 8-channel pipettes were from Organon Teknika (Holland). The spectrophotometer was an SLT 210 (Kontron; Switzerland).

Methods

Preparation of coating antibody. The IgG fraction of a guinea pig anti-hGH antiserum (GP 16-20) was prepared by binding to and elution from Protein A-Sepharose (Pharmacia; Sweden).

Preparation of peroxidase-labelled antibody. The IgG fraction of a guinea pig anti-hGH antiserum (GP 2-7) was prepared as above. This IgG was either peroxidase-labelled directly by the periodate method [1] or fragmented into monovalent $F_{ab'}$-fragments, which were peroxidase-labelled by the "maleimide method I" of Ishikawa et al. [2]. Both peroxidase anti-hGH conjugates were separated from free peroxidase by size-exclusion chromatography on Ultrogel ACA-34 (IgG-conjugate) or ACA-44 ($F_{ab'}$-conjugate). The column was 2.6 cm i.d. and 92 cm long. The conjugates were stored at −20°C without further treatment.

Preparation of samples. The bacteria from 100 μl of bacterial culture were collected by centrifugation and the pellet was resuspended in 85 μl of lysozyme buffer. After lysis for 30 min on ice, 15 μl of DNase buffer was added and incubation was continued for a further 30 min at room temperature. Diluted solutions of these lysates were analysed for their hGH content by e.l.i.s.a.

Procedure. A portion (125 μl) of coating antibody diluted to 6 μg ml^{-1} in coating buffer was pipetted into each hole on the micro-test plate. The plate

was covered with tape and incubated at 4°C for at least 3 days before use (stability is 1 month).

For antigen incubation, the coated plate was washed 4 times, each with 350 μl of wash solution; 125-μl portions of appropriately diluted standards, controls and samples were pipetted in duplicate into the holes on the washed plate. Samples and controls were assayed at two dilutions. In modifications A and C the standard range was 0—8 ng ml^{-1}; in B the standard range was 0—1 ng ml^{-1} (8 concentrations). The test plate was covered with tape and incubated for 2 h at room temperature (ca. 20°C) in modification A. In B and C the incubation proceeded overnight at 4° C.

For labelled antibody incubation, the test plate was washed 4 times as above and 125 μl of $F_{ab'}$-peroxidase conjugate diluted 1:3000 with labelled antibody incubation buffer (A and C) or 1:1200 (B) was pipetted into each hole on the plate. The test plate was covered with tape and incubated for 2 h at room temperature (A and C) or overnight at 4°C (B).

To measure the enzyme activity, the test plate was washed 4 times as above and 125 μl of freshly prepared enzyme substrate was pipetted into each hole. The test plate was incubated at room temperature in the dark for 60 min, whereafter the enzymatic reaction was stopped with 150 μl of 2.5 M sulphuric acid. The absorbance was measured at 486 nm, and corrected for the absorbance at 620 nm, the net absorbance was plotted against hGH concentration to obtain a calibration graph.

RESULTS AND DISCUSSION

In the experimental section, three modifications of the e.l.i.s.a. procedure are described. Method A is the fast version, in which results from a limited number (ca. 20) of samples can be obtained within 6 h. Method B has a detection limit of 4 ng l^{-1} hGH, allowing determination (after dilution) of hGH in samples containing seriously interfering materials. Method C is for use when hundreds of samples are to be screened for hGH, leaving sufficient time for sample preparation "the day before". Versions A and C have similar detection limits (50 ng hGH l^{-1}). This flexibility of application is based on the use of an optimally coated solid-phase and choice of incubation conditions. The choice of conjugation reaction is also important.

A solid phase with the maximum number of binding sites is needed to give the fastest possible antigen incubation. This is achieved by making a monolayer of antibody molecules on the solid phase [3, 4]. Attempts to use higher antibody concentrations in the coating solution than are needed for monolayer formation lead to protein—protein adsorption rather than protein—polystyrene adsorption, without a larger number of binding sites on the resulting coated solid phase. As the adsorptive forces seem weaker between two proteins than between a protein and polystyrene, excessive coating leads to a coated solid-phase which is less stable to washing [4]. Generally, protein concentrations within the range 1—10 μg ml^{-1} lead to an optimally coated solid phase; in this procedure, 6 μg ml^{-1} was used.

An increase in temperature and incubation time in both immunological reactions leads to higher enzyme activity bound to the solid phase. This also results when the concentration of conjugate in the labelled antibody incubation is increased (Fig. 1). The extent to which these parameters can be increased depends mainly on the spectrophotometer used, because the substrate used for peroxidase is not rate-limiting. The recommended method produces an absorbance of 2.0 at 486 nm when the standard with the highest hGH concentration is incubated (in all modifications). Achieving less absorbance by decreasing the enzyme/substrate reaction time to <1 h is not recommended because the pipetting time might become critical.

As demonstrated in Fig. 2, the use of different conjugate preparations may give rise to marked differences in the performance of the final e.l.i.s.a. method. The differences between conjugates prepared by the periodate and maleimide methods are not likely to be so large in other systems. Thus, although $F_{ab'}$-peroxidase is also superior to IgG-peroxidase conjugates in an e.l.i.s.a. for Coagulation Factor VIII coagulant antigen [4], the difference is small. The steep dose—response curve obtainable in hGH-e.l.i.s.a. with a $F_{ab'}$-peroxidase conjugate prepared by the maleimide method I of Ishikawa et al. [2] is a result of the (generally seen) low non-specific binding of this

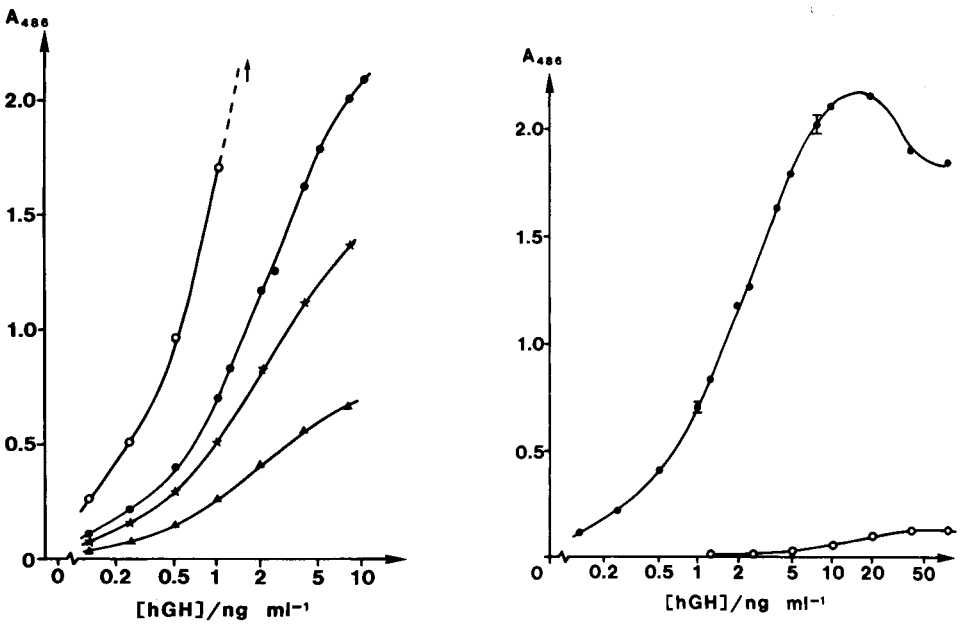

Fig. 1. Calibration graphs for hGH at different conjugate dilutions. Conjugate dilution: (○) 1:2000; (●) 1:5000; (×) 1:10 000; (▲) 1:20 000.

Fig. 2. Effect of different conjugates on the hGH calibration graph: (○) 027 II, dilution 1:5, prepared by the periodate method [1]; (●) 022, dilution 1:5000, prepared by the maleimide method [2].

type of conjugate. After size-exclusion chromatography on Ultrogel ACA-44, this $F_{ab'}$-peroxidase conjugate appeared as a single population of molecules, with an average of 1.15 peroxidase molecules per $F_{ab'}$ fragment [2]. The amount was sufficient for 10^6 single estimations.

Interferences

The influence of protein concentration in the antigen incubation buffer was studied. Calibration graphs prepared for solutions in antigen incubation buffer alone, and in the same buffer with albumin concentration raised to 5% or with both 5% albumin and 1.2% human IgG added were compared. In the fast version (A), the buffer with both albumin and IgG caused a 13% decline in resulting solid phase-bound enzyme activity compared to the antigen incubation buffer. This decline was intermediary using the buffer with 5% albumin. In the sensitive version (B), the inhibitory effects of large protein concentrations were smaller.

The influence of related peptides is shown in Fig. 3, where human prolactin (hPRL) and human placental lactogen (hPL) show limited cross-reactivity. This is due to the similarity in primary structure of these hormones to hGH [5]. The other peptides tested showed negligible interference. Figure 4 shows the inhibitory effect of very large amounts of hGH on the e.l.i.s.a. method. This type of effect (also evident in Fig. 2) is generally termed a "High-dose hook effect" [6]. Because e.l.i.s.a. is capable of producing this type of dose-response curve, it is advisable to assay samples at more than one dilution. Figure 4 shows that this immunological assay does not discriminate between pituitary hGH and methionine-hGH produced in *E. coli*. This indicates that these guinea pig anti hGH antibodies are insensitive to the amino terminal part of hGH.

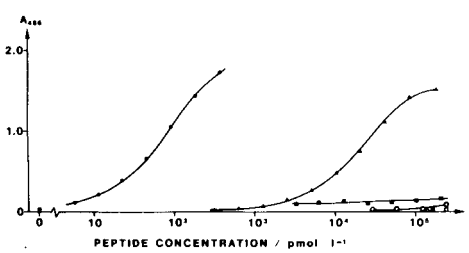

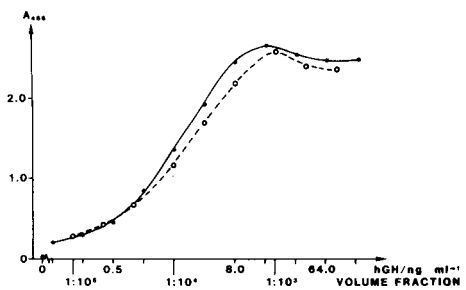

Fig. 3. Response of the method to various peptides: (•) hGH; (▲) human prolactin (<0.27% response of hGH); (■) human placental lactogen (<0.05%), (○) luteinizing hormone (<0.003%); (□) follicle-stimulating hormone; (■) thyroid-stimulating hormone; (△) human chorionic gonadotropin.

Fig. 4. Dose-response curves obtained using: (○) volume fraction data; (•) hGH data.

From Anal. chim. Acta, 171 (1985) 389

corrected.
ch.8
8/ma.21

TABLE 1

Reproducibility of the various e.l.i.s.a. modifications

Modification	hGH conc. (μg ml^{-1})		n	R.s.d. (%)
	Mean ± s.d.	Range		
A: fast	13.1 ± 0.8	12.2—14.5	12	6.5
B: sensitive	12.8 ± 0.2	12.6—13.0	3	1.3
C: convenient	13.7 ± 0.7	12.1—14.8	13	5.0
All	13.3 ± 0.8	12.1—14.8	28	6.0

Reproducibility

Table 1 shows the control results obtained over 4 months. Even when control data (one result per plate) from assays with different modifications were combined, the between-plate relative standard deviation was only 6%.

Application

The method was used for optimization of the production of methionine hGH in *E. coli* containing a hGH cDNA clone, brought under the control of the promoter from the lactose operon. This promoter is normally strongly repressed; therefore, there is no significant production of protein from the following gene. Removal of the repression is possible by addition of the inducer IPTG to the growth medium. Increasing concentrations of IPTG were added to different bacterial cultures, in order to establish the concentration of inducer required for maximum methionine-hGH production. The resulting hGH production was estimated by e.l.i.s.a. As demonstrated in

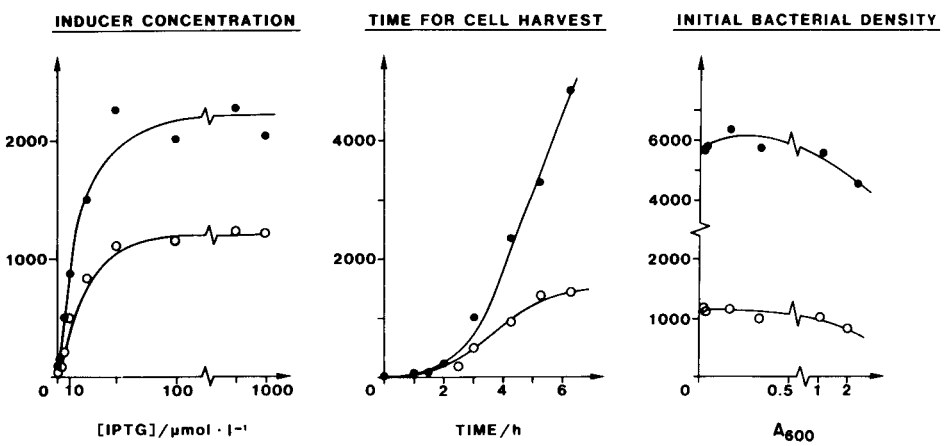

Fig. 5. Optimization of methionine-hGH production in *E. coli*. For the ordinate: (•) hGH concentration (ng ml^{-1}) in *E. coli* supernatant liquid; (○) hGH concentration (ng ml^{-1}) normalized to $A_{600} = 1$.

Fig. 5, an IPTG concentration of 100 μmol l^{-1} leads to a fully active promoter, and therefore maximum production of hGH. This inducer concentration was used in the following experiments. A bacterial culture was induced at a bacterial concentration corresponding to an absorbance of 0.05 at 600 nm. Samples for hGH estimation by e.l.i.s.a. were taken at the times indicated. After 6 h, the bacterial concentration reached an absorbance of 3.5, and hGH production per cell was at a maximum. The cells produced the same amount of hGH after 6 h in culture, if the cultures were initiated at any bacterial concentration corresponding to an absorbance at 600 nm between 0.05 and 0.5. This is also shown in Fig. 5, as is the fact that induction at higher bacterial concentrations leads to a decline in the amount of hGH produced per cell.

REFERENCES

1 M. B. Wilson and P. K. Nakane, in W. Knapp, K. Holubar and G. Wick (Eds.), Immunofluorescence and Related Staining Techniques, Elsevier, Amsterdam, 1978, p. 215.
2 E. Ishikawa, M. Imagawa, S. Hashida, S. Yoshitake, Y. Hamaguichi and T. Ueno, J. Immunoassay 4 (1983) 209.
3 L. A. Cantarero, J. E. Butler and J. W. Osborne, Anal. Biochem., 105 (1980) 375.
4 B. Dinesen and C. Feddersen, Thromb. Res., 31 (1983) 707.
5 W. L. Miller and N. L. Eberhardt, Endocrine Rev., 4 (1983) 97.
6 L. E. M. Miles, D. A. Lipschitz, C. P. Bieber and J. D. Cook, Anal. Biochem., 61 (1974) 209.

Analytica Chimica Acta, 163 (1984) 127—133
Elsevier Science Publishers B.V., Amsterdam — Printed in The Netherlands

MONITORING OF METHANOGENIC PROCESSES WITH AN IMMOBILIZED MIXED CULTURE IN COMBINATION WITH A GAS-FLOW METER

ULLA DISSING, TORBJÖRN G. I. LING and BO MATTIASSON*

Department of Pure & Applied Biochemistry, Chemical Center, University of Lund, P.O. Box 124, S-221 00 Lund (Sweden)

(Received 17th May 1984)

SUMMARY

A sensitive gas-flow meter is described for use in combination with a preparation of immobilized methanogenic bacteria. Upon administration of substrate, the gas formed is quantified by using this gas-flow meter. When a high density of the extremely slow growing and metabolizing methanogenic bacteria was added, it was possible to quantify and correlate samples with respect to their content of biodegradable matter.

The development of modern biotechnology places higher demands on productivity and control of biotechnological processes than in former days. New organisms, which may be genetically modified, may be more sensitive to changes in environmental conditions. Furthermore, the technology for operating with increased cell densities by using immobilized cells [1] or recirculating the cells by means of centrifugation or membrane filtration [2] creates systems that need a high degree of external control fully to capitalize the potential that increased cell density offers.

The development of sensors has been focussed mainly on applications in the area of clinical analysis and reports have only recently started to appear concerning the use of such sensors for process control. The first sensors to be developed were enzyme-based (so-called enzyme electrodes, etc.) [3] and later it also turned out that cells could be used for such analytical purposes [4]. The use of cells, however, laid some constraints on the system and it was clearly demonstrated that it gave problems with the selectivity of the analytical unit. There are reports on the use of immobilized cells for measuring BOD equivalents [5, 6]. The advantage of using immobilized cells in conjunction with a transducer has been that the high cell density gives a faster response than that normally achieved with enzymes.

The present paper deals with the development of a system to monitor metabolic behaviour in an immobilized, or otherwise enriched, culture. The system was initially developed to monitor and control methanogenic processes, but proved to be of general applicability. This paper deals with the basic characteristics of this sensor system and presents examples of its use in studying methanogenic processes.

0003-2670/84/$03.00

EXPERIMENTAL

Materials

Alginate (BDH Chemicals) and agarose 15/45, ultralow gelling temperature (FMC Corporation, Portland, ME, U.S.A.) were used. Concentrated sugar beet molasses was a generous gift from Sorigona AB, Staffanstorp, Sweden. Other solvents and chemicals were analytical reagents or laboratory-grade materials. Deionized water was used in all procedures. The polyurethane foam was of commodity quality, purchased in a local store.

Cultures of microorganisms and immobilization

A methanogenic microbial population was selected from the anaerobic digester at the sugar factory, Örtofta, Sweden. The culture was grown to high cell density and held active by feeding once a day with 5 ml of molasses (COD 67 500 mg l^{-1}) in 0.01 M sodium phosphate buffer, pH 7.0. A 1-l stirred (100 rpm) fermentor thermostated at 35° C was used. The pH, measured in the fermentor, was found to be constant at 7.0.

For the immobilization of microorganisms, cells from the active culture were harvested by centrifugation (2500 g). Immobilizations in alginate [7] and agarose [8] were done in the conventional manner, except that anaerobic conditions were applied with a plastic bubble under nitrogen.

For the immobilization in polyurethane, a flow of fermentation broth from a fermentor with an active methanogenic culture was continuously recirculated over a column (5 cm × 2 cm inner diameter) filled with polyurethane foam. The bacteria became attached within a few hours and a thick slime of bacterial culture developed in the foam.

Gas-flow meter

The gas-flow meter used is shown schematically in Fig. 1. A solenoid microvalve (Brunswick Technetics, Cedar Knolls, NJ, U.S.A.) is connected to a U-shaped glass tube filled with an aqueous solution of methylene blue. An optical sensor is connected to the tube, consisting of a light-emitting diode (giving red light) and a phototransistor. A tube is connected from the methanogenic process medium to the solenoid microvalve. Initially A is open and B closed and the gas evolved pushes the meniscus from position *a* to *b*. A signal is generated when the meniscus moves through the light path of the optical sensor and conceals the light beam. The signal is registered as a pulse in a microcomputer (ABC 80, Luxor AB, Motala, Sweden) and the input A closes and B opens for 1 s. The meniscus moves back to position *a* and the procedure can start again. The volume of each pulse was measured by introducing a given volume of gas and counting the number of pulses.

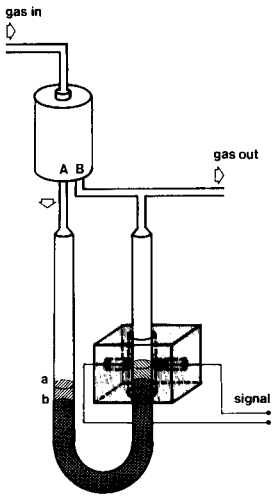

Fig. 1. Gas-flow meter (for description, see text).

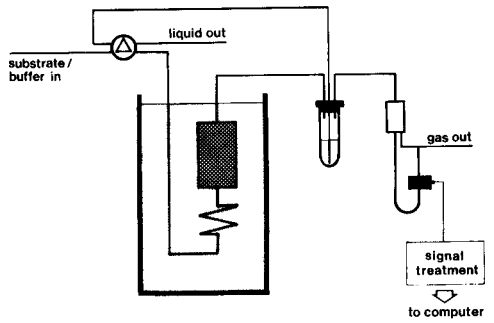

Fig. 2. Arrangement for the experiments with immobilized methanogenic bacteria. The column with the bacteria was thermostated in the water bath at 35° C.

Procedures

Batch experiments. The gas-flow meter was connected to a fermentor containing methanogenic bacteria. A sample of a concentrated solution of molasses (COD 67 500 mg l^{-1}) in 0.01 M sodium phosphate buffer, pH 7.0, was introduced and the evolved gas was monitored with the gas-flow meter. After each run, the gas in the fermentor was analysed and the content of methane was found to be ca. 70%.

Methane was quantified by gas chromatography (Varian Aerograph) with thermal conductivity detection. The column, 1 m × 2 mm inner diameter, was packed with Porapak Q (60—80 mesh). The carrier gas was helium at a flow rate of 25 ml min^{-1}. The column temperature was 30° C, the detector current 150 mA and the detector temperature 175° C.

Chemical oxygen demand (COD) was estimated by the American Standard Methods [9].

Immobilized system. The set-up is illustrated in Fig. 2. Liquid was continuously pumped into and out of the system at the same rate (7.5 ml h^{-1}) with a two-channel peristaltic pump (Microperpex; LKB, Bromma, Sweden). The gas evolved from the column followed the outgoing liquid as small gas bubbles into a small gas-tight unit outside the water bath. This 3.5-ml unit was half-filled. The column was equilibrated with 0.01 M sodium phosphate buffer, pH 7.0, before pulses of substrate (molasses in 0.01 M sodium phosphate buffer, pH 7.0) were introduced. Gas evolved in the column was monitored with the gas-flow meter and the metabolic activity was given as the gas production rate. The methane content in the gas was quantified, and was found to be between 50 and 70%.

RESULTS AND DISCUSSION

Several methods for monitoring methanogenic processes have been developed. In order to record gas production, van den Berg et al. [10] used a modified Warburg apparatus [10]. They were able to follow the process in a small aliquot under very well standardized conditions. Equipment such as the Warburg apparatus is very useful for batch experiments when gas is produced or consumed. It was, however, not developed to be used for continuous measurements and is thus not useful, for example, for process control.

In an earlier report [11] a calorimetric approach was used to follow methanogenic processes. The small amounts of heat generated in this reaction did not make flow calorimetry the ideal method. At the outlet from the calorimeter, gas bubbles were observed long before a heat signal started to emerge. Thus, a gas-flow meter was constructed instead. The construction and experimental set up are shown in Figs. 1 and 2.

The gas-flow meter was constructed so that both the gas flow and the total amount of gas generated could be measured. When U-tubes with an inner diameter of 2.5 mm were used, the meniscus had to move a distance of ca. 6 mm before the positions of the valve were changed, the fluid in the test tube came back to the starting position, and the electronic counter recorded another gas quantum produced when 30 μl of gas had been formed. This means that 1 μmol of gas was measured by the gas-flow meter. Provided that optical components of different geometric properties are used, this volume can be even smaller; a narrower tube can be used and an even more sensitive assay can be set up. For the studies in this report, the sensitivity was adequate with the equipment used, and no attempts were made to improve the performance.

Measuring methanogenic activity in a batch fermentor with high cell densities

A mixed culture was grown as described above. A dense cell population was transferred to a stirred batch reactor, which was connected to a gas-flow meter in which the U-tube had an inner diameter of 3.5 mm. After additions of pulses of substrate, the amount of gas evolved was quantified. In these experiments, the carbon dioxide formed in the reaction was not removed. Because the microbial system is known to be a mixed culture of unknown complexity, it was important to evaluate the reproducibility of the results obtained for the system.

In this context, it should be stressed that, as is mentioned elsewhere [4], when starved cells are used in analysis, they often demonstrate a memory effect in the sense that the first pulse helps to activate an earlier resting metabolic potential, start new syntheses, etc. These memory effects make starved cells unsuitable for quantitative work where a major part of their metabolism is involved. This is why a methanogenic mixed culture which was in good condition was used; the reproducibility shown by the two sets of

results in Fig. 3 was obtained. It is interesting to note that not only was the total amount of gas produced almost identical in each assay, but the curves illustrating the time-dependence were also almost identical, indicating that no drastic changes had taken place between the two assays. Using the same equipment, various amounts of substrate were added. The relationship between the substrate added and the total gas formed was found to be linear over the range 0.5—8 ml of substrate. Furthermore, the gas production correlated well with the COD, as shown in Table 1.

As can be seen in Fig. 4, each sample took 10—30 h to process. To improve the analytical performance, an immobilized system was used, as described below.

Monitoring methanogenic activity in an immobilized system

Initially, a methanogenic mixed culture was immobilized under anaerobic conditions in calcium alginate. During the first stage of the subsequent experiment the cells behaved as expected by converting the substrate added into methane and carbon dioxide. However, after 2—3 days of operation, the gel beads became severely eroded and eventually vanished. The mixed culture degraded the polymer backbone making up the matrix. An identical situation was found when agarose was used. To avoid biodegradation, an inert support, polyurethane foam, was used. The plug of polyurethane was placed in a holder and connected to a pump so that it was continuously perfused with broth from a fermentor with actively growing methanogenic culture.

After some time, the polymer foam was filled with a black mass of cells and, when the fluid was recovered from the fermentor and buffer was passed over the cell preparation instead, most of the cells were found to stay in the foam and were still metabolically active. The cell preparation was washed

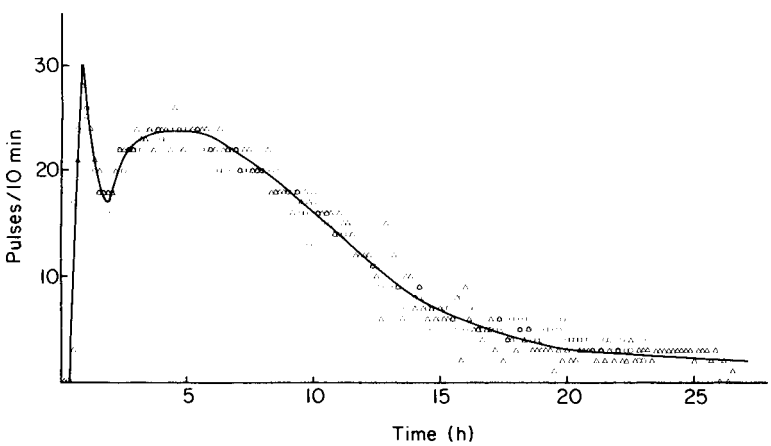

Fig. 3. Gas production rate as a function of time after addition of a 7.5-ml pulse of molasses (COD 67 500 mg l^{-1}) in 0.01 M sodium phosphate buffer, pH 7.0; (○) and (△) indicate two experiments 1 week apart.

TABLE 1

Correlation of gas production rate with COD

Substrate (ml)	0.5	1.0	2.5	5.0	7.5
No. of pulses	130	265	600	1125	1760
ml gas/mg COD	0.31	0.31	0.28	0.27	0.28

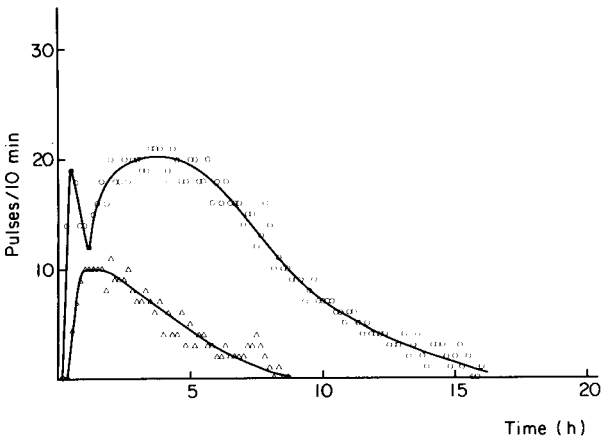

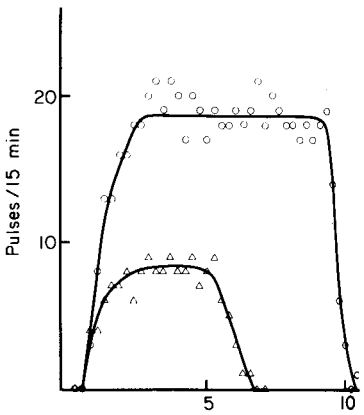

Fig. 4. Gas production rate as a function of time after pulses of (○) 5 ml and (△) 2.5 ml of molasses (COD 67 500 mg l^{-1}) in 0.01 M sodium phosphate buffer, pH 7.0.

Fig. 5. Gas production rate as a function of time for pulses of molasses with (○) COD 13.5 mg ml^{-1} and (△) COD 6.75 mg ml^{-1}, in 0.01 M sodium phosphate buffer, pH 7.0.

with buffer before assays started. The experimental arrangement is shown in Fig. 2. The immobilized system contained a very high cell density and thereby had a high metabolic potential. A high cell density gave the conditions for faster analysis. When pulses of substrate were added, each assay took only 5—10 h with pulses long enough to give steady-state conditions. However, it is clearly seen from Fig. 5 that the maximum level is attained after 2 h. Provided that non-equilibrium conditions are used, considerably shorter periods may be satisfactory. There was a linear correlation between added substrate and gas formed over the COD range 1—13 g l^{-1}.

Because of the short contact time between the immobilized cell preparation and the sample, incomplete metabolism could be expected. The lower gas yield in these experiments compared to that of the batch experiments is now under investigation. It should be stressed that the organisms studied here are extremely slow growing; when other systems are studied, a much faster response can be expected. This concept of using sensitive and fast gas-flow measurements opens up new possibilities for monitoring events in biotechnological processes.

This project was supported by the National Swedish Board for Technical Development.

REFERENCES

1 B. Mattiasson (Ed.), Immobilized Cells and Organelles, Vols. I and II, CRC Press, Boca Raton, FL, 1983.
2 A. S. Michaels, Desalination, 35 (1980) 329.
3 L. C. Clark, Jr., Biotechnol. Bioeng. Symp., 3 (1972) 377.
4 B. Mattiasson, in B. Mattiasson (Ed.), Immobilized Cells and Organelles, CRC Press, Boca Raton, FL, 1983, pp. 95—123.
5 I. Karube, T. Matsunata, S. Mitsuda and S. Suzuki, Biotechnol. Bioeng., 19 (1977) 1535.
6 B. Mattiasson, P.-O. Larsson and K. Mosbach, Nature (London), 268 (1977) 519.
7 M. Kierstan and C. Bucke, Biotechnol. Bioeng., 19 (1977) 387.
8 T. Matsunaga, I. Karube and S. Suzuki, Anal. Chim. Acta, 99 (1978) 233.
9 Annual Book of ASTM Standards, American Society for Testing and Materials, Philadelphia, PA, Part 31, Water, 1980.
10 L. van den Berg, C. P. Lentz, R. J. Athey and E. A. Rooke, Biotechnol. Bioeng., 14 (1974) 1459.
11 U. Dissing, T. G. I. Ling and B. Mattiasson, Poster Presented at Third Int. Symp. Anaerobic Digestion, August 1983, Boston, MA.

Analytica Chimica Acta, 163 (1984) 135—141
Elsevier Science Publishers B.V., Amsterdam — Printed in The Netherlands

EVALUATION OF A DIALYSIS PROBE FOR CONTINUOUS SAMPLING IN FERMENTORS AND IN COMPLEX MEDIA

C. F. MANDENIUS, B. DANIELSSON* and B. MATTIASSON

Department of Pure & Applied Biochemistry, University of Lund, Box 124, S-221 00 Lund (Sweden)

(Received 17th May 1984)

SUMMARY

A dialysis probe is described for continuous sampling from complex solutions, such as fermentation broth, milk or waste water, to yield samples suitable for liquid chromatography, flow injection analysis, enzyme calorimetry, etc. The analyte is transferred to a flow stream separated from the sample by a dialysis membrane that is protected from fouling by a strong tangential flow of the sample solution. This flow is accomplished by placing a magnetic stirring bar close to the membrane surface. The device is constructed of materials permitting the probe to be steam-sterilized when mounted inside a fermentor.

In recent years several analytical techniques have emerged as suitable for continuous or intermittent monitoring of biotechnological processes and similar systems in which it is desirable to follow the concentration of a compound in a complex mixture. It may concern the determination of penicillin concentration during fermentation, analysis for different sugars during cellulose or starch degradation or measurement of a pollutant during waste-water treatment. Furthermore, there is a trend today in biotechnology from batch processes towards continuous processes for which the demand for continuous monitoring and control is even more important.

Microbiological processes taking advantage of the progress made in gene technology for the production of, for instance, hormones, require rapid results from analysis for proper process control, especially because the concentration of the metabolite produced often decreases rapidly from its maximum value. A rapidly growing need for specific determinations in such areas as those mentioned can be foreseen, stressing the associated problems of continuous sampling and sample treatment.

Special interest has been focussed on the use of biosensors for such measurements. In a biosensor, a biocatalyst (an enzyme or a cell preparation) is immobilized onto a support material or held within a membrane close to a suitable transducer to detect the reaction governed by the biocatalyst. In the enzyme thermistor [1], a temperature transducer (thermistor) is used; in the enzyme electrode [2], various selective electrodes can be used, e.g., pH, pCO_2 or pO_2 electrodes. In addition, it has become increasingly common to

0003-2670/84/$03.00

apply high-resolution techniques such as h.p.l.c. [3] as well as flow-injection analysis (f.i.a.) [4] to analysis in biotechnology. These procedures have a common feature in that they require representative samples to be drawn from the process solution and also they usually require that the sample be freed at least from particulates, which otherwise would quickly clog flow channels, columns, etc. in the instrument used. For occasional samples, it may be possible to use manual operation of a sterilizable sampling valve followed by filtration or centrifugation or both prior to quantifying the analyte. For more frequent or continuous sampling, however, an automatic sampling device should be very useful.

Various attempts to solve these problems have been reported. A common approach is to let low-molecular-weight analytes pass a dialysis membrane. One example of this is given in a design in which a plastic probe is covered by dialysis tubing. The probe is inserted into the test solution and the permeated solution is recovered through a spiral groove machined around the surface of the probe [5]. An advantage of such systems is that the process solution is simultaneously protected from infection. This is, of course, a most important point and for this reason a membrane was chosen as a sterility barrier in the present work. Another problem connected with sampling in complex biological mixtures is fouling of the membrane, which will change its performance. In the present design, an attempt is made to minimize the effects of fouling by creating a tangential flow across the membrane surface either by a built-in impeller or by directing existing turbulent flow inside the fermentor over the membrane surface.

The tangential flow also brings fresh sample continuously to the dialysis membrane. After passage through the membrane, the analyte is free from cells and particulate contaminants and also from macromolecules that otherwise might interfere with the procedure. The analyte is furthermore directly obtained in a solution with suitable and constant composition with respect to pH, ionic strength, etc. Dilution of the sample is often required and this step is also done automatically by the dialysis probe by proper selection of dialysis membrane, its area and the dialysis fluid flow rate. To be useful for monitoring of fermentation processes, the sample probe should have a constant performance over a sufficiently long period of time. The first goal in the present study was to have the probe in operation for a week without change of membrane. Furthermore, all parts should be made in such materials that the probe could be steam-sterilized and mounted inside a fermentor.

EXPERIMENTAL

Glucose oxidase (EC 1.1.3.4) type V from *Aspergillus niger* and catalase (EC 1.11.1.6) (cat. No. C-100 from bovine liver) were obtained from Sigma Chemicals and peroxidase (EC 1.11.1.7) from horse radish was from Boehringer-Mannheim. Other materials were cellulose (Solkafloc; Brown Co., Berlin, NH, USA) and polyethylene glycol (PEG 20 000; Serva, Heidelberg,

West Germany). Controlled pore glass (CPG; pore diameter 130 nm, alkylamino derivatized) was a generous gift from Corning Glass Works.

The yeast suspensions used for testing the dialysis probe were made by suspending baker's yeast in distilled water to give a final concentration of 1—4 g l^{-1}. The buffer used as the dialysis solution was 0.1 M sodium phosphate, pH 6.0. All chemicals used were of analytical grade.

A cross-section of the dialysis probe is shown in Fig. 1. All parts were made of autoclavable materials: acid-proof steel, polycarbonate and polytetrafluoroethylene. The probe was equipped with an autoclavable Maxon d.c. motor type 2326 (Interelectric AG, Sachseln, Switzerland). The motor was powered from an external speed control, variable from 0 to 1000 rpm. Various 25-mm diameter ultrafiltration membranes (Millipore, polysulfon, with cut-off at 30 000), dialysis membranes (Cuprofan) and Spectrapore dialysis tubing were used.

Glucose was used as the analyte in all experiments, and it was assayed by a modified Barham/Trinder method [6] using sequentially operated 0.1-ml immobilized enzyme reactors containing 40 mg of glucose oxidase and 40 mg of peroxidase per g of CPG. The colour reagent for the peroxidase reaction was 2,4-dichlorophenol-6-sulfonate and 4-aminoantipyrine. Glucose samples (40 or 100 μl) were injected via a timer-controlled valve into a flow-injection system operated at 1.6 ml min^{-1}. The detector was a Zeiss PM2

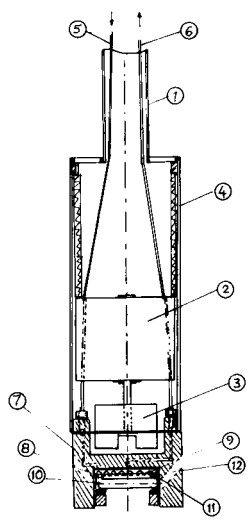

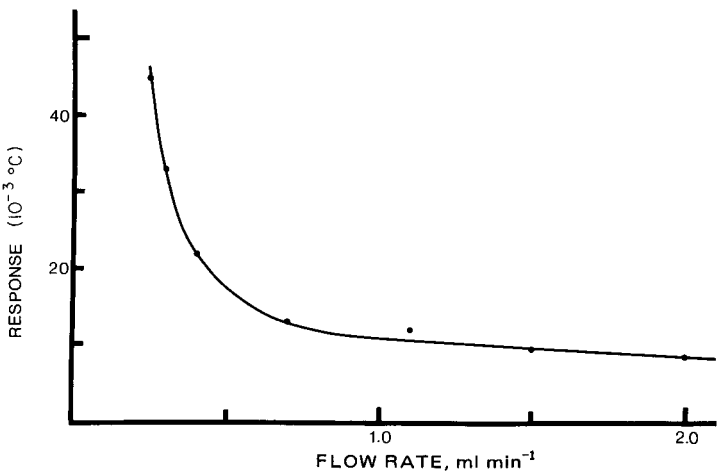

Fig. 1. Cross-section of the dialysis probe: (1) stainless steel shaft; (2) autoclaveable d.c. motor; (3) permanent magnet; (4) stainless steel housing; (5, 6) in- and out-going dialysis solution; (7) polycarbonate membrane holder; (8) membrane; (9) membrane support with spiral groove; (10) magnetic stirring bar; (11) thin teflon washer; (12) channels for air escape and improved circulation.

Fig. 2. Effect of dialysis solution flow rate (for details, see text).

photometer equipped with a flow cell. This system gave a linear response in the range 0—150 g l^{-1}. A glucose sample containing 0.1 g l^{-1} gave an absorbance change of 0.235 at 514 nm.

Alternatively, the glucose concentration was measured with an enzyme thermistor [1] equipped with a 1-ml co-immobilized glucose oxidase/catalase column (1000 U glucose oxidase and 300 000 U catalase applied). The flow rate was 1 ml min^{-1}. The glucose samples were continuously pumped through the enzyme thermistor unit after 4-fold dilution. The response was linear up to 0.6 mM.

RESULTS AND DISCUSSION

Performance of the probe

The performance of the dialysis probe was investigated under various working conditions, with different membranes, and for longer and shorter periods to see if it could be useful for sampling for fermentation monitoring over one week or more. After its general properties had been established, the way in which the function of the probe was affected by changes in stirring speed, flow rate of the dialysis fluid, temperature, concentration of macromolecular solutes, such as cellulose or polyethylene glycol, as well as the content of yeast cells in the sample solution, and finally, the long-term performance in complex mixtures, were examined. As an example, the performance in cellulose suspensions is described below.

Stirring speed. The stirring speed of the magnetic bar sweeping the membrane of the probe was varied from 0 to 1000 rpm, with other parameters fixed, while the concentration of analyte in the dialysate was measured. A major increase in analyte concentration was noted when the speed was raised from zero to a few rpm and then the increase in concentration became slower when the speed was further increased. Above 300—400 rpm the transmission rate of the analyte was constant. To ensure good long-term operation, the speed was usually set at 600 rpm.

Flow rate. The concentration of analyte in the dialysate depends on the flow rate of the dialysis solution. It is also affected by the properties of the membrane and the analyte itself, e.g., its molecular weight. Figure 2 summarizes the results of an experiment with the probe equipped with a Millipore Pellicon membrane type PS (cut-off 30 000) immersed in a 4 mM glucose solution. The flow rate of the dialysis solution was varied from 0.25 to 2.0 ml min^{-1}, while the glucose concentration of the dialysate was continuously measured with an enzyme thermistor charged with a glucose oxidase/catalase column. There was a drastic decrease in glucose concentration between 0.25 and 0.5 ml min^{-1}, but at flow rates higher than 1 ml min^{-1} the glucose concentration did not change much. By varying the flow rate, the analyte concentration in the dialysate could be varied over a 5-fold range. This possibility is valuable if the analytical procedure has a narrow operable concentration range.

Temperature. The temperature-dependence of the yield of analyte in the dialysate was investigated for penicillin V samples measured by a β-lactamase thermistor. Over the range 20—40° C the yield increased by about 4% per degree. This dialysis probe will, however, normally be used in very large volumes in which the temperature variations can be expected to be small.

Operation in complex solutions

The performance of the dialysis probe in various media was investigated by automatically drawing a 40 μl sample from the dialysate every 10 min. In these experiments, glucose was used as the analyte as it could easily and accurately be determined by a spectrophotometric f.i.a. procedure with use of sequentially operating columns of immobilized glucose oxidase and peroxidase. The membrane was a polysulfon ultrafilter with cut-off at 30 000. In some experiments, this membrane was covered with an outer Cuprophan membrane as this sometimes seemed to decrease the degree of fouling. Thus the experiments reported in this section were done with double membranes. In contrast, the long-term studies reported in the next section were performed with the ultrafilter alone.

Figure 3 shows how the permeability of the glucose was affected by the presence of three different concentrations of polyethylene glycol, cellulose and yeast cells. Especially in polyethylene glycol, the glucose transport was rather severely affected, probably because of the higher viscosity. In the other two cases, the glucose readings were less influenced by changes in the amount of bulk material. For practical use, however, this feature is less important because the matrix composition is likely to be more or less constant.

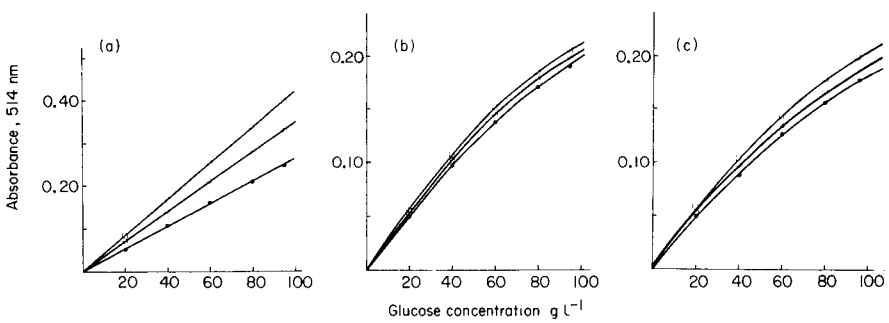

Fig. 3. Effect of macromolecules and cells. Known additions of glucose were made to the test solution and the glucose concentration in the dialysis solution was measured by f.i.a. giving an absorbance at 514 nm of 0.235 for 0.1 g l^{-1} of glucose. The distilled water test solutions were as follows: (a) polyethylene glycol (M = 20 000) at (□) 5%, (○) 10%, (●) 15% (w/v); (b) cellulose (Solkafloc) at (□) 5%, (○) 10%, (●) 15% (w/v); (c) yeast cells at (□) 1%, (○) 2%, (●) 4% (w/v) dry yeast.

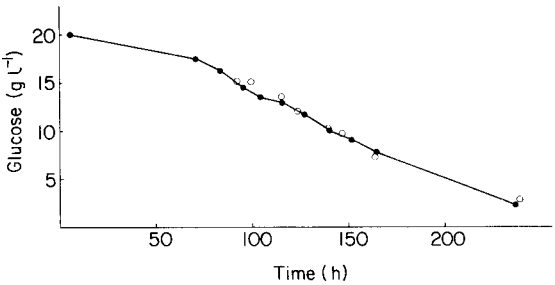

Fig. 4. Long term experiment with the dialysis probe equipped with a polysulfon ultrafiltration membrane (cut-off 30 000) operated in a mixture of 10.5% polyethylene glycol (M = 40 000), 0.2% dextran (M = 40 000) in 50 mM sodium acetate, pH 4.8, containing 0.03% sodium azide. The glucose concentration was determined in samples obtained via the probe (•) and taken directly from the crude solution after dilution (○).

Long-term stability

The long-term stability of the probe was tested in 1—2 week runs in different crude solutions. The curve shown in Fig. 4 was obtained with a mixture of polyethylene glycol, dextran and cellulose. The glucose concentration in the dialysate was checked regularly with the f.i.a. system on 40-μl samples drawn by the automatic sampling valve. For control of the function of the probe, samples drawn directly from the crude solution at regular intervals were diluted and injected into the f.i.a. system. As can be seen in Fig. 4, the plots representing the glucose concentration measured directly and via the dialysis probe coincide quite well, which indicates a constant permeation of analyte through the membrane during the test period.

Consequently, it can be concluded that this dialysis probe can be used for sampling of low-molecular-weight analytes in crude solutions for at least one or two weeks without change of membrane. During this time the anti-fouling action of the stirrer ensures constant and reliable operation. The membrane also provides a sterile barrier between the sample solution and the surroundings, and furthermore, the whole device is autoclavable, which should make it highly interesting for direct sampling and continuous monitoring of metabolites in fermentors.

The skillful technical assistance by Ms M. B. Larsson and Mr. L. Johansson is gratefully acknowledged. This study was in part supported by the National Swedish Board for Technical Development. We thank Drs H. Lundbäck and B. Olsson for valuable suggestions.

REFERENCES

1 B. Danielsson, B. Mattiasson and K. Mosbach, in L. Wingard, Jr., E. Katchalski-Katzir and L. Goldstein (Eds.), Applied Biochemistry and Bioengineering, Vol. 3, Academic Press, New York, 1981, p. 97.

2 G. G. Guilbault, Ion-Selective Electrode Rev., 4 (1982) 187.
3 R. A. Mowery, Jr., in D. P. Manka (Ed.), Automated Stream Analysis for Process Control, Vol. 1, Academic Press, New York, 1982, p. 119.
4 C. B. Ranger, in D. P. Manka (Ed.), Automated Stream Analysis for Process Control, Vol. 1, Academic Press, New York, 1982, p. 39.
5 U.S. Pat. No. 3, 830, 106; 1974.
6 D. Barham and P. Trinder, Analyst (London), 97 (1972) 142.

Analytica Chimica Acta, 163 (1984) 143—149
Elsevier Science Publishers B.V., Amsterdam — Printed in The Netherlands

DETERMINATION OF UREA WITH AN AMMONIA GAS-SENSITIVE SEMICONDUCTOR DEVICE IN COMBINATION WITH UREASE

F. WINQUIST*, A. SPETZ and I. LUNDSTRÖM

Laboratory of Applied Physics, Linköping Institute of Technology, S-581 83 Linköping (Sweden)

B. DANIELSSON

Department of Pure and Applied Biochemistry, Chemical Centre, University of Lund, S-220 07 Lund (Sweden)

(Received 3rd April 1984)

SUMMARY

An ammonia gas-sensitive Ir/Pd MOS capacitor is used for urea determinations with the aid of urease in two different systems. One combination utilizes a reaction column with immobilized urease in a flow-injection system. The lower limit of urea detection for 150-μl samples was 0.2 μM. Urea in whole blood and blood serum was determined after a 500-fold dilution, and 15 samples per hour could be assayed. The relative standard deviation was 4.6% (n = 10). Recovery tests were satisfactory. Values obtained for urea in serum correlated well with those from a spectrophotometric method. The other combination is based on a small flow cell with free urease enclosed between a dialysis membrane and a gas-permeable membrane. Urea was determined in the concentration range 0.01— 50 mM. The enzyme probe could be used for up to four days without changes of behaviour.

The determination of urea is a very important routine test, widely used in clinical laboratories. Spectrophotometric methods are most commonly used, such as the indophenol method [1] or the glutamate dehydrogenase method [2]. Other methods are based on the combination of urease with different kinds of sensors, such as potentiometric enzyme electrodes [3], ammonia gas sensors [4] or a Stark microwave cavity resonator [5]. Simple fast methods for the determination of urea are still in demand, however, and a procedure based on a sensitive ammonia sensor in combination with urease would be valuable.

Much attention has lately been given to sensors based on semiconductor technology, because of their smallness and simplicity. Recently, a new type of ammonia gas-sensitive semiconductor structure was described [6—8]. The sensor was made by evaporating a thin film (nominal thickness 3 nm) of iridium over and outside the palladium gate in a Pd MOS capacitor, and the lower limit of detection for ammonia gas in air was 1 ppm. The Ir/Pd MOS capacitor has also been used for the determination of ammonium in aqueous solutions [8]. Because the sensor operates in the gas phase, a flow-injection

0003-2670/84/$03.00

system utilizing a gas-permeable membrane was developed. The detection limit for ammonium in aqueous solutions was 2×10^{-7} M.

This paper deals with the use of an ammonia-sensitive Ir/Pd MOS capacitor in combination with urease for urea determinations. A reaction column, containing immobilized urease is inserted in a flow-injection system for ammonium determinations, and urea can be determined in whole blood and serum samples. A simple enzyme probe, based on free urease enclosed between a dialysis membrane and a gas-permeable membrane is also described. With this probe, urea can be determined in buffered solutions.

EXPERIMENTAL

Chemical and samples

All reagents used were of analytical grade. L-Glutamate dehydrogenase (type III from bovine liver, E.C. 1.4.1.3.) and urease (type III from jack beans, E.C. 3.5.1.5.) were obtained from the Sigma Chemical Company. (One unit of L-glutamate dehydrogenase will reduce 1 μmol of α-ketoglutarate to L-glutamate per minute at pH 7.3 at 25°C. One unit of urease is defined as the amount of enzyme necessary to liberate 1 μmol of ammonia from urea per minute at pH 7.0 at 20°C.) Oxirane-acrylic beads, trade name Eupergit C, were obtained from Röhm-Pharma (Darmstadt). Distilled deionized water was used throughout.

The buffer used during immobilization was 0.05 M potassium phosphate, pH 7.0; the working buffer was 0.05 Tris —HCl, pH 8.5, which was prepared freshly every 3 days. Stock standard solution (20 mM) was prepared by dissolving 0.120 g of urea in 100 ml of water. Working standards were prepared by serial dilution, every 3 days.

Whole blood samples were taken from 4 healthy adults. The serum samples were taken from these specimens after clotting.

Preparation of sensors and equipment

The sensors were made of *p*-type silicon with a 100-nm layer of thermally grown dry oxide. Palladium was resistively evaporated through a 1×2 mm T-shaped mask on the oxide to a nominal thickness of 200 nm. Iridium was then evaporated over the upper part of the T-shaped palladium gate to a nominal thickness of 3 nm. An aluminium back contact was made prior to the gate metallization. The size of the active area was 1.5×2.0 mm. The structure was mounted on a temperature-controlled sample holder, adjusted to 35°C. The shift of the C—V characteristics of the capacitor along the voltage axis on exposure to ammonia gas was measured with a constant capacitance regulator, connected to an X-t recorder. The temperature-controlled sample holder and the constant capacitance regulator were built at the laboratory. The pump used was a MicroPerpex (LKB, Bromma, Sweden), and the six-way valve was obtained from Rheodyne. The polytetrafluoroethylene gas-permeable membrane used was SM-33 with pore size

5 μm (Sartorius). All tubings used in the flow-injection system were made of teflon (0.5 mm i.d.).

The flow-injection system

This system was developed from the system used for determination of ammonia in aqueous solutions [8], and is shown in Fig. 1. Working buffer is continuously pumped at a flow rate of 0.5 ml min^{-1} through the system via a six-way valve with a sample loop to a reaction column, containing immobilized urease. The column is made from a teflon tubing (3 mm i.d., 43 mm long) containing 0.3 ml of enzyme preparation, corresponding to about 400 U. The buffer then enters the upper part of the cell with the gas-permeable membrane. This cell is made from a circular teflon rod (8 mm diameter, 30 mm long) with a 0.5 mm diameter hole along the centre axis, through which the buffer enters; at the other end is a 20 mm deep circular channel (7.0 mm i.d., 7.5 mm o.d.). A 0.5-mm diameter hole is drilled from the side of the rod to the inside of the channel, and a gas-permeable membrane is attached over the end of the rod. Buffer flows radially from the centre hole to the channel between the membrane and the plane end of the rod, through the channel and out from the cell via the hole in the side of the rod. The back-pressure is increased by attaching some tubing (0.5 m long, 0.2 mm i.d.) to the outlet so that diffusion of ammonia through the membrane is enhanced [8]. The Ir/Pd MOS capacitor is placed with the active area of the sensor directly opposite the centre of the gas-permeable membrane, and the air gap between the sensor and the membrane is 0.3 mm.

Calibration graphs were obtained by injecting 150-μl standard solutions into the system via the sample loop. For the determination of urea in whole blood and serum samples, portions of 10 μl were diluted 500-fold with the working buffer to a final volume of 5.0 ml; 150 μl of these dilutions was then injected in the system.

For immobilization of the enzyme, 600 U of urease was added to a suspended solution of 250 mg of oxirane acrylic beads in 0.05 M potassium phosphate buffer (pH 7.0). The mixture was gently shaken at room temperature for 48 h and then washed with water three times. The suspension was

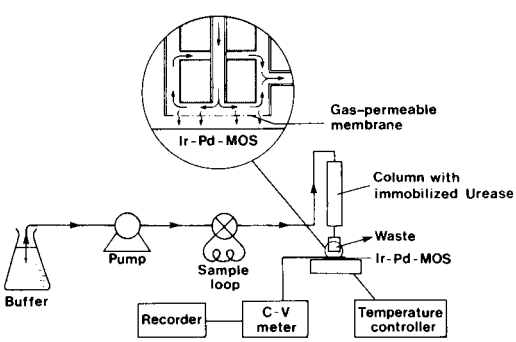

Fig. 1. Schematic diagram of the flow-injection system for urea.

finally shaken with 20 ml of 1 mM alanine in 0.05 M potassium phosphate buffer (pH 7.0) for 12 h in order to cap all unreacted groups on the matrix.

The enzyme probe

A cross-section of the enzyme probe is shown in Fig. 2. Free enzyme, approximately 50 U of urease, was enclosed between a dialysis membrane (molecular weight cut-off at 10 000) and a gas-permeable membrane. This arrangement was one of the sides in a thin, circular teflon cell (10 mm diameter, 0.5 mm high) with an inlet and an outlet on the opposite side. The sensor was placed 0.1 mm from the centre of the gas-permeable membrane. Working buffer was then pumped through the cell at a flow rate of 0.1 ml min^{-1}.

Spectrophotometric assay for urea

The sample (5 μl) was added to 3 ml of a solution buffered at pH 7.0 and containing 1.2 mM α-ketoglutarate, 0.18 mM NADH and 50 U of L-glutamate dehydrogenase. The concentration of urea was calculated from the decrease in absorbance caused by NADH consumption in the enzyme-catalyzed reaction.

RESULTS AND DISCUSSION

The steady-state response characteristics of an Ir/Pd MOS capacitor for ammonia follow an equation of the form $\Delta V = K_1 (P_{NH_3})^x$, where ΔV is the voltage drop across the capacitor, P_{NH_3} is the partial pressure of ammonia gas and K_1 and x are constants. Under non-equilibrium conditions, i.e., if the sensor is exposed to ammonia for a short time, Δt, then $\Delta V = K_2 P_{NH_3} \Delta t$, where K_2 is a constant. In the flow-injection system for ammonium determinations in aqueous solutions, the sample volume injected is directly related to Δt, and it was found [8] that a sample volume of 150 μl (at a flow rate of 0.5 ml min^{-1}) was preferable. By combining this system with immobilized urease, it is possible to determine urea concentrations by means of the ammonia released in the enzyme-catalyzed reaction. The pH of the working buffer was chosen as 8.5. As is well known, the equilibrium between NH_4^+ and NH_3 is pH-dependent: increased pH favors ammonia formation, but the pH optimum for urease activity is 7.0 and a compromise has to be made. Experiments made clear, however, that complete substrate conversion was obtained even at pH 8.5 because of the high enzyme activity of the column (approximately 400 units) and the low substrate concentration (<50 μm).

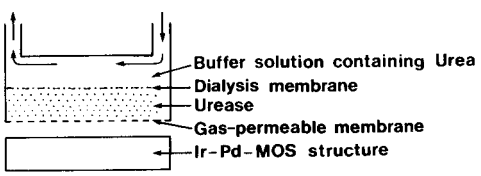

Fig. 2. Schematic cross-section of the enzyme probe cell.

The pH should not be raised above 8.5 in measurements on blood samples, because ammonia may be liberated from labile compounds [9].

The experimental arrangement is shown in Fig. 1. The calibration plot for 150-μl standard solutions was linear up to 50 μM urea and followed the equation $C = 1.41\ \Delta V$, where C is the concentration in μM and ΔV is the response of the sensor in mV. The lower limit of detection (defined as S/N = 3) was 0.2 μM urea.

The normal concentration range of urea in whole blood and serum is 3.2—6.8 mM [10]. The high sensitivity of the system therefore allows a sample to be diluted up to a 1000-fold before injection; practically, a 500-fold dilution was found to be satisfactory. This large dilution is advantageous, first because clogging of column and tubings is minimized and secondly because only a very small volume of sample is required. The volume of the sample loop is 150 μl, so that only 0.3 μl of the original sample is used. Samples of both whole blood and serum were collected from healthy members of the laboratory and the urea concentrations were determined. The results obtained are shown in Table 1; also shown in the table are results obtained for the same serum samples by using the conventional glutamate dehydrogenase method for the determination of urea. A reasonable correlation was observed. Recovery studies were done on whole blood samples spiked with various amounts of urea. These results are summarized in Table 2. Precision data were obtained from ten successive determinations on whole blood. The mean value of urea concentration was 4.53 mM with a relative standard deviation of 4.6%. The reaction column could be used for over a month with unchanged performance.

The flow-injection method described is independent of the optical properties of the sample, which allows whole blood to be analyzed without any pretreatment except for a dilution step. One sample can be analyzed in less than 4 min, so that the method is very simple and fast.

As an alternative to the flow-injection system, an enzyme probe was devel-

TABLE 1

Urea determinations in whole blood and serum (for the serum samples, the values obtained with the present method are compared with values from a conventional spectrophotometric method)

Sample	Urea concentration found (mmol l^{-1})		
	Whole blood Present method[a]	Serum Present method[a]	Serum Spectrophotometric[b]
1	3.70	3.76	3.58
2	4.30	4.43	4.60
3	4.56	4.66	5.06
4	5.23	5.33	5.10

[a]Mean of triplicate determinations. [b]Single measurement.

TABLE 2

Recoveries from whole blood spiked with various amounts of urea

Urea concentration (mmol l^{-1})		Recovery (%)
Added	Found	
0	4.36	—
0.5	4.89	106
1.0	5.20	85
1.5	5.80	97
2.0	6.42	104

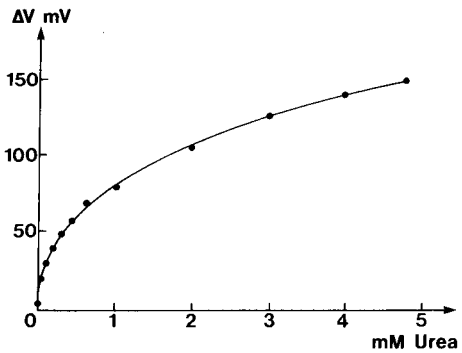

Fig. 3. Calibration plot obtained for steady-state values of urea determined with the enzyme probe.

oped for the determination of urea. The probe is based on the enzyme urease in close proximity to the Ir/Pd MOS capacitor, as shown in Fig. 2. Working buffer solutions containing urea at various concentrations were introduced into the cell. The urea diffuses through the dialysis membrane, and ammonia is produced when the urease acts on it. A calibration plot, obtained for steady-state values of urea could thus be obtained (Fig. 3). The nonlinearity of the plot is due to the response characteristics of the sensor and diffusional limitations over the two membranes. The time required for steady-state values to be attained was about 3 min, and urea in standard solutions could be determined up to 5 mM. The lowest detectable concentration was 0.01 mM. The enzyme probe could be used up to four days; after that, the efficiency of the system was markedly reduced because of enzyme deactivation and/or bacterial growth on the dialysis membrane.

These experiments indicate possibilities for determining many other important nitrogen-containing compounds with similar systems using other enzymes.

This work was supported by the National Swedish Board for Technical Development.

REFERENCES

1 H. McCullough, Clin. Chim. Acta, 19 (1968) 101.
2 C. J. Hallet and J. G. H. Cook, Clin. Chim. Acta, 35 (1971) 31.
3 P. W. Alexander and J. P. Joseph, Anal. Chim. Acta, 131 (1981) 103.
4 M. Mascini and G. Guilbault, Anal. Chem., 49 (1977) 795.
5 S. Hirose, M. Hayashi, N. Tamura and T. Kamidate, Anal. Chim. Acta, 151 (1983) 377.
6 A. Spetz, F. Winquist, C. Nylander and I. Lundström, Proc. Int. Meet. Chemical Sensors, Kodansha, Japan, 1983.
7 F. Winquist, A. Spetz, M. Armgarth, C. Nylander and I. Lundström, Appl. Phys. Lett., 43(9) (1983) 839.
8 F. Winquist, A. Spetz, I. Lundström and B. Danielsson, Anal. Chim. Acta, 164 (1984) 000.
9 J. I. Routh, in Fundamentals of Clinical Chemistry, N. W. Tietz (Ed.), W. B. Saunders, Philadelphia, 1976.
10 W. R. Faulkner and J. W. King, in Fundamentals of Clinical Chemistry, N. W. Tietz (Ed.), W. B. Saunders, Philadelphia, 1970.

Analytica Chimica Acta, 163 (1984) 151—160
Elsevier Science Publishers B.V., Amsterdam — Printed in The Netherlands

INTERPRETATION OF STATIC AND DYNAMIC RESPONSES OF A DISSOLVED OXYGEN ELECTRODE IN VISCOUS BROTHS

C. G. DUSSAP and J. B. GROS*

Laboratoire de Génie Chimique Biologique, Université de Clermont II, B.P. 45, 63170 Aubière (France)

(Received 9th April 1984)

SUMMARY

The response of an amperometric oxygen electrode is studied theoretically and experimentally for the case of significant liquid film resistance at the outer side of the membrane. The behaviour of the probe in a gas stream is predicted by using a transfer function which involves an electrode model including oxygen diffusion within the electrode. The effects of the liquid film which exists at the membrane surface when dissolved oxygen concentrations are measured, are taken into account by modifying the transfer function. The new expression obtained is used to model the step response of the probe in a 2-l stirred tank fermentor filled with water or xanthane solutions at different concentrations. First, the results are used to correct automatically the steady-state voltage readings of the probe. Secondly, the probe transfer function is used to evaluate k_1a by dynamic measurements: the response to a step change in the gas concentration is transformed via the fast Fourier transform algorithm and k_1a is identified in the Fourier domain by a Gauss—Newton algorithm. Data acquisition, Fourier transform and k_1a identification are implemented on-line on a HP-87 computer. This method of obtaining k_1a values appears to be a generalized moment method. It is shown that it is necessary to consider the liquid film dynamics around the probe in the actual fermenting conditions to evaluate k_1a successfully.

Since its introduction by Clark in 1956, the membrane-covered dissolved oxygen electrode has been widely used both in research and in industry [1]. In aerobic submerged fermentations, the data obtained from dissolved oxygen (DO) measurements not only give information on microbial physiology, but also form the basis for assessing the kinetics of microbial growth and product formation, for yield calculations, for monitoring aeration, and in the comparison of aeration devices and fermentor control. It is obviously important that the output signal of the probes be interpreted correctly so that they can be used effectively in these particular applications.

The purpose of this paper is to propose and describe a generally applicable model of the dynamic behaviour of the probe in a gas stream and in the liquid phase of an aerated fermentor. This model is applied in measuring the aeration capacity of a fermentor, the value of which is characterized by the volumetric mass-transfer coefficient k_1a, which is the most important parameter in scaling up aeration devices.

0003-2670/84/$03.00

THEORY

Modelling of the probe

According to Lee, Luk and Tsao [2, 3], whether the polarization voltage for the membrane-covered DO probe is applied internally (galvanic) or externally (amperometric), the operating principles of the electrode remain the same: provided that the oxygen diffusion is controlled by the membrane covering the cathode, the current output of the probe is proportional to the oxygen partial pressure in the gas or the oxygen activity in the liquid medium. For a mathematical treatment, the following assumptions are made: (1) the thickness of the electrolyte layer between the membrane and the cathode is negligible; (2) the partial pressure of oxygen at the membrane surface is the same as that of the bulk medium; (3) transport of oxygen occurs by diffusion only in the direction perpendicular to the membrane surface. This is the so-called monolayer model, but it can be extended if assumption (1) is not valid by adding a second layer corresponding to the electrolyte thickness.

If the electrode, originally in a fast moving gas stream with a known concentration of oxygen C_1, is rapidly transferred to another gas stream with oxygen concentration C_2, then according to Fick's second law, the unsteady mass balance of oxygen in the probe can be described by

$$\partial C/\partial t = D_0 \partial^2 C/\partial x^2 \tag{1}$$

The initial and boundary conditions are (Fig. 1A):

$$\begin{cases} t = 0, \ x > 0, \ C = mC_1 x/\delta_0 \\ t > 0, \ x = 0, \ C = 0 \\ t > 0, \ x = \delta_0, \ C = mC_2 \end{cases}$$

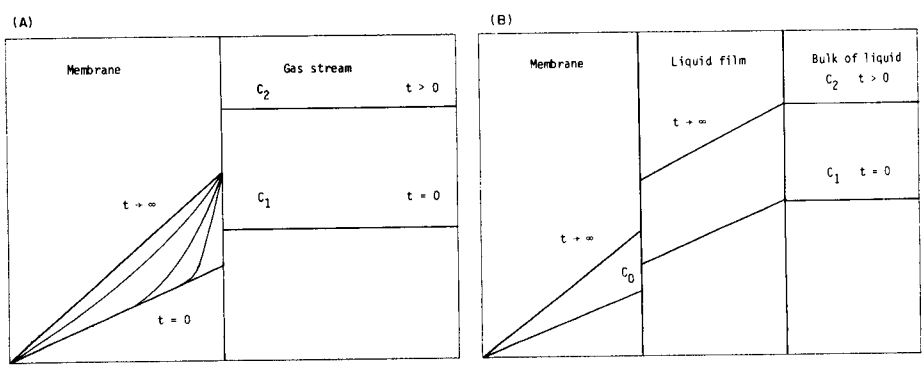

Fig. 1. Schematic diagram of oxygen concentration profiles: (A) within the probe for a step change of concentration in a gas stream; (B) within the probe and the liquid phase for a step change of concentration in the liquid.

(Symbols are defined in Table 1.) The solution to Eqn. 1 with the above conditions has been published by Heineken [4] and independently by Robinson and Wilke [5] as an infinite series of exponential terms. In this paper, the transfer function approach [6] is preferred, Eqn. 1 being the response of the probe system to a step input. The Laplace transform of Eqn. 1 with the corresponding boundary conditions yields

$$p\bar{C} - mC_1 x/\delta_0 = D_0 \mathrm{d}^2\bar{C}/\mathrm{d}x^2 \tag{2}$$

$$\begin{cases} x = 0, & \bar{C} = 0 \\ x = \delta_0, & \bar{C} = mC_2/p \end{cases}$$

which, after integration, gives

$$\bar{C} - mC_1/p = \{\sinh[(p/D_0)^{1/2}x]/\sinh[(p/D_0)^{1/2}\delta_0]\}m(C_2 - C_1)/p \tag{3}$$

From this expression, it becomes possible to calculate the Laplace transform of the oxygen flux at the cathode which is directly proportional to the output voltage of the probe:

$$\bar{E} = km(\mathrm{d}\bar{C}/\mathrm{d}x)_{x=0} = km\{(D_0p)^{1/2}/\sinh[(p/D_0)^{1/2}\delta_0]\} + km(D_0/\delta_0)(C_1/p)$$

If E_0 and $E_{\infty g}$ are the output voltages of the probe at $t = 0$ and $t \to \infty$, respectively, then

$$\bar{E}_0 = E_0/p = km(D_0/\delta_0)(C_1/p)$$

$$\bar{E}_\infty = E_{\infty g}/p = km(D_0/\delta_0)(C_2/p)$$

which leads to

TABLE 1

Symbols used

Symbol	Definition	Symbol	Definition
a	Specific interfacial area for mass transfer	L	Ratio of the oxygen mass-transfer resistance in the membrane to the mass-transfer resistance in the film
C	Oxygen concentration inside the membrane		
C'	Oxygen concentration in the liquid film		
C^*	Oxygen concentration in the liquid at saturation	m	Distribution coefficient
		p	Laplace variable
D	Oxygen diffusion coefficient in the liquid film	t	Time
		x	Abscissa
D_0	Oxygen diffusion coefficient in the membrane	δ	Thickness of the liquid film around the probe
E	Output voltage of the probe	δ_0	Thickness of the membrane
E_0	Output voltage of the probe at $t = 0$	ν	Frequency (Fourier domain)
E_∞	Output voltage of the probe in the liquid at $t \to \infty$	τ	Time constant of the probe in the liquid
		τ_0	Time constant of the probe in a gas stream
$E_{\infty g}$	Output voltage of the probe in the gas at $t \to \infty$	τ_1	Time constant of the liquid film
		τ_2	Time constant for the mass-transfer step
$H(p), H_0(p)$	Transfer functions		
j	Imaginary unit $j^2 = -1$		
k	Proportionality constant		
k_1	Mass-transfer coefficient		

$$\overline{E} - \overline{E}_0 = \{(p/D_0)^{1/2}\delta_0/\sinh[(p/D_0)^{1/2}\delta_0]\}\,(E_{\infty g} - E_0)/p \tag{4}$$

The transfer function of the probe is then given by

$$H_0(p) = (p/D_0)^{1/2}\delta_0/\sinh[(p/D_0)^{1/2}\delta_0] \tag{5}$$

It is worth noting that this function can be expanded in a Taylor's series at $p = 0$ which, limited to the leading term (i.e., the first moment of the transfer function), gives

$$H_0(p) \approx 1/(1 + 1/6\,\delta_0^2 p/D_0) \tag{6}$$

In this case the electrode is characterized by a first-order transfer function with a time constant τ_0 equal to $\delta_0^2/6D_0$. This is why Eqn. 5 will be written as

$$H_0(p) = (6p\tau_0)^{1/2}/\sinh(6p\tau_0)^{1/2} \tag{7}$$

Effect of the liquid film

The probe, when immersed in a stirred liquid, produces a diffusion gradient extending outside the hydrodynamic boundary layer created next to the solid surface of the membrane. The reading of the probe then depends on the rate of diffusion of dissolved oxygen molecules through the boundary layer or film and then through the permeable membrane. Because the level of agitation and fluid properties such as viscosity and oxygen diffusivity will all affect the rate of oxygen transfer across the boundary layer, the response of the probe has a flow dependency. All commercial probes presently available for fermentation use have such behaviour.

If the electrode, originally in a liquid of known oxygen concentration C_1, is rapidly transferred to a liquid at C_2, the unsteady mass balance in the probe and in the stagnant liquid film can be described by

$$\begin{cases} \partial C/\partial t = D_0\partial^2 C/\partial x^2 & (0 \leqslant x < \delta_0) \\ \partial C'/\partial t = D\partial^2 C'/\partial x^2 & (\delta_0 \leqslant x \leqslant \delta + \delta_0) \end{cases} \tag{8}$$

with the initial and boundary conditions (Fig. 1B):

$$\begin{cases} t = 0, & 0 \leqslant x \leqslant \delta_0, & C = mC_0 x/\delta_0 \\ t = 0, & \delta_0 \leqslant x \leqslant \delta + \delta_0, & C' = (C_1 - C_0)(x - \delta_0)/\delta + C_0 \\ t > 0, & x = 0, & C = 0 \\ t > 0, & x = \delta + \delta_0, & C' = C_2 \\ t \geqslant 0, & D_0(\partial C/\partial x)_{x=\delta_0} = D(\partial C'/\partial x)_{x=\delta_0} & \end{cases}$$

The solution of these equations in the Laplace domain gives the following transfer function:

$$H(p) = [b_0 + m(D_0/D)^{1/2}b]\,/[\sinh(b_0)\cosh(b) + m(D_0/D)^{1/2}\sinh(b)\cosh(b_0)] \tag{9}$$

where $b_0 = (6\tau_0 p)^{1/2}$ and $b = (p/D)^{1/2}\delta = (6\tau_1 p)^{1/2}$.

Equation 9 can be reduced to

$$H(p) = H_0(p)/(1 + \tau p) \tag{10}$$

where τ is a time constant that can be expressed as a function of τ_0 and τ_1

$$\tau = [1/(L + 1)][2\tau_0 + (3L + 1)\tau_1] \tag{11}$$

Here, L represents the ratio of the oxygen mass-transfer coefficient through the liquid film (D/δ) to that through the membrane (D_0/δ_0) multiplied by the distribution coefficient m [7, 8]:

$$L = (1/m)(\delta_0/D_0)(D/\delta) = (1/m)(D/D_0)^{1/2}(\tau_1/\tau_0)^{1/2} \tag{12}$$

The value of L can be found experimentally from the steady-state outputs of the probe in air ($E_{\infty g}$) and in air-saturated liquid (E_∞) in given hydrodynamics conditions:

$$L = E_\infty/(E_{\infty g} - E_\infty) \tag{13}$$

It it is assumed that $1/L$ remains small compared with unity, Eqn. 11 can be approximated by $\tau = 3\tau_1$. Combining this with Eqns. 12 and 13 yields

$$(E_{\infty g} - E_\infty)/E_\infty = m(D_0/D)^{1/2}(3\tau_0/\tau)^{1/2} \tag{14}$$

When the probe has been set to 100 in a fast moving air stream, knowledge of the time constant in the second term in Eqn. 14 makes it possible to estimate the output value given by the probe in the liquid saturated with air. The actual value in a fermentation broth can be obtained.

Evaluation of the volumetric oxygen transfer coefficient

If perfect mixing in both liquid and gas phases in the vessel can be assumed, then the oxygen balance in the bulk of liquid can be written as

$$dC/dt = k_1a(C^* - C) \tag{15}$$

At $t = 0$, $C = C_0$. The Laplace transform of Eqn. 15 is

$$\overline{C} - \overline{C_0} = (C^*/p)/(1 + \tau_2 p) \tag{16}$$

where $\tau_2 = 1/k_1a$. The Laplace transform of the output voltage of the probe during the evaluation of k_1a is obtained by the product of the transfer function of the probe and the transfer function of the system (Eqns. 9 and 16 or Eqns. 10 and 16) so that

$$\overline{E} - \overline{E_0} = H(p)(E_\infty/p)/(1 + \tau_2 p) \tag{17}$$

In the case of more complex situations, such as electrolyte resistance to transfer, chemical reaction in the liquid film or imperfectly mixed gas phase, it remains easy to derive relationships in the Laplace domain for the transient response of the system. This is one of the advantages of the approach in the Laplace domain compared to modelling in the time domain by integration of the probe and mass transfer equations [4, 5, 7, 8].

EXPERIMENTAL

The vessel used was a fermentor with a working volume of 2 l (Setric, Model Set 2) fitted with baffles and agitated by a four-bladed turbine stirrer. The dissolved oxygen was measured by a steam-sterilizable amperometric oxygen electrode (Ingold Electrode) and the signal was amplified by an Ingold 4C-501 oxygen-measuring system. The output signal of the electrode, between 0 and +10 V was automatically converted, every 1/28 s, by an analog/digital converter (Hewlett Packard, model 3421-A data acquisition unit) and stored in a digital computer (Hewlett Packard, model HP87).

The air flow rate into the vessel was controlled by a gas flow controller (Air Liquide, model Dynamal 56) and measured by a Brooks rotameter (model R2-15C).

A set of experiments was done to determine the constants for the electrode and for the liquid film, and the volumetric mass-transfer coefficient k_1a. In order to obtain the values of the constant in the transfer function of the electrode, the electrode was suddenly transferred from a nitrogen stream to an air stream at the same temperature or vice versa. The time constant in the liquid film was determined as follows: the step-change response was obtained when the probe, initially in a pure nitrogen stream was suddenly immersed in agitated water saturated with air. Various agitation rates were applied for measurements in the liquid phase. Viscous broths were obtained by use of xanthane solutions (Rhone Poulenc, Rhodopol 23) at different concentrations. For k_1a measurements, the aeration was stopped and the oxygen concentration in the fermentor was set at a very low level (but not to zero) by adding a known amount of sulphite reducing mixture (1 ml of 0.8 M sulphite solution with 10^{-3} M $CoSO_4$ as catalyst). Upon renewed aeration, the oxygen concentration gradually increased as time passed.

For each experiment, the step-response curve stored in the computer was first interpolated by Newton's interpolation formula with divided differences of fifth order [9] to obtain a curve defined by 64 or 128 points. The identification of the constants τ_0, τ_1, τ and k_1a can be done in the frequency domain, provided that the experimental responses given by the probe are transformed in the Fourier domain. This is done by the fast Fourier transform algorithm (FFT) [10]. The analogy between the Laplace transform and the Fourier transform is valid whenever the functions studied are piecewise regular: in our case this implies that the experimental curve transformed is $(E_\infty - E(t))$ instead of $E(t)$. The theoretical, real and imaginary parts are separated analytically by setting $p = 2\pi j\nu$ in the corresponding expression of the Laplace transform:

$$(\overline{E}_\infty - \overline{E})_{th} = [1 - H(p)]E_\infty/p$$

The parameters were then identified by minimization of a quadratic criterion by the Gauss—Newton algorithm. The criterion was expressed as the sum of the squares of the differences between the theoretical and experimental

values of both real and imaginary parts. For data acquisition, data storage and processing, all programs were written in BASIC.

RESULTS AND DISCUSSION

Dynamics of the probe in a gas stream

A typical experiment on the response of the probe is shown in Fig. 2. The real and imaginary parts of the experimental Fourier transform are reported in Fig. 3. Four experiments including up and down step responses were conducted. The mean value of τ_0 obtained after identification with Eqn. 7 is τ_0 = 8.7 s with a mean standard deviation of 0.4 s. The identification with a first-order model (Eqn. 6) leads to the same value for τ_0, but with a criterion value which is 100-times greater. The continuous lines on Fig. 3 correspond to the model (Eqn. 7) for τ_0 = 8.7 s.

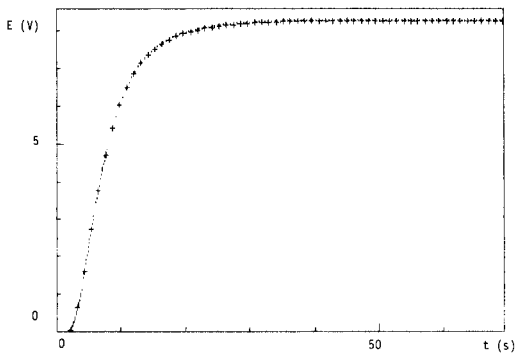

Fig. 2. Experimental response of the probe to a step change of oxygen concentration in the gas phase: output voltage as a function of time (s).

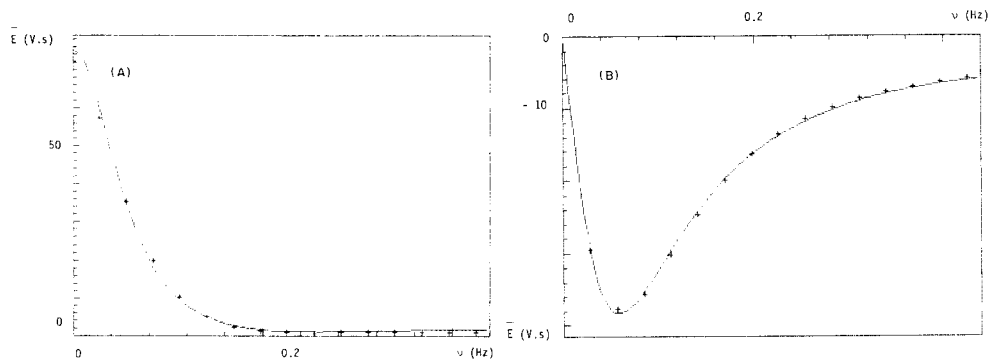

Fig. 3. Real (A) and imaginary (B) parts of the Fourier transform of the experimental response outlined in Fig. 2 compared to the calculated real (A) or imaginary (B) parts of the model (Eqn. 5).

Dynamics of the probe in a liquid medium

The treatment of the experimental data which were obtained to quantify the influence of the liquid film around the probe showed that the two models proposed (Eqns. 9 and 10) were adequate and equivalent; Eqn. 10 will be used below to account for the effect of hydrodynamic conditions in the vicinity of the probe. As mentioned by Lee and Tsao [3], the up and down step responses were not found to be symmetrical, leading to different values for τ. Furthermore, the value of τ is very sensitive to the boundary conditions of the model, particularly the initial concentration profile inside the liquid film and in the membrane which are difficult to control experimentally. This point has been emphasized by Linek et al. [11] who criticized the experimental procedures for the determination of the transient characteristics of oxygen probes adopted by many workers.

The k_1a *determination*

Experimental results in water and in xanthane solutions, an example of which is given in Fig. 4, were treated with Eqn. 17 to obtain k_1a values. First, only τ_2 (i.e., k_1a) was identified, τ_0 and τ being fixed at the values obtained from the former experiments. Secondly, τ and τ_2 were identified simultaneously. The results are presented in Table 2. Whatever the agitation speed and the viscosity of the liquid may be, the results show that, when an oxygen electrode is used in liquid in a fermentor, the liquid film on the membrane surface is unavoidable; this is due to the inherent coupling effect between the mass transfer resistance in the vessel and the liquid film resistance around the probe. However, it may be noted that the increase in the time constant τ in viscous liquids is more than offset by the increase in τ_2, which corresponds to a decrease in k_1a values.

When τ is of the same order of magnitude as τ_2, the accuracy obtained for k_1a values becomes very dependent on the accuracy on τ [12]. The simultaneous identification of the two parameters makes it possible to avoid the ambiguities in the τ determination caused by separate experiments [11]. An

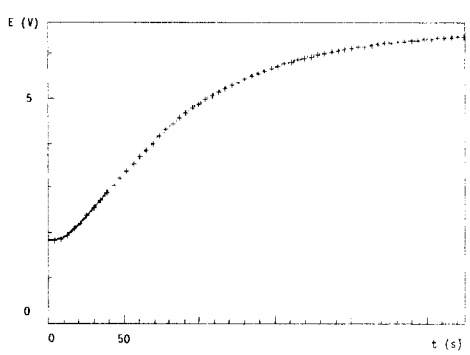

Fig. 4. Experimental response of the probe for k_1a measurement in a 3 g l^{-1} xanthane solution. Volume 1.75 l, gas flow rate 105 l h^{-1}, agitation speed 750 rpm.

TABLE 2

Time constants and k_1a values in water and xanthane solutions (working volume 1.75 l; aeration rate 105 l h^{-1})

Liquid medium	Agitation rate (rpm)	Parameters identified	τ_0 (s)	τ (s)	τ_2 (s)	k_1a (h^{-1})	Criterion value
Water	150	τ_2	8.7	23.4	106.5	33.9	15.20
		τ and τ_2	8.7	16.5	113.4	31.7	6.40
	300	τ_2	8.7	17	64.5	55.8	2.60
		τ and τ_2	8.7	14.9	67.8	53.1	1.12
	750	τ_2	8.7	11.4	26	138	0.207
		τ and τ_2	8.7	11.9	25.5	141	0.183
	950	τ_2	8.7	9.6	13.4	269	0.713
		τ and τ_2	8.7	6.2	17.1	211	0.103
Xanthane (1 g l^{-1})	300	τ_2	8.7	26.3	92.9	38.8	44
		τ and τ_2	8.7	17.7	95.1	37.8	22.6
	750	τ_2	8.7	21.4	23.3	154	2.65
		τ and τ_2	8.7	12.8	32.3	111	0.377
Xanthane (3 g l^{-1})	750	τ_2	8.7	15.5	64.0	56.3	7.60
		τ and τ_2	8.7	16.7	62.8	57.3	7.20
	950	τ_2	8.7	15.5	38.5	93.5	2.23
		τ and τ_2	8.7	17.6	36.3	99.2	2.06

interesting experimental consequence is that k_1a and τ can be determined accurately from the sole knowledge of the dynamic characteristics of the probe in a gas stream.

This method of obtaining k_1a values appears to be a generalized moment method as introduced by Nicolaev et al., cited by Lee and Tsao [3], and used by Linek and co-workers [8, 11]. In fact, the zero-order moment method is deduced directly from the expression of the transfer function at $p = 0$; the experimental zero-order moment corresponds to the first point of the real part of the Fourier transform at $\upsilon = 0$. Finally, this method has the advantage, compared to the frequency response analysis presented by Vardar and Lilly [13], of eliminating the need to create a sinusoidal pressure input in the fermentor.

REFERENCES

1 M. L. Hitchman, Measurement of Dissolved Oxygen, Wiley, New York, 1978.
2 Y. H. Lee and S. Luk, in G. T. Tsao (Ed.), Annual Reports on Fermentation Processes, Vol. 6, Academic Press, New York, 1983.
3 Y. H. Lee and G. T. Tsao, in T. K. Ghose, A. Fiechter and N. Blakebrough (Eds.), Advances in Biochemical Engineering, Vol. 13, Springer-Verlag, Berlin, 1979.
4 F. G. Heineken, Biotechnol. Bioeng., 12 (1970) 145.
5 C. W. Robinson and C. R. Wilke, Lawrence Berkeley Laboratory, Report UCRL, 20472, 1971.

6 D. H. Himmelblau and K. B. Bischoff, Process Analysis and Simulation: Deterministic Systems, Wiley, New York, 1968.
7 V. Linek and V. Vacek, Biotechnol. Bioeng., 18 (1976) 1537.
8 V. Linek and J. Sinkule, Biotechnol. Bioeng., 25 (1983) 1401.
9 R. H. Perry and C. H. Chilton, Chemical Engineers' Handbook, 5th edn. MacGraw-Hill, New York, 1973.
10 C. Demars, Micro-Systemes, 155 (1981) September—October.
11 V. Linek, V. Vacek and J. Sinkule, Biotechnol. Bioeng., 25 (1983) 1195.
12 K. Van't Riet, Ind. Eng. Chem. Process Des. Dev., 18 (1979) 357.
13 F. Vardar and M. D. Lilly, Biotechnol. Bioeng., 18 (1982) 1711.

Analytica Chimica Acta, 163 (1984) 161—174
Elsevier Science Publishers B.V., Amsterdam — Printed in The Netherlands

CARBON MONOXIDE:ACCEPTOR OXIDOREDUCTASE FROM *PSEUDOMONAS THERMOCARBOXYDOVORANS* STRAIN C2 AND ITS USE IN A CARBON MONOXIDE SENSOR

A. P. F. TURNER*, W. J. ASTON and I. J. HIGGINS

Biotechnology Centre, Cranfield Institute of Technology, Cranfield, Bedfordshire MK43 0AL (Great Britain)

J. M. BELL and J. COLBY

Department of Biology, Sunderland Polytechnic, Chester Road, Sunderland SR1 3SD (Great Britain)

G. DAVIS and H. A. O. HILL

Inorganic Chemistry Laboratory, University of Oxford, South Parks Road, Oxford, OX1 3QR (Great Britain)

(Received 16th April 1984)

SUMMARY

The carbon monoxide:acceptor oxidoreductase from autotrophically-grown *Pseudomonas thermocarboxydovorans* strain C2 was purified to 95% homogeneity and found to contain flavin, iron, acid-labile sulphide and possibly molybdenum; its molecular weight was 2.7×10^5. The enzyme catalyzed the oxidation of CO to CO_2 with various electron acceptors including phenazine ethosulphate, methylene blue, hexacyanoferrate(III) and ferrocene derivatives (ferrocene monocarboxylic acid, 1,1'-dimethylferrocene and horse heart cytochrome C) but not viologen dyes, NAD(P) and oxygen. The optimum pH and temperature for enzyme activity in the in vitro assay were 7.5 and 80°C, respectively. Carbon monoxide is the only known electron donor (apparent K_m 5×10^{-7} M) and acetylene, cyanide, 8-quinolinol and sulphydryl reagents inhibited the enzyme. Second-order homogeneous rate constants for the reaction between the reduced enzyme and either cytochrome C (3.0×10^4 l mol^{-1} s^{-1}) or the ferricinium ion of ferrocene monocarboxylic acid (4.0×10^5 l mol^{-1} s^{-1}) were calculated by using cyclic voltammetry. The latter reaction was exploited by incorporating 1,1'-dimethylferrocene in a carbon electrode and retaining carbon monoxide oxidoreductase behind a membrane at the surface. The probe gave a linear current response to aqueous concentrations of carbon monoxide up to 65 μM and achieved a steady current in <15 s. A similar configuration was used to detect gaseous carbon monoxide. With a fuel cell mode, 20 nmol could be detected.

Gram-negative, aerobic carboxydotrophic bacteria contain carbon monoxide (CO): acceptor oxidoreductases (CO dehydrogenases) which catalyse the oxidation of carbon monoxide to carbon dioxide. The enzymes from the mesophilic bacteria *Pseudomonas carboxydovorans* and *Pseudomonas carboxydohydrogena* have been purified and studied in some detail by classical chemical procedures, u.v.-visible spectrophotometry and e.p.r. spectroscopy [1—4]. Both enzymes contain FAD, iron, acid-labile sulphide and

0003-2670/84/$03.00

molybdenum, are specific for CO, use similar electron acceptors and have a similar apparent K_m for CO ($5.3 - 6.3 \times 10^{-5}$ M). The molecular weights of the enzymes from *P. carboxydovorans*, *P. carboxydohydrogena*, *P. carboxydoflava*, *Comomonas compransoris* and unidentified strains OM2, OM3 and OM4 are about 230 000 [5]. In contrast, however, Kim and Hegeman [4] reported a value of 400 000 for the molecular weight of the CO oxidoreductase from *P. carboxydohydrogena* and gave [6], a possible explanation for this disparity. The CO dehydrogenase from *Achromobacter carboxydus* is smaller with a molecular weight of 170 000 [5].

The enzyme from *P. carboxydovorans* is composed of two identical subunits [2], whereas the enzyme from *P. carboxydohydrogena* is apparently composed of at least three different types of subunit [4]. Despite the reported differences between the enzymes from different mesophilic carboxydobacteria, immunological investigations have shown that the enzymes from *P. carboxydohydrogena*, *P. carboxydovorans* and *Azomonas* sp. 2 are structurally similar [6, 7]. Anaerobic bacteria, however, possess a CO dehydrogenase that contains nickel and uses low-potential electron acceptors such as the viologen dyes, ferredoxin and rubredoxin [8—11]. The only CO dehydrogenase isolated from a Gram-positive bacterium, the aerobic, moderately thermophilic actinomycete *Streptomyces* G26 [12] also uses low-potential electron acceptors in vitro.

Enrichment cultures for thermophilic bacteria, able to utilise mixtures of CO and hydrogen, yielded several strains of a Gram-negative, aerobic, moderately thermophilic bacterium named *Pseudomonas thermocarboxydovorans* [13]. When grown with CO as carbon and energy source, this organism contains a CO:acceptor oxidoreductase that is similar to the enzyme from *P. carboxydovorans* whilst showing significant differences in its thermal stability, electron acceptor range and apparent K_m for CO. Such properties make this enzyme particularly suitable for biotechnological applications such as CO scrubbers, CO enzyme-based biofuel cells and CO detectors [14, 15].

A cheap miniature carbon monoxide sensor would have important implications for combustion control, as a fire alarm and for the detection of hazardous concentrations of the gas in domestic, public and industrial situations. A limited range of such sensors is commercially available, operating either by direct electro-oxidation of carbon monoxide or by adsorption on coated semiconductor devices. In the analysis of authentic samples, the most important limitation of these devices is lack of selectivity. Even when it is appropriate to use more costly analytical techniques such as i.r. spectrometry, mass spectrometry and gas—liquid chromatography, analysis of biological samples can be difficult, particularly when low aqueous concentrations of carbon monoxide have to be determined [15].

Several biosensor configurations have been reported that are capable of responding to gases such as neurotoxins [16], methane [17, 18], ammonia [19], nitrogen dioxide [20] and formaldehyde [21]. Most biosensors depend on a secondary transducer, quite separate from the main reaction, which is

capable of detecting the consumption of substrates or the formation of products [14]. Biological redox catalysts, however, may be coupled more simply and effectively to electronic systems by the use of promotors and/or mediators facilitating electron transfer between the catalyst and an electrode. The rapid reversible electrochemistry of horse heart cytochrome C at a 1,2-bis(4-pyridyl)ethene-modified gold electrode has been used to couple the enzyme-catalyzed reduction of dioxygen to an electrode [22]. Oxidative enzyme electrodes based on carbon modified with insoluble ferrocene derivatives have been produced and used to measure methanol [23] and glucose [24].

This paper reports the purification and characterization of CO dehydrogenase from *P. thermocarboxydovorans*, the electrochemical coupling of the enzyme-catalyzed oxidation of CO to a gold electrode via cytochrome C and the construction of a ferrocene-mediated enzyme electrode for amperometric determination of carbon monoxide.

EXPERIMENTAL

Chemicals

Acetylene was prepared by treating calcium carbide with water. Bottled gases were obtained from BOC Special Gases (London). The carbon monoxide supplied to the fermenter as growth substrate was technical grade (99.5%); other gases were of the following purity: carbon monoxide for biochemical studies (99.9%), argon for electrochemical studies (99.998%), hydrogen (99.999%), ethylene (99.8%), methane (99%), nitrous oxide (99.6%). Horse heart cytochrome C, type IV (Sigma Chemical Co.) was purified prior to use by ion-exchange chromatography on carboxymethylcellulose resin (CM32, Whatman) to remove all polymeric and deamidated forms. 1,2-Bis(4-pyridyl)-ethene (Aldrich) was recrystallized from ethanol/water.

Other chemicals and biochemicals were of the highest grade available and were supplied by BDH Chemicals, Sigma, Aldrich, Boehringer Corporation, and Strem Chemicals (Newburyport, MA). Bovine superoxide dismutase (EC 1.15.1.1.) was the kind gift of Dr. J. Bannister (Oxford University).

Culture of the bacteria and enzyme separation

Growth of organisms. The *Pseudomonas thermocarboxydovorans* strain C2 is a thermophilic carboxydobacterium isolated from sewage by enrichment culture under carbon monoxide and hydrogen. The characteristics of the organism have been described elsewhere [13]. The bacteria were grown in batch culture in a magnetically-driven 4-l fermenter (Ultroferm; LKB Instruments) housed in a fume cupboard. The fermenter contained 3 l of mineral base E [25], with twice the usual concentration of ammonium sulphate and supplemented with *p*-aminobenzoic acid (0.1 mg ml^{-1}). The medium was inoculated with 100 ml of an exponential-phase culture of *P. thermocarboxydovorans* C2 and gassed with a mixture of carbon monoxide

(60 ml min^{-1}) and air (100 ml min^{-1}); the dissolved oxygen concentration in the culture was kept low (below 30%). The culture was maintained at 50°C and pH 7.0 (by addition of sterile 1M sodium hydroxide solution) until the absorbance of the culture at 540 nm reached 1.2; the bulk of the culture was then harvested and the remainder used as inoculum for the next culture.

Harvesting and cell breakage. All enzyme extraction and purification work was done at 2—4°C. the culture was harvested by centrifugation at 2000 g for 90 min, washed once with a 10 mM Tris—HCl buffer, pH 7.0/5 mM magnesium chloride solution and stored as a pellet at −20°C until required. For enzyme extraction, the pellet from 3 l of culture was resuspended to a final volume of 20 ml in the above buffered magnesium chloride solution containing deoxyribonuclease (0.1 mg ml^{-1}) and passed once through a French press at 11 000 psi (137 MPa). The crude cell extract was diluted to 50 ml in the same buffer, centrifuged at 30 000*g* for 60 min and at 100 000 g for 30 min; in both cases the supernatant liquids (S30 and S100, respectively) were retained. The CO oxidoreductase activity in crude extracts was determined by using an oxygen electrode.

Enzyme purification. The S100 fraction was pumped on to a 2.5 × 15 cm column of DEAE-cellulose equilibrated with 10 mM Tris—HCl buffer, pH 7.0 and eluted with a 500-ml gradient of 0—0.3 M sodium chloride in the same buffer at 100 ml h^{-1}. The eluant from the column was assayed for CO oxidoreductase activity by the standard spectrophotometric assay (see below) and the active fractions were combined. The DEAE eluant was concentrated and fractionated with ammonium sulphate, the protein precipitating between 35% and 55% saturation being retained and resuspended in a small volume of 10 mM Tris—HCl buffer, pH 7.0. The ammonium sulphate fraction was briefly dialysed against 1 l of the same buffer and pumped on to a 2.5 × 90 cm column of Ultragel AcA34 (LKB Instruments) and eluted with the same buffer at 12 ml h^{-1}. The active fractions were combined and pumped on to a second DEAE—cellulose column (1.5 × 6 cm) equilibrated with 10 mM Tris—HCl buffer, pH 8.0. The column was eluted with a 300-ml linear gradient of 0—0.5 M sodium chloride in the same buffer at a flow rate of 30 ml h^{-1}. The final enzyme preparation was obtained by concentrating the active fractions from the second DEAE—cellulose column with 60%-saturated ammonium sulphate followed by dialysis of the concentrated material against 1 l of 20 mM Tris—HCl buffer, pH 7.0 for 3 h. Enzyme for metal and sulphide analysis was dialyzed overnight against Tris-HCl buffer, 1 mM in EDTA, followed by dialysis against Tris buffer alone. When necessary, enzyme could be stored for prolonged periods at −20°C with little loss of activity after treatment with ice-cold 50% ethanediol.

Purity checks and composition of the enzyme

Polyacrylamide gel electrophoresis. The purity of CO oxidoreductase preparations was determined by slab-gel electrophoresis under non-denaturing

conditions. Enzyme solution (about 1 mg protein ml^{-1}) containing 6% (w/v) sucrose and bromophenol blue marker dye was placed in wells in the stacker gel over a 6.5% (w/v) acrylamide slab gel. The gel was run at room temperature and pH 8.5 at a constant current of 20 mA; the methods and apparatus used were similar to those of O'Farrell [26]. Gels were stained for protein with Coomassie Brilliant Blue R.

The purity of some enzyme preparations was determined by fast protein liquid chromatography (Pharmacia FPLC System), using an anion-exchange resin, and elution with a gradient of 0—1.0 M KCl in 20 mM Tris—HCl buffer, pH 7.

Determination of the molecular weight of CO oxidoreductase. This was done by gel filtration as described by Andrews [27] but on a 2.5 cm × 90 cm column of Ultragel AcA34. Thyroglobulin (m.w. 640 000), ferritin (m.w. 440 000), catalase (m.w. 230 000), yeast alcohol dehydrogenase (m.w. 150 000) and *Escherichia coli* alkaline phosphatase (m.w. 75 000) were the standards.

Spectrophotometry. All spectrophotometric measurements were done with a SP8150 or PU8800 spectrophotometer (Pye-Unicam) fitted with constant-temperature cuvette housings.

Protein, iron and copper were determined as described by Colby and Dalton [28] and flavin and acid-labile sulphide (ALS) as described by Colby and Dalton [29], except that commercial xanthine oxidase was used as standard in the ALS assay. Molybdenum was determined with toluene-3,4-dithiol against molybdenum trioxide as standard [30].

Determination of CO oxidoreductase activity

Unless stated otherwise, the spectrophotometric assay was used. Enzyme activity in crude extracts could not be determined by this assay because of reoxidation of the reduced dyes by molecular oxygen; the oxygen electrode assay was used instead. The latter was also used to determine the apparent K_m for phenazine ethosulphate (PES) because the auxiliary dye in the spectrophotometric assay, 2,6-dichlorophenolindophenol (DCPIP), is also an electron acceptor.

Spectrophotometric assay. Teflon-capped glass cuvettes were charged with 3 ml of solution, which contained 0.15 mmol Tris—HCl buffer (pH 7), 0.015 mmol PES, 2.6×10^{-4} mmol DCPIP, and 0.5 ml of CO-saturated water. The cuvettes were prewarmed to 50° C and the reaction was started by the injection of enzyme solution through the cap. The decrease in absorbance at 600 nm was monitored; the molar absorptivity for DCPIP was taken as 20 650 l mol^{-1} cm^{-1} under the conditions of the assay. Control reaction mixtures contained 0.5 ml of nitrogen-saturated water in place of the CO-saturated water, or contained boiled enzyme solution.

Oxygen-electrode assay. Assays were done in a Tank oxygen electrode chamber (Rank Bros, Bottisham, Cambs.) at 50° C. Reaction mixtures were as above except that the DCPIP was omitted. The output from the electrode

was calibrated by using gas mixtures of known oxygen partial pressures; the solubility of oxygen in water at 50° C was taken to be 2.46 ml per 100 ml.

Enzyme units. One unit of CO oxidoreductase activity is defined as the amount of enzyme catalysing the reduction of 1 μmol DCPIP min^{-1} in the spectrophotometric assay or the uptake of 1 μmol of oxygen in the oxygen-electrode assay at 50° C.

Electrochemistry

Conventional d.c. cyclic voltammetry experiments were done with a two-compartment glass cell of 1 ml volume separated by a Luggin capillary containing a 4-mm diameter gold disc working electrode, a 1-cm^2 platinum gauze counter electrode and a saturated calomel electrode (SCE) as reference [24, 31]. The working electrode was polished with an alumina-water paste (particle size 0.3 μm) to remove contaminants prior to experiments. Voltammograms were obtained with a potentiostat (Oxford Electrodes, Oxford) and were recorded on a X-Y 26000 A3 chart recorder (Bryans, Mitcham). The reversible electrochemistry of horse heart ferricytochrome C (433 μM) in the presence of 1,2-bis(4-pyridyl)ethene (1 mM), and of ferrocene monocarboxylic acid (200 μM) in argon-saturated Tris—HCl buffer (pH 7, 0.1 M), was established by recording voltammograms at different scan rates (1—100 mV s^{-1}) over the range —200 to 500 mV.

The electrolyte was saturated with carbon monoxide and the experiment repeated in order to assess the effect of the substrate on the electrochemistry of the mediator. Enzyme was then added, to give final concentrations in the range 10—100 μM, and the enhanced anodic current obtained was recorded as a function of the voltage scan rate. The experiment was repeated after addition of carbon monoxide as the final component to ensure that the reaction was substrate-dependent. Superoxide dismutase (20 I.U.) was added to the cytochrome C-coupled system to test for the involvement of the superoxide radical.

The construction of a CO biofuel cell was based on a previously described design for a methanol biofuel cell [32]; in this case, however, the anode compartment contained Tris—HCl buffer (0.5 M, pH 7.5) and CO oxidoreductase (2 mg) with either phenazine ethosulphate or methylene blue as mediator. The voltage across a 10-ohm resistance was recorded.

A homogeneous coulometric assay for carbon monoxide was produced by replacing the methanol dehydrogenase in a previously described configuration [31] with CO oxidoreductase. *N,N,N',N'*-tetramethyl-4-phenylenediamine (TMPD) was used as mediator and the platinum working electrode was poised at 110 mV vs. SCE.

Construction and testing of enzyme probes

Carbon monoxide-sensing probes were constructed by bonding a platinum disc and connecting wire (1 mm diameter) inside the wide end of a Pasteur pipette (Fig. 1). The electrode was polished with alumina and covered with a

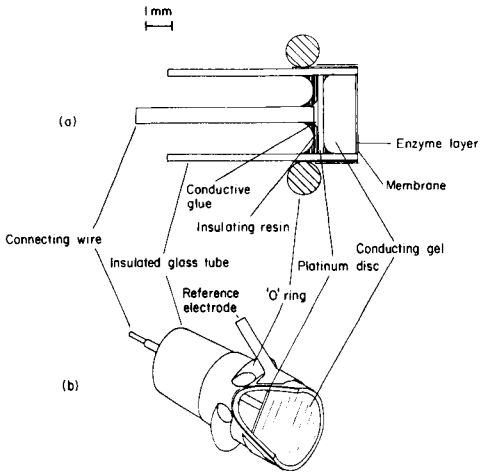

Fig. 1. An enzyme-based CO probe.

conductive paste containing graphite (2.5 g), 1,1′-dimethylferrocene (125 mg) and liquid paraffin (1.5 ml). The CO oxidoreductase (27 μg) was pipetted onto the paste and retained by a disc of polycarbonate membrane (0.03 μm, Nuclepore) held in place by an O-ring. An Ag/AgCl reference electrode, consisting of a cylindrical piece of silver foil, was incorporated into the probe (Fig. 1b). Probes were calibrated at 160 mV (vs. Ag/AgCl) in buffer (5 ml) maintained at 25° C to which aliquots of CO-saturated buffer were added.

A four-channel programmable interface package was designed by A.P.F.T. in association with Artek (59, Langlands, Lavendon, Bucks) for use with a BBC model B microcomputer (Acorn, Cambridge). The interface provided 12-bit software control of the voltage applied simultaneously to four enzyme electrodes and allowed the amperometric response of each to be continuously recorded. Statistical treatment of the data was done within the program which was written principally in BBC BASIC.

RESULTS

Purification and composition of CO oxidoreductase

The results of a typical purification run are shown in Table 1. The procedure resulted in a 15-fold purification with 30% yield. Polyacrylamide gel electrophoresis on non-denaturing slab gels showed the preparation to contain one major band and a second minor contaminating band. Fast protein liquid chromatography gave a similar result; the enzyme preparation contained a major component eluting at 0.45 M KCl and a second minor protein eluting at a slightly lower salt concentration. The minor component represented about 5% of the total protein but none of the CO oxidoreductase activity.

The molecular weight was estimated to be 310 000 by gel-filtration chromatography on a column of Ultrogel AcA34. Sedimentation velocity

TABLE 1

Purification of CO:PES oxidoreductase
(Enzyme activity in the crude extract was determined by the oxygen electrode assay; otherwise the standard spectrophotometric assay was used)

Fraction	Volume (ml)	Activity (U)	Protein (mg)	Specific activity (U mg^{-1} protein)	Recovery (%)	Purification factor
S_{35} extract	38	1400	1750	0.8	100	1.0
DEAE—cellulose eluate I	68	994	160	6.2	71	7.7
35—55% $(NH_4)_2SO_4$ fraction	4.2	952	148	6.4	68	8.0
Ultragel AcA34 eluate	70	714	77	9.3	51	10.4
DEAE—cellulose eluate II	4.7	434	37	11.6	31	14.5

determined by ultracentrifugation of the purified enzyme preparation suggested a lower molecular weight of 230 000 [12]. For the purposes of calculating cofactor compositions, the molecular weight of the enzyme is assumed to be 270 000.

The purified enzyme preparation showed absorption maxima at 270, 335 and 420 nm with a distinct shoulder at 460 nm. Boiling with 1% (w/v) sodium dodecyl sulphate solution caused a change in the absorption spectrum to that typical of free flavin. Assuming the cofactor to be FAD, and the molar absorptivity for FAD to be 11 300 l mol^{-1} cm^{-1} [33], the average FAD content of several different preparations was 1.8 mol mol^{-1} enzyme.

Spectrophotometric assays of several different preparations showed that the average contents of copper, iron, molybdenum and acid-labile sulphide (per mol of enzyme) were 0.7, 6.9, 0.7 and 6.9 mol, respectively.

Properties of the enzyme

The pH—activity dependence for CO oxidoreductase is shown in Fig. 2. The enzyme exhibits greatest activity at pH 7.5 but the peak is broad with >60% of maximum activity observed at pH values between 6.0 and 8.8.

The temperature—activity dependence is shown in Fig. 3. Under the conditions of the assay, maximum activity was observed at 80°C although denaturation at and above this temperature was rapid. A plot of log(velocity) vs. K^{-1}(temperature) was linear between 30 and 65°C, and from the slope the Arrhenius activation energy was calculated to be 36.5 kJ mol^{-1} (8.7 kcal mol^{-1}) with a Q_{10} value of 1.55.

Oxidisable substrates. Potential substrates were tested in the spectrophotometric assay. Gases were tested by adding 0.5 ml of saturated aqueous solutions; cyclohexanol, diethyl ether and n-butylformate were tested by adding 10 μl of the liquid: others were tested at 1 mM and 10 mM concentrations. The following were tested: formaldehyde, methanol, methylammonium chloride, methane, sodium formate, sodium azide, sodium cyanate, sodium malonate, ammonium chloride, sodium nitrite, acetone, potassium cyanide, nitrous oxide, hydrogen, ethylene, acetylene, cyclohexanol, diethylether,

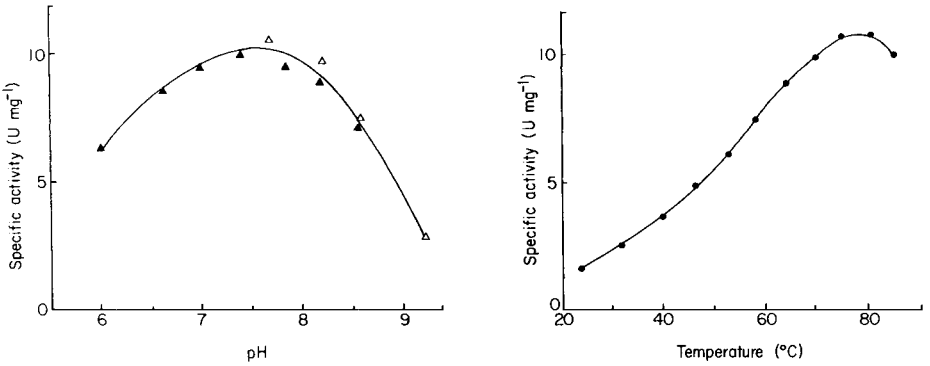

Fig. 2. The pH-activity dependence for CO oxidoreductase: (▲) 50 mM sodium phosphate buffer; (△) 50 mM sodium pyrophosphate buffer.

Fig. 3. Temperature-activity dependence for CO oxidoreductase.

n-butylformate, xanthine, hypoxanthine and adenine. None of these compounds stimulated DCPIP reduction in the assay. On addition of CO to initiate the reaction, only acetylene (70% inhibition) and potassium cyanide (64% inhibition of 10 mM) significantly inhibited CO oxidoreductase.

Apparent K_m *values.* The K_m for CO was estimated by the addition of various volumes of CO-saturated water (saturated and kept at 20° C) during the spectrophotometric assay. The solubility of carbon monoxide at atmospheric pressure and 20° C was taken to be 1.04 mM. Many measurements were made at each concentration and Lineweaver–Burke plots of the data from three different experiments yielded values of 3.1×10^{-7}, 6.1×10^{-7} and 5.3×10^{-7} M; K_m is therefore taken to be 5×10^{-7} M.

The apparent K_m values for PES and PMS were determined by assaying CO oxidoreductase activity in the presence of various concentrations of the acceptors by using the oxygen-electrode assay; the spectrophotometric assay could not be used because the secondary dye, DCPIP, is also an acceptor. Lineweaver–Burke plots were linear with correlation coefficients (r^2) of 0.992 and 0.994 (8 results each or $n = 8$) and yielded apparent K_m values of 5.1×10^{-6} and 6.0×10^{-6} M for PES and PMS, respectively. The V_{max} values were 26.2 and 22.3 unit mg^{-1} protein for PES and PMS, respectively.

Effect of inhibitors and electron acceptors. Enzyme activity was unaffected by the carbonyl reagents, semicarbazide–HCl (1 mM) and hydroxylammonium chloride (1 mM). Of the chelating agents tested, EDTA (1 mM), neocuproin (1 mM) and 1,10-phenanthroline (1 mM) were ineffective whereas 8-quinolinol (1 mM) caused 58% inhibition. The sulphydryl reagents *p*-hydroxymercuribenzoate (0.2 mM), sodium iodoacetate (10 mM) and 2,2-dithio-bis-dinitrobenzoic acid (1 mM) caused 100%, 89% and 84% inhibition, respectively. As reported above, the enzyme was also inhibited by cyanide.

TABLE 2

Activity of CO oxidoreductase with different electron acceptors
(Enzyme purified from *Pseudomonas thermocarboxydovorans* strain C2. Non-autoxidizable acceptors tested spectrophotometrically; autoxidizable acceptors in the oxygen-electrode assay. Positive results confirmed in a modified, anaerobic spectrophotometric assay in which the reaction mixture was saturated with CO, and catalase (1 U), glucose oxidase (1 U) and glucose (0.1 mM) were added to remove residual oxygen. The values quoted (as % of rate with PMS) were obtained by the oxygen-electrode assay)

Electron acceptor	E^0 (mV vs. NHE)	Relative rate	Electron acceptor	E^0 (mV vs. NHE)	Relative rate
Methyl viologen	−440	0	Thionin[a]	+70	38
Benzyl viologen	−359	0	PMS	+80	100
NAD/NADP	−320	0	DCPIP	+217	23
FAD/FMN	−319	0	Cytochrome C (horse heart)	+245	32
Methylene blue[a]	+11	50	Hexacyanoferrate(III)	+429	47

[a]Autoxidizable acceptors.

A range of artificial electron acceptors was tried. Autoxidizable acceptors were tested in the oxygen-electrode assay; the others in the spectrophotometric assay. The results are shown in Table 2. Highest reaction rates were observed with PES and phenazine methosulphate (PMS), although the concentrations of the different acceptors used varied and no attempt was made to measure the maximum rate for each acceptor. The active acceptors all had positive electrode potentials (11—429 mV vs. normal hydrogen electrode). Superoxide dismutase did not inhibit enzyme activity measured with any of the active electron acceptors listed in Table 2.

Stability. Purified enzyme solution (6 mg protein ml^{-1}) lost activity slowly (about 10% activity in 4 days) when kept at 2°C, but lost all activity on freezing and thawing. The enzyme preparation has a half-life of 48 h at 45°C and 50 min at 70°C and solutions lost little or no activity over several weeks when stored at −20°C in 50% (v/v) ethanediol. Enzyme probes lost activity on continual operation at a rate of ca. 12% h^{-1}.

Electrochemical studies

Cyclic voltammetry. The cyclic voltammetric experiments showed no indication of direct electroactivity of either CO oxidoreductase or its substrate; CO had no discernible effect on the voltammetry of either horse heart cytochrome C or ferrocene monocarboxylic acid (Fig. 4a). The addition of enzyme to the system in the presence of either cytochrome C or ferrocene monocarboxylic acid resulted in an enhanced anodic current (Fig. 4b). Quantitative kinetic data for these reactions were obtained under conditions of substrate excess by using the theory developed by Nicholson and Shain [34]. A second-order homogeneous rate constant was calculated for the reaction between either cytochrome C (3.0×10^4 l mol^{-1} s^{-1}) or the ferricinium ion

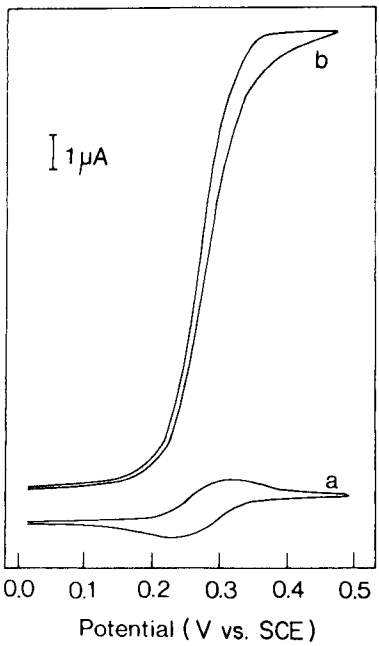

Fig. 4. Cyclic voltammogram of ferrocene monocarboxylic acid (0.2 mM) in argon-saturated Tris/HCl buffer, pH 7.0, saturated with CO: (a) alone; (b) with the addition of 10 μM CO oxidoreductase.

(4.0×10^5 l mol^{-1} s^{-1}) and the reduced enzyme (pH 7, 20° C). These reactions were unaffected by the addition of superoxide dismutase.

Biofuel cell. When the anode compartment of the CO biofuel cell was continuously sparged with CO, the cell produced a current of approximately 1 mA for several hours. Although the cell responded to aliquots of CO, the apparent coulombic efficiency of the system was poor (14%).

Homogeneous CO detector. Aliquots of CO-saturated buffer were added to a stirred solution of TMPD and CO oxidoreductase. The oxidized form of the mediator was regenerated at a platinum electrode poised at 110 mV (vs. SCE) and the charge passed was calculated by integration of the current/time curve. The charge passed bore a linear relationship to the amount of CO up to the maximum of 0.35×10^{-6} mol of CO added. A plot of typical data showed a gradient of $14.4 \pm 0.4 \times 10^3$ C mol^{-1} and an intercept of $0.8 \pm 69.9 \times 10^{-3}$ C (correlation coefficient 0.9982; $n = 7$). These data are consistent with the two-electron stoichiometry of CO oxidation.

Enzyme probe. The four-channel programmable interface was used to test up to four enzyme electrodes simultaneously. The selected voltage was applied to the probes (normally a continuous 160 mV vs. Ag/AgCl) and the steady-state current was recorded for various CO concentrations. Least-squares regression within the program produced the data in the form of a

calibration graph for each probe. Probes responded very rapidly to the addition of aliquots of CO-saturated buffer reaching a steady-state current in less than 15 s. The current obtained was directly proportional to CO concentration up to 68 μM. A typical plot had a gradient of $21.4 \pm 0.5 \times 10^{-3}$ A M^{-1} CO with an intercept of $-6.1 \pm 18.7 \times 10^{-3}$ A (correlation coefficient = 0.9989; $n = 7$).

DISCUSSION

Prior to the work of Lyons et al. [13], studies with carboxydobacteria had been largely confined to mesophilic species with optimum growth temperatures of 25—30°C [6, 35—37]. The CO:acceptor oxidoreductases responsible for the oxidation of CO to CO_2 in two such mesophilic species, *P. carboxydovorans* and *P. carboxydohydrogena*, have been purified and characterized [1—4]. In this study, CO:PES oxidoreductase from *Pseudomonas thermocarboxydovorans* was purified to 95% homogeneity with 30% yield. The specific activity of the final preparation (11.6 unit mg^{-1} protein) lies between the values quoted for the analogous enzyme from the mesophilic carboxydobacteria *P. carboxydovorans* (1.9 unit mg^{-1} [1]) and *P. carboxydohydrogena* (180 unit mg^{-1} [4]).

In many of its properties, CO:PES oxidoreductase resembles the enzymes from mesophilic bacteria as reported by Meyer and his colleagues. Its molecular weight of 270 000 is close to the value of 230 000 quoted for the enzyme from a number of mesophiles [2, 5] and it probably contains 2FAD, 8Fe and 8ALS per mole together with smaller amounts of molybdenum and copper. Further work is required to confirm the presence and catalytic function of molybdenum but it seems likely that CO:PES oxidoreductase is a molybdeno-flavoprotein of the xanthine oxidase type [2, 3].

The enzyme from *P. thermocarboxydovorans* has some novel properties [1, 4]. It is considerably more heat-stable than the mesophilic enzyme with a higher optimum temperature in the spectrophotometric assay (80°C vs. 63°C [1]). The Arrhenius activation energy (36.5 kJ mol^{-1}) reported here is very similar to the value of 36.8 kJ mol^{-1} determined with the enzyme from *P. carboxydovorans* [1]. Unlike the enzymes from the mesophiles, that from *P. thermocarboxydovorans* is rapidly denatured on freezing and thawing although it can be stored for long periods at −20°C in 50% ethanediol. Its apparent K_m for CO (5×10^{-7} M) is two orders of magnitude smaller than previously reported values and the best electron acceptors are PES and PMS rather than methylene blue or thionin. Meyer [2] demonstrated through spectral studies that the enzyme from *P. carboxydovorans* could donate electrons to hexacyanoferrate(III) although the latter was ineffective when tested as an acceptor in the spectrophotometric assay. Similarly, Kim and Hegeman [4] reported that hexacyanoferrate(III) was ineffective as an electron acceptor for the CO:thionin oxidoreductase from *P. carboxydohydrogena.* The present study, however, has shown that hexacyanoferrate(III)

can replace PES as an electron acceptor for the thermophilic enzyme. Unlike the enzyme from *P. carboxydohydrogena*, CO:PES oxidoreductase can use 2,6-dichlorophenolindophenol as acceptor and is markedly inhibited by sulphydryl reagents. In addition, reduction of horse heart cytochrome C by CO:PES oxidoreductase did not appear to be mediated by the superoxide radical because the reaction proceeded under anaerobic conditions and was not inhibited by the presence of superoxide dismutase [37].

The coupling of an oxidative enzyme to an electrode via cytochrome C allows a number of biosensor configurations to be considered. By exploiting the direct electrochemistry of cytochrome C, the need for low-molecular-weight mediators is avoided and electron transfer from enzymes via this protein may be envisaged according to the general scheme

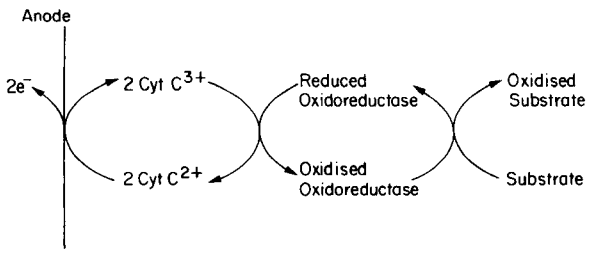

The ferrocene-mediated reaction was, however, an order of magnitude faster.

The construction of the CO biofuel cell illustrates an important principle because it exploits the complete biological oxidation of a practical fuel by a single enzyme. The inefficiencies observed were presumably associated with the problems of handling CO in a cell designed for less volatile substrates; CO could easily be lost from the anode both to the atmosphere and through the membrane separating the two half-cells. For quantitative measurements, the single-compartment poised potential configuration was preferred, demonstrating coulombic efficiencies of ca. 75%.

A probe configuration would have many obvious advantages over a homogeneous assay system for detection of carbon monoxide in the field. The rapid reaction between CO oxidoreductase and the ferricinium ion provided a route to an oxygen-independent sensor [24] based on a carbon electrode modified with the insoluble ferrocene derivative, 1,1-dimethylferrocene. The present data show that such an approach is feasible for the detection of carbon monoxide in either solution or gas phase. The response time and range of the sensor were good, but work is required to improve the stability of the system. Alternative enzyme immobilizations, the use of intact micro-organisms and improvements in the design and operation of the probe are being investigated in order to achieve a stable detector.

A.P.F.T. is a Senior Research Fellow of the British Diabetic Association. J. Colby thanks the SERC for financial support.

REFERENCES

1 O. Meyer and H. G. Schlegel, J. Bacteriol., 141 (1980) 74.
2 O. Meyer, J. Biol. Chem., 257 (1982) 1333.
3 R. C. Bray, G. N. George, R. Lange and O. Meyer, Biochem. J., 211 (1983) 687.
4 Y. M. Kim and G. D. Hegeman, J. Bacteriol., 148 (1981) 904.
5 H. Cypionka, O. Meyer and H. G. Schlegel, Arch. Microbiol., 127 (1980) 301.
6 Y. M. Kim and G. D. Hegeman, Int. Rev. Cytol., 81 (1983) 1.
7 Y. M. Kim, S. Kirkconnell and G. D. Hegeman, FEMS Microbiol. Lett., 13 (1982) 219.
8 R. K. Thauer, G. Fuchs, B. Kaufer and U. Schnitker, Eur. J. Biochem., 45 (1974) 343.
9 H. L. Drake, S. I. Hu and H. G. Wood, J. Biol. Chem., 255 (1980) 7174.
10 S. W. Ragsdale, J. E. Clark, L. G. Ljungdahl, L. L. Lundie and H. L. Drake, J. Biol. Chem., 258 (1983) 2364.
11 S. W. Ragsdale, L. G. Ljungdahl and D. V. DerVartanian, J. Bacteriol., 155 (1983) 1224.
12 J. Bell, E. Williams and J. Colby, in R. K. Poole and C. S. Dow (Eds.), Microbial Gas Metabolism, SGM Symposium, Academic Press, London, 1984, in press.
13 C. M. Lyons, P. Justin, J. Colby and E. Williams, J. Gen. Microbiol., 130 (1984) 1097.
14 W. J. Aston and A. P. F. Turner, in G. E. Russel (Ed.), Biotechnology and Genetic Engineering Reviews, Vol. 1, Intercept, Newcastle upon Tyne, 1984, p. 89.
15 A. P. F. Turner, W. J. Aston, G. Davis, I. J. Higgins, H. A. O. Hill and J. Colby, in R. K. Poole and C. S. Dow (Eds.), Microbial Gas Metabolism, SGM Symposium, Academic Press, London, 1984, in press.
16 L. H. Goodson and W. B. Jacobs, in E. K. Pye and L. B. Wingard, Jr. (Eds.), Enzyme Engineering, Vol. 2, Plenum Press, New York, 1974, p. 393.
17 T. Okada, I. Karube and S. Suzuki, Europ. J. Appl. Microbiol. Biotechnol., 12 (1981) 122.
18 I. Karube, T. Okada and S. Suzuki, Anal. Chim. Acta, 135 (1982) 61.
19 M. Hikuma, T. Kubo, T. Yasuda, I. Karube and S. Suzuki, Anal. Chem., 52 (1980) 1020.
20 T. Okada, I. Karube and S. Suzuki, Biotechnol. Bioeng., 25 (1983) 1641.
21 G. G. Guilbault, Anal. Chem., 55 (1983) 1682.
22 H. A. O. Hill, N. J. Walton and I. J. Higgins, FEBS Lett., 126 (1981) 282.
23 W. J. Aston, R. E. Ashby, I. J. Higgins, L. D. L. Scott and A. P. F. Turner, in M. J. Allen and P. N. R. Usherwood (Eds.), Charge and Field Effects in Biosystems, Abacus Press, Tunbridge Wells, 1984, p. 491.
24 A. E. G. Cass, G. Davis, G. D. Francis, H. A. O. Hill, W. J. Aston, I. J. Higgins, E. V. Plotkin, L. D. L. Scott and A. P. F. Turner, Anal. Chem., 56 (1984) 667.
25 J. D. Owens and R. M. Keddie, J. Appl. Bacteriol., 322 (1969) 338.
26 P. H. O'Farrell, J. Biol. Chem., 250 (1975) 4007.
27 P. Andrews, Biochem. J., 96 (1965) 595.
28 J. Colby and H. Dalton, Biochem J., 171 (1978) 461.
29 J. Colby and H. Dalton, Biochem J., 177 (1979) 903.
30 J. Cardenas and L. E. Mortenson, Anal. Biochem., 60 (1974) 372.
31 G. Davis, H. A. O. Hill, W. J. Aston, A. P. F. Turner and I. J. Higgins, Enzyme Microb. Technol., 5 (1983) 383.
32 A. P. F. Turner, W. J. Aston, I. J. Higgins, G. Davis and H. A. O. Hill, Biotechnol. Bioeng. Symp., 12 (1982) 401.
33 H. Beinert, Enzymes, 2 (1960) 339.
34 R. S. Nicholson and I. Shain, Anal. Chem., 36 (1964) 706.
35 A. N. Nozhevnikova and L. N. Yurganev, in M. Alexander (Ed.), Advances in Microbial Ecology, Vol. 2, Plenum, New York, 1978, p. 203.
36 B. Bowien and H. G. Schlegel, Ann. Rev. Microbiol., 35 (1981) 405.
37 O. Meyer and H. G. Schlegel, Ann. Rev. Microbiol., 37 (1983) 277.

Analytica Chimica Acta, 163 (1984) 175—183
Elsevier Science Publishers B.V., Amsterdam — Printed in The Netherlands

APPLICATION OF ^{13}C-n.m.r. SPECTROSCOPY TO STUDY THE MECHANISM OF *N*-DEMETHYLATION OF [*N*—Me—^{13}C] CODEINE BY CELL-FREE EXTRACTS OF *CUNNINGHAMELLA BAINIERI*

MARK GIBSON, COLIN J. SOPER* and ROBERT T. PARFITT
School of Pharmacy and Pharmacology, University of Bath, Bath BA2 7AY (Great Britain)
(Received 3rd April 1984)

SUMMARY

Codeine was synthesized with 90% enrichment of the *N*-methyl group with carbon-13. *N*-Demethylation of this substrate by cell-free extracts of *Cunninghamella bainieri* in an n.m.r. tube gave norcodeine and ^{13}C-labelled formaldehyde. Fourier-transform ^{13}C-n.m.r. spectroscopy was used to observe the *N*-demethylation process at selected temperatures. The labelled formaldehyde liberated was trapped with sodium sulphite, and the sulphite adduct, as well as intermediates, were located in the n.m.r. spectrum at each temperature. Intermediate resonances assignable to codeine-*N*-oxide were not detected during these enzyme-transformation studies. These data suggest that the observed ^{13}C-n.m.r. signals correspond to the chemically labile carbinolamine intermediate formed during *N*-demethylation. A methine ^{13}C signal was not observed. Thus, *N*-demethylation of codeine by *Cunninghamella bainieri* occurs by direct *C*-oxidation and not via an *N*-oxide intermediate.

The *N*-dealkylation of pharmaceutically important molecules is often an important intermediate step in drug synthesis and manufacture but such reactions can be difficult or hazardous to achieve by direct chemical means, often resulting in variable yields and involving toxic reagents [1]. However, *N*-dealkylation of *N*-methyl substituted compounds is a common metabolic pathway in many microbial and mammalian species [2]. The use of micro-organisms may offer an alternative means of preparing *N*-dealkylated drug intermediates.

It has been demonstrated [1] that both viable cells and cell-free extracts from several species of the fungus *Cunninghamella* are capable of *N*-demethylating drug molecules: for example, the tertiary amine codeine is transformed to afford the *N*-demethyl derivative norcodeine and formaldehyde. Evidence has also been reported [3] that the *N*-demethylase enzyme from *Cunninghamella* is probably membrane-bound. Furthermore, a peak in the u.v. carbon monoxide-reduced difference spectrum around 450 nm suggested the involvement of a cytochrome P450-linked monooxygenase [4], which requires NADPH, NADH and Fe^{2+} for the *N*-demethylation of codeine.

Although *N*-dealkylation has been observed widely in both mammalian and microbial metabolism, the mechanism has been disputed, primarily

0003-2670/84/$03.00

because in most instances intermediates are not readily observable because of their lability. Tertiary amines are susceptible to two routes of oxidation [5] (Fig. 1). In the first, primary oxidative attack is thought to occur upon the carbon α to nitrogen (α-C oxidation) to give a carbinolamine which, because of its inherent instability, decomposes rapidly to the secondary amine and a corresponding carbonyl product, possibly via the unstable azmethine. An alternative mechanism involves metabolic attack on the nitrogen (*N*-oxidation) to produce an *N*-oxide which in certain limited cases may undergo dealkylation to yield the corresponding secondary amine and carbonyl products. Additionally, tertiary amine *N*-oxides are readily reduced to the parent drug [6—8] and some may undergo a rearrangement to the corresponding α-carbinolamines.

Proton, ^{31}P- and, more recently, ^{13}C-n.m.r. spectroscopy have been developed as elegant methods for biochemical and metabolic studies and have the advantage of being non-destructive techniques [9—11]. In the past, the low natural abundance of carbon-13 (1.1%) has restricted its experimental use, but with the advent of high-resolution Fourier-transform n.m.r. spectrometers, and the development of ^{13}C-enrichment techniques, this is no longer an impediment.

In the past, biosynthetic pathways have been studied by feeding ^{13}C-labelled substrates to different micro-organisms and measuring the ^{13}C-n.m.r. spectra of the extracts [12—15]. Such n.m.r. studies have also been done with intact cells in suspension [16], and even with whole organ preparations [17, 18]. Carbon-13 is used as a tracer, and chemical shift changes resulting from the biochemical transformations are observed. The applications of ^{13}C-n.m.r. to metabolic studies have been reviewed by Scott and Baxter [19]. Similar techniques have been used to observe metabolic pathways involving enzyme-catalysed reactions where unstable or transient intermediates were involved [20—24].

This paper reports the use of ^{13}C-n.m.r. spectroscopy to detect the intermediates in the *N*-demethylation of codeine. Enriched [*N*—Me—^{13}C] codeine

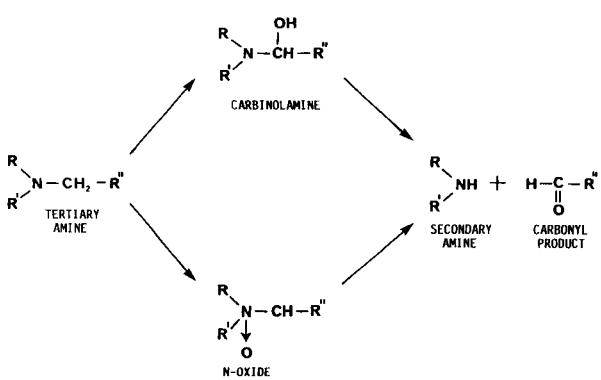

Fig. 1. Mechanisms of *N*-dealkylation of tertiary amines.

was *N*-demethylated in the n.m.r. tube by cell-free extracts of *Cunninghamella bainieri* so that the intermediates, and subsequently the formaldehyde liberated, were also ^{13}C-enriched. Carbon-13 spectra constructed at progressive times during the enzyme reaction show signals for the carbon-enriched species only, which are identified by their chemical shift values and their off-resonance splitting patterns. Natural abundance ^{13}C-signals are too weak to be detected under the conditions of the experiment.

EXPERIMENTAL

Cunninghamella bainieri (C43) was maintained on malt extract agar slopes at 4° C, and grown in liquid media using the 2-stage procedure of Sewell [25]. Codeine (1 mM) was added to the stage 2 cultures as an enzyme inducer. The microbial cells from 10-day cultures were extracted as previously reported [3] to produce the "cell-free extract". This was stored at 4° C in an atmosphere of nitrogen until required for use. Protein in the cell-free extract was determined by the method of Sedmak and Grossberg [26].

Codeine *N*-oxide standard was prepared from codeine base by the method of Groutas et al. [27]. Codeine [*N*—Me—^{13}C] was synthesized in two stages. In the first stage normethylcodeine was prepared from codeine base by the method used by Montzka et al. [28] to *N*-demethylate morphine, as described by Sewell [25]. Then, codeine [*N*—Me—^{13}C] was prepared from normethylcodeine by the method of Anderson and Woods [29] but employing ^{13}C-formaldehyde with 90% atom enrichment. The hydrochloride of the resulting codeine (*N*—Me—^{13}C) was prepared and was used in the transformation studies.

A Jeol FX-90Q high-resolution Fourier-transform n.m.r. spectrometer operating at 22.5 MHz was used to observe ^{13}C resonances, and a Jeol JES-VT temperature controller was used to vary the probe temperature from 5° to 40° C (±0.5° C). For temperature control below 21° C, nitrogen gas evaporated from liquid nitrogen in a 10-l metal Dewar flask was employed; the evaporation rate was controlled automatically. For temperature control above 21° C, air from an air compressor passed through a heat blasting pipe was used; the temperature of the air was automatically controlled.

For an average spectral width of 5000 Hz, a 4-μs pulse corresponding to a tilt angle of 30° was employed, with a 1.8192 s interval (acquisition time + 1-s pulse delay) between pulses. The n.m.r. sample tubes were 10 mm in diameter. A sealed D_2O capillary was used to provide the lock signal.

Concentrated solutions of the standards (100 mg in 0.5 ml) prepared in a suitable solvent (see below) were used for spectral measurements. Complete decoupled spectra (COM) and off-resonance spectra (OFR) were constructed for each solution, and the chemical shifts calculated with reference to tetramethylsilane (TMS) (0 ppm). Spectra were obtained from mixtures of ^{13}C-labelled formaldehyde solution (50 μl) in the presence of each of the trapping agents listed in Table 1 to produce 3 mM solutions in D_2O. The sodium hydrogensulphite solution was prepared freshly from sodium metabisulphite

solution (5% w/v) to give a final concentration in the formaldehyde—D_2O solution of 1% w/v. Alcohol dehydrogenase (2 I.U.) and NADH (1×10^{-4} M) were added to the formaldehyde solution (50 μl) in 0.5 ml of D_2O.

The enzyme reaction was initiated by adding codeine [N—Me—^{13}C] hydrochloride (10 mg) in a solution (0.2 ml) of iron(II) sulphate (1×10^{-4} M), NADH (1×10^{-4} M), NADPH (1×10^{-4} M) and sodium sulphite (3×10^{-3} M) in Sorensen's phosphate buffer (0.066M, pH 7.0) [30], to a cell-free extract (1.8 ml) contained in a 10-mm diameter n.m.r. sample tube. The spectrometer was locked onto the D_2O capillary, placed coaxially inside the n.m.r. tube, and accumulation of spectra was commenced in the COM mode. The ^{13}C-n.m.r. spectra were constructed at frequent intervals to observe the progress of the enzyme transformation. The operation was repeated in the OFR mode, and at different temperatures in the range 5—40°C.

RESULTS AND DISCUSSION

Carbon-13 n.m.r. spectra in the COM and OFR modes were determined for solutions of codeine hydrochloride and codeine N-oxide standards in D_2O. The spectra were interpreted with the aid of references [31] and chemical shift values assigned for the N-methyl carbons of codeine hydrochloride and codeine N-oxide. These were 41.5 ppm and 58.3 ppm, respectively, with TMS as reference.

Microbial N-demethylation of codeine produces norcodeine and an equimolar concentration of formaldehyde. Free formaldehyde is capable of combining with other components in the transformation mixture to produce various ^{13}C-labelled artefacts. To prevent this occurring, formaldehyde may be trapped by the addition of a reagent to the reaction mixture with which it will react to give a single product. The trapping agents most commonly used are carbonyl scavenger compounds, which have the ability to react rapidly and quantitatively with compounds such as formaldehyde to form non-volatile adducts [32].

Signals from ^{13}C-n.m.r. spectra determined for ^{13}C-labelled formaldehyde with various trapping agents selected for their ability to react rapidly with aldehydes [33] are shown in Table 1. The chemical shifts of the N—$^{13}CH_3$ of codeine hydrochloride and codeine N-oxide are included for comparison.

The trapping agents investigated, except semicarbazide and hydrazine, produced a single resonance in the COM spectra. Semicarbazide and formaldehyde react to form a semicarbazone and produced a doublet at 56.9 and 59.9 ppm. Both signals were triplets in the OFR spectra, implicating methylene groups. The signals are believed to occur because the carbonyl group of the semicarbazone can rotate to form two different ring conformations which are stabilised by hydrogen bonds. The magnetic environment of the methylene group will differ in each conformation resulting in the different chemical shifts. Similarly, the reaction of formaldehyde with hydrazine affords three signals (Table 1) arising from the hydrazone, and further

TABLE 1

Chemical shifts of various trapping agents with formaldehyde

Substance[a]	Species present	Chemical shift of ^{13}C-enriched species (ppm vs. TMS)
Codeine—HCl [*N*—Me—^{13}C] alone	$[R_2—\overset{H^+}{\underset{|}{N}}—\overset{*}{C}H_3]Cl^-$	41.6
Codeine *N*-oxide alone	$R_2—\underset{\underset{O}{\downarrow}}{N}—\overset{*}{C}H_3$	58.3
Semicarbazide—HCl[b] + $H\overset{*}{C}HO$	$NH_2CONH—N=\overset{*}{C}H_2$	56.9, 59.9
Hydrazine hydrate[b] + $H\overset{*}{C}HO$	$NH_2—N=\overset{*}{C}H_2$	137.8, 75.9, 70.8
Phenylhydrazine—HCl[b] + $H\overset{*}{C}HO$	$PhNH—N=\overset{*}{C}H_2$	82.4
1% $NaHSO_3$ + $H\overset{*}{C}HO$	$\overset{*}{C}H_2\begin{matrix}\diagup OH \\ \diagdown SO_3\end{matrix}$	74.7
Na_2SO_3[b] + $H\overset{*}{C}HO$	$\overset{*}{C}H_2\begin{matrix}\diagup ONa \\ \diagdown SO_3\end{matrix}$	79.4
Alcohol dehydrogenase + NADH + $H\overset{*}{C}HO$	$\overset{*}{C}H_3OH$	49.5

[a]The enriched carbon is shown by an asterisk. [b]AnalaR grade, (BDH, Poole, England).

reaction of the hydrazone with a second molecule of formaldehyde to give an azine [34].

Alcohol dehydrogenase (ADH), in the presence of NADH, converts formaldehyde to methanol:

$$HCHO + NADH + H^+ \xrightarrow{ADH} CH_3OH + NAD^+$$

The ^{13}C-enriched methanol produces a singlet at 49.5 ppm in the ^{13}C-n.m.r. spectra (Table 1).

For the enzyme transformation studies, it was desirable that the product formed between the trapping agent and formaldehyde possessed one signal in the COM spectra, well displaced from the codeine hydrochloride [*N*—Me—^{13}C] and possible intermediates in the *N*-demethylation reaction. At the concentrations used, it should not interfere with the *N*-demethylation process. Determination of the transformation activity of the cell-free extract, in the presence of each trapping agent, showed that only phenylhydrazine impaired the *N*-demethylation of codeine. The ADH system was disfavoured, as the methanol signal at 49.5 ppm might conceal intermediates in this region

of the spectrum. Because both semicarbazide and hydrazine produce multiplet peaks in the COM spectra, the most suitable trapping agents were sodium sulphite or sodium hydrogensulphite. The sulphite was preferred, because kinetic studies have shown that it reacts with formaldehyde much more rapidly than hydrogensulphite [35] and its signal in the COM spectrum is further downfield from codeine [*N*—Me—^{13}C] hydrochloride.

The rate of an enzyme-catalysed reaction can be influenced markedly by temperature. At sub-optimum temperatures, the decreased rate may enable transient intermediates to appear for longer periods of time. Sewell [25] has demonstrated that *N*-demethylation of codeine by cell-free extracts from *Cunninghamella* species exhibits an optimum between 30° and 32°C. Enzyme denaturation occurred above 40°C. The optimum temperature for the growth of the organism is 27°C. Chemical shifts for codeine [*N*—Me—^{13}C] hydrochloride and the formaldehyde adduct were therefore measured in the presence of all the test mixture components between 5° and 40°C. The chemical shift values did not vary significantly over this temperature range.

N-Demethylation of codeine was initiated by adding codeine [*N*—Me—^{13}C] hydrochloride in solution to the cell-free extract in an n.m.r. tube. A typical series of COM spectra produced at progressive time intervals is shown in Fig. 2. A signal corresponding to the *N*-methyl group of codeine [*N*—Me—^{13}C] hydrochloride (A) was seen above the noise level after only 6 pulses. A signal (C) at +37 ppm relative to codeine was observed after 250 pulses. This corresponds to the formaldehyde—sulphite adduct, and shows that the *N*-methyl group has been completely cleaved. Resonances from intermediates in the *N*-demethylation reaction would occur downfield from codeine if the *N*-methyl group were to be oxidised by the *N*-demethylase enzyme in the cell-free extract. The signal (B) in Fig. 2 at +26 ppm relative to codeine can be seen clearly at 500 pulses, which corresponds to a possible intermediate.

Figure 3 shows the OFR spectrum of the same transformation mixture at 27°C, accumulated for a longer period of time (28 200 pulses). The codeine [*N*—Me—^{13}C] hydrochloride signal (A) is a quartet, typical of the splitting pattern of an *N*-methyl group. The sulphite adduct (C) is a triplet, due to the methylene group. The signal at +26 ppm (B) is also a triplet, again implicating a methylene group. Spectra of control transformation mixtures containing boiled enzyme showed no product or intermediate peaks.

Experiments done at temperatures from 5° to 40°C produced spectra similar to those shown in Fig. 3. Data from the COM and OFR spectra produced from these experiments are shown in Table 2. These results demonstrate that codeine is *N*-demethylated at all the temperatures studied. The signals, which are triplets in the OFR spectra, centred at about +37 ppm, confirm the presence of the formaldehyde—sulphite adduct. Various possible intermediate signals were also observed, but only one occurred in all the spectra at each temperature. This was a triplet in the OFR spectra, in each case centred at +26 ppm relative to codeine.

The two proposed mechanisms for the *N*-dealkylation of tertiary amines are shown in Fig. 1. The tertiary amine, codeine, is *N*-demethylated by a

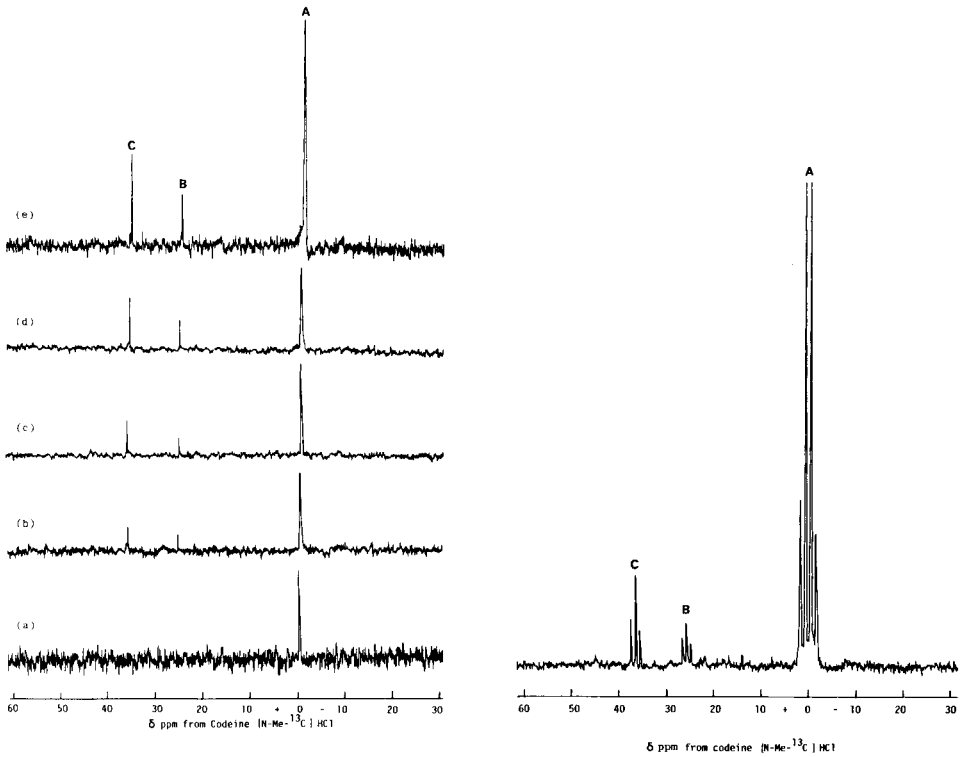

Fig. 2. Time-dependent ^{13}C-n.m.r. spectra (COM mode) for the *N*-demethylation of [*N*—Me—^{13}C]codeine by a cell-free extract of *Cunninghamella bainieri* (27° C, pH 7.0): (a) 6 pulses; (b) 250 pulses; (c) 500 pulses; (d) 1000 pulses; (e) 1500 pulses. (A) Codeine N—$\overset{*}{C}H_3$; (B) intermediate; (C) sulphite adduct HO—$\overset{*}{C}H_2$—SO_3Na.

Fig. 3. ^{13}C-n.m.r. spectrum (OFR mode) for the *N*-demethylation of [*N*—Me—^{13}C]-codeine by a cell-free extract of *Cunninghamella bainieri* (27° C, pH 7.0, 28 200 pulses): (A) codeine N—$\overset{*}{C}H_3$, quartet; (B) intermediate, triplet; (C) sulphite-adduct HO—$\overset{*}{C}H_2$—SO_3Na, triplet.

putative cytochrome P450-type mixed function oxidase extracted from *Cunninghamella* sp. in the presence of molecular oxygen, to yield the secondary amine, norcodeine, and formaldehyde [25]. If *N*-demethylation of codeine was occurring by *N*-oxidation, then an *N*-methyl signal in the OFR spectra would be seen as a quartet centred at 58.3 ppm (or +16.7 ppm relative to codeine) and no such signal is observed (Table 2). Alternatively, the mechanistic route might involve a carbinolamine intermediate generated by direct α-carbon oxidation with an *N*-hydroxymethyl function giving a triplet in the OFR spectrum. The triplet at +26 ppm in Table 2 may well correspond to this. Confirmation cannot be obtained by chemical synthesis because *N*-hydroxymethyl codeine is unstable.

Comparison of the data with those for other compounds containing the carbinolamine moeity is not possible because stable carbinolamines are rare,

TABLE 2

Chemical shifts of signals relative to codeine produced during *N*-demethylation of [*N*—Me—^{13}C]codeine by a cell-free extract of *Cunninghamella bainieri* at various temperatures (pH 7.0)

Temp. of n.m.r. probe (°C)	Chemical shift (ppm relative to codeine)[a]	OFR splitting pattern	Temp. of n.m.r. probe (°C)	Chemical shift (ppm relative to codeine)[a]	OFR splitting pattern
5	+7.2	—[b]	27	+14.8	—[b]
	+25.95	triplet		+26.0	triplet
	+36.8	triplet		+36.96	triplet
10	+25.99	not recorded	30	+26.1	not recorded
	+36.96	not recorded		+36.9	not recorded
21	+12.3	—[b]	40	+26.2	triplet
	+26.1	triplet		+37.0	triplet
	+37.2	triplet			
	+43.4	—[b]			

[a]Codeine *N*-oxide gave a quartet centred at +16.7 ppm relative to codeine; the protein concentration determined for each cell-free extract varied from 0.75 to 1.1 mg ml^{-1}. [b]The splitting pattern could not be interpreted.

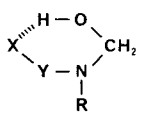

I

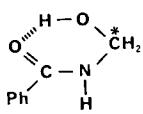

II

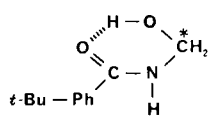

III

Fig. 4. Chemical shifts of stable *N*-hydroxymethyl compounds. I, Basic structure of a stable carbinolamine, with Y—X as the electron-withdrawing group. II, *N*-(Hydroxymethyl)-benzamide with δ_C ($\overset{*}{C}H_2$) = 63.0 ppm vs. TMS or 21.5 ppm vs. codeine. III, 4-(t-Butyl)-*N*-(hydroxymethyl)benzamide with δ_C ($\overset{*}{C}H_2$) = 69.66 ppm vs. TMS or 28.16 ppm vs. codeine.

and for those that are known no ^{13}C-n.m.r. data are available. Gorrod and Temple [36] have reported a series of carbinolamines found as stable metabolites in various mammalian metabolic studies. A prerequisite for their stability appears to be the presence of an electron-withdrawing group (such as carbonyl) adjacent to the nitrogen (Fig. 4). The stability is afforded by the formation of hydrogen bonds between the electron-withdrawing group X and the hydroxyl group to form a ring structure.

In the search for possible anti-tumour agents, Stevens [37] has synthesised a series of stable *N*-(hydroxymethyl) compounds related to formamide. Values for the *N*-(hydroxymethyl) carbon for two of these compounds are listed in Fig. 4. The nitrogen of the codeine carbinolamine intermediate is tertiary and part of the phenanthrene ring, with no electron-withdrawing group adjacent to the nitrogen to stabilise it, so that the chemical shift of the

carbon is likely to be slightly different from the values shown in Fig. 4. However, all these values are similar and suggest, but cannot confirm, that the intermediate at +26 ppm (67 ppm against TMS) observed during the microbial *N*-dealkylation of codeine, could be the carbinolamine proposed.

REFERENCES

1 G. J. Sewell, C. J. Soper and R. T. Parfitt, J. Pharm. Pharmacol., 31 (1979) 90P.
2 J. Rosazza and R. V. Smith, Adv. Appl. Microbiol., 25 (1979) 169.
3 M. Gibson, Ph.D. thesis, Bath University, 1984.
4 T. Omura and R. Sato, J. Biol. Chem., 239 (1964) 2370.
5 J. Rose and N. Castagnoli, Jr., Med. Res. Rev., 3 (1983) 73.
6 J. W. Gorrod and D. J. Temple, Xenobiotica, 5 (1975) 465.
7 P. Hlavica and G. Aichinger, Biochim. Biophys. Acta, 54 (1978) 185.
8 M. Sugiura, K. Iwasaki, H. Noguchi and R. Kato, Life Sciences, 15 (1974) 1433.
9 S. J. Opella, Science, 198 (1977) 158.
10 I. C. Calder, Prog. Drug Metab., 3 (1979) 303.
11 D. E. Case, Xenobiotica, 3 (1973) 451.
12 M. Tanabe, Biosynthesis, 2 (1973) 241.
13 V. Sequin and A. I. Scott, Science, 186 (1974) 101.
14 A. G. McInnes and J. L. C. Wright, Acc. Chem. Res., 9 (1975) 313.
15 A. G. McInnes, J. A. Walter, J. L. C. Wright and L. C. Vining, in G. C. Levy (Ed.), Topics in Carbon-13 NMR Spectroscopy, Vol. 2, Wiley-Interscience, New York, 1976, p. 123.
16 R. G. Shulman, T. R. Brown, K. Ugurbil, S. Ogawa, S. M. Cohen and J. A. den Hollander, Science, 205 (1979) 160.
17 S. M. Cohen, R. G. Shulman and A. C. McLaughlin, Proc. Nat. Acad. Sci., U.S.A., 76 (1979) 4808.
18 A. Bailey, D. G. Baiden, P. M. Matthews, G. K. Radda and P. J. Seeley, FEBS. Lett., 123 (1981) 315.
19 I. A. Scott and R. L. Baxter, Ann. Rev. Biophys. Bioeng., 10 (1981) 151.
20 K. Ugurbil, T. R. Brown, J. A. den Hollander, P. Glynn and R. G. Shulman, Proc. Nat. Acad. Sci., U.S.A., 75 (1978) 3742.
21 J. A. den Hollander, T. R. Brown, K. Ugurbil and R. G. Shulman, Proc. Natl. Acad. Sci., U.S.A., 76 (1979) 6069.
22 S. M. Cohen, S. Ogawa and R. G. Shulman, Proc. Nat. Acad. Sci., U.S.A., 76 (1979) 1603.
23 A. I. Scott, G. Burton and P. E. Fagerness, J. Chem. Soc. Chem. Commun., (1979) 199.
24 G. Burton, P. E. Fagerness, S. Hosozawa, P. M. Jordan and A. I. Scott, J. Chem. Soc. Chem. Commun., (1979) 202.
25 G. J. Sewell, Ph.D. thesis, Bath University, 1982.
26 J. J. Sedmak and S. E. Grossberg, Anal. Chem., 79 (1977) 544.
27 W. C. Groutas, M. Essawi and P. S. Portoghese, Synth. Commun., 10 (1980) 495.
28 T. A. Montzka, J. D. Matiskella and R. A. Martyka, Tetrahedron Lett., 14 (1974) 1325.
29 K. S. Anderson and L. A. Woods, J. Org. Chem., 24 (1959) 274.
30 S. P. L. Sorensen, Biochem. J., 21 (1909) 131.
31 W. F. Wherli, Adv. Mol. Relax. Proc., 6 (1974) 39.
32 National Research Council on Aldehydes (N.R.C.C.) in Formaldehyde and other Aldehydes, National Academic Press, Washington, DC, 1981, p. 132.
33 R. P. Bell and P. G. Evans, Proc. R. Soc., Ser. A., (1966) 297.
34 R. O. C. Norman, in Principles of Organic Synthesis, 2nd edn., Chapman and Hall, London, 1978, p. 315.
35 A. Skrabel and A. Skrabel, Sitz. Akad. Wiss. Wien, 145 (1936) 617.
36 J. W. Gorrod and D. J. Temple, Xenobiotica, 6 (1976) 1265.
37 M. F. G. Stevens, Personal Communication, University of Aston, Birmingham, 1983.

Analytica Chimica Acta, 163 (1984) 185—191
Elsevier Science Publishers B.V., Amsterdam — Printed in The Netherlands

MASS SPECTROMETRIC MONITORING OF 2-OXOGLUTARIC ACID IN FERMENTATION BROTH

E. PUNGOR Jr.*, M. PECS, L. SZIGETI and L. NYESTE

Department of Agricultural Chemical Technology, Technical University, Budapest (Hungary)

J. SZILAGYI

Biogal Pharmaceutical Works, Debrecen (Hungary)

(Received 16th April 1984)

SUMMARY

A mass spectrometric method for monitoring 2-oxoglutaric acid (an essentially non-volatile compound) in aqueous solutions is described. Silicone rubber membranes are used for mass spectrometric sampling; the acid is esterified with methanol. The assay was applied to monitoring 2-oxoglutaric acid in penicillin fermentation broths. Three ion peaks of the ester were suitable for measurements. Preliminary work on faster esterification with diazomethane in diethyl ether is reported.

The ease of controlling a particular process depends strongly on how efficiently the process variables can be measured. Thus, improvements in process control can be expected by reducing the dead time and the sampling time of the measurements, by increasing the frequency of sampling and by improving the reproducibility and accuracy of the measurement [1]. In the case of fermentations, reduction of the dead time and the reproducibility of the measurements cause the biggest technical problems. Compounds must be monitored selectively in the fermentation broth, i.e., in an environment where in most cases very few of the other compounds present are even identified, and this must be done without any (or without time-consuming) separation steps to lower dead time. In addition, the sensors used have to be very stable so that they can operate without recalibration, or with minimal recalibration, during the fermentation. Consideration of these problems makes it easy to understand why so few on-line measurements of chemicals are used routinely in the control of fermentations (partial pressures of O_2 and CO_2 in the gas phase, pH and dissolved oxygen in the broth).

The use of a relatively inexpensive mass spectrometer provides a very flexible approach to multiple compound monitoring without preliminary separations (e.g., chromatography). Mass spectrometry (m.s.) can be used to quantify a variety of volatile compounds in gaseous and liquid samples. In addition, an appropriately selected internal standard makes it possible to

0003-2670/84/$03.00

recalibrate the system continuously to overcome drift problems. In these applications, m.s. systems are used as programmable selective sensors rather than as spectrometers for chemical identification or structural elucidation.

Considerable early work was done on the measurement of dissolved gases in blood [2, 3] and on the direct use of m.s. for monitoring respiratory gases [4, 5]. Other workers have described the use of m.s. for monitoring a number of nondissociating dissolved volatile compounds [6, 7]. Other successful m.s. applications include monitoring dissolved gases and volatile chemicals in fermentation broths [8—11].

The key problem of the application of m.s. to fermentation process monitoring is the sampling of the fermentation broth. In the sampling devices coupled to the spectrometer, the microorganisms must be prevented from entering the vacuum system, i.e., on-line filtration is essential. In some cases, filtration and sampling can be combined by using membrane-covered sampling probes as was done in all the above-cited applications to fermentation.

To extend the range of compounds that can be monitored by m.s., appropriate membranes must be selected and/or volatility conditions must be modified. This latter may involve physical methods (e.g., modification of the temperature of sampling [11] or adjusting the pH of the sample to be able to measure dissolved volatile acids and bases [12]) or chemical and/or enzyme-catalyzed reactions to convert non-volatile compounds to volatile products [13].

The goal of the present work was to develop a method for m.s. monitoring of 2-oxoglutaric acid, an essentially non-volatile compound having no boiling point, by using chemical conversion and to use this method in penicillin fermentation.

EXPERIMENTAL

Hardware and software configuration

An Atomki Model NZC-820 (Atomki, Debrecen, Hungary) quadrupole mass spectrometer was used. This instrument can measure ion peaks in the range 1—300 daltons. The spectrometer was interfaced to a TRS-80 (Tandy Co., TX) personal computer. The computer monitors the output current from the spectrometer and controls the peak selection by generating the programming voltage input of the spectrometer and the gain and low-pass filter of the instrument. Selected ion monitoring was done by taking 120 data points for each ion peak of interest; peak areas were calculated by using the trapezoid rule and the average of 5 consecutive readings was accepted as the measurement result. The control and data acquisition modules of the program were written in Z-80 Assembler language to provide fast execution whereas program modules for interaction with the operator were written in BASIC. Parts of the spectra or entire spectra could also be recorded on a strip-chart recorder.

The spectrometer was equipped with a sampling port to which different sampling probes could be attached. In this study, two types of probe were

used, a perforated stainless steel capillary with a tubular membrane and a flat membrane probe (Fig. 1). The sampling probes were separated from the vacuum system by a safety valve. The total pressure of the system with the valve closed was below 5×10^{-8} mbar and in the range 5×10^{-6}—2×10^{-5} mbar with the valve open, depending on the actual sampling circumstances and the membrane used. The sampling probes were thermostatted all the way to the safety valve by immersing them in the circulating water bath held at the same temperature as that of the sample analyzed.

Additional procedures

Fermentation broth samples obtained from an industrial penicillin production plant at nine different points of the 103-h process were kindly donated by the BIOGAL Pharmaceutical Works. Broth samples were filtered and cooled to 4° C for storage.

The 2-oxoglutaric acid content of the samples was measured after esterification (58.5% filtered broth, 38.5% methanol and 3% sulphuric acid thermostatted at 60° C for 1 h) in a Pye 105 gas chromatograph fitted with a 3% Dexsil/97% Anakrom-Q 90/100 column and a flame ionization detector.

RESULTS AND DISCUSSION

Development of the mass spectrometric method

Preliminary experiments were done with a pure aqueous solution of 2-oxoglutaric acid (62.5 g l^{-1}) to check if there was any m.s. response to a simple acidification of the sample to pH 1. Volatile and involatile acids (formic, acetic, sulphuric and phosphoric acids) were tested for acidification. These experiments yielded negative results: no differences were obtained even at sample temperatures of 60° C when the spectra of the samples were compared to the background spectra obtained by processing the same solutions without 2-oxoglutaric acid. No decay products characteristic of the

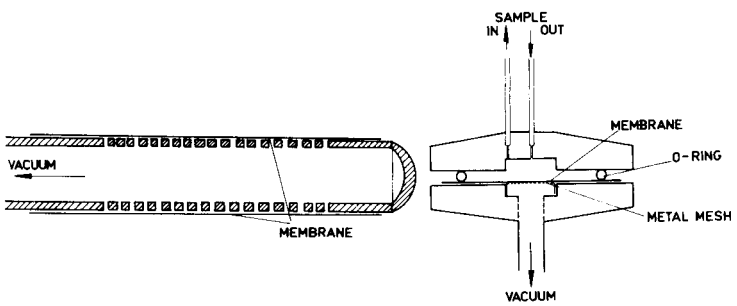

Fig. 1. Sampling probes. The internal diameter of the perforated stainless steel capillary used for the tubular membrane probe is 1.2 mm. The housing and tubing of the flat membrane probe are made of stainless steel; the tubes for transferring the sample are of 1.2 mm diameter.

2-oxoglutaric acid were observed within this temperature range explored (2-oxoglutaric acid itself does not have a boiling point).

Accordingly, experimental work was concentrated on finding a suitable method for the conversion of 2-oxoglutaric acid to a volatile compound and on finding a membrane that could be used to sample the conversion product. Esterification seemed to be the most obvious choice. The ultimate goal was to establish a procedure that could be used for continuous monitoring of 2-oxoglutaric acid requiring no separations, apart from filtration of the broth. Thus the following points had to be considered: (a) the esterification had to be done in aqueous solution in a large excess of water; (b) the reagent had to be easily miscible with water, to avoid partition between phases and the problems with sampling and data-acquisition that would occur if the membrane were exposed to two phases simultaneously; (c) the membrane used had to withstand the esterification conditions, so that separation procedures between the chemical reaction and the sampling for m.s. would not be needed.

To meet these requirements, methanol was used for esterification with acid catalysis (3% v/v sulphuric acid). Different membrane materials were tested (teflon, polyethylene, polypropylene and silicone) for their transmission properties for the methyl ester of 2-oxoglutaric acid. Silicone rubber membranes showed the best selectivity for the ester over the other compounds present (water and methanol) and were used in further work. A study of their solvent resistance showed that a tubular membrane (wall thickness 200 μm) was stable for over 100 h in a 3:2 mixture of water and methanol; this was the best solvent resistance found for the tested membranes. (Screening experiments for transmission were done with 4:1 mixtures of aqueous solution of 2-oxoglutaric acid and methanol with 3% sulphuric acid added, at a controlled temperature of 67.0 ± 0.2° C and mass spectrometry was conducted one hour after the start of the reaction.) When the spectra of solutions treated in this way were compared to the blank spectra (from the same reaction mixture without 2-oxoglutaric acid), ion peaks were observed at m/z (mass/charge) = 60, 75, 86, 88, 116 and 144; the biggest peak was at m/z = 116, which probably corresponds to the ionization product $[M-(COOCH_3) + 1]^+$.

In further experiments, the optimal temperature and methanol concentration for the esterification were established. Figure 2 shows the correlation between the ester signal at m/z = 116 and the concentration of methanol in the reaction mixture; as can be seen the signal can be almost doubled by increasing the concentration of methanol from 20 to 40%. Considering that the total pressure (the total flux of compounds through the membrane is closely correlated with the total pressure) showed a three-fold increase as the methanol concentration increased from 20% to 40%, it is clear that the methanol concentration in the mixture has a greater effect on the equilibrium concentration of the ester than on the total flux through the membrane. The concentration of methanol could not be increased above 40% (v/v) because the stability of the membrane was dramatically decreased by the solvent uptake.

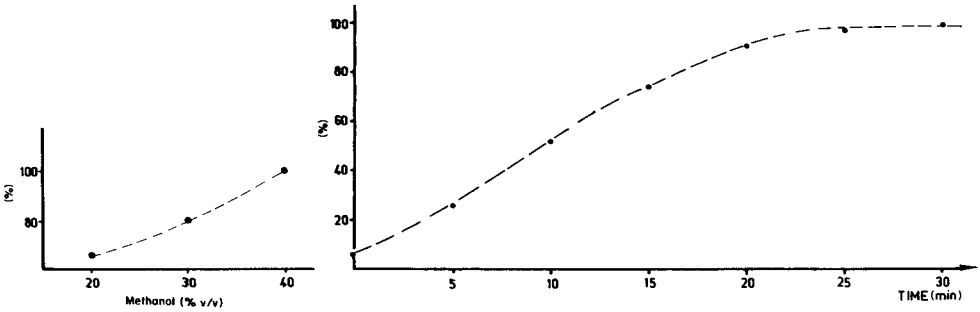

Fig. 2. The effect of methanol concentration on the ester signal at m/z 116.

Fig. 3. The time profile of the ester signal at m/z = 116 during esterification of 2-oxoglutaric acid at 76.5° C.

The temperature had a large effect on the speed of the reaction; 97% response at m/z = 116 was obtained after 57.5 min at 67.5° C but after only 22.5 min at 76.5° C. Therefore, for calibration and measurement, the temperature was controlled at 76.5 ± 0.2° C, just 0.5° C below the observed boiling point of the mixture. The time dependence of the ester signal at m/z = 116 during the course of the reaction at this temperature is shown in Fig. 3. The measured response time of the mass spectrometer was approximately 20 s.

Calibration

Calibration experiments were done under the above optimal conditions. Preliminary experiments showed that for periods of <24 h, the stability of the peak areas was good, e.g., with 100 mM 2-oxoglutaric acid in the initial solution, the ion peak at m/z = 116 deviated by 2.6% (relative) in 8 h. For longer periods, however, it is advisable to use ion peaks from an internal standard in the measurements; the ion peaks of methanol at m/z = 31 and water at m/z = 18 were used successfully.

The calibration curve for the ion peak at m/z = 116 is presented in Fig. 4. (Here and in the further experiments, calibration and measurement data are related to the original concentration of 2-oxoglutaric acid in the aqueous solution before addition of methanol.) For 7 mM 2-oxoglutaric acid, the observed relative standard deviation of five consecutive readings was 5.57%; for a 0.7 mM solution, the relative standard deviation was 7.97% in another experiment when the detection limit was investigated. The calibration curves obtained for the other characteristic ion peaks had the same shape, but the statistical properties were different because of the differences in peak areas.

Measurements in penicillin fermentation broth samples

The filtered samples from penicillin fermentation were treated the same way as the solutions for calibration. Mixtures of 58.5% filtered broth, 38.5%

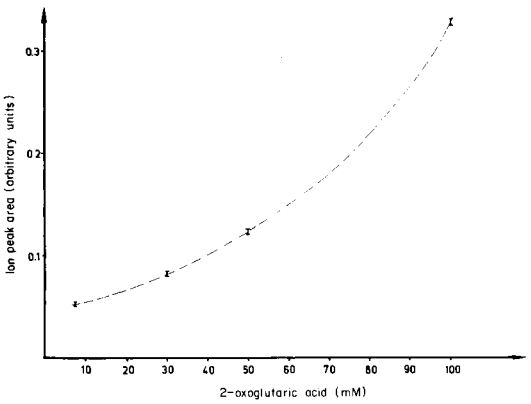

Fig. 4. Calibration curve for 2-oxoglutaric acid based on the ion peak at m/z = 116.

methanol and 3% sulphuric acid were prepared in test tubes which were immersed in a water bath thermostatted at 76.5 ± 0.2° C, for 30 min before spectrometric measurement at the same temperature. All six characteristic ion peaks for 2-oxoglutaric acid were monitored simultaneously.

The performance of the m.s. method was investigated by comparing the results with those obtained by gas chromatography of the same samples (see Experimental). Correlation analysis of the ion peak areas showed that only the peaks at m/z = 86, 116 and 144 behaved similarly. The other three ion peaks showed positive biases (predicting higher concentrations than the real values), probably because of spectral overlap by the ionization fragments of other compounds present in the broth sample. The slopes and correlation coefficients obtained for the computed concentrations by using calibration data of ion peaks at m/z = 86, 116 and 144 are shown in Table 1. In the calibration experiments, the greatest sensitivity was obtained by using the ion peak at m/z = 116, thus this ion peak was accepted for monitoring 2-oxoglutaric acid in penicillin fermentation. The computed concentrations based on the calibration data of ion peak at m/z = 116 are listed in Table 2. These data were also checked by gas chromatography.

It can be concluded that this monitoring technique for 2-oxoglutaric acid is sensitive enough to be applicable to penicillin fermentations. The time delay between sampling and the m.s. measurement is approximately 20 min, which means that the method can be used for control only when the time constant of the process for this variable is large (>40 min). Further studies are now being directed to finding a faster means of esterification. Application of diazomethane in diethylether might be suitable. There is partition of the ester in this process, but preliminary results indicate that this method can also be used in a large amount of water, because esterification is much faster than the hydrolysis of diazomethane, reaching equilibrium within 3 min. For solvent resistance, teflon membranes are needed for this method.

TABLE 1

Slopes and correlation coefficients obtained by comparing the concentrations of 2-oxoglutaric acid predicted by different ion-peak calibrations

Ion peak at *m/z*	vs. ion peak at *m/z*	Slope	Correlation coefficient
116	86	1.092	0.96
116	144	0.933	0.91

TABLE 2

Concentration of 2-oxoglutaric acid, based on calibration at m/z = 116, in the broth samples of penicillin fermentation at different ages

Age (h)	0	9	22	31	55	70	79	95	103
Conc. (mM)	45	44	65	71	70.5	76	81.5	81	82.5

This work was supported by the BIOGAL Pharmaceutical Works and by the Hungarian Academy of Sciences (Grant No. 470-82-12).

REFERENCES

1 G. Kateman and F. W. Pijpers, in P. J. Elvina (Ed.), Chemical Analysis, Vol. 60, Wiley-Interscience, New York, 1981.
2 S. Woldering, F. Owens and D. C. Woolford, Science, 153 (1966) 885.
3 D. Delpy and D. Parker, The Lancet, May 3 (1975) 1016.
4 K. Muysers and V. Schmidt, in G. R. Waller (Ed.), Biochemical Applications of Mass Spectrometry, Vol. 22, Wiley-Interscience, New York, 1972.
5 I. E. Sodal and G. D. Swanson, in J. S. Gravenstein, R. S. Newbower, A. K. Ream, N. T. Smith and J. Barden (Eds.), Essential Noninvasive Monitoring in Anesthesia, Vol. 2, Gruner and Statton, New York, 1980.
6 L. B. Westover, J. C. Tou and J. H. Mark, Anal. Chem., 46 (1974) 568.
7 J. P. Mieure, G. W. Mappes, E. S. Tucker and M. W. Dietrich, in L. H. Keith (Ed.), Identification and Analysis of Organic Pollutants in Water, Vol. 8, Ann Arbor Science, Ann Arbor, 1976.
8 M. Reuss, H. Piehl and F. Wagner, Eur. J. Appl. Microbiol., 1 (1975) 323.
9 E. Pungor Jr., E. Schaefer, J. C. Weaver and C. L. Cooney, Proc. 6th Int. Fermentation Symp., London, Ontario, Canada, 1980.
10 E. Pungor Jr., E. Schaefer, C. L. Cooney and J. C. Weaver, Eur. J. Appl. Microbiol., 18 (1983) 135.
11 E. Heinzle, I. J. Dunn and J. R. Bourne, Proc. 2nd European Cong. Biotechnol., Eastbourne, England, 1981.
12 J. C. Weaver and J. H. Abrams, Rev. Sci. Instrum., 50 (1976) 478.
13 J. C. Weaver, C. R. Perley, F. M. Reames and C. L. Cooney, Biotechnol. Lett., 2 (1980) 133.

Analytica Chimica Acta, 163 (1984) 193—205
Elsevier Science Publishers B.V., Amsterdam — Printed in The Netherlands

MASS SPECTROMETRIC AND FACTOR DISCRIMINANT ANALYSIS OF COMPLEX ORGANIC MATTER FROM THE BACTERIAL CULTURE ENVIRONMENT OF *BACTEROIDES GINGIVALIS*

JAAP J. BOON*, A. TOM, B. BRANDT, G. B. EIJKEL and P. G. KISTEMAKER

Mass Spectrometry of Macromolecular Systems Unit, FOM Institute for Atomic and Molecular Physics, Kruislaan 407, 1098 SJ Amsterdam (The Netherlands)

F. J. W. NOTTEN and F. H. M. MIKX

Preventieve Tandheelkunde, Faculty of Dentistry and Medical Sciences, Catholic University of Nijmegen, P.O. 9101, 6500 HB Nijmegen (The Netherlands)

(Received 17th April 1984)

SUMMARY

Curie point evaporation and pyrolysis mass spectrometry were applied to the analysis of samples from cultures of *Bacteroides gingivalis*, an anaerobic microorganism isolated from the dental sulcus of human patients. Gaseous metabolites were sampled on ferromagnetic wires with an absorbent coating of activated carbon. Smears of bacteria and media after growth were analysed on normal ferromagnetic wires. The mass spectra from analyses at the Curie-point temperatures of 358°C and 510°C were examined with a specially adapted factor discriminant analysis program based on ARTHUR. The bacteria were characterised mainly by their volatile fractions. Mass spectra of the media after growth reflected physiological differences between the strains. The absorbent wire technique proved useful for evaluation of gaseous metabolites. Curie-point evaporation and pyrolysis mass spectrometry was found to be especially useful for preliminary screening of samples of organic matter from the various compartments of the bacterial environment.

Mass spectrometry is an important technique for the characterisation of gases, liquids and solids sampled from natural and artificial environments, such as culture vessels and biotechnological production units. Commercially available equipment can now be used for molecular systems up to 10 000 dalton provided that the sample can be made "vacuum-borne" in an ionised state. Gases and liquids are usually introduced via chromatographic ports to the ion source. Some solid samples can be desorbed and ionised by using special methods such as field-, laser- or fast atom bombardment-desorption. Most solid samples such as whole bacteria, yeasts, fungi, plants and animal cells and their macromolecular fractions are too complex and too large for direct mass spectrometric analysis and must first be transformed to smaller but still characteristic chemical units. The possibilities of using a Curie-point evaporation and pyrolysis direct probe as an inlet to a fast scanning mass spectrometer for the analysis and characterisation of such samples have been investigated and a suitable automated instrument has been developed [1].

0003-2670/84/$03.00

The essential elements of the Curie-point probe are a high-frequency coil and power supply for generation of an oscillating magnetic field and ferromagnetic sample wires which are rapidly heated to their Curie-point in an active high-frequency magnetic field. The wires are disposable and can be used in the analysis of solids, liquids and, with the modification of a coating of absorbent material [2], for gases as well. The Curie temperature of the wires depends on their metallurgical composition; wires with temperatures of 358, 510, 610 and 770°C are available. The fast heating rates obtained in this probe (5000 K s^{-1}) and the rapid removal of the thermal degradation products from the reaction zone guarantee the formation of primary pyrolysis products which carry information about the composition of the macromolecular system under study. Use of a wire end temperature of <360°C leads to a full spectrum of the volatiles contained in the sample (Curie-point evaporation), because thermal degradation of the macromolecules has not yet taken place.

Methods in use for pyrolysis mass spectrometry have been adequately reviewed [3]. An atlas with fingerprints of a great variety of macromolecular samples [4] has greatly facilitated wider use of the Curie-point pyrolysis/electron impact/mass spectrometric (m.s.) technique. A comparative study of various techniques of pyrolysis m.s. (both high and low resolution) and pyrolysis g.c./m.s. applied to the amino-carbohydrate polymer chitin in this laboratory has shown that the results from these methods are highly compatible. Most of the individual components in the pyrolysates of the samples can be identified by chromatographic separation on highly apolar capillary columns prior to mass spectrometry.

Many computer programs for chemometric analysis have been developed or adapted from existing data-analysis packages. A factor-discriminant analysis (f.d.a.) procedure [5] is now applied routinely to series of mass spectral fingerprints in order to identify and quantify characteristic differences between the spectra of the samples. This allows rapid evaluation of relatively large series of complex organic matter samples, but the gain in time is obtained by sacrifice of resolution. The general scheme used here is to evaluate the sample series by the pyrolysis m.s./f.d.a. followed by an elaborate pyrolysis g.c./m.s. program to understand the chemical causes underlying differences between the samples.

This paper describes the results of a Curie-point evaporation/pyrolysis mass spectrometric study of several *Bacteroides gingivalis* strains. An accompanying pyrolysis high resolution g.c./m.s. study will be published separately. Whole bacterial colonies, gaseous waste products and the solid growth media after bacterial growth were analysed in order to understand the chemical ecology of these organisms. *Bacteroides gingivalis* is a potentially pathogenic microorganism, which is associated with periodontal diseases [6]. A selection of strains from several patients was analysed in order to evaluate the possibility of using this technique for characterisation of individual strains in epidemiological studies.

EXPERIMENTAL

Bacterial strains and culture conditions

Bacteroides strains were isolated from dental plaques and sulci from human patients and Beagle dogs. The plaque samples were cultured on BBM agar [7] and incubated in an anaerobic chamber with an atmosphere of 5% hydrogen, 10% carbon dioxide and 85% nitrogen at 37°C for 7 days. The composition of the BBM agar was 2.7% trypticase soy broth (BBL), 0.3% yeast extract (BBL), 5% sheep blood, 2% agar (Difco), 0.25% liver digest (Oxoid), 0.05% sodium thioglycolate, 0.01% sodium carbonate, 0.05% haemin and a 0.005% Menadion. The BBM agar was also used for the agar slants used in the incubation experiments. The human *B. gingivalis* strains Ny 468, Ny 467 and Ny 469 are coded in the text as A, D, and E. The *B. intermedius* strain (Ny 460) isolated from the beagle dog is coded as H.

Sampling for mass spectrometric analysis

Odours. The bacterial odours were sampled by introduction of a ferromagnetic wire with a Curie-point temperature of 358°C coated with activated carbon (Norit SX-1) in the culture environment. A schematic diagram of the system is shown in Fig. 1. The bacterial culture tube is introduced into a glass incubator with a teflon stopper. The wire is inserted in the stopper and kept suspended magnetically about 2 cm above the surface of the solid medium. The absorbent coating on each wire is applied by glueing Norit powder on a thin film of an aqueous saturated sodium silicate solution [2]. The absorbent was activated in an activation unit by Curie-point heating of the coated wire in an inert atmosphere using a high-frequency field. Activated wires were incubated in the bacterial culture environment for 24 h at 4°C. The wires were analysed immediately after removal from the incubators.

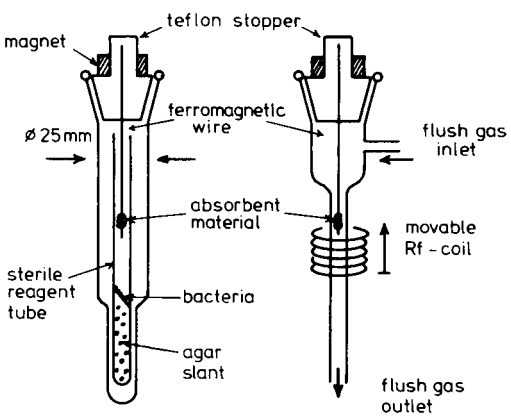

Fig. 1. Schematic diagram of the activation unit for the absorbent wires and the incubator with the bacterial culture in a reagent tube. The absorbent wire is incubated after activation above the living bacterial culture on the agar slant.

Medium and bacteria. Bacteria and solid media were sampled by a sterile platinum needle and applied on ferromagnetic wires with a Curie-point temperature of 358 or 510°C. Bacteria were removed from the surface by careful scraping to avoid contamination of the sample with medium. Samples of the media were taken after removal of the upper 3 mm of the solid medium. The samples were dried briefly in vacuo at 1 mbar and inserted in glass liners for analysis.

Curie-point pyrolysis mass spectrometer

The Curie-point evaporation or pyrolysis mass spectra were obtained with an instrument made in this Institute, equipped with an automatic sampling exchange system, a Curie-point pyrolysis unit, a heated expansion volume and inlet system, a liquid nitrogen-cooled ion chamber, a quadrupole mass analyser (Balzers QMA 150/QMG 511) and an ion-counting detection system [1]. Conditions were as follows: batch size 36 samples. Curie-point temperature 358 and 510°C, temperature rise time 0.1 s, total heating time 0.8 s, expansion chamber temperature 150°C, electron-impact ionisation at 15 eV, mass range 24—180, scan speed 10 scans s^{-1}, total number of averaged spectra 200; samples were analysed in quadruplicate. A Curie-point high-frequency generator (model 9425; Fischer, 5309 Meckenheim bei Bonn, F.R.G.) was used to generate the magnetic field. The ferromagnetic wires were from Philips (5300 PB, Eindhoven, The Netherlands).

Multivariate treatment of the mass spectra by factor-discriminant analysis

The raw data, expressed in ion counts/mass channel, are normalised by expression of the mass intensities as percentages of the total ion counts. Multivariate analysis of the spectra is done on files of selected spectra, using a modified ARTHUR package (Infometrix, Seattle, W.A.); the modifications and expansion of this package with linear discriminant analysis have been described [5]. Principles of the application of this procedure to pyrolysis mass spectra have been described by Windig et al. [8]. The essential elements of the f.d.a. procedure are shown in Table 1. After definition of the file (training set), an overall average spectrum (zero point) is calculated which serves as the reference point for comparison of the individual spectra. This spectrum is also used for scaling of the data set. Positive and negative differences with respect to this reference are evaluated by the f.d.a. program. Covariant mass peaks are linearly combined to new independent variables (discriminant functions). The dissimilarity between the categories (groups of multiplicate spectra) is qualitatively expressed in these discriminant functions, which are represented graphically by reconstructed mass spectra. Dissimilarity is quantitatively expressed in discriminant function scores, which can be plotted as scores curves or maps (in two dimensions).

TABLE 1

Steps in the factor discriminant analysis for the Curie-point mass spectrometer based on an adapted ARTHUR program package expanded with discriminant analysis capabilities

a. Choose the mass spectra for training set and test set.
b. Determine overall average spectrum: zero point.
c. Scale data on $(X-\bar{X})/\sigma$.
d. Run principal components analysis: factors (groups of correlated mass peaks) are found and ordered according to the amount of variance explained.
e. Quantify each factor in each mass spectrum: factor scores.
f. Express each mass spectrum with factors as new variables. Average each category.
g. Repeat c and d: discriminant functions (groups of correlated factors = groups of correlated mass peaks) are found, which describe differences between the categories.
h. Quantify D-functions in each category and pyrolysis mass spectrum: D-scores.

RESULTS AND DISCUSSION

The *Bacteroides* strains investigated in this study consist of anaerobic, Gram-negative, non-sporulating, rod-shaped bacteria, which produce black pigmented colonies when incubated on blood agar plates. Strains of black pigmented *Bacteroides* can be isolated from various parts of the body [9] and appear to be frequently associated with forms of periodontal disease [6]. The precise taxonomy and the biochemical characteristics needed for a meaningful taxonomical differentiation are still under investigation [10—12]. Several metabolic waste products such as indole, phenylacetic acid and C_2—C_5 fatty acids are in use for this discrimination. The present study on some *Bacteroides gingivalis* strains was designed to evaluate the potential application of a Curie-point pyrolysis m.s. system for direct characterisation of the bacterial organic matter; this method had been successful in the differentiation of *Mycobacteria* [13, 14]. The complexity of the metabolism of *Bacteroides gingivalis* and the possible contribution of bacterial metabolites to the mass spectral fingerprints called for characterisation of organic matter in all the environmental compartments of the microorganism, shown schematically in Fig. 2. Gaseous metabolites were collected on absorbent sample wires, samples from the bacteria and the media were applied as smears to normal sample wires and analysed both for volatiles

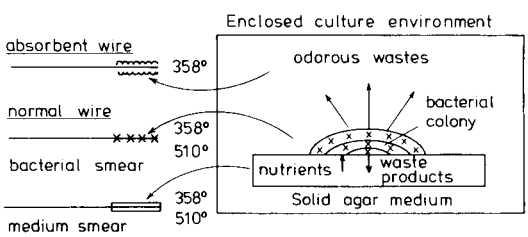

Fig. 2. Outline of the sampling plan for the enclosed bacterial culture of *Bacteroides gingivalis*.

evaporation mass spectrometry) and for macromolecular characteristics (pyrolysis mass spectrometry). Isolates from dental plaques were available from three human patients and one from a dog. Emphasis is given to the analytical aspects here; a more clinically orientated microbiological study will be reported elsewhere.

Mass spectrometry of the bacterial culture environment

Isolated *Bacteroides* strains grown on agar slants in stoppered reagent tubes could be introduced easily in the incubator with the absorbent wire for sampling the head-space gases. A teflon stopper on the incubator was essential to avoid contamination from the incubator itself. Figure 3 shows the mass spectral fingerprint of the gaseous environment of *Bacteroides gingivalis* strain A. The highest peak in this spectrum, m/z 117, corresponds to 60 000 counts, which was about 2000-fold above background. Gaseous products

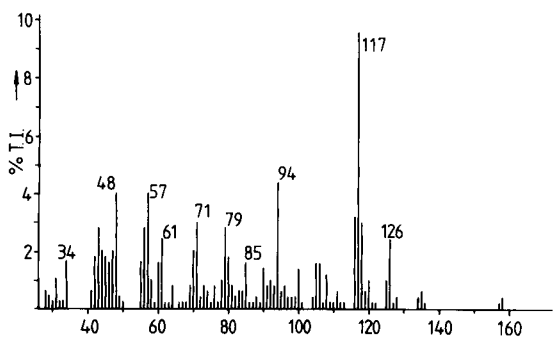

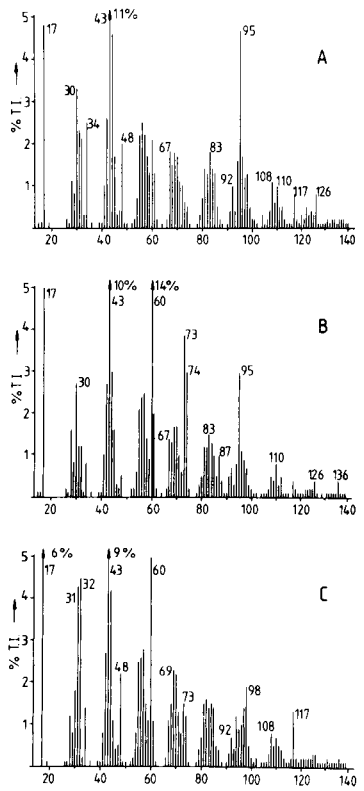

Fig. 3. Curie-point evaporation m.s. fingerprint of the gaseous atmosphere above *Bacteroides gingivalis* (human strain A).

Fig. 4. Curie-point mass spectral fingerprints: (A) the medium before growth; (B) the medium after growth of *B. gingivalis* (human strain A); (C) *B. gingivalis* (human strain A). The Curie-point temperature was 510°C.

were evidently trapped effectively by the absorbent wire and did not seem to be affected appreciably by a short period under vacuum prior to the spectrometry. The low-voltage mass spectrum shown is complex because of its cumulative nature. It shows fragment ions of aliphatic hydrocarbons (i.e., *m/z* 43, 57, 71, 85, 99), the molecular ions and fragment ions of aromatic hydrocarbons (i.e., *m/z* 92 from toluene, *m/z* 105, 106 from xylene, *m/z* 120 and 134 from alkylbenzenes), the molecular ion of indole (*m/z* 117 with a fragment ion at *m/z* 90), a series of mass peaks which point to dimethyl disulphide (*m/z* 94, 79, 61, 47) and dimethyl trisulphide (*m/z* 128, 126, 111, 79) [17], a minor contribution of hydrogen sulphide (*m/z* 34) and possibly methanethiol with a molecular ion at *m/z* 48. No tentative identification can be given for *m/z* 100 and 108. Indole is a well known metabolite of some *Bacteroides* species [10]; hydrogen sulphide, methanethiol and dimethyl disulphide have been shown to be present in the head-space above liquid cultures of *B. gingivalis* [15]. The other compounds need further study.

The pyrolysis mass spectra of the bacterium and the medium before and after growth are shown in Fig. 4. The spectra obtained at 510°C reflect both evaporated and the pyrolytic fractions. The spectrum of the medium before growth (Fig. 4A) closely resembles the pyrolysis mass spectrum of agarose [4], the major constituent of the agar medium, with a relatively high peak at *m/z* 95 and associated mass peaks characteristic for hexose polymers [16]. These carbohydrate-derived peaks in the spectrum can be used conveniently as an internal standard. Other mass peaks (*m/z* 34, 48, 56, 59, 67, 68, 83, 92, 94, 108 and 117) are generated from the various protein fractions [4] and the sheep blood used in the medium. The medium after growth (Fig. 4B) shows, apart from the agar-derived mass peaks and peaks from proteins, several new intense mass peaks, which must result from the bacterial metabolism. Examples are *m/z* 60, 73 and 74, pointing to acetic and propionic acid. These peaks are even more intense in the evaporation mass spectrum obtained at 358°C (not shown). Less intense peaks which are not present in the medium prior to growth are *m/z* 87, 88, 91 and 136 from butanoic and phenylacetic acid. The presence of these acids was confirmed by pyrolysis g.c. The spectrum of the bacterium (Fig. 4C) differs considerably from Fig. 4B because of the absence of the agar derived mass peak series. Peak *m/z* 60 from acetic acid is rather intense. The intensities of peaks *m/z* 117 (indole) and 98 (unknown, but also rather intense in the 358°C spectrum) are relatively high. The mass peaks from other volatile acids known to occur in *B. gingivalis* (propionic, butyric, isobutyric, valeric and isovaleric acid) appear as *m/z* 73, 74, 87 and 102 in the spectrum.

The general conclusion is that indole is present in high concentration in the gaseous phase and to some extent in the bacterium, but absent from the medium after growth. Volatile C_2—C_5 acids are preferentially concentrated in the medium, but small amounts can be volatilised from the bacterial sample. There is evidence for the presence of phenylacetic acid in the bacterium and

the medium after growth. The macromolecular fraction of the bacterium is mostly characterised by proteinaceous material. Further work is needed to establish the detailed composition of the product mixtures and to confirm tentative identifications.

Factor-discriminant analysis

Comparison of the media and bacteria. A file consisting of mass spectra of the media and bacteria from both temperatures was examined by the factor-discriminant procedure. The results are shown in Fig. 5 as a discriminant score map which describes the differences between the spectra quantitatively and accounts for 70% of the characteristic outer/inner variance. Media and bacteria are clearly separated as two elongated clusters. There are clear differences between the individual bacterial strains of human origin, but the *B. intermedius* strain H from the dog plots on top of human *B. gingivalis* strain A under both evaporation and pyrolysis conditions. These strains are discriminated by functions of the third and fourth dimension. All media from the human strains (large triangles enclose 4 replicates) lie close together regardless of the temperature used. There is a clear difference between the spectra of the medium from the dog and from the human strains, which is related to the difference in physiology between *B. gingivalis* and *B. intermedius* strains. Details on the distribution of these sample points and underlying mass spectrometric characteristics expressed in discriminant function spectra were investigated further by examining several subfiles.

Dissimilarity of evaporation and pyrolysis mass spectra. A subfile of evaporation and pyrolysis spectra of the bacteria was examined by the f.d.a. procedure to identify and quantify the contributions of evaporation and pyrolysis products to the mass spectral fingerprints. The difference between the Curie-point analyses at 358°C and 510°C was found to be described in the first factor, which results from unsupervised analysis of all spectra as independent data. This implied that the differences between the spectra were very obvious. Figure 6 shows the reconstructed factor spectra and the distribution of the factor scores of the strains. The division in two groups correlates well with the analysis temperatures. The greater spread in factor scores for the 358°C spectra was probably caused by different residence times of the replicates in the vacuum of the sample exchanger causing some loss of volatile fractions. The differences between the two temperatures are qualitatively expressed in the factor spectra. The mass peaks in Fig. 6A are practically all pyrolysis products of proteins [4]. The peaks at m/z 31, 32, 58, 110 and 112 may relate to a small contribution of pyrolysis products from carbohydrates. The mass peaks in Fig. 6B pertain to molecular ions and fragment ions of the volatile fatty acids (m/z 60, 73, 74, 87, 88 and 102), phenylacetic acid (m/z 91 and 136), indole (m/z 90 and 117) and an unknown volatile compound with m/z 98. These compounds are metabolites of the bacteria as discussed above. Both the factor spectra and the factor scores show that no pyrolysis occurred at 358°C. Unpublished observations on many

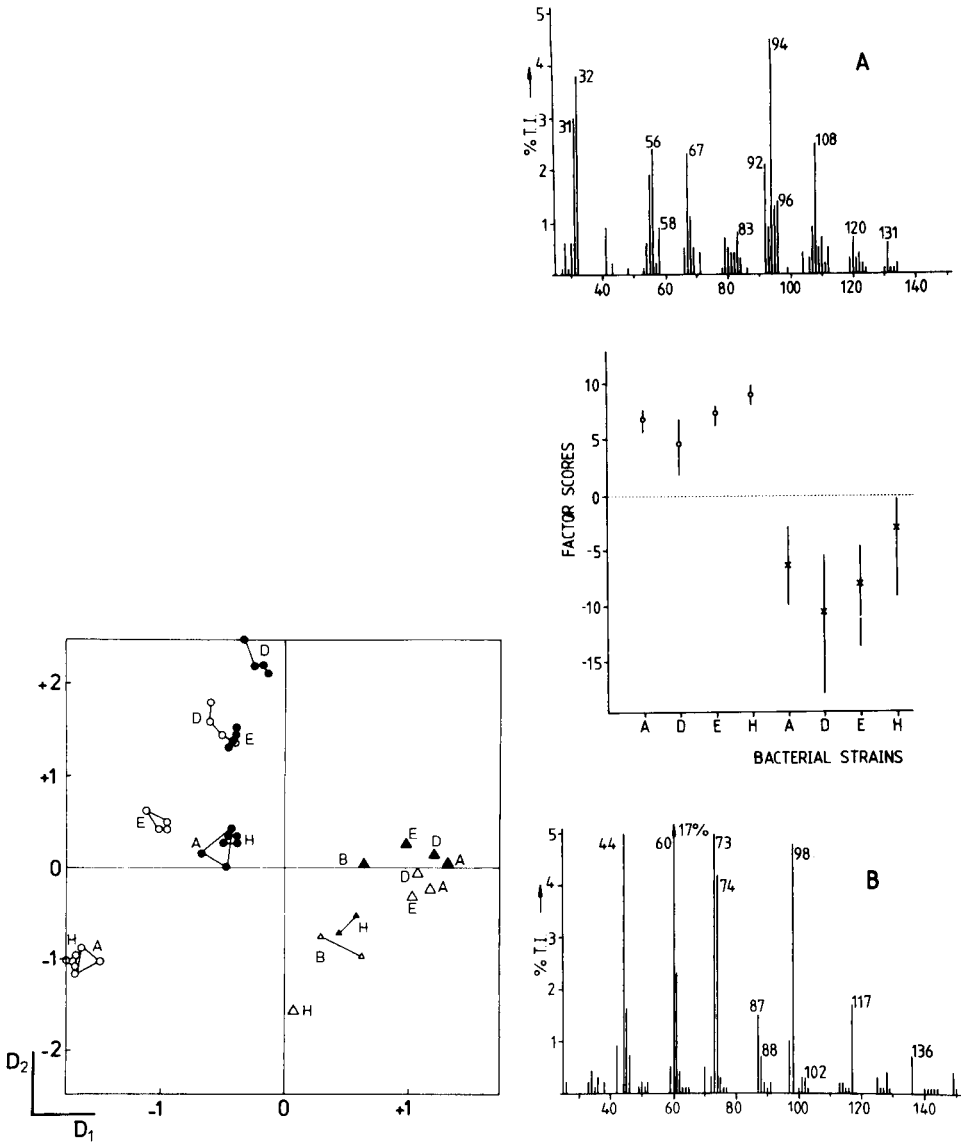

Fig. 5. Discriminant function score plot of Curie-point evaporation (358°C) and Curie-point pyrolysis (510°C) mass spectra for (○) bacterial colonies and (△) media underneath these colonies; open symbols relate to 358°C and filled symbols to 510°C. The *B. gingivalis* strains coded A, D and E were isolated from human patients. The strain coded H isolated from a beagle dog is a *B. intermedius*; B indicates the medium before growth.

Fig. 6. Positive (A) and negative (B) factor spectra of the first factor and its factor scores for a subfile consisting of mass spectra obtained by Curie-point pyrolysis and evaporation of the different *Bacteroides* strains; (○) 510°C: (×) 358°C. The bars on the symbols are error bars (4 replicates).

samples including reference biopolymers confirm this. The f.d.a. treatment of this file produced the D_1, D_2 score map in Fig. 7; discrimination between the individual strains is clearly more pronounced with the 358°C temperature. This indicates that the volatile compounds are more important for classification than the pyrolysis products from macromolecular fractions. The discriminant function spectra showed that the dog *B. intermedius* strain produces less volatile acids and indole than the human *B. gingivalis* strains; accordingly, it is plotted remote from the human strains in Fig. 7. These relative differences were less pronounced when the whole file was used (Fig. 5) because the differences between H and A were expressed in the third and fourth discriminant function.

Comparison of evaporation and pyrolysis mass spectra of the media before and after growth. In order to estimate differences in the physiological patterns of nutrient use and production of metabolic wastes between the strains, a subfile of evaporation and pyrolysis spectra of the media before and after growth of the four strains investigated was examined by the f.d.a. procedure. Three discriminant functions were found to be almost equally viable. Only the second and third functions are relevant here. Figure 8 shows that the difference between the media before and after growth was expressed in the third function of this file. The reconstructed discriminant function spectra (not shown) indicated that the discrimination is based mainly on the mass peaks from the volatile acids and phenylacetic acid; these spectra offered no evidence for any major changes in composition of the nutrient substances, probably because of their relatively high abundance in the media. The relative positions in Fig. 8 for the various media after growth indicate differences in the physiology of the human and dog strains; the positions

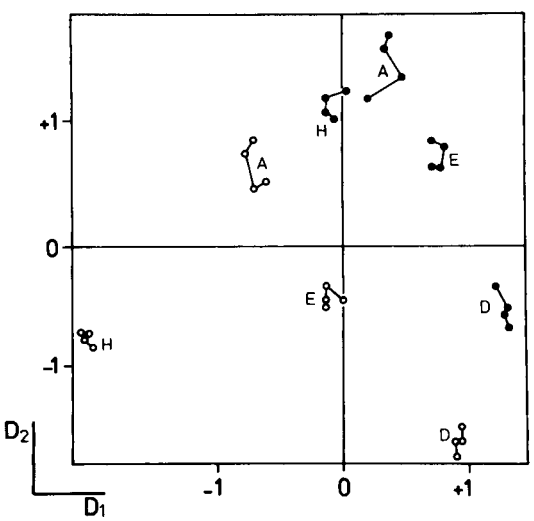

Fig. 7. Discriminant function score map (D_1, D_2) produced for a subfile of Curie-point evaporation and pyrolysis mass spectra of the *Bacteroides* strains; (○) 358°C; (●) 510°C.

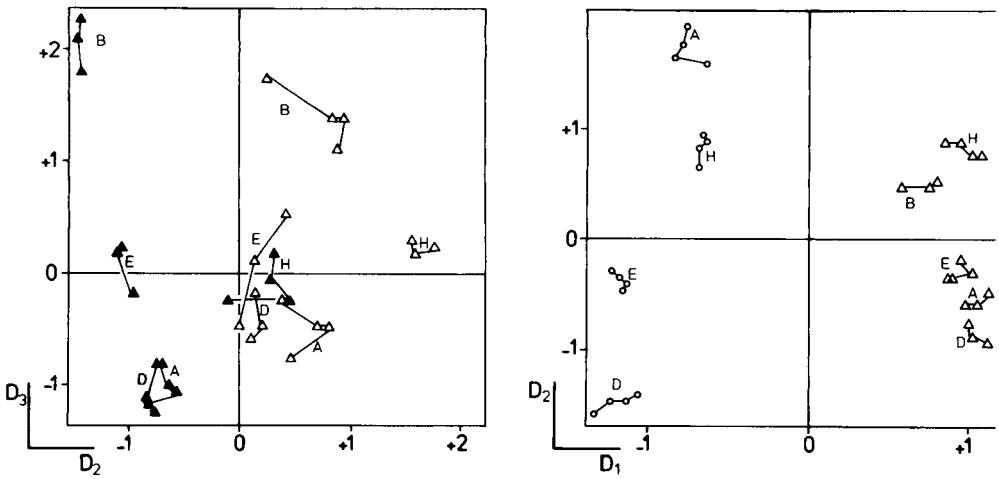

Fig. 8. Discriminant function score map (D_2, D_3) for a subfile of Curie-point evaporation and pyrolysis mass spectra of the media after growth of the *Bacteroides* strains; (△) 358°C; (▲) 510°C. The medium before growth is indicated by B.

Fig. 9. Discriminant function score map (D_1, D_2) for a subfile of Curie-point evaporation mass spectra (358°C); (○) bacterial strains; (△) their media after growth.

were similar for both Curie-point temperatures. The dog strain medium is well separated from the human strain media. Physiological tests confirm that the dog strain is a *Bacteroides intermedius* which secretes acetic and succinic acid.

Comparison of evaporation spectra of bacteria and media. As shown above, characteristic differences between the individual strains are to be found in samples from the bacterial colonies themselves and in samples from the media after growth. In both types of samples, the volatile fractions were found to be very important for discrimination; these data were therefore compared. The results of the f.d.a. treatment of the subfile of evaporation mass spectra of bacteria and media are shown in Fig. 9. The two discriminant functions describe 84% of the available outer/inner variance in the data set. The first discriminant function separates bacteria from media (cf. Fig. 5). The second function describes the difference of the dog strain and medium relative to the human strains and their media. In the reconstructed mass spectra of the first discriminant function (not shown) the media were differentiated from the bacteria by mass peaks of the volatile acids and the agar derived peaks; the spectra for the bacteria spectra had a higher relative intensity of indole mass peaks (m/z 117 and 90) and m/z 34, 48, 55, 59, 69, 70, 81, 82, 97 and 98, the latter peaks coming from various compounds. The spectrum of the second discriminant function suggested m/z 31, 32 and 46 from methanol and ethanol for discrimination between human strain A and the dog strain; there was also a higher relative intensity of m/z 117 in human

strain D and E. The differences between the dog medium and human media were again caused mainly by the intense mass peaks of volatile acids in the latter strains. The spectrum of the bacterium isolated from the dog was discriminated in the fourth dimension by the mass peaks m/z 56 and 84 of unknown origin.

Conclusions

The simple Curie-point wire technique is valuable for desorption and analysis of gases, liquid and solids from bacterial environments. Wires are mounted in a pyrolysis unit which is used as an inlet for a mass spectrometer or a gas chromatograph (coupled to a mass spectrometer). When a rapid-scanning mass spectrometer is used, an elaborate chemometric analysis of the data is needed to demonstrate quantitative relationships between the data obtained. Qualitative differences between the samples are deduced from series of correlated mass peaks and generally need pyrolysis g.c. and pyrolysis g.c./m.s. for confirmation. It would clearly be better to use complete g.c./m.s. data files for the data evaluation. The fast fingerprinting instrument used here sacrifices this resolution for the sake of multiple analyses and relatively large batches of samples. Instrumental improvements would include more complete sample transfer from the pyrolysis unit to the ion source and a softer ionisation technique.

The potential of the approach has been shown for the example of *Bacteroides* strains. It should be generally applicable to all kinds of bacterial, plant and animal systems. Practically all compounds involved in the culture system can be evaluated directly from the mass spectra and the chemometric analysis shows that there are distinct differences between the bacterial strains. In the above study, the pyrolysis mass spectral fingerprint turned out to be mainly an evaporation fingerprint because the spectra were dominated by volatile fractions from the bacteria. Such analytical aspects of a clinically orientated microbiological survey need attention in the evaluation of the stability of the characteristics found. A complete understanding of the chemical compounds involved in the differentiation of strains and in their metabolic patterns may lead eventually to more specific methods of analysis. The above Curie-point method, however, allows easy sampling with a high degree of automation.

The pyrolysis work in this investigation was supported by the Foundation for Fundamental Research on Matter (FOM), a subsidiary of the Netherlands Organisation for the Advancement of Pure Research (ZWO).

REFERENCES

1 H. L. C. Meuzelaar, P. G. Kistemaker, W. Eshuis and H. A. J. Boerboom, in N. R. Daly (Ed.), Advances in Mass Spectrometry, Vol. 78, Heyden, London, 1977, 452.
2 J. D. Twibell, J. M. Home and K. W. Smalldon, Chromatographia, 14 (1981) 366.
3 J. Haverkamp and P. G. Kistemaker, Int. J. Mass Spectrosc. Ion Phys., 45 (1982) 273.

4 H. L. C. Meuzelaar, J. Haverkamp and F. D. Hileman, Pyrolysis Mass Spectrometry of Recent and Fossil Biomaterials, Elsevier, Amsterdam, 1982, p. 293.
5 R. Hoogerbrugge, S. J. Willig and P. G. Kistemaker, Anal. Chem., 55 (1983) 1711.
6 J. Slots, in R. J. Genco and S. E. Mergenhagen (Eds.), Host—Parasite Interaction in Periodontal Diseases, Am. Soc. Microbiol., Washington, DC, 1982, p. 27.
7 F. J. W. Notten, E. W. J. Meys, P. M. van Zandvoort and F. H. M. Mikx, Anth. v. Leeuwenhoek, 49 (1983) 607.
8 W. Windig, J. Haverkamp and P. G. Kistemaker, Anal. Chem., 55 (1983) 81.
9 B. I. Duerden, J. G. Collee, R. Brown, A. G. Deacon and W. P. Holbrooks, J. Med. Microbiol., 13 (1980) 231.
10 T. J. M. Van Steenbergen, Ph.D. Thesis, Free University, Amsterdam, 1981.
11 A. G. Deacon, B. I. Duerden and W. P. Holbrook, J. Med. Microbiol., 11 (1978) 81.
12 H. N. Shah, R. A. D. Williams, G. H. Bowden and J. M. Hardie, J. Appl. Bacteriol., 41 (1976) 473.
13 G. Wieten, Ph.D. Thesis, University of Amsterdam, 1983.
14 G. Wieten, H. L. C. Meuzelaar and J. Haverkamp, in G. Odham, L. Larsson and P-A. Mardh (Eds.), Gas Chromatography/Mass Spectrometry Applications in Microbiology, Plenum Press, New York, 1984, p. 335.
15 J. Tonzetich and B. C. McBride, Arch. Oral Biol., 26 (1981) 963.
16 A. Van der Kaaden, J. Haverkamp, J. J. Boon and J. W. deLeeuw, J. Anal. Appl. Pyrol., 5 (1983) 199.
17 W. A. Konig, K. Ludwig, S. Sievers, M. Rinken, K. H. Stotting and W. Gunter, J. HRCC. and CC., 3 (1980) 415.

Analytica Chimica Acta, 163 (1984) 207—217
Elsevier Science Publishers B.V., Amsterdam — Printed in The Netherlands

AUTOMATION OF AN EXPERIMENTAL SYSTEM FOR THE MICROBIAL EPOXIDATION OF PROPENE AND 1-BUTENE

L. E. S. BRINK*, J. TRAMPER and K. VAN 'T RIET

Department of Food Science, Food and Bioengineering Group, Agricultural University Wageningen, De Dreyen 12, 6703 BC Wageningen (The Netherlands)

K. CH. A. M. LUYBEN

Laboratory of Bioengineering, Delft University of Technology, Julianalaan 67, 2628 BC Delft (The Netherlands)

(Received 14th April 1984)

SUMMARY

An experimental set-up for automatic gas chromatographic analysis of circulation gas in a batch-reactor system is described. Gas sampling, substrate addition, data acquisition and data reduction are done with a coupled programmable integrator and microcomputer. On-line monitoring of the microbial oxidation of the gaseous alkenes, propene and 1-butene, to the corresponding epoxides is used to illustrate the operation of the experimental system. Measured gas concentrations of alkene and alkene oxide can be converted readily to quantify the reaction course in the liquid phase(s) of the circulation system. Results are presented for both one liquid phase (water) and two liquid phases (water and organic solvent) present in the reactor. The operational stability of the immobilized-cell system used for the epoxidations can be assessed by computer-controlled addition of gaseous alkene.

The use of water-immiscible organic solvents has recently been given increasing attention as a possible approach to diminishing the fundamental restrictions often inherent in biotechnological processes. Some of these restrictions are the low solubility of (gaseous) substrates and/or products in water, product inhibition, product hydrolysis and laborious product recovery [1, 2]. In order to study the potential of an additional organic phase, the epoxidation of the gaseous alkenes, propene and 1-butene, by immobilized cells in a multiphase bioreactor has been studied as a model. The system consists of a solid biocatalyst, an aqueous phase, an organic solvent, and a gas phase containing the gaseous substrates oxygen and propene or 1-butene [3]. Selecting an optimal composition for this multiphase system involves careful weighing of many different factors and their possible mutual interactions. Factors such as the technique of immobilization, type of organic solvent, microbial aspects (bacterial strain, co-factor regeneration) and process engineering aspects (hydrodynamics, reactor design) allow a vast number of combinations, which requires automation of the experiments, especially the monitoring of alkene and alkene oxide concentrations in the liquid phases.

0003-2670/84/$03.00

The choice of a well-established technique like gas chromatography (g.c.) for separation and determination of the various components in the multiphase system is obvious. Gas chromatography may be used for on-line monitoring by using a small sampling interval in combination with the proper chromatographic conditions. Direct g.c. of the aqueous and/or organic liquid phase has several disadvantages: it is difficult to quantify small quantities of organic compounds in water because of overloading the column and the detector by water; the various solvents (and their impurities) used may interfere seriously and contaminate the g.c. column; and the automation of liquid-sample withdrawal is expensive. The need for intimate contact between gas and liquid phases to supply the gaseous substrates, however, makes it feasible to follow the reaction course in the reactor by measuring the gas-phase concentrations. The easily detectable gaseous substrates and volatile alkene oxides and the low concentrations of water, solvent and impurities in the gas phase, and the simple automation of a gas-sampling valve, are further considerations which make gas analysis preferable to liquid analysis. This technique, head-space gas chromatography (h.s.g.c.), has found practical applications in trace analysis and in the measurement of thermodynamic data [4], and has been used recently to monitor batch and continuous alcoholic fermentations with ethanol concentrations in the liquid phase up to 110 g l^{-1}, and acetone/butanol fermentation with acetone and butanol concentrations in the liquid phase up to 20 g l^{-1} [5, 6].

An inherent disadvantage of quantitative h.s.g.c., compared with direct g.c., stems from the need to convert the measured gas concentrations to liquid concentrations so that additional parameters must be considered [4]. The conversion is mostly based on the assumption of thermodynamic equilibrium between the gas and liquid phase(s). Henry's law may be used for poorly soluble gases like oxygen and propene to correlate the partial vapour pressure (p_i) of a component i in the gas phase and its mole fraction (x_i) in the liquid (aqueous or organic) phase: $p_i = H_i x_i$, where H_i is the Henry constant of component i. For less volatile, better soluble compounds like alkene oxides, non-ideality in the liquid phase is taken into account by specifying an activity coefficient γ_i of the dissolved component i. If ideal behaviour of the gas phase can be assumed, the activity coefficient relates the partial vapour pressure to liquid mole fraction by the equation

$$p_i = p_i^0 \gamma_i x_i \qquad (1)$$

in which p_i^0 is the vapour pressure of the pure component i. The activity coefficient depends not only on temperature and, to a lesser extent, on pressure, but also on the interaction between component i and the other components present. Successful quantitative interpretation based on the p_i equation, and the experimental determination of the calibration factor $p_i^0 \gamma_i$, must therefore take into account possible changes in the activity coefficient caused by variations in the composition of the liquid phase. At low concentrations of the component of interest, a linear relation between signal (p_i)

and the mole fraction in the liquid (x_i) is expected, because the activity coefficient of a very dilute solution is nearly constant [4, 7]. Comberbach and Bu'Lock [5] found that for ethanol/distilled water mixtures, a linear relation exists between the h.s.g.c. signal and the actual ethanol concentration in the liquid phase from 2 to 80 g l^{-1}.

EXPERIMENTAL

Batch reactor with gas circuit

Cells were entrapped in calcium alginate gel for immobilization. Details of the immobilization technique and of microbial aspects such as substrate specificity of the *Mycobacterium* strain E3 used for the epoxidations, are reported elsewhere [3]. Experiments with the biocatalyst beads (ca. 25 ml) were done with a small bubble-column bioreactor, containing an aqueous 0.05 M calcium chloride solution and in some cases an organic solvent phase (total volume of beads and liquid phases, 250 ml). An aerated flask containing 250 ml of (0.05 M) potassium phosphate buffer of pH 7.0 was used in measurements with suspended cells. Air (25 ml s^{-1}) from a gas supply vessel (300 ml) containing 1.7% alkene (v/v) was circulated through the suspension of immobilized or free cells by means of a gas diaphragm pump (Fig. 1). Reaction and gas supply vessel (total gas volume 570 ml) were thermostated at 30°C in a water bath. Errors produced by leakage of gaseous components were minimized by using only materials with low gas permeability, like glass,

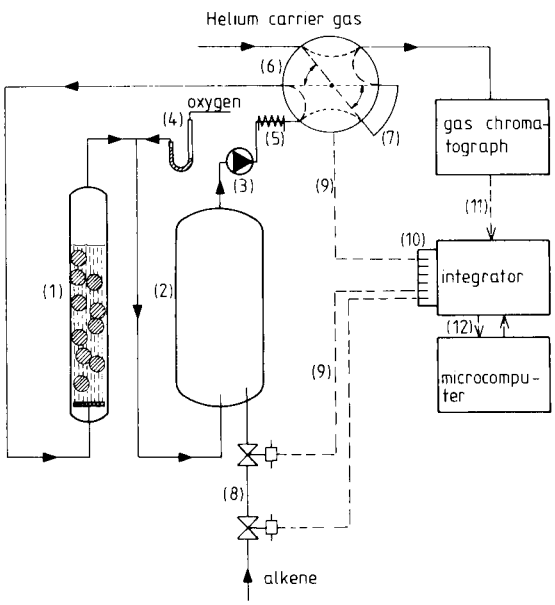

Fig. 1. Schematic representation of circulation batch reactor and control system: (1) bubble-column bioreactor; (2) gas-supply vessel; (3) diaphragm pump; (4) oxygen inlet with water seal; (5) heating; (6) two-position gas-sampling valve showing the normal (---) and inject (———) mode; (7) sample loop; (8) magnetic valves; (9) control signals; (10) external-control option; (11) analog g.c. signal; (12) digital communication. See also text and Fig. 2.

teflon (compared with other plastics) and viton for tubing. As the gaseous substrates were consumed in the reaction, the pressure in the system decreased; atmospheric pressure was maintained by introducing pure oxygen through a water seal, which also maintained an excess of oxygen.

Gas samples (0.48 ml) were withdrawn from the gas circuit every 30 min by a computer-controlled electropneumatic two-position gas-sampling valve. Problems of water condensation were averted simply by heating the gas entering the valve to 50°C and isolating the sampling valve and sample loop, which resulted in a reasonably constant valve temperature (about 35°C).

Measurements of the operational stability of the immobilized-cell system were facilitated by controlling the substrate level in the circulation system. Gaseous alkene was added by sequential computer-controlled opening and closing of two magnetic valves. The amount of gas added per sequence was determined by separate calibration.

Gas chromatograph

A gas chromatograph (Carlo Erba 4200) equipped with flame-ionization and thermal-conductivity detectors was used. Helium was used as carrier gas (0.33 ml s^{-1}); the column (2 m, 3 mm o.d.) was packed with Porapak-Q (80–100 mesh). Oven and flame-ionization detectors were held at 200 and 210°C, respectively. Alkene and alkene oxide were quantified regularly by computer-controlled switching of the two-position valve into the inject mode, upon which the content (0.48 ml) of the sample loop was carried into the column.

The partial vapour pressures of (excess) oxygen and nitrogen were verified by manual injection of gas samples (50 μl) onto a column packed with molecular sieve 13X (60–80 mesh) and using the thermal-conductivity detector. This column was positioned outside the gas chromatograph and used at ambient temperatures.

Response factors relating peak areas to gas phase concentrations were evaluated by adding known quantities of alkene or alkene oxide to the system described above (without biocatalyst), and/or to known gas volumes (not in contact with a condensed phase), and subsequent analysis of the gas phase. Likewise, addition of a known quantity of alkene oxide to the batch-reactor system (also no biocatalyst) made it possible to establish relationships between liquid and gas phase concentrations of the epoxide in question.

Integrator and microcomputer

Processing of the analog g.c. signals and control of the electropneumatic and magnetic valves were done with a programmable integrator (Spectra-Physics 4270) coupled to a microcomputer (Hewlett-Packard 86-B). The integrator was equipped with an interface (RS-232) for serial communication with the computer, and with external controls (6 per channel of integration) for on/off-switching of valves and, if necessary, of other equipment (see Fig. 2). Implementation of a second channel for peak integration is optional. The interfacing capabilities could be extended for data acquisition from various instruments (e.g., pH and oxygen electrodes).

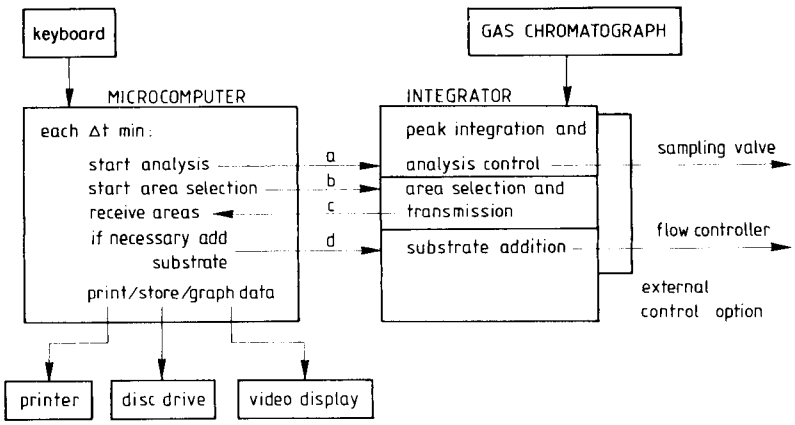

Fig. 2. Signal flow diagram showing the coupling of integrator and microcomputer. Serial interfaces (RS-232) were used for the communication signals (a, b, c, d). See text for discussion.

Data handling

At regular time intervals Δt (e.g., 30 min) the sampling sequence (Fig. 2) is initiated by the built-in timer of the microcomputer. The analysis is started (arrow *a* in Fig. 2) by transmitting an inject command to the integrator; this has the same effect as pressing the "start" or "inject" knob of the integrator. The analysis and peak integration are controlled by built-in standard programs. The parameters needed are stored in the integrator memory before the experiment. Typical values are: at 0.01 min (almost zero), switch gas-sampling valve to the inject mode; at 4.9 min, switch gas-sampling valve to the normal mode; at 5 min, terminate the signal integration. The main program in the microcomputer then initiates a simple user-written program for area selection at 5.2 min (step b); only the areas of the required components are selected and subsequently transmitted (step c) back to the computer. Required unit conversions (e.g., area to partial vapour pressure) and calculations are then done. In experiments with a constant level of alkene, the alkene area or concentration of the latest sample and, if wanted, of previous samples are compared with a user-defined setpoint. If the deviation exceeds a certain value, a small quantity of substrate is added to the batch-reactor system by initiating (step d) another user-written program section in the integrator memory, which in turn activates the substrate valve(s). Sample number, sampling time, areas or concentrations, number of substrate additions and total amount of substrate consumed are then printed and stored (computer memory and/or disc drive) and can be reproduced graphically on the video display (e.g., alkene (oxide) concentration versus time).

RESULTS AND DISCUSSION

Quantitative h.s.g.c.

The consumption of the alkene substrates could be quantified by using as reference the first measurement taken very shortly after the addition of a known amount of alkene (10 ml). The conversion factor between peak area and total amount of gaseous alkene present in the various phases of the circulation system was determined thus. The peak areas during the remainder of the experiment were converted to ml of alkene by using this factor. It was assumed that decreasing alkene concentrations did not affect the value of the Henry constants of interest (alkene/water, alkene/solvent). Gas and liquid concentrations were calculated with the absolute values of the Henry constants. For example, from the constant for propene in water (1.24×10^6 kPa at 30°C [8]), it was calculated that 4.6% of the total amount of propene present would dissolve in the 250-ml aqueous phase (water and hydrophilic gel), while the rest remained in the 570-ml gas phase. The low salt concentrations used (0.05 M calcium chloride) showed no significant effect on the fraction of propene present in the gas phase.

Activity coefficients are needed to convert the measured gas concentrations to liquid concentrations of the produced alkene oxides. In experiments with only one (aqueous) liquid phase (no organic solvent), propene oxide was quantified by addition of a known quantity of propene oxide N_{PO} to the circulation system. Separate calibration (only gas phase present) of the measured peak areas of propene oxide for conversion of areas to gas mole fractions y_{PO} (see Table 1) made it possible to determine the liquid mole fraction x_{PO} by using a simple mass balance

$$x_{PO} = (N_{PO} - y_{PO}N_g)/N_l \qquad (2)$$

TABLE 1

Equilibrium data for propene oxide

N_{PO}[a] (10^{-6} mol)	y_{PO}[b] (10^{-3})	$y_{PO}N_g/N_{PO}$[c]	x_{PO}[d] (10^{-4})	γ_{PO}[e]
713	0.795	0.026	0.50	18.2
1426	1.52	0.024	1.00	17.4
2139	2.23	0.024	1.50	17.0
2852	3.08	0.025	2.00	17.6
3565	3.84	0.025	2.50	17.6
4278	4.63	0.025	3.00	17.7
			Average	17.6

[a]Total number of moles of propene oxide present in the circulation system. [b]Gas-phase mole fraction (h.s.g.c. signal). [c]Fraction of propene oxide in the gas phase. [d]Liquid mole fraction. [e]Activity coefficients.

in which N_g and N_l are the total number of moles in the gas and liquid phase, respectively (570 ml or 0.0229 mol of gas phase and 250 ml or 13.9 mol of demineralized water). Activity coefficients, γ_{PO}, were estimated by using the equation (obtained from Eqn. 1)

$$\gamma_{PO} = p_{PO}/x_{PO}p^0_{PO} = y_{PO}P_t/x_{PO}p^0_{PO} \quad (3)$$

with the system pressure P_t = 100 kPa, and the vapour pressure of pure propene oxide at 30°C, p^0_{PO} = 87.25 kPa [9].

From Table 1 it may be concluded that for the dilute aqueous solutions of propene oxide considered ($\leqslant 3 \times 10^{-4}$), the activity coefficient is independent of epoxide concentrations, and that there is a linear relationship between y_{PO} (h.s.g.c. signal) and the liquid-phase mole fraction x_{PO}. Quantification of the propene oxide is also facilitated by the linear relationship between the h.s.g.c. signal or gas-phase mole fraction y_{PO} and the total number of moles of propene oxide N_{PO} present in the batch-reactor system (Table 1): y_{PO} = 1.08 N_{PO} − 2 × 10^{-5} (standard error of estimate 0.04 × 10^{-3}; correlation coefficient 0.999). In most of the tests, the total amount of biologically produced liquid propene oxide did not exceed 29.2 μl (416 μmol, the maximum theoretical production from 10 ml of gaseous propene), thus Table 1 shows that a single factor suffices for the conversion of peak areas to produced amounts of epoxide, and also to liquid epoxide concentrations.

Similar behaviour has already been found for dilute aqueous solutions of alcohols, ketones, aldehydes, esters and sulfides [7], thus it can be assumed that the same linear relationship will hold for 1-butene oxide. It was found that the small fraction of the total amount of this epoxide that was contained in the gas phase (3.2%) was slightly higher than the corresponding fraction of propene oxide (2.5%).

As the solubility of propene oxide and 1-butene oxide in the water-immiscible organic solvents used is mostly higher than the corresponding solubility in water, replacement of part of the aqueous phase by these solvents will decrease the gas-phase and aqueous phase concentrations of the epoxide. The epoxide activity coefficients will be affected considerably by the mutual solubility of water and the organic solvent. Accordingly, conversion of gas concentrations to aqueous and organic liquid concentrations, and the distribution of the epoxide between the two liquid phases, cannot be evaluated from activity coefficients of separate gas/water and gas/solvent calibrations. Although not required in the present investigation, epoxide concentrations in the liquid phases may be deduced from separate gas/water/solvent calibrations.

Monitoring alkene consumption and alkene oxide production

The microbial epoxidation of propene and 1-butene was investigated as described above. Typical gas chromatograms for the propene epoxidation, at the start and finish of the experiment, are shown in Fig. 3. Methane was used to check the sealing of the recirculation system. Separate blank mea-

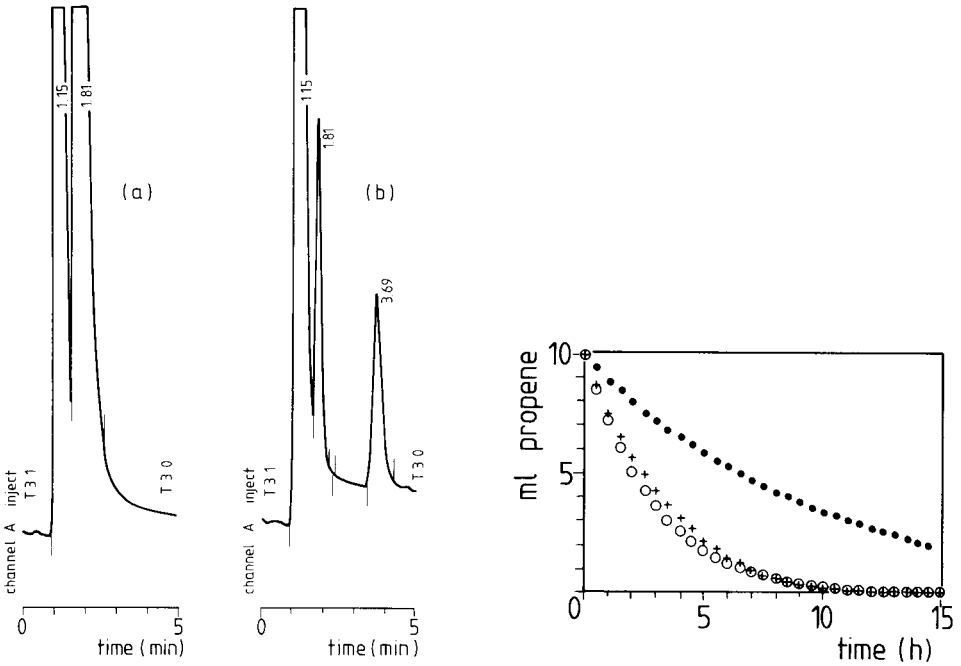

Fig. 3. Typical chromatograms from a propene epoxidation experiment: (a) only methane (1.15 min) and propene (1.81 min) are present at the start; (b) at the end, propene was mostly converted to propene oxide (3.69 min). Peak markers show the start and end of peak integration. Switching of the gas-sampling valve is indicated by "T3 1" (inject mode) and "T3 0" (normal mode).

Fig. 4. Amount of unconverted propene in the system versus time: (○) free cells; (+) cells immobilized in 0.7-mm alginate beads; (•) cells immobilized in 2.5-mm alginate beads.

surements, without biocatalyst, showed that the leakage rate of propene at the maximum propene level (1.7% v/v) was several times higher than the leakage rate of methane (also 1.7% v/v). In these experiments, alkene leakage rates were always less than 5% of the alkene consumption rates. Retention times of 1-butene and 1-butene oxide for the same chromatographic conditions were 2.5 and 6.4 min, respectively. The total time required for one sampling sequence was about 5.5 min for propene epoxidation, but may be reduced to 2 min or even less by increasing carrier flow and oven temperature and/or reducing column length and diameter.

Results of propene consumption by free and immobilized cells in an aqueous environment are given in Fig. 4. Equal amounts of cells (ca. 1 g dry weight) were used in each case. Propene levels are given in ml (gaseous) propene present in the total circulation system. Multiplication by appropriate factors would give the number of moles present, partial vapour pressure, gas or liquid mole fraction as the unit of the *Y*-axis. Compared to the curve for 2.5 (±0.2)-mm beads, there is only a small difference in propene consumption

rate between free suspended cells and cells immobilized in alginate beads with an average diameter of 0.7 ± 0.1 mm, obviously because of diffusion limitation.

The kinetic parameters can be estimated by different methods, including non-linear regression, and the diffusion limitation can be modelled by using the same microcomputer system; details will be given elsewhere. For example, the kinetic parameters of the integrated Michaelis—Menten equation, estimated by a non-linear regression of substrate versus time, were used to characterize the alkene consumption rates. Illustrations of this regression method are given in Figs. 5 and 6. It did not seem necessary to make these calculations during the experiments.

Measured values of propene oxide and 1-butene oxide production by cells immobilized in alginate beads are compared with values calculated from propene and 1-butene consumption rates in Fig. 7 (1 ml of gaseous propene gives 2.92 μl of liquid propene oxide; 1 ml of gaseous 1-butene gives 3.58 μl of liquid 1-butene oxide). Epoxide levels are given as the total amount in the circulation system, but most of it is in the aqueous phase (see above). Despite the small quantities of propene oxide and 1-butene oxide in the gas phase, the trend of the epoxide concentrations is clear. The increasing difference between the epoxide concentrations found and those calculated from alkene consumption rates confirms that the bacterial strain used can consume the alkene oxides [3]. Decreasing the sampling time interval will improve the reliability even further. The relative influence of the experimental error in the alkene oxide concentrations (10—20% in Fig. 7) is smaller at higher epoxide levels (see below).

Propene epoxidation was also monitored in the presence of a second liquid phase consisting of a water-immiscible organic solvent (10 ml). Some results are summarized in Fig. 8. As reported for other cells [10], the very inert perfluoro compound used (FC-40; 3M, St. Paul, MN) caused little or no

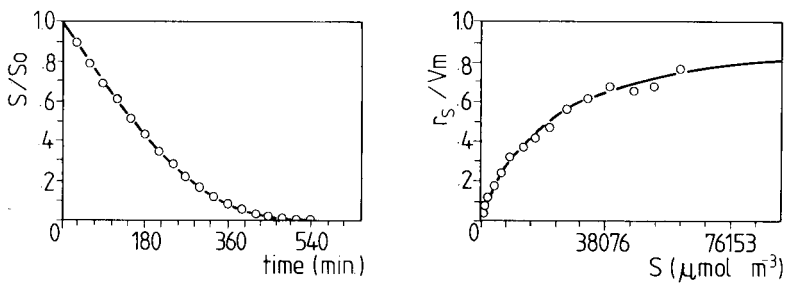

Fig. 5. Dimensionless substrate (propene) concentrations, S/S_0, versus time for cells (0.8 g dry weight) immobilized in 1.0-mm alginate beads. Smooth line depicts the Michaelis—Menten model approximation (V_m = 2.30 μmol min^{-1} g dry weight^{-1}; K_m = 20900 μmol m^{-3}).

Fig. 6. Dimensionless propene consumption rates r_s/V_m versus substrate (propene) concentration S for immobilized cells (as in Fig. 5). Smooth line depicts Michaelis—Menten model approximation as in Fig. 5.

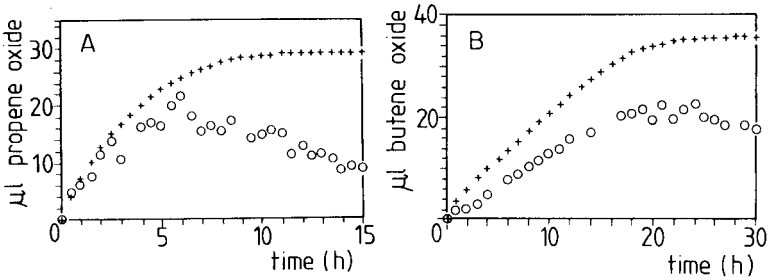

Fig. 7. Amount of liquid epoxide produced in the circulation system versus time: (A) propene oxide with 0.7-mm beads; (B) butene oxide with 0.8-mm beads. (○) Measured values, (+) values calculated from substrate consumption.

inactivation of the cells compared to a blank measurement without solvent. Commoner solvents (phthalic acid dibutyl ester and di-isopentyl ether) caused some cell inhibition, and hexane and trioctylamine rapidly inactivate the immobilized-cell system.

Substrate level control

The operational stability of the immobilized cells was verified by monitoring the substrate level. The propene concentration was held constant within about 10% of a user-defined setpoint (10 ml in these tests) by computer-controlled opening and closing of two magnetic valves each time the measured propene concentrations of two consecutive analyses both fell below the setpoint. Such variations in propene level are unlikely to affect the substrate consumption rate as the enzymatic reaction order at this substrate level is close to zero. Again, an increasing difference was found between the measured

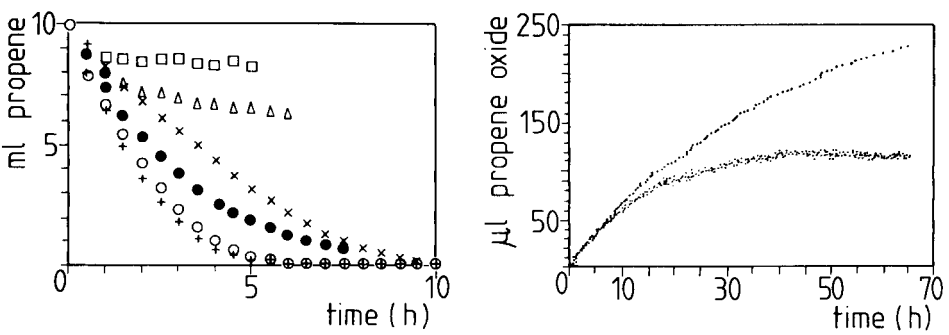

Fig. 8. Amount of unconverted propene in the system versus time with 10 ml of organic liquid phase present (cells immobilized in alginate): (+) blank measurement; (○) FC-40; (•) phthalic acid dibutyl ester; (×) di-isopentyl ether; (△) n-hexane; (□) trioctylamine.

Fig. 9. Amount of propene oxide produced in the reactor with control of propene level (cells immobilized in alginate). Lower points represent measured values; upper points represent values calculated from cumulative amount of propene addition.

amount of liquid propene oxide and the calculated production, obtained by multiplying the number of substrate additions by the amount of propene added (0.74 ml) in one valve-switching sequence (Fig. 9).

From the number of analyses (each 10 min), the volume of the gas phase in the circulation system, and the internal volume of the sample loop of the gas-sampling valve (0.48 ml), it can be deduced that the maximum cumulative experimental error arising from sampling losses of propene is about 5%. Minimizing this error, and preventing the oxygen partial vapour pressure from becoming too low, is possible by increasing the interval between sampling times, reducing the sample loop volume and/or increasing the volume of the gas phase.

Further research will concentrate on factors of importance for the optimization of this multiphase system.

REFERENCES

1 E. Antonini, G. Carrea and P. Cremonesi, Enzyme Microb. Technol., 3 (1981) 291.
2 M. D. Lilly, J. Chem. Technol. Biotechnol., 32 (1982) 162.
3 A. Q. H. Habets-Crützen, L. E. S. Brink, C. G. van Ginkel, J. A. M. de Bont and J. Tramper, Eur. J. Appl. Microbiol. Biotechnol., in press.
4 H. Hachenberg and A. P. Schmidt, Gas Chromatographic Headspace Analysis, Heyden, London, 1977.
5 D. M. Comberbach and J. D. Bu'Lock, Biotechnol. Bioeng., 25 (1983) 2503.
6 D. M. Comberbach, J. M. Scharer and M. Moo-Young, Biotechnol. Lett., 6 (1984) 91.
7 S. Özeris and R. Bassette, Anal. Chem., 35 (1963) 1091.
8 Landolt-Börnstein, Gleichgewicht der Absorption von Gasen in Flüssigkeiten, IV. Band, 4. Teil, Bandteil c, Springer-Verlag, Berlin, 1976.
9 B. Gutsche and H. Knapp, Polish J. Chem., 54 (1980) 2261.
10 P. Adlercreutz and B. Mattiasson, Eur. J. Appl. Microbiol. Biotechnol., 16 (1982) 165.

Analytica Chimica Acta, 163 (1984) 219—229
Elsevier Science Publishers B.V., Amsterdam — Printed in The Netherlands

ON-LINE MASS SPECTROMETRY IN FERMENTATION

E. HEINZLE*, J. MOES, M. GRIOT, H. KRAMER, I. J. DUNN and J. R. BOURNE

Chemical Engineering Department, Eidgenössische Technische Hochschule, CH-8092 Zurich (Switzerland)

(Received 17th April 1984)

SUMMARY

The on-line application of mass spectrometry (m.s.) includes analysis of the fermentor gas phase by using a capillary inlet and analysis of the liquid phase by using membrane probes. Gas-phase measurements with a capillary inlet are fast and accurate for all gases of interest (O_2, N_2, CO_2, H_2, etc.). Liquid-phase measurements are done with steam-sterilizable membrane inlet probes, permitting direct analysis of dissolved gases and various volatiles. With these two inlets, automatic measurement of both the liquid and gas phases is possible when a microcomputer is used. This was applied to the batch fermentation of *Bacillus subtilis*. A further application of the membrane probe is evaluation of fermentation process state; this involves measuring the spectra of all detectable volatiles and correlating this information with the process state (e.g., product formation). Sufficient characteristic volatiles were found in various industrial fermentation samples. When mass spectra are treated by factor analysis, useful correlations are found with the product concentrations measured off-line. Calibration depending on the process conditions is necessary for this method, but it is widely applicable and allows automatic monitoring.

One of the main limitations for on-line process analysis and control is the lack of reliable sensors for relevant process variables. Few probes are available for chemical quantities (electrodes for dissolved oxygen, pH and redox potential, i.r. analyzer for CO_2, paramagnetic analyzer for O_2). Because of recent developments in equipment for mass spectrometry (m.s.), this technique is likely to become a standard on-line method for fermentation. It can be used for gas analysis with a continuously operating capillary inlet, described as early as 1949 by Hunter et al. [1] and later applied to fermentation [2].

The liquid phase can also be monitored by introducing the molecules into the high vacuum of the m.s. via a membrane probe, which was first used to monitor blood gas partial pressures [3]. Such probes have been used in fermentation to monitor dissolved gases [2—7], partial pressures in the gas phase [8], methanol [4], ethanol [2, 9] and acetone/butanol [10]. Many compounds are only volatile under certain conditions (e.g., pH), but by shifting conditions these can also be detected by a membrane probe [11]. Each fermentation produces various by-products, some of which are volatile;

their synthesis depends on the process conditions. Thus monitoring of the volatiles should give useful information. Most of the compounds in fermentation are not volatile and so are not directly accessible to m.s. However, any chemical reaction which can produce volatile products from these compounds could be used in conjunction with m.s. One of the most widely applicable methods of chemical volatilization is pyrolysis [12].

Although m.s. has a wide range of applications in fermentation it is still relatively little used. This is no doubt due to the earlier high costs and user difficulties.

EXPERIMENTAL

Two quadrupole m.s. (Balzers, Liechtenstein) were used in this work. A small, inexpensive model (QMG 64), especially designed for residual gas analysis with a direct ion detector (Faraday cup) and with a turbomolecular pump (TSU 40), was equipped with a capillary gas inlet (GES 10). Because no serial interface was available to control this m.s. with a computer, a connection to the m.s. was built to a microcomputer, which supplied the voltage (0—10 V) for the mass scan and measured the resulting ion currents from the electrometer amplifier, the range of which was automatically controlled by the m.s. itself. Electrical signals were checked for transients and only measurements at stable ion currents were used for further evaluation. Analog/digital conversion was done with a 12-bit A/D converter. For each measurement, at least 100 A/D conversions were made to filter out electrical noise. This system was used only for gas analysis with a capillary inlet.

A more powerful spectrometer (QMG 311) with gas-tight ion source, secondary electron multiplier and a turbomolecular pump (TPU 270), was equipped with a capillary gas inlet and a membrane inlet, both via pneumatic valves (BK series Nupro, Willoughby, OH). For connection of the membrane probe with the spectrometer, gold-plated copper tubing (4 mm i.d.) was used. Silicone rubber membranes (0.125 or 0.062 mm thick, Silastic sheeting, Dow Corning; or 0.12 mm thick, Wacker Chemie) were used. The membrane probe contained a porous stainless steel plate to support the membrane. Sealing was done by pressing the membrane onto the socket of the probe with a screw cap. This spectrometer was controlled via a data processor (QDP 101, Balzers, Liechtenstein), which was connected to an Apple-II microcomputer via a serial interface.

The data acquisition system was of essentially the same type for both spectrometers and consisted of an Apple-II microcomputer additionally equipped with a clock, two disk drives, a matrix printer and a process interface for A/D and D/A conversion as well as digital I/O (Andi, Zahner Elektrik, Kronach, FRG). Additionally, a serial card was used to connect the m.s. data processor with the CDC-6000 computer of the ETH computer center. All matrix calculations for factor analysis were done with the FACTOR/PA1 program (without rotation) of the Statistical Package for Social Sciences [13].

Fermenters used were from Bioengineering (Wald, Switzerland) with essentially the same equipment as described elsewhere [14] and from Chemap (Maennedorf, Switzerland). Gas flows were measured with mass flow meters (Brooks, Hatfield, PA). Culture conditions for batch cultures of *Bacillus subtilis* and methods of off-line analysis for concentration of biomass (absorbance), glucose and volatiles will be described elsewhere. Samples from industrial fermentations were supplied by Ciba-Geigy (Basel), Sandoz (Basel) and the Swiss Serum Institute (Thoerishaus) in a filtered and frozen state. Their spectra were measured in a thermostated stirred cell (3 ml) after proof of steady conditions. Analyses of product concentration were done by the companies and relative data were given to the authors.

Error analysis for gas balancing

For determining specific reaction rates for gases (O_2, CO_2), mass balances around the reactor must be written. For the gas phase,

$$V_G dC_{G,out}/dt = F_{G,in} C_{G,in} - F_{G,out} C_{G,out} - K_L a(C_L^* - C_L)V_L \quad (1)$$

and for the liquid phase

$$V_L dC_L/dt = K_L a(C_L^* - C_L)V_L - Q_i X V_L \quad (2)$$

where C is concentration, V volume, F_G gas flow, $K_L a$ the volumetric mass transfer coefficient and C^* the equilibrium concentration. Q is the specific gas reaction rate and X is the biomass concentration. Subscripts L and G indicate liquid and gas phase, respectively; in and out refer to the entrance and exit of the reactor. Under near steady-state conditions where the accumulation terms dC/dt are negligibly small, the equations reduce to

$$Q_i X V_L = F_{G,in} C_{G,i,in} - F_{G,out} C_{G,out} \quad (3)$$

Balancing inert gases yields

$$F_{G,out} = F_{G,in} C_{G,inert,in}/C_{G,inert,out} \quad (4)$$

which finally yields

$$Q_i X V_L = F_{G,in} C_{G,i,in} - F_{G,in} C_{G,inert,in} C_{G,i,out}/C_{G,inert,out} \quad (5)$$

For oxygen balancing, the question of the limits of accuracy of measuring Q_{O_2} is often important, especially under unfavorable conditions, where $C_{O_2,in}$ and $C_{O_2,out}$ are only slightly different. This is true for dilute cultures or generally for conditions with a high ratio of gas flow to mass transfer capacity of the reactor. This error in measuring Q_i can be estimated with Eqn. 5, using error propagation by Taylor series expansion. By defining $a = F_{G,in}$, $b = C_{G,inert,in}$, $c = C_{G,i,in}/C_{G,inert,in}$, $d = C_{G,i,out}/C_{G,inert,out}$ and $f = Q_i X V_L$, Eqn. 5 becomes

$$f = ab(c - d) \quad (6)$$

Introducing the relative error $s_f' = s_f/f$, $s_a' = s_a/a$, etc. (s is standard deviation)

and calculating error propagation gives

$$s_f'^2 = s_a'^2 + s_b'^2 + (c^2 s_c'^2 + d^2 s_d'^2)/(c - d)^2 \quad (7)$$

With air at the inlet $s_b' = s_c' = 0$ and

$$s_f'^2 = s_a'^2 + d^2 s_d'^2/(c - d)^2 \quad (8)$$

If the measurement of gas flow is accurate ($s_a'^2 \ll d^2 s_d'^2/(c - d)^2$, Eqn. 8 reduces to

$$s_f' = d\, s_d'/(c - d) \quad (9)$$

Table 1 gives the relative error in measuring d for specified relative differences in concentration of component i between inlet and outlet ($\Delta C_i'$) necessary to reach a maximal final relative error of $s_f = 5\%$ in determinations of $Q_i X V_L$ and the final expected error for a relative error in gas analysis, $s_d' = 1\%$.

For gas mixtures at the fermenter inlet, where gas concentrations must be measured at both inlet and outlet, Eqn. 7 can be applied, assuming $s_a' \ll s_f'$ and $s_b' \ll s_f'$ and by setting $s_c' = s_d'$, which means that results for both inlet and outlet gases have the same error. This gives

$$s_f' = s_c'(c^2 + d^2)^{1/2}/(c - d) \quad (10)$$

With the same conditions for required error and relative difference in concentration ($\Delta C_i'$), the results shown in Table 1 are obtained. It can be seen that almost double the precision in the measured concentration is needed compared to the case of air or another gas mixture of constant known composition at the inlet.

Next the above situation in which ratios of concentration are measured with one instrument (m.s., g.c., etc.) is compared with the situation where two independent instruments are used to determine C_{O_2} and C_{CO_2} (e.g., paramagnetic and infrared). In the latter case, the concentrations of the inert

TABLE 1

Imprecision of determination of specific oxygen uptake rate (Q_{O_2}) according to Eqns. 9, 10 and 12

$\Delta C_{O_2}'$ (%)[a]	50	10	5	1	Eqn.	Condition
s_d' (%)	4.4	0.67	0.32	0.13	9	for s_f' = 5%
s_f' (%)	1.1	7.5	16	40	9	if s_d' = 1%
s_c' (%)	2.1	0.44	0.22	0.09	10	for s_f' = 5%
s_f' (%)	2.4	11	23	57	10	if s_c' = 1%
s_c' (%)	2.2	0.33	0.16	0.06	12	for s_f' = 5%
s_f' (%)	2.3	15	31	80	12	if s_c' = 1%

[a] Relative oxygen concentration difference between inlet and outlet $[2(C_{O_2,in} - C_{O_2,out})/(C_{O_2,in} + C_{O_2,out})]$.

gases are obtained by difference between the whole gas and the sum of CO_2 and O_2.

Starting with Eqn. 5, using the same substitutions for f and a, and substituting $b = C_{G,i,in}$; $c = C_{G,inert,in}$; $d = C_{G,i,out}$ and $e = C_{G,inert,out}$ gives

$$f = a(b - cd/e) \tag{11}$$

The error analysis for air at the reactor inlet, by analogy with the above treatments, and making the same assumptions, finally yields

$$s'_f = 2s'_d cd/(be - cd) \tag{12}$$

Table 1 shows the relative difference in concentration ($\Delta C'_i$), the precision of the concentration measurement required to get a final result for $Q_i X V_L$ with a relative error s'_f = 5% and the result if the error in the concentration measurement s'_c = 1%. Comparison of these results with those from Eqn. 10 shows that independent measurements of concentration require double the precision compared to the situation where only ratios of concentration have to be evaluated. The latter case applies to both m.s. and g.c. methods of determining gas concentration.

Gas analysis with m.s.

As shown above, the limits of precision of the determination of $Q_i X V_L$ by gas balancing for small differences in concentration between the inlet and the outlet are given by the precision of measurement of the ratio of two ion currents (e.g., I_{32} for oxygen and I_{14} or I_{28} for nitrogen or I_{40} for argon). Therefore, the stability of measurement of such ratios with the two m.s. (QMG 64 and QMG 311) was investigated. Typical results for measurement of air during several hours are given in Table 2. It is clear that the absolute stability of the ion currents is considerably worse than the ratio of intensities. Absolute intensities are known to be influenced by temperature and total pressure, as well as electronic instabilities. The results shown here indicate

TABLE 2

Measurement of nitrogen (*m/z* 28), oxygen (*m/z* 32) and argon (*m/z* 40) in air

	I_{28}	I_{32}	I_{40}	I_{32}/I_{28}	I_{40}/I_{28}	Method[b]
Mean	422.8×10^{-7}	971.8×10^{-8}	549.1×10^{-9}	0.2299	0.012979	I
(A)	$1{,}5097 \times 10^{-7}$	3.2704×10^{-8}	2.3161×10^{-9}	0.2166	0.015336	II
s[a]	0.69	0.80	1.20	0.17	0.59	I
(%)	0.68	0.95	1.73	0.098	0.30	II

[a]Standard deviation. [b]Method I: QMG 64, 50 measurements each the mean of 1000 A/D conversions, measured in ambient air. Method II: QMG 311, single measurements at gas inlet into the fermenter during fermentation with about 5000 A/D conversions in the quadrupol data processor using secondary electron multiplier (700 scale units), data transfer with 11-bit mantissa.

that even the smaller QMG 64 instrument would be suitable in practically any situation of interest.

Concentrations of oxygen, carbon dioxide and argon were calculated from

$$C_i = k_{i,j}(I_j - I_{j,\,BG}) \tag{13}$$

whereas nitrogen concentrations were calculated from

$$C_{N_2} = k_{N_2,\,28}(I_{28} - I_{28,\,BG} - C_{CO_2} k_{28,\,CO_2}) \tag{14}$$

where k's are calibration constants and BG indicates background.

For the calculation of concentration, both m.s. were first calibrated with helium to measure the background intensities, then with air to get calibration factors for O_2, N_2 and Ar, and then with a suitable calibration gas containing air and CO_2 to calibrate for CO_2. The contribution of CO_2 to the ion current at m/z 28 was determined in advance by using pure CO_2. With the small m.s., calibration was only done at the beginning of fermentation. With the bigger one, calibration was done at regular intervals. As it was clearly proved during fermentation that measurement of air gives very constant results for relative signals (Table 2), it will usually be sufficient, at least for short-term batch fermentation, to calibrate only initially.

Results of off-line analysis and measurement of dissolved oxygen (DO) of a batch fermentation of *Bacillus subtilis* are shown in Fig. 1. With the QMG 64 for gas analysis, specific reaction rates for oxygen (Q_{O_2}) and for carbon dioxide (Q_{CO_2}) were measured as shown in Fig. 2. Shortly before hour 4 in the fermentation, the gas flow was changed. These results show that even with a rather dilute culture, useful results can be obtained for the

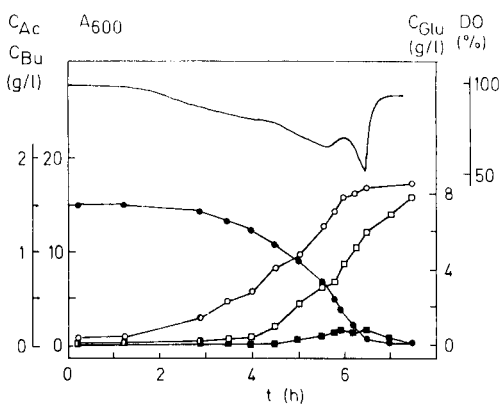

Fig. 1. Batch fermentation of *Bacillus subtilis* in the Chemap fermenter (14 l, 30°C, pH 7.0). DO, dissolved oxygen concentration in % of air saturation; A (○) absorbance of the culture at 600 nm; C_{Ac} (□) concentration of acetoin (g l^{-1}); C_{Bu} (■) concentration of D,L-butandiol (g l^{-1}); C_{Glu} (●) concentration of glucose (g l^{-1}).

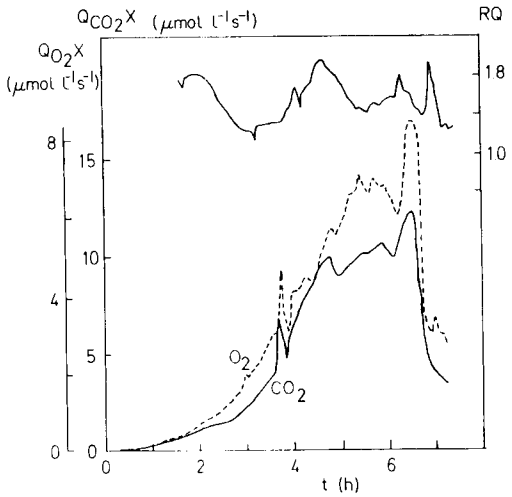

Fig. 2. Results of gas analysis of the same batch fermentation as described in Fig. 1. Q_{O_2X}, specific oxygen uptake rate multiplied by biomass concentration (μmol l^{-1} s^{-1}); Q_{CO_2X}, specific carbon dioxide production rate multiplied by biomass concentration (μmol l^{-1} s^{-1}) RQ, respiratory quotient (Q_{CO_2}/Q_{O_2}).

specific gas reaction rates as well as for the respiratory quotient. It is also clear that some irregularities in the absorbance measurements are not measurement errors but real changes in the culture; careful interpretation of the gas analysis results shows that shortly before hour 5 there is decreased growth and increased excretion of reduced products (increased RQ). The gas analysis also indicates some excretion of butandiol just after hour 6.

Results of another culture of *Bacillus subtilis* under different conditions with the QMG 311 also showed the usefulness of the proposed method in problem-solving.

Fingerprinting with m.s. membrane probe

The basic idea behind this general method of fermentation analysis is that probably all microorganisms excrete various products depending on culture conditions and the physiological state of the culture. Amongst these are volatile compounds which might be useful for on-line monitoring of the state of the culture and so for monitoring products that are not directly accessible.

Several samples from industrial fermentations were analyzed for volatile compounds and correlation of these with product formation was evaluated. Tested organisms included *Streptomyces* sp., *Clostridium tetanii* and *Actinomyces* sp. Filtered samples were measured with the membrane probe using a small stirred cell. All of the samples tested showed significant peaks in the m.s. An example with *Clostridium tetanii* showed a large number of very intense peaks (Fig. 3). As in all other spectra, the water peak (*m/z* 18)

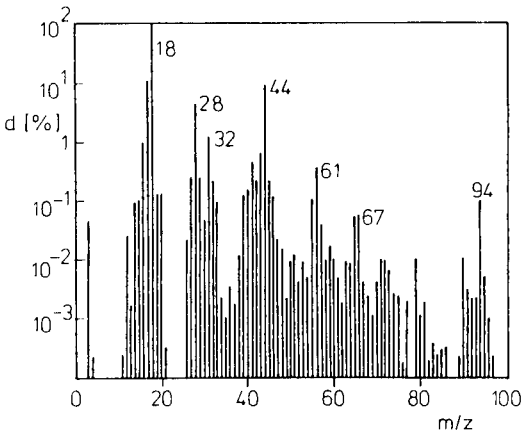

Fig. 3. Spectrum from *Clostridium tetanii* fermentation. $I_{18} = I_{max} = 1.29 \times 10^{-6}$ A; d is normalized intensity.

predominated. Peaks of dissolved gases (N_2 m/z 28, O_2 m/z 32 and CO_2 m/z 44) were also always very large.

The quantification of specific volatile components is not necessary if single m.s. peaks or groups of them could indicate product formation. Changes of single-peak intensities are difficult to detect and would often be misleading because mixtures of volatiles give an overlap of fragments originating from different compounds. On the assumption of linear superposition of peak intensities from different compounds, factor analysis of spectra should give a means of useful data reduction. This condition will not always be satisfied when mixtures of volatiles are measured with a m.s. membrane probe, especially at high concentrations of volatiles where nonlinearities have been observed [10].

Factor analysis was used to treat data from a sequence of samples from various batch fermentations. Since primarily only data reduction was required, the principal components method was used without factor rotation. All peaks with m/z <31 and peaks with m/z 32(O_2), 40(Ar) and 44(CO_2) and those having variance <3.5% were rejected. Intensities were first normalized to the water peak by applying $d_{i,j} = I_{i,j}/I_{18,j}$. Then the data matrix was transformed by taking intensities of each mass ($d_{i,j}$) around its mean (d_i) and normalizing it with its standard deviation (s_i): $d^*_{i,j} = (d_{i,j} - d_i)/s_i$. The resulting data matrix was then processed by the SPSS program [13]. Factor spectra were calculated from $r_{i,j} = r^*_{i,j} s_i$, where r is the transformation matrix. Factor scores $f_{i,j}$ were then plotted together with actual product concentration. Samples from three different batches of a *Streptomyces* fermentation (Ciba-Geigy) were analyzed (Fig. 4). Even with no knowledge of the fermentation conditions and product formation, it is clear that batch B6 differed considerably from batches B3 and B4, which seemed to be similar. The actual product analysis verified these differences.

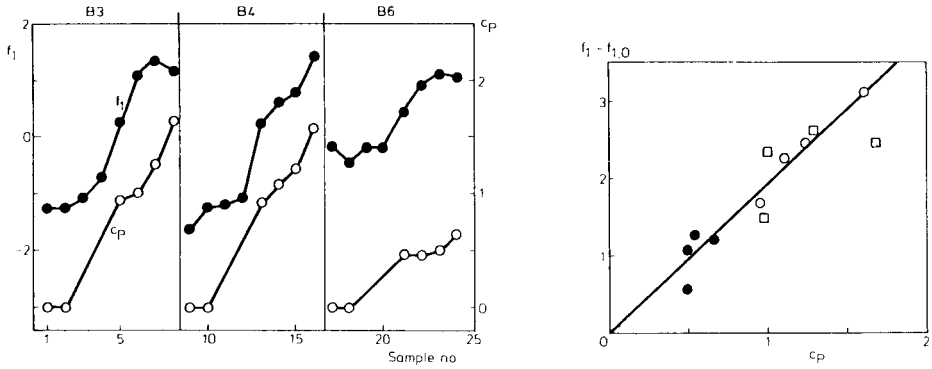

Fig. 4. Comparison of product concentration (○, C_P) with factor 1 (●, f_1) in three different batch fermentations of *Streptomyces* sp.

Fig. 5. Correlation of increase in factor 1 and product concentration: (□) batch 3 (B3); (○) batch 4 (B4); (●) batch 6 (B6).

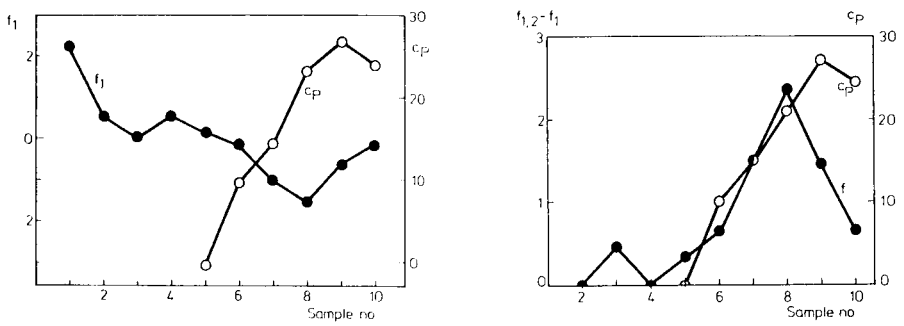

Fig. 6. Comparison of another batch fermentation of *Streptomyces* sp. Symbols as in Fig. 4; C_P in mg l^{-1}.

Fig. 7. Correlation of factor value $f_{1,2}$ of sample no. 2 in Fig. 6. minus actual factor f_1 with the product concentration. Symbols as in Fig. 4; C_P in mg l^{-1}.

A plot of each factor (f_i) minus the factor score at the beginning of the fermentation (f_0) against product concentration showed a reasonable linear correlation (Fig. 5).

Another *Streptomyces* fermentation (Sandoz) producing a different product, an intracellular oligopeptide, showed completely different behaviour (Fig.6). Here the first sample (medium before inoculation) and sample 2 (broth immediately after inoculation) differed considerably. Plotting the difference of each factor score (f_i) minus f_2 (sample after inoculation) against product concentration yielded the results shown in Fig. 7. Here the drastic drop of the factor score just before the end of product formation could be a useful on-line indicator for harvesting culture broth. On-line

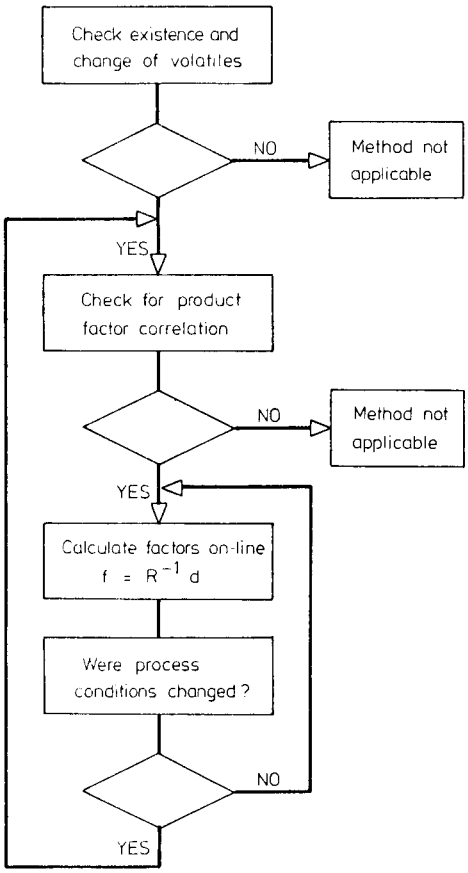

Fig. 8. Scheme for on-line fingerprinting of fermentations with the m.s. membrane probe and factor analysis.

use of this fingerprinting method with factor analysis is possible after prior factor score correlation with product concentration. The procedure for using this method on-line is shown schematically in Fig. 8. The first step involves checking for volatile compounds (peaks in the mass spectrum of the liquid phase) followed by a check for a product/factor correlation. Then rapid on-line calculation only with a microcomputer is possible.

The authors thank Ciba-Geigy (Basel) and Sandoz (Basel) for supplying samples and data, and Balzers (Liechtenstein) for supplying the QMG 64 mass spectrometer.

REFERENCES

1 J. A. Hunter, R. W. Stacy and F. A. Hitchcock, Rev. Sci. Instrum., 20 (1949) 333.
2 E. Heinzle, K. Furukawa, I. J. Dunn and J. R. Bourne, Bio/technology, 1 (1983) 181.
3 S. Woldring, G. Owens and D. Woolford, Science, 153 (1966) 885.
4 M. Reuss, H. Piehl and F. Wagner, Eur. J. Appl. Microbiol. Biotechnol., 1 (1975) 323.
5 J. S. Lundsgaard, L. C. Peterson and H. Degn, in H. Degn and R. Brook, (Eds.), Measurement of Oxygen. Proc. Interdisc. Symp., Elsevier, Amsterdam, 1976, p. 168.
6 E. Heinzle and R. M. Lafferty, Eur. J. Appl. Microbiol. Biotechnol., 11 (1980) 17.
7 Y. Jouanneau, B. C. Kelly, Y. Berlier, P. A. Lespinat and P. M. Vignais, J. Bacteriol., 143 (1980) 628.
8 E. Pungor Jr., C. R. Perley, C. L. Cooney and J. C. Weaver, Biotechnol. Lett., 2 (1981) 409.
9 E. Pungor Jr., E. Schaefer, J. C. Weaver and C. L. Cooney, in M. Moo-Young, C. W. Robinson and C. Vezina (Eds.), Advances in Biotechnology, Vol. 1, Pergamon Press, Toronto, 1981, p. 393.
10 P. Doerner, J. Lehmann, H. Piehl and R. Megnet, Biotechnol. Lett., 4 (1982) 557.
11 J. C. Weaver and J. H. Abrams, Rev. Sci. Instrum., 50 (1979) 478.
12 H. L. C. Meuzelaar, J. Haverkamp and F. D. Hileman, Pyrolysis Mass Spectrometry of Recent and Fossil Biomaterials, Elsevier, Amsterdam, 1982.
13 N. H. Nie, B. H. Dale and H. C. Hull, Statistical Package for Social Sciences — SPSS, McGraw-Hill, New York, 1970.
14 K. Furukawa, E. Heinzle and I. J. Dunn, Biotechnol. Bioeng., 25 (1983) 2293.

Analytica Chimica Acta, 163 (1984) 231—236
Elsevier Science Publishers B.V., Amsterdam — Printed in The Netherlands

Short Communication

HIGH-RESOLUTION CONFOCAL SCANNING LIGHT MICROSCOPY IN BIOLOGY

G. J. BRAKENHOFF,* H. T. M. VAN DER VOORT and N. NANNINGA

Department of Electron Microscopy and Molecular Cytology, University of Amsterdam, Muldergracht 14, 1018 TV Amsterdam (The Netherlands)

(Received 31st March 1984)

Summary. Confocal scanning light microscopy provides an appreciable improvement in resolving power compared with classical light microscopy; the amount of information that can be extracted from a specimen is increased by a factor of 3. When a laser serves as light source and u.v. wavelengths are used, resolutions of 140 nm are possible. Applications are the study of biological structures in the sub-μm region, for instance, the replicating nucleoid (DNA) morphology of live *Escherichia coli* and eukaryotic chromosomes.

Confocal scanning light microscopy (c.s.l.m.) has been developed [1—3] in order to study hydrated specimens at higher resolutions than conventional light microscopy. Electron microscopy has of course much better resolving capabilities, but can in practice only deliver high-resolution images of chemically fixed, dehydrated biological material. Some observations of hydrated specimens by electron microscopy with the "wet cell" method have been published [4], but this technique is rather complicated, and the object is exposed to a high, probably lethal, radiation dose during observation. High-resolution immersion c.s.l.m. is currently the only technique available that can supply morphological information on live specimens below the resolution limit of standard light microscopy. A scanning x-ray microscope [5] may eventually achieve a better resolution than c.s.l.m. However, it can be shown that the radiation dose per image point needed for image formation with acceptable signal-to-noise conditions, will exceed the tolerance limits of many, if not all, live specimens.

In comparison with conventional light microscopy, c.s.l.m. provides not only a fundamentally improved resolution but an extended dynamic range because of the absence of glare as well as possibilities for image processing. These properties can be exploited in a number of unusual imaging modes. With the use of high-aperture immersion optics, it is in principle possible to achieve resolutions down to 60 nm at a wavelength of 200 nm (the lower limit for refraction optics). Because of the relative newness of the c.s.l.m. technique, a short account of its mode of operation is given, before some high-resolution images of biological specimens are presented and the general aspects and further prospects of this imaging technique are discussed.

0003-2670/84/$03.00

Principle and construction of the c.s.l. microscope

The basic idea behind the c.s.l. microscope is simple. As indicated in Fig. 1, exactly the same point in the object is both optimally illuminated and imaged on the detector pinhole. It can be shown [1] that when there is a point light source and a point detector, and the imaging is diffraction-limited, there is a fundamental improvement in linear resolution by a factor of 1.4. This modest improvement in linear resolution means, nevertheless, that as the depth of the field is also reduced by the same factor, the information relating to an image point corresponds to a volume which is smaller by a factor of about 3 (1.4^3) than in conventional light microscopy.

The c.s.l. microscope built and in use in this institute [2] may be described briefly as follows. To maximize the profit from the gain in resolution, it is necessary to equip the instrument with optics with the highest possible apertures (i.e., oil-immersion objectives). This leads to the construction and positioning of the object as shown in Fig. 2. The immersion oil stays in place during the mechanical scanning up to the highest scan amplitudes used (1 mm). The mechanical scan has to meet very high standards of stability with regard to both height positioning of the specimen in relation to the confocal optics, and the repeatability of the scan line during the scan movement. Both need to be appreciably better than the resolution (100—200 nm) which is defined by the diffraction-limited imaging. In the approach used here, where there is scan table "skating" on an attached ruby over a polished hard metal surface, the system is stable within 10 nm for a period more than sufficient for observation and recording of the images. Technical details are available elsewhere [6].

Because of its power, a laser is the most suitable light source for a c.s.l. microscope. As a few milliwatts suffice for adequate image formation, gas lasers (HeNe, λ = 633 nm; HeCd, λ = 442 and 325 nm) or low-power argon ion lasers (λ = 488 nm and 514 nm and others) are suitable. With dye lasers and doubling techniques, light with virtually any wavelength in the visible and u.v. range can be made, though at considerable expense.

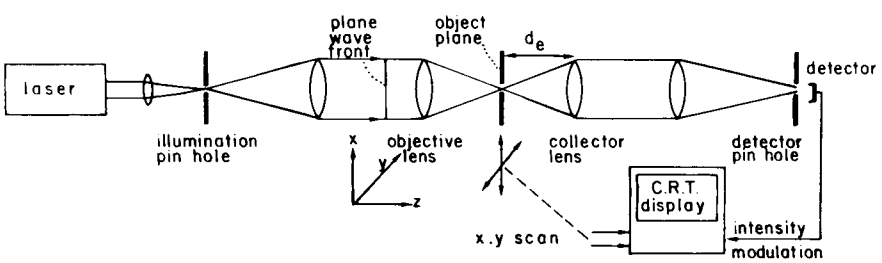

Fig. 1. Principle of image formation in c.s.l.m. A plane light wave generated by a laser light source and an illumination pinhole is focused in the object by the objective lens. The collector lens is adjusted so that the back projected image of the point detector coincides exactly with the point of focus in the object. The object is scanned mechanically through this communal focal point in the object, modulating the light intensity on the detector which in turn modulates the cathode ray tube on which the image is created.

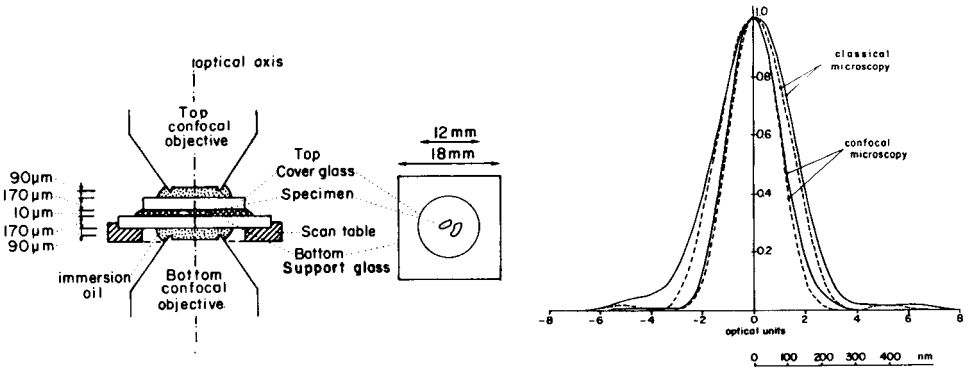

Fig. 2. Construction of the objective and positioning of the scan table between the two confocally arranged objectives. The indicated distances and thicknesses of the support glass and cover glass are determined by the optical requirements of the immersion objectives used.

Fig. 3. The response as a function of position during the scan of a small hole through the confocal area: (—) measurement; (---) theory. The response measured at λ = 633 nm is close to the theoretical expectation for the optics used (NA = 1.3). For comparison, the respective responses in classical microscopy are shown.

Image formation in c.s.l.m.

The actual improvement in resolution beyond the classical limit can be demonstrated on the point response of the c.s.l.m. system to the test object of a small hole (10 nm) in a gold film (Fig. 3). The point resolution (response width at half intensity) in c.s.l.m. is wavelength-dependent. The minimum so far achieved here is 140 nm at a wavelength of 325 nm. The image of a grating replica (Fig. 4) obtained at 325 nm is in accordance with this point resolution and shows that the image is free from artefacts down to this resolution limit.

Comparison of images of live bacteria (Fig. 5) shows a remarkable increase in observable detail in the structure of the bacterial genome (light areas). The somewhat "ladder"-like structure is in agreement with structures observed by electron microscopy in fixed material and this is the first time they have been observed in living material. The c.s.l.m. absorption contrast image was produced with the help of electronic contrast enhancement. This is not possible in classical microscopy where one has to use phase contrast to visualize weakly absorbing objects. The c.s.l.m. technique provides a remarkable increase in observable detail in the banding pattern of *Drosophila hydei* polytene chromosomes (Fig. 6). It is possible to count 60% more bands from c.s.l.m. images compared to conventional light microscopy [7]; further applications may include the study of integrated electronic circuits and submicron fat/oil suspensions (butter, margarine).

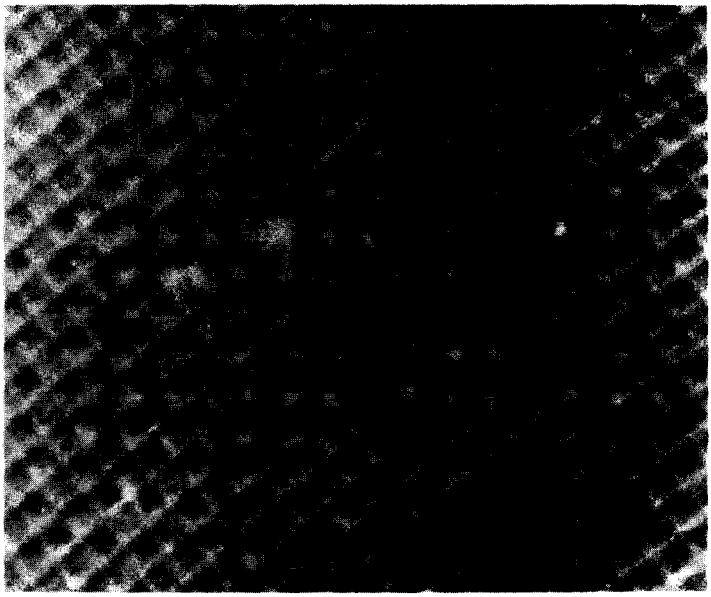

Fig. 4. The c.s.l.m. image of the replica of a waffle-type grating (grating distance 463 nm) at $\lambda = 325$ nm.

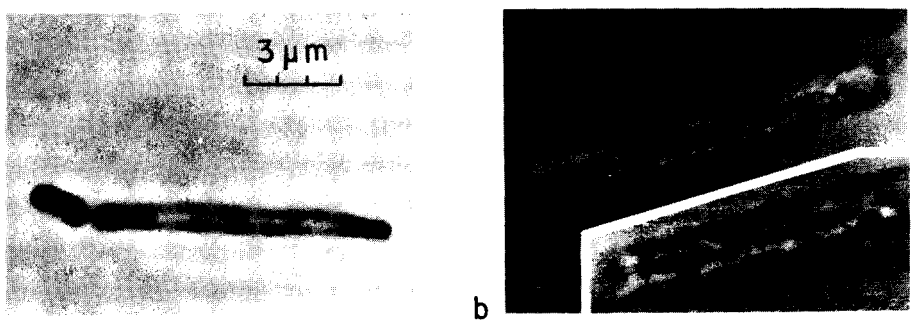

Fig. 5. (a) Image of a live bacterium by classical light microscopy with phase contrast; (b) image at $\lambda = 325$ nm of a bacterium from same preparation by c.s.l.m. with absorption contrast. The inset shows further magnification of the internal structure.

Scanning aspects and discussion

The fundamental increase in resolution in c.s.l.m. is accompanied by a number of important properties. In c.s.l.m. only light emanating from the illuminated spot can contribute efficiently to the signal detected by the point detector, thus glare caused by light scattered elsewhere in the microscope (on lens flaws, off focus areas in the specimen, etc.) is virtually absent. Hence, the dynamic range, i.e., the intensity range between the brightest and the darkest areas in the microscope image, is increased from typically 100 in normal light microscopy to 10 000 in c.s.l.m.

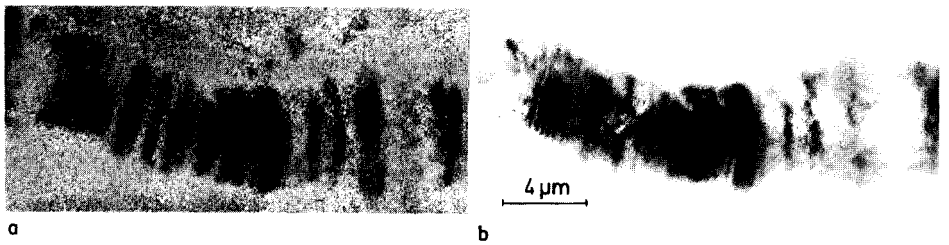

Fig. 6. The banding pattern in a segment of the *Drosophila hydei* polytene chromosome observed (a) in classical light microscopy with absorption contrast and (b) in c.s.l.m. at $\lambda = 442$ nm with absorption contrast.

The scanning aspect of the microscope contributes the following properties. First, quantitative image data are available, hence image processing is possible in various forms. Secondly, the detection efficiency of the detectors used is higher (±0.1—0.3) than that of the photographic plate (±0.01) which leads, together with the fact that only the area of interest is illuminated, to a lower radiation dose on a sensitive specimen. Thirdly, the field of view of the microscope is not fixed by the optics, but depends on the amplitude of the mechanical scan and can be adjusted as required; for the same reason, the magnification is continuously variable. Finally, the plane imaged does not have to be perpendicular to the optical axis but can be chosen at will, because the height position of the specimen can be varied during the transverse scan. Thus, inclined or even bent surfaces may be imaged, depending on the sophistication of the control electronics.

The above properties can be used in various imaging modes [3] among which various forms of differential contrast and high-resolution stereo imaging may be mentioned. The c.s.l.m. can also operate in the reflection mode which will be useful for the investigation of living biological specimens situated (or growing) on a glass surface. In this mode, an area of the specimen close to the glass interface with a thickness of about 10 µm at high numerical aperture (NA) (more at lower NA) can be investigated with high resolution. During such viewing the specimen is fully accessible, which opens up possibilities for experiments on live specimens. The illuminating and detecting wavelengths do not have to be identical which, for instance, makes fluorescence c.s.l.m. possible, and further improvement in resolution can be expected [8].

The c.s.l.m. has a number of disadvantages with respect to normal light microscopy. For instance, the entire image is not immediately viewable and the mode of operation is definitely more complicated. These handicaps should be overcome by operating the instrument under computer control, which would take care of the procedures for automatic confocal alignment and image contrast adjustment. Also a continuous "viewing" image could be generated from a digital image frame store, periodically extended by the signals obtained during the relatively slow mechanical scan in c.s.l.m. Image subtraction and various forms of filtering are of course also possible on the data in this frame store.

We thank J. A. C. Valkenburg from our institute, J. Grond and J. Derksen from the University of Nijmegen for supplying specimens. We are greatly indebted to the Foundation for Fundamental Biological Research (BION), which is subsidized by the Netherlands Organization for the Advancement of Pure Research (ZWO) and by the Foundation of Technical Sciences (STW) who support this project.

REFERENCES

1 C. J. R. Sheppard and T. Wilson, J. Microsc., 114 (1978) 179.
2 G. J. Brakenhoff, P. Blom and P. Barends, J. Microsc., 117 (1979) 219.
3 G. J. Brakenhoff, J. Microsc., 117 (1979) 233.
4 D. F. Parsons, Proc. 6th Eur. Congr. Electron Microscopy, Jerusalem, 1976, Vol 2, p. 79.
5 E. Spiller, In E. A. Ash (Ed.), Scanned Image Microscopy, Academic Press, London, 1980, p. 365.
6 H. J. B. Marsman, R. Stricker, R. W. Wijnaends van Resandt, G. J. Brakenhoff and P. Blom, Rev. Sci. Instrum., 54 (1983) 1047.
7 C. J. Grond, J. Derksen and G. J. Brakenhoff, Exp. Cell. Res., 138 (1982) 458.
8 J. Cox, C. J. R. Sheppard and T. Wilson, Optik, 60 (1982) 391.

Analytica Chimica Acta, 163 (1984) 237—242
Elsevier Science Publishers B.V., Amsterdam — Printed in The Netherlands

Short Communication

EXTRACTION AND GAS—LIQUID CHROMATOGRAPHY OF MICROBIAL *N*-DEALKYLATION SYSTEMS

G. J. SEWELL*[a], C. J. SOPER and R. T. PARFITT

School of Pharmacy and Pharmacology, University of Bath, Bath BA2 7AY (Great Britain)

(Received 3rd April 1984)

Summary. Methods are described for the extraction and qualitative gas-liquid chromatography of a series of microbial transformation systems in which various *Streptomycetes* and fungi were screened for *N*-dealkylation activity against a variety of drug molecules. The possibility that microbial transformation products could react under extraction conditions to form gem-diamines was investigated. Rapid on-column acetylation permitted the resolution of *N*-dealkylated products from starting substrate. Incomplete acetylation under the conditions used ensured that each *N*-dealkylated transformation product formed at least two species with characteristic retention times; with careful standardization, this increased confidence in the identifications.

The potential benefits of microbial *N*-dealkylation in the preparation of drug intermediates have been described previously [1]. Various *Streptomycetes* and species of the fungus *Cunninghamella* were screened for *N*-dealkylation activity against a variety of drug molecules including amitriptyline, chlorpromazine, codeine and two 6,7-benzomorphans. These compounds are all tertiary amines possessing *N*-methyl functions in alkylamine chains and piperidine ring structures. The transformation systems studied are listed in Table 1. This communication describes methods for the isolation and characterisation of *N*-dealkylated transformation products.

Transformation products and unchanged substrate were extracted from basified transformation cultures into organic solvents. On the basis of experiments with hepatic microsomes [2, 3], it was expected that microbial *N*-demethylation of tertiary amines would proceed via a carbinolamine intermediate which would cleave to yield a secondary amine transformation product and formaldehyde. It was envisaged that the formaldehyde by-product would remain dissolved in the aqueous culture medium, the water—air partition coefficient being 500 [4]. Kalaus et al. [5] showed that under alkaline conditions, two molecules of a secondary amine can react with one molecule of formaldehyde to form a gem-diamine. To test the significance of this reaction in the extraction of microbial transformation mixtures, two

[a]Present address: Quality Control Laboratory, Manor Park Hospital, Bristol, Great Britain.

TABLE 1

Microbial transformation systems with required *N*-dealkylated transformation products

Transformation system	Substrate	Required transformation product
1	Amitriptyline	Nortriptyline
2	Chlorpromazine	Desmethylchlorpromazine
3	Codeine	Norcodeine
4	Metazocine	Normetazocine
5	Pentazocine	Normetazocine

model secondary amines were extracted from a microbial culture medium under basic conditions in the presence of formaldehyde. Piperidine and norcodeine, the *N*-demethylation products of *N*-methylpiperidine and codeine, respectively, were the model secondary amines selected.

Studies on the mammalian metabolism of drug molecules have shown that derivatization is usually required to facilitate the separation of *N*-demethylated metabolite from the parent molecule by gas-liquid chromatography (g.l.c.) [6]. Rapid on-column derivatization has been used successfully to identify drug metabolites in biological fluids [6] and was therefore considered applicable to microbial *N*-dealkylation systems. The sample extract and acetic anhydride are injected concurrently onto the column; the available secondary amine and/or hydroxyl functions of some, but not all, of the analyte molecules are acetylated. On the non-polar stationary phase used, the derivatized fraction exhibited a peak shift to longer retention times than the underivatized fraction. This simple procedure was expected to resolve selectively secondary amine transformation products from the starting material and to produce at least two species for each analyte possessing one or more sites available for acetylation. Retention data for transformation culture extracts were compared with those obtained from authentic standards of starting material and the expected transformation product(s). Because at least two species eluted for each *N*-dealkylated product, confidence in product identification was increased.

Experimental

Examination of extracts for gem-diamine formation. Microbial growth medium (50 ml) containing either piperidine (0.02 M) or norcodeine hydrochloride (0.02 M) and formaldehyde (0.01 M) was vigorously stirred and adjusted to pH 10.5 with 2 M sodium hydroxide and extracted into 1,2-dichloroethane (2 × 50 ml). The combined organic phase was separated, dried (anhydrous $MgSO_4$) and filtered, and the filtrate was evaporated to an oily residue. The residue was dissolved in deuterated chloroform and subjected to ^{1}H-n.m.r. spectroscopy.

On-column derivatization g.l.c. Microbial transformation cultures (50 ml) containing a combined substrate and transformation product concentration of 1 mM were extracted as described above, with the organic solvents detailed in Table 2. The residues obtained after evaporation of extraction solvents were reconstituted with 2 ml of either n-hexane (transformation system 1) or a mixture of equal parts of methanol and tetrahydrofuran. Acetic anhydride (2 μl) and the reconstituted sample (2 μl) were drawn into a 5-μl syringe and injected into the gas chromatograph (Perkin-Elmer F-11) fitted with a 2 m × 4 mm i.d. glass column packed with 3% SE-30 Ultraphase on Chromosorb W-HP, 100/120 mesh (Phase Separations, Clwyd, U.K.). The column was conditioned for 12 h at 275°C and silanized before use. Isothermal conditions were used throughout; the operating temperatures used for each transformation system are shown in Table 2. In each case the carrier gas was nitrogen at 124 ml min^{-1}. Detection was by flame ionization. Reference solutions of the required transformation products, nortriptyline (Eli Lilly), desmethylchlorpromazine (Merck, Sharp and Dohme), norcodeine (prepared by the method of Montzka et al. [7]) and normetazocine (Sterling Organic) were chromatographed under the same conditions.

Results and discussion

Examination of extracts for gem-diamine formation. The ^{1}H-n.m.r. (60 MHz) spectrum of the extract of piperidine in the presence of formaldehyde showed peaks at δ1.50 (m, 12H, —CH_2—), δ2.45 (m, 8H, N—CH_2—) and δ2.85 (s, 2H, N—CH_2—N) vs. TMS. Addition of D_2O did not alter this spectrum. The ^{1}H-spectrum (100 MHz) of the extract of norcodeine in the presence of formaldehyde was unchanged from that of norcodeine. The piperidine extract spectrum exhibited double the number of piperidine ring protons and a signal from two deshielded methylene protons indicative of a methylene bridge linking two tertiary nitrogen atoms. The absence of an exchangeable proton in the extraction product implies the loss of the

TABLE 2

Extraction solvents and g.l.c. operating temperatures used in the analysis of microbial transformation systems

Transformation system[a]	Extraction solvent	Oven temp. (°C)	Injection temp. (°C)
1	n-Hexane	210	215
2	1,2-Dichloroethane	215	220
3	10% 2-Methylpropanol in 1,2-dichloroethane	210	215
4, 5	20% 2-Methylpropanol in 1,2-dichloroethane	195	200

[a]See Table 1.

secondary amine function of piperidine (which provides a proton exchangeable with D_2O). These data are consistent with gem-diamine formation under the extraction conditions. The n.m.r. spectrum of the norcodeine extract was concordant with that of a norcodeine standard, suggesting that dimer formation had not occurred and that norcodeine was extracted without complication in the presence of formaldehyde.

These observations cannot readily be explained by steric considerations because the piperidine ring is positioned perpendicular to the plane of the norcodeine molecule and the nitrogen atom is unhindered. It is more plausible that vigorous stirring of the extraction mixture afforded instant partitioning of the norcodeine base into the organic phase where it was protected from the formaldehyde in the aqueous phase. Conversely, the piperidine base is water-miscible and remained in the aqueous phase where it reacted with formaldehyde. The gem-diamine produced by this reaction partitioned into the organic phase. It appears that if the base form of the nor-compound is not water-miscible, and if the organic and aqueous phases are well mixed, extraction of *N*-demethylated product in the presence of formaldehyde proceeds without difficulty. However, these results suggest that the extraction of *N*-demethylated metabolites of polar, water-miscible bases under basic conditions could result in gem-diamine formation and severe loss of product from the microbial transformation cultures.

On-column derivatization for g.l.c. Retention data obtained with the on-column derivatization procedure are shown for standard compounds of substrates and the corresponding *N*-dealkylated product in Table 3. In each case, peaks corresponding to derivatized transformation product species were clearly resolved from the parent substrate, even when retention times of the underivatized analytes were identical. Compounds with more than one derivatization site gave rise to several characteristic peaks as species of various

TABLE 3

Retention data (g.l.c.) for substrates and required transformation products

Transformation system[a]	Analyte	Retention times (min)
1	Amitriptyline	3.10
	nortriptyline	3.10, 9.61
2	Chlorpromazine	6.42
	desmethylchlorpromazine	6.42, 20.67
3	Codeine	4.50, 6.12
	norcodeine	4.50, 6.12, 12.11, 16.88
4	Metazocine	2.65
	normetazocine	2.65, 3.00, 7.10
5	Pentazocine[b]	6.70
	normetazocine	2.65

[a]See Table 1. [b]Analytes not derivatized.

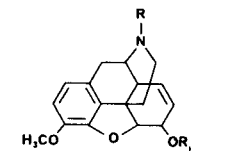

Compound	R	R_1
A	CH_3	H
B	CH_3	$COCH_3$
C	H	H
D	H	$COCH_3$
E	$COCH_3$	H
F	$COCH_3$	$COCH_3$

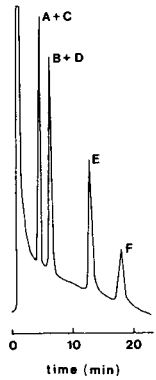

Fig. 1. Derivative species and gas-liquid chromatogram obtained by on-column acetylation of codeine and norcodeine.

derivative combinations exhibited different affinity for the SE-30 stationary phase. The various species formed by the on-column derivatization of codeine and norcodeine are shown in Fig. 1. A fraction of the codeine molecules present in a mixture with its transformation product, norcodeine, would be esterified at the 6-hydroxyl function, resulting in a mixture of species A and B (see Fig. 1). The chromatogram (Fig. 1) shows that the parent compound (A) is eluted before the acetyl derivative (B). Norcodeine has two active sites, the 6-hydroxyl group and the secondary amine group; underivatized norcodeine (C) will elute before the mono-acetylated species (D). These would not be resolved from the corresponding codeine species and are not significant. However, acetylation of the amine group (E) and diacetylation of both the amine and hydroxyl groups (F) produce two well-separated peaks characteristic of norcodeine. The peak assignments shown in Fig. 1 were made on the basis of retention data for standards of codeine and norcodeine completely acetylated with acetic anhydride and pyridine before injection.

These procedures facilitated the rapid separation and identification of *N*-dealkylated transformation products in screening experiments with a variety of drug molecules. Analysis of all of the transformation systems described was possible with essentially one g.l.c. system, requiring only variation of operating temperatures to achieve resolution. Because at least two species with characteristic retention times eluted for each *N*-dealkylated analyte, confidence in product identity was increased. These procedures could readily be made quantitative by derivatizing the sample analytes to completion prior to chromatography, and so should be useful in quantitative microbial *N*-dealkylation experiments.

REFERENCES

1 G. J. Sewell, C. J. Soper and R. T. Parfitt, J. Pharm. Pharmacol., 31 (1979) 90.
2 R. E. McMahon, J. Pharm. Sci., 55 (1966) 334.

3 E. Gram, Handb. Exp. Pharmacol., 28 (1971) 334.
4 H. Knight and R. W. G. Tennant, Lab. Pract., 22 (1973) 169.
5 G. Y. Kalaus, L. Toke and C. S. Szantay, Acta Chim. Acad. Sci. Hung., 63 (1970) 443.
6 M. W. Anders and G. J. Mannering, Anal. Chem., 34 (1962) 730.
7 T. A. Montzka, J. D. Matiskella and R. A. Partyka, Tetrahedron Lett., 14 (1974) 1325.

Analytica Chimica Acta, 163 (1984) 243—248
Elsevier Science Publishers B.V., Amsterdam — Printed in The Netherlands

Short Communication

TECHNICAL IMPROVEMENTS IN PROTEIN MICROSEQUENCING

POR-HSIUNG LAI
Amgen, 1900 Oak Terrace Lane, Thousand Oaks, CA 91320 (U.S.A.)
(Received 9th April 1984)

Summary. Improved techniques for preparing samples and sequencing reagents have been developed to achieve highly sensitive protein sequencing. These improvements include a new sequencing buffer system which gives extremely low chromatographic background, a method for preparing polybrene, a key chemical in gas-phase protein microsequencing, and techniques for preparing protein samples suitable for microsequencing.

Protein microsequencing is important in protein characterization for production of recombinant DNA-derived protein products. In the past few years, the sensitivity of protein sequencing has been remarkably increased by improvements in sequencer design, methods of determining phenylthiohydantoin amino acids (PTH amino acids) and sample preparation. The most significant improvement in sequencer design has been the gas-phase sequencer which uses polybrene, a polymeric quaternary ammonium salt, for the physical immobilization of a protein sample in the reaction chamber and aqueous trimethylamine (TMA) and anhydrous trifluoroacetic acid (TFA) in coupling and cleavage steps, respectively [1]. Both reagents are delivered as gases. Both the polybrene and TMA can cause problems. Commercially available polybrene contains impurities which interfere with Edman degradation. Polybrene can be purified by running Edman degradation cycles in the presence of a dipeptide prior to sample application [1, 2]. The precycling of polybrene takes 8—12 h for each analysis which significantly reduces the time available for actual analysis.

In the case of TMA, water vapor is delivered with TMA vapor causing the partial degradation of phenylisothiocyanate. Secondly, dimethylamine can be formed from TMA during storage in the sequencer; it reacts with phenylisothiocyanate to form phenylthiocarbamyldimethylamine which interferes with PTH-amino acid analysis [3].

To improve the overall performance of protein sequence analysis, several approaches were made to improve sequencer usage, to eliminate interference caused by degraded sequencing reagents, and to remove contaminating salts in the protein sample by liquid—liquid extraction.

0003-2670/84/$03.00

Experimental

Preparation of polybrene. Polybrene (Aldrich; 1 g) was dissolved in 10 ml of distilled water. The aqueous solution was extracted three times, each with 100 ml of spinning-band distilled ethyl acetate (Burdick & Jackson) by vigorous stirring for 48 h. The organic phase was then removed by suction. The extraction was repeated three times using a total of 300 ml of ethyl acetate. The residual ethyl acetate was removed under vacuum. The aqueous solution was diluted with 10 ml of distilled water and added dropwise to 100 ml of a mixture (1 + 4) of methanol and ethyl acetate while stirring. After standing overnight, the upper phase was removed and the lower phase containing polybrene was dried under vacuum. A solution containing 60 mg of the purified polybrene per ml of water was prepared for sequencing use. For each sample analysis, 30 μl of the polybrene solution was applied to the filter disc. No short peptide is needed for scavenging.

Preparation of new coupling buffer for gas phase sequencing. Anhydrous TMA (50 g; Eastman Kodak) was mixed with 150 ml of h.p.l.c.-grade 2-propanol at −20°C. Ninhydrin (2 g) and hydrindantin (0.2 g) were added and the mixture was stirred for 12 h at 25°C and stored at −20°C.

Peptide/protein sample preparation. Samples were prepared by h.p.l.c. or sodium dodecyl sulfate/polyacrylamide gel electrophoresis. In the latter, samples were eluted from the gel according to the method of Hunkapiller and Hood [3]. Samples prepared by this method may contain some dodecyl sulfate and buffer salts. These can be removed by extraction with absolute methanol and, if necessary, with 50—80% (v/v) methanol in water, depending on the solubility of the contamination salts and the protein sample in the aqueous methanol solvent.

Protein sequencing. Sequencing was done with a gas-phase sequencer (Applied Biosystems) fitted with a regular conversion flask, using the modified standard protein program which has shorter R1 delivery time (4 s) and extended S3 (75 s) and S4 (90 s) washing; S4 was modified to contain 10% acetonitrile. Reagents and solvents used for gas-phase sequencing are listed in Table 1. Prior to sample loading, the filter disc containing pre-purified polybrene was taken through 0—6 precycles depending on the amount of protein to be analyzed. The smaller the amount of protein to be applied, the more precycles are needed. No more than six precycles are necessary for any sample. The PTH-amino acids are identified by reverse-phase h.p.l.c. using IBM cyano columns [4].

Results and discussion

The use of purified polybrene remarkably increased the overall efficiency of the gas phase sequencer. Usually, when the amount of sample to be analyzed is >5 nmol, no precycling for further cleaning is necessary. The initial and repetitive yields remain high enough for extended sequence analysis. Since the number of precycles for polybrene was reduced to the minimum, in a year of operation, the gas-phase sequencer was able to process 165 samples, a total of 3300 peptide residue cycles. Compared to the recently

TABLE 1

Comparison of reagents/solvents used in the published and modified procedures

Reagent/ solvent	Published procedure [1][a]	Modified procedure	Improvement
Immobilizing carrier	polybrene + dipeptide	prepurified polybrene	50% more analysis >50% reduction in cost
R1	15% PITC[b] in n-heptane	same	—
R2	25% TMA in water	25% TMA in 2-propanol + 2 g ninhydrin 0.2 g hydrindantin	20-fold reduction in levels of DPTU and PTCDMA; no distillation required; 15-fold reduction in cost; more sensitive analysis
S4	methanol/0.001% dithiothreitol	10% acetonitrile in methanol/0.001% dithiothreitol	less overlap

[a]No changes were made to R3 (TFA), R4 (1 M HCl/methanol), S2 (ethyl acetate) or S3 (n-butyl chloride). [b]Phenylisothiocyanate.

reported evaluation of a gas-phase sequencer (i.e., 110 analyses per year [2]), the gas-phase sequencer using prepurified polybrene can be used for 50% more analyses. The use of prepurified polybrene also significantly improved the cost efficiency. The cost of precycling is reduced by at least 50% compared to the cost for precycling commercial polybrene. It is also possible to do two sequence analyses with one sequencer in a day. This is particularly important for testing the purity of peptide or protein samples before an extended sequence analysis is conducted.

The improved R2 can achieve the same coupling efficiency as the original one (Table 1), yet it uses no purification apparatus and greatly reduces the formation of two major gas-phase sequencing artifacts, i.e., diphenylthiourea and phenylthiocarbamyldimethylamine (PTCDMA), as shown in Fig. 1. 2-Propanol, which replaces water in the original R2, decreases the formation of diphenylthiourea, the hydrolysis product of phenylisothiocyanate. Ninhydrin is added to react with contaminating primary and secondary amines such as dimethylamine and prevents them from being delivered to the reaction chamber. As shown in Fig. 1, the levels of diphenylthiourea and PTCDMA observed with the improved R2 are only about 5% of those obtained with the original R2. The diphenylthiourea interferes with the identification of PTH—methionine and PTH—proline, while PTCDMA coelutes with PTH—glutamine when the system described by Hunkapiller and Hood [3] is used. Although the h.p.l.c. gradient system can be modified to separate PTCDMA from PTH—glutamine and diphenylthiourea slightly from PTH—methionine, it loses some resolution between certain pairs of PTH amino acids, such as PTH—tyrosine and PTH—valine, and PTH—leucine and PTH—phenylalanine. The ability to determine PTH—glutamine and

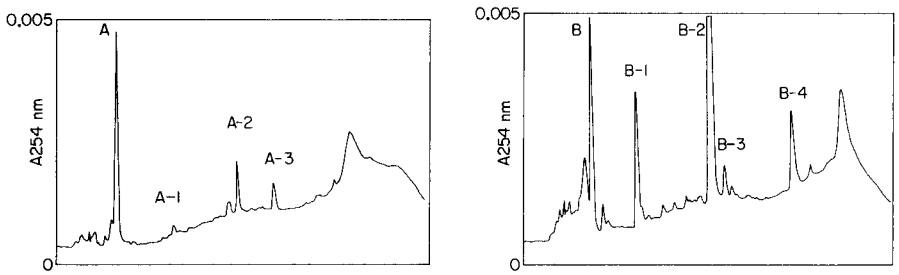

Fig. 1. H.p.l.c. traces from analyses of gas-phase sequencer artifacts using the commercial R2 and improved reagent. Prepurified polybrene was applied to the filter disc and precycled through four sequencing cycles. Fractions collected from cycle 4 in each analysis were dried under vacuum. The residue was redissolved in 30 μl of h.p.l.c.-grade methanol; 10 μl was injected for reversed-phase h.p.l.c. (A) Data with improved R2; peaks A-1 and A-2 are PTCDMA and DPTU, respectively, peak A-3 is unidentified. (B) Data with commercial R2; peaks B-1 and B-2 are PTCDMA and DPTU, respectively, peaks B-3 and B-4 are unidentified.

PTH—methionine without ambiguity is particulary important for recombinant DNA research for the detection of post-translational modification of proteins and for obtaining protein sequences that contains single codon amino acid residues such as methionine. Other organic solvents such as methanol and ethyl acetate were also tried as the solvent for TMA. They produced about the same concentration of PTCDMA as 2-propanol did, but yielded more diphenylthiourea (DPTU).

The original R2 ages during storage. The levels of diphenylthiourea and PTCDMA became unacceptable when the original R2 was stored at 4°C for several months or at 25°C for several weeks. This is not a problem for the improved R2, because fresh ninhydrin and hydrindantin can be added to the modified R2 whenever necessary. The overall advantages of using purified polybrene and improved R2 are also shown in Table 1.

Because sodium dodecyl sulfate (SDS) is soluble in methanol, and almost all proteins are insoluble in methanol even in the presence of SDS, methanol can be used to remove the contaminating SDS from protein samples prepared by SDS—Page. The residual salts, which may not be soluble in methanol, can be extracted with a methanol—water mixture. Usually 20—50% of water in methanol gives enough polarity to extract residual salts such as Tris—HCl and glycine buffers. The extracts can be saved for protein assay if necessary. Such treatment significantly increases the initial and repetitive yields during Edman degradation cycles.

The overall performance of the gas-phase sequencer has been greatly enhanced by using these improved procedures. Table 2 lists some of the peptides and proteins examined by the improved procedures. Most of the samples contained less than 1 nmol of protein and some contained less than 50 pmol. Most of the peptides listed were sequenced through to the carboxyl terminal residue. The capability of the sequencer with the improved

TABLE 2

Polypeptides studied with the gas-phase sequencer using improved procedures

Sample	Residues identified/ total residues	Amount (pmol)
Yeast-secreted β-endorphin peptides [5][a]		
Peptide I	12/12	880
Peptide II	19/19	140
Peptide IIIa	13/13	150
Tryptic peptides derived from human erythropoietin		
T13	4/4	35
T25	6/6	30
T35	7/7	50
T28	15/15	45
T38	21/21	60
E. coli *Colicin Ib [6]*	38/625	1800
rDNA-derived chicken growth hormone [7][b]	68/191	15000

[a]β-Endorphin peptides I: $\overset{20}{\text{N}}$AIIKNAYKKG$\overset{31}{\text{E}}$; II: $\overset{1}{\text{Y}}$GGFLTSEKSQTPLLVTLF$\overset{19}{\text{K}}$ and III: $\overset{-4}{\text{E}}$AEA$\overset{1}{\text{Y}}$GGFLTSE$\overset{9}{\text{K}}$. [b]rDNA-derived chicken growth hormone: $\overset{1}{\text{M}}$FPAMPLSNLFANAVLRAQHLHLLAAETYKEFERTYIPEDQRYTNKNSQAAFXY(S)ETIXAPT(G)KXXAXQKXX$\overset{71}{\text{M}}$.

techniques is clearly illustrated in Table 2 and was particulary important in the structural determination of human erythropoietin and rDNA-derived β-endorphin peptides. Sequence information obtained from a tryptic peptide derived from human erythropoietin has been used to synthesize DNA probes and finally has led to the successful cloning and expression of this protein [8]. Using the improved microsequencing techniques, it was also possible to identify and determine the β-endorphin peptides secreted and proteolytically processed by genetically engineered yeast [5]. Sequencing of 15 nmol of intact rDNA-derived chicken growth hormone yielded the structure of the amino terminal 68 residues, which is 36% of the entire protein molecule [7].

Reproducible and highly sensitive protein sequencing with high resolution is crucial for productive recombinant DNA research. Although its most important role is in the determination of the sequence of minute amounts of biologically important proteins, protein microsequencing has many other applications. It is required to identify the amino terminus of secreted protein and in the determination of the coding regions of genomic sequences containing introns. It can be used to identify post-translational modifications of proteins and to confirm DNA sequence analysis [9—13]. In addition, it is required in elucidating the structure of proteins produced by recombinant DNA techniques.

REFERENCES

1 R. M. Hewick, M. W. Hunkapiller, L. E. Hood and W. J. Dreyer, J. Biol. Chem., 256 (1981) 7990.
2 F. S. Esch, Anal. Biochem., 136 (1984) 39.
3 M. W. Hunkapiller and L. E. Hood, Science, 219 (1983) 650.
4 M. W. Hunkapiller, E. Lujan, F. Ostrander and L. E. Hood, in C. H. W. Hirs and S. N. Timasheff (Eds.), Methods in Enzymology, 91 (1983) 227.
5 G. A. Bitter, K. K. Chen, A. R. Banks and P.-H. Lai, Proc. Nat. Acad. Sci., U.S.A., 81 (1984) 5330.
6 J. A. Mankovich, P.-H. Lai, N. Gokul and J. Konisky, J. Biol. Chem., 259 (1984) 8764.
7 T. Boone, D. Murdock, M. Tallen, F. Martin, H. Hockman, B. Altrock, L. DeOgny, P.-H. Lai, J. Wypych, K. Langley, C. Rudman, N. Stebbing and L. Souza, DNA, 2 (1983) 74.
8 F. K. Lin, C. H. Lin, P.-H. Lai, J. Egrie, E. Goldwasser, F. F. Wang and M. Castro, J. Cell. Biochem., Suppl. 8B, (1984) 45.
9 G. M. Air, F. Sanger and A. R. Coulson, J. Mol. Biol., 108 (1976) 519.
10 D. C. Shaw, J. E. Walker, F. D. Northrop, B. G. Barrell, G. N. Godson and J. C. Fiddes, Nature (London), 272 (1978) 510.
11 B. G. Barrell, A. Bankier and J. Drouin, Nature (London), 282 (1979) 189.
12 B. Noyes, M. Mevarech, R. Stein and K. Agarwal, Proc. Nat. Acad. Sci., U.S.A., 76 (1979) 1770.
13 M. Steinmetz, K. Minard, S. Horvath, J. McNicholas, J. Srelinger, C. Wake, E. Long, B. Mach and L. Hood, Nature (London), 300 (1982) 35.

Analytica Chimica Acta, 163 (1984) 249—255
Elsevier Science Publishers B.V., Amsterdam — Printed in The Netherlands

Short Communication

TIME-RESOLVED FLUORESCENCE MICROSCOPY FOR MEASURING SPECIFIC COENZYMES IN METHANOGENIC BACTERIA

H. SCHNECKENBURGER* and B. W. REUTER

Gesellschaft für Strahlen- und Umweltforschung mbH München, Abteilung für Angewandte Optik, D-8042 Neuherberg (West Germany)

S. M. SCHOBERTH

Kernforschungsanlage Jülich, Institut für Biotechnologie, D-5170 Jülich (West Germany)

(Received 30th March 1984)

Summary. Measurements of time-resolved photobleaching and nanosecond fluorescence decay from microscopic samples of methanogenic bacteria are reported. From cultures of *Methanobacterium thermoautotrophicum* and *Methanosarcina barkeri*, decay times of 1 ns and 3 ns were obtained for the specific coenzymes F_{420} and 7-methylpterin, respectively. In contrast to methylpterin, the fluorescence of F_{420} was bleached selectively, with a time constant of about 160 s, at an irradiation power density of 5 mW mm^{-2}. Similar time constants were found for samples of sewage sludge containing methanogenic bacteria. Active and inactive bacterial cells could be differentiated by following the course of photobleaching.

Anaerobic digestion of biomass to methane plays an important role in nature and has become a very interesting facet of biotechnology. At the end of the anaerobic food chain, methanogenic bacteria convert hydrogen, carbon dioxide and acetic acid to methane. These organisms are therefore the most essential microbial group for biogas production from organic substances, such as are found in sewage sludge, agricultural residues and certain industrial effluents.

Methanogenic bacteria are often identified on the basis of their autofluorescence [1] which is due to specific coenzymes. In particular, the fluorescence of coenzyme F_{420} which is present in all methanogens investigated [2] has been suggested for monitoring the activity of these bacteria [3, 4]. However, overlap with the fluorescence of 7-methylpterin, another coenzyme identical to F_{342} and F_{350} [5], and other organic or inorganic compounds within complex samples has so far prevented the direct determination of F_{420}, unless it was first extracted and purified. To distinguish the microfluorescence of coenzyme F_{420} directly from that of 7-methylpterin and the background luminescence, the time-resolved bleaching and the nanosecond decay of bacterial fluorescence have been measured. Preliminary experiments carried out with microscopic samples from cultures of *Methanobacterium thermoautotrophicum* [6] were confirmed and extended to

0003-2670/84/$03.00

cultures of *Methanosarcina barkeri* as well as to sludge samples from a digester of a sewage treatment plant. *Acetobacterium woodii*, a non-methanogenic anaerobe lacking F_{420} [2], was used for comparison.

Experimental

Materials and preparation. Methanobacterium thermoautotrophicum strain BHK-1 was isolated from a thermophilic mixture [7] and grown at 60°C in medium 119 of the Deutsche Sammlung für Mikroorganismen (DSM) in Göttingen [8] placed in 100-ml serum vials or 25-ml Hungate tubes. *Acetobacterium woodii* (DSM 1030) was grown on fructose at 30°C, as described previously [9]. The samples of methanol-grown *Methanosarcina barkeri* (DSM 804) were a gift from E. Heine. In addition, sludge samples from a digestor of a sewage treatment plant containing different species of methanogenic bacteria were used.

For fluorescence microscopy, wet mounts were prepared from single droplets of the supernatant liquid over the sludge samples after several hours of sedimentation or directly from the bacterial cultures. For *Methanobacterium thermoautotrophicum*, a 20-fold increase in cell concentration was obtained by centrifugation. No special precautions to prevent the presence of oxygen were taken. Cells were regarded as inactive after treatment with formaldehyde (4 ml/100 ml culture), exposure to air for at least 24 h, or removal of the energy source for several days [6].

Fluorescence microscopy. Bacterial fluorescence was investigated using a Leitz Orthoplan microscope with an MPV photometer unit, a Ploemopak illuminator and an oil immersion objective (40/1.30). The light sources were a 50-W high-pressure mercury lamp with an excitation maximum at 405 nm (Ploemopak filter system D) and an argon ion laser operated at 364 nm, corresponding to the absorption maxima of coenzyme F_{420} [2] and 7-methylpterin [5], respectively. For both light sources, the power density at the samples was adjusted to about 5 mW mm^{-2}, while the illuminated area was 80—100 μm in diameter.

After appropriate spectral filtering [6], the fluorescence was detected by using a time-resolving single photon counting system (Fig. 1). For measurements of the nanosecond decay curves, the samples were excited by 100-ps pulses from the modelocked laser. A repetition rate of 250 kHz was adjusted by means of an electro-optical shutter. For measuring fluorescence bleaching, continuous wave excitation by the argon ion laser or the mercury lamp (not shown in Fig. 1) was used instead.

The time resolution of the entire detection system was about 0.8 ns. For the measurements of photobleaching, however, an adjustment to 600 ms was sufficient.

Results

Fluorescence of similar intensity was obtained from all samples of *Methanobacterium thermoautotrophicum* and *Methanosarcina barkeri*

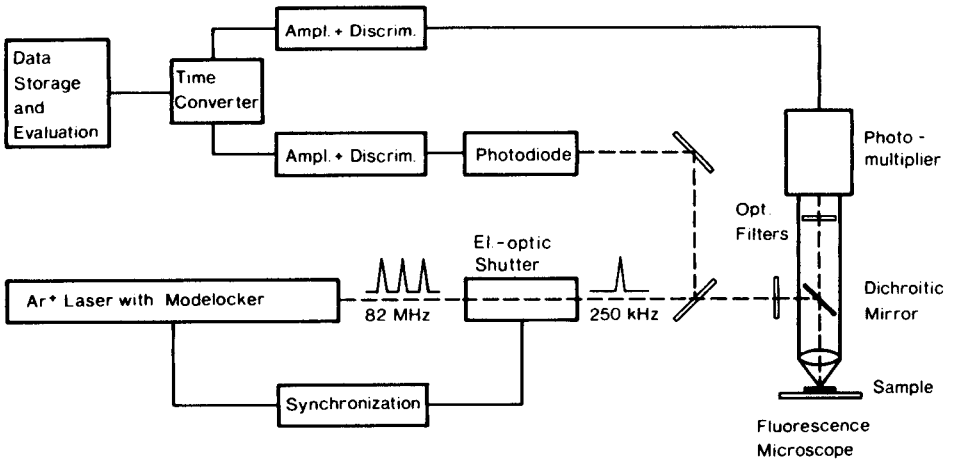

Fig. 1. Experimental set-up for time-resolved fluorescence microscopy.

when the two excitation sources were used. For active bacteria of both species, this intensity remained almost constant under argon laser u.v. excitation, but decreased rapidly due to photobleaching during irradiation by the mercury lamp. The bleaching curves obtained after discrimination from a constant fluorescent background were mono-exponential for all active samples with a time constant of 160 ± 80 s. However, for bacteria which had lost their metabolic activity, two bleaching time constants of t_1 = 30 ± 15 s and t_2 = 160 ± 80 s were measured. This different photobleaching behaviour between active and inactive bacterial cells is demonstrated in Fig. 2 for *Methanobacterium thermoautotrophicum*. Similar curves were measured for the samples of *Methanosarcina barkeri*.

Although fading of the fluorescence of active samples was slight under laser u.v. excitation, the influence of photobleaching on the nanosecond decay curves was significant. This effect, previously observed for *Methanobacterium thermoautotrophicum* [6], was also measured for *Methanosarcina barkeri* (Fig. 3). Whereas the integral fluorescence, which is proportional to the area below the decay curve, decreased only slightly under irradiation, the photon counting rate at the maximum of the curve was decreased considerably. The fluorescence decay was found to be bi-exponential with time constants of τ_1 = (3.0 ± 1.0) ns and $\tau_2 \leqslant 1$ ns, indicating selective photobleaching of the short-lived component. In contrast to these findings, considerable photobleaching of the integral fluorescence intensity was measured for inactive bacterial cells. This is demonstrated in Fig. 4 by the fluorescence decay curves of *Methanosarcina barkeri*. Comparative measurements with *Acetobacterium woodii* did not show any photobleaching effect, and a significant fluorescent signal was obtained only after laser u.v. excitation. The decay time of 4.0 ± 1.0 ns was, within the limits of error, the same as that of the longer-lived component of the methanogenic bacteria.

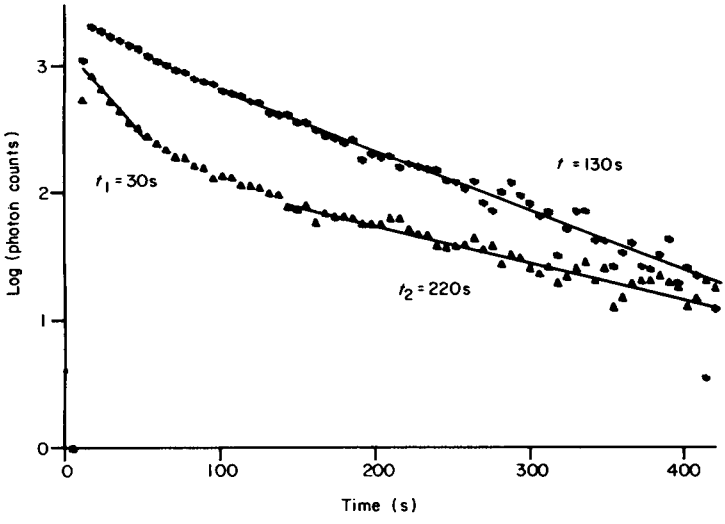

Fig. 2. Fluorescence bleaching of *Methanobacterium thermoautotrophicum* in (*) active and (▲) inactive states (wavelength of irradiation 405 nm, power density 5 mW mm^{-2}).

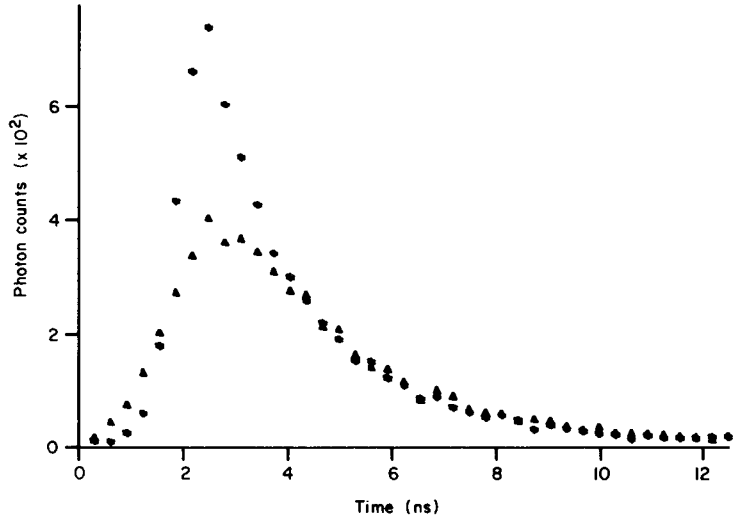

Fig. 3. Time-resolved fluorescence of *Methanosarcina barkeri* in an active state: (*) before bleaching; (▲) after photobleaching for 8 min (excitation wavelength 364 nm, power density 5 mW mm^{-2}).

The interesting results obtained from different bacterial cultures stimulated a study of the fluorescence of microscopic sludge samples from a sewage treatment plant containing a mixed population of non-methanogenic and methanogenic bacteria. When an excitation wavelength of 405 nm was used,

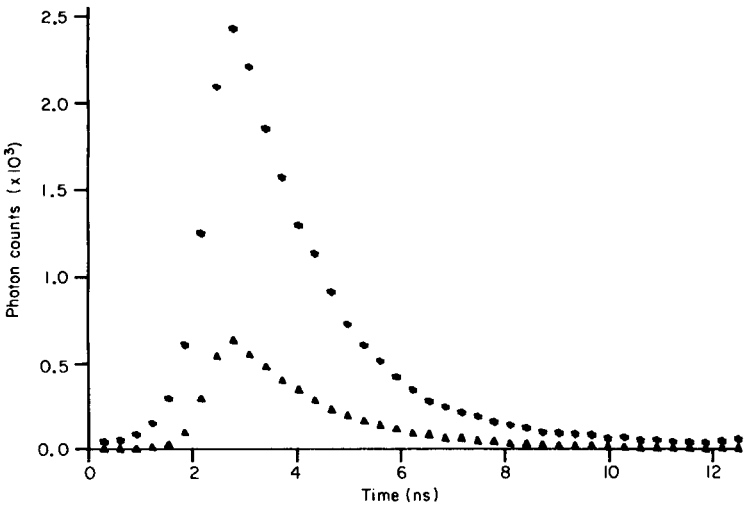

Fig. 4. Time-resolved fluorescence of *Methanosarcina barkeri* in an inactive state: (*) before bleaching; (▲) after photobleaching (conditions as for Fig. 3).

the fluorescence of the methanogens was bleached more rapidly than the fluorescence of other kinds of bacteria, but apparently more slowly than parts of the fluorescent sludge. The bleaching curves from samples with different physiological states of methanogenic bacteria are shown in Fig. 5. The samples of substrate-saturated methanogens were obtained by supplying

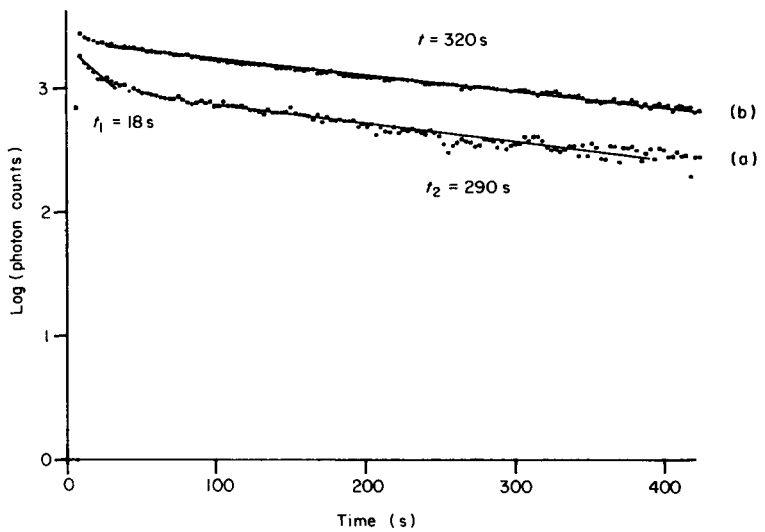

Fig. 5. Fluorescence bleaching from samples of sewage sludge: (a) substrate-limited methanogenic bacteria; (b) substrate-saturated methanogenic bacteria (wavelength of irradiation 405 nm).

the sewage sludge for 3 days with hydrogen and carbon dioxide, which are specific substrates for methanogens. The microscopic image of these samples showed an increased concentration of methanogenic bacteria, compared to samples which had received no substrates (substrate-limited methanogens). The bleaching curves of the starved samples showed at least two, possibly three, different time constants with preliminary values of $t_1 = 20 \pm 10$ s, $t_2 = 250 \pm 150$ s and possibly $t_3 = 500$—1000 s. The short time constant t_1 was detected even from parts of the sludge samples without microscopically detectable methanogens and was about the same as that obtained from the pure cultures of *Methanobacterium thermoautotrophicum* and *Methanosarcina barkeri* in an inactive state. The time constant t_2 was the same for lower and higher concentrations of methanogenic bacteria. In the substrate-saturated samples only this component was detected, similarly to the cultures of active methanogens.

Discussion

The different fluorescence and photobleaching properties of the methanogenic bacteria irradiated with the argon ion laser and the mercury lamp can be explained by assuming that different coenzymes, 7-methylpterin and F_{420}, were excited at 364 nm and 405 nm, respectively. Whereas F_{420} fluorescence was bleached out almost completely, 7-methylpterin was stable within the range of irradiating power applied. The small photobleaching effect under laser excitation can be attributed to superimposed fluorescence by coenzyme F_{420} corresponding to the short-lived component of the nanosecond decay curves.

For inactive methanogenic bacteria, an additional fluorescent component was detected which was bleached more rapidly than F_{420}, and which showed significant photobleaching also under laser u.v. excitation. This component might be a decomposition product which so far has not been identified from the optical spectra.

By using the experimental methods described above, it seems possible to determine the state of activity of methanogenic bacteria and also to separate the fluorescence of coenzyme F_{420} from 7-methylpterin and additional fluorescent compounds. Quantitative measurements of the content of F_{420} and other specific coenzymes may, however, be difficult, if complex samples are used, e.g., from anaerobic digestors. In this case, components of the fluorescent background with similar time constants may interfere with the fluorescence signals arising from the specific coenzymes or their decomposition products. It seems possible, however, to overcome this problem, e.g., by activating the methanogenic bacteria within the samples as described above. Therefore the experimental methods described may become important for practical applications such as surveying the activity of the methanogenic bacteria during biogas production.

The authors thank K. Striegel and A. Popowitsch for excellent technical assistance and E. Heine, Forschungsanstalt für Landwirtschaft, Braunschweig, for providing the samples of *Methanosarcina barkeri*.

REFERENCES

1 R. W. Mink and P. R. Dugan, Appl. Environ. Microbiol., 33 (1977) 713.
2 L. D. Eirich, G. D. Vogels and R. S. Wolfe, J. Bacteriol., 140 (1979) 20.
3 R. A. Binot, H. P. Naveau and E. J. Nyns, Biotechnol. Lett., 3 (1981) 623.
4 P. van Beelen, A. C. Dijkstra and G. D. Vogels, Eur. J. Appl. Microbiol. Biotechnol., 18 (1983) 67.
5 J. T. Keltjens, P. van Beelen, A. M. Stassen and G. D. Vogels, FEMS Microbiol. Lett., 20 (1983) 259.
6 H. Schneckenburger, B. W. Reuter and S. M. Schoberth, FEMS Microbiol. Lett., 22 (1984) 205.
7 H. P. Bochem, S. M. Schoberth, B. Sprey and P. Wengler, Can. J. Microbiol., 28 (1982) 500.
8 D. Claus, P. Lack and B. Neu, DSM Catalogue of Strains, 3rd edn., Gesellschaft für Biotechnologische Forschung mbH, Braunschweig, 1983, p. 280.
9 F. Mayer, R. Lurz and S. M. Schoberth, Arch. Microbiol., 115 (1977) 207.

Analytica Chimica Acta, 163 (1984) 257—261
Elsevier Science Publishers B.V., Amsterdam — Printed in The Netherlands

Short Communication

APPLICATION OF A CLINICAL ANALYSER IN BIOTECHNOLOGY

B. G. HENSHAW
Sturge Biochemicals, Denison Road, Selby, North Yorkshire YO8 8EF (Great Britain)
(Received 2nd April 1984)

Summary. High sample throughput of often perishable samples in relatively consistent matrices is needed in both clinical and biotechnological analysis. Higher levels of accuracy and precision are normally required for quality/process control in fermentation work. Assessment of discrete clinical analysers for application in fermentation work is discussed. Methods of measuring precision, accuracy and carryover are outlined. Several assay procedures are used routinely for research and process and quality control with satisfactory results.

Automated systems of analysis have become increasingly used over the past 20 years. Continuous flow systems have found wide applicability but commercial discrete analysers have generally been developed to meet the increasingly large demands of clinical analysis. These discrete analysers have several attractive features in terms of throughput, reagent usage, measurement procedures and data handling; they are also versatile, usually requiring only modification or development of operating procedures. Their main limitation lies in the nature of the workload in many wet-chemical laboratories [1] where small numbers of very different samples are assayed. This limitation does not apply to the workload of a fermentation production/research laboratory where the requirements are strikingly similar to those of a clinical laboratory. In both environments, numerous samples which are often urgent and perishable must be processed. This necessitates a high throughput of samples, a rapid response service, and good data handling to minimise time-consuming manual data transformations. In addition, the analytes are contained in a relatively consistent matrix of physiological fluid (serum, urine) in clinical work, or fermentation media, broth or formulated product in biotechnology.

A wide range of assays, often with several analytes to be quantified in the same sample, is required for clinical and fermentation work, which means considerable instrumental flexibility in measurement procedures (e.g., kinetic, end-point, end-point with sample blanking (see Fig. 1)). The use of kinetic or reaction-rate modes is particularly advantageous in quantifying enzymes produced by fermentation. Because the rate of change of absorbance is measured rather than the absolute absorbance, problems with variable sample blanks are avoided. Continuous segmented-flow analysers are limited to

0003-2670/84/$03.00

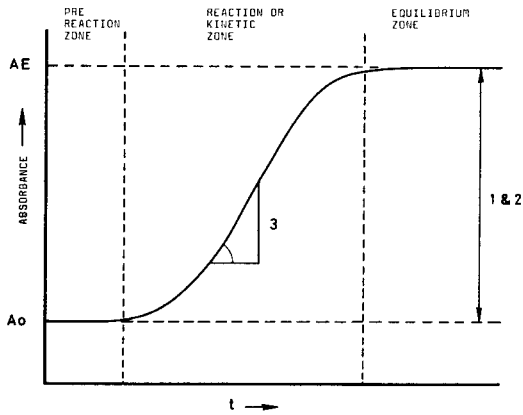

Fig. 1. Measurement modes of the clinical analyser used. (1) The end-point mode assumes minimal sample blank, measures A_0 (reagent blank) and computes $A_E - A_0$ to calculate analyte concentration; (2) the end-point mode with individual sample blanks measures A_0 for each sample and uses $A_E - A_0$ to calculate analyte concentration; (3) the kinetic mode measures rate of change dA/dt and uses this to calculate analyte concentration. All these procedures can be done by using measurement against standards or a factor based on molar absorptivity.

measuring kinetic reactions by a "two point" procedure, which can lead to large errors if the response is non-linear. In discrete analysers, the response linearity is usually closely monitored and a best-fit line is used to determine the reaction rate. Unsegmented flow analysers can also monitor kinetic measurements by stopped-flow procedures but the choice of commercial systems is small. In addition to reaction-rate measurements, the provision of a mode by which individual sample blanks are measured in the discrete systems is particularly suitable for fermentation research work.

Two other similarities between clinical and fermentation work are apparent. An on-demand service is necessary to cope with emergencies, which means that method changeover time or start-up time must be short, and expensive enzymatic reagents are often used so that small reaction volumes are desirable. These similarities make clinical analyser attractive for fermentation work, but there are still some significant differences in the requirements. The most important is that relatively low levels of precision and accuracy are usually acceptable for clinical analyses because the prime interest is whether or not analyte levels fall outside a physiologically normal range. Rigorous control of accuracy and precision is not regarded as essential, despite vigorous attempts to improve this situation [2—5]. For some applications in fermentation analysis, the relatively poor performance of some clinical discrete analysers may be adequate, e.g., in "shake-flask" screening of organisms where gross differences in organism performance are sought. It is not adequate for studies of organisms giving marginal (but commercially valuable) improvements, or in process or quality control.

Selection of a suitable instrument

A discrete analyser for clinical work consists of four main components which may be integral or in modular form: a volumetric (dilution and dispensing) stage, sample transport, optical system, and computerised control and data-handling functions. Only the optical and volumetric systems can be compared on a numerical basis, though the sample transport procedure may contribute to the overall error. The inaccuracy and imprecision of the photometric system is best assessed by processing $\geqslant 20$ aliquots of, e.g., 10^{-3} N potassium dichromate and calculating the mean and relative standard deviation. The corresponding data for the volumetric system are obtained by making $\geqslant 20$ dilutions (100-fold) of a concentrated solution, e.g., 0.1 N dichromate with dilute acid, and comparing the data with those obtained from manual dilutions. Carryover is best monitored by alternate loading of acidic potassium dichromate solution and water in groups of three, to check carryover from high to low concentrations and vice versa. Other matters must also be considered in the choice of an optical system. Filter and spectral-line photometers and grating spectrophotometers are available in the various instruments: the grating spectrophotometer is obviously the most versatile but also the most expensive; the spectral-line photometer has a stable high energy output but a limited range of wavelengths; filter photometers are not versatile, but are relatively inexpensive.

Linear and carousel types of sample transport are available. In the linear type, samples can generally be added on to a run already underway; this is not true for the carousel type, which are batch rather than continuous analysers, with a consequent loss of productivity.

In-built programming (ROM) and data handling varies very much between instruments. The inability to change some minor parameters can be irritating, but the main point is to ensure that the most useful measurement modes in Fig. 1 are available. Data handling on all the instruments has been designed to avoid confusion between samples.

Various guides on cost/benefit analysis for instrumental selection are available [1, 5, 6] but the weighting of intrinsic (non-monetary) benefits such as faster service and better flexibility, will obviously depend on the particular situation. On-site evaluation of the best candidate instruments at an appropriate cost is essential despite the staff time involved. Most high-throughput clinical analysers have in-built checking procedures which detect gross problems in performance and diagnostic systems for major instrumental faults. Procedures for checking the inaccuracy and imprecision of the optical and volumetric systems and the carryover from sample to sample must be applied as outlined above, however. Good instruments should give relative standard deviations of $<0.1\%$ for checks on the photometric systems, and about 0.5% for the volumetric system with inaccuracies of $<1\%$; carryover should be $<1\%$. Further, it is necessary to check which of the normally used assays is transferable to the analyser without excessive development time.

TABLE 1

Assays currently used on the clinical analyser

Analyte	Description of method	Method type	Samp
$K_2Cr_2O_7$	Imprecision and inaccuracy measurements	End-point	220
NAD	NAD reduction to NADH with alcohol dehydrogenase and ethanol	End-point[a]	100
Citric acid	BCL test kit adaption	End-point	200+
Citric acid with sample blanks	BCL test kit adaption	End-point[a]	90
Titratable acidity	Reaction of NaONP[c] in buffered solution	End-point	170
β-Glucosidase	Hydrolysis of PNP[d] β-glucoside with cellulase	End-point	170
β-Galactosidase	Hydrolysis of ONP[c] β-galactoside with lactase	End-point	140
Amyloglucosidase	Hydrolysis of starch, measurement of glucose produced	Kinetic[b]	170
Glucose oxidase	Oxidation of glucose, H_2O_2 measured	Kinetic	110
Glucose	Glucose oxidase/peroxidase reaction	Kinetic	170

[a]With individual sample blanks. [b]After an initial incubation. [c]ONP-*ortho* nitrophenol. [d]PNP-*para* nitrophenol.

In this laboratory, the capacity required was 1000—3000 assays per week, which meant, when reagent/preparation time was allowed for, sample throughputs of 100—200 h^{-1}. A cost recovery time of 1—2 years was regarded as realistic. Various discrete clinical analysers were considered; some were rejected as being of unsound design philosophy and five were evaluated on-site. None of the instruments was perfect for application to fermentation work; the most appropriate instrument was the Gilford 203-S, which is a 60-place carousel batch instrument, capable of three reagent additions and with a flow-cell measuring system contained within a grating spectrophotometer. The spectrophotometer can also be used off-line.

Application of the discrete analyser

The Gilford 203-S has excellent accuracy, precision and carryover characteristics and a generally satisfactory range of measurement procedures. It can be readily applied to many fermentation laboratory assays. Temperature control in the flow cell (peltier block) is good, but the air-bath temperature control in the carousel is inefficient. This becomes significant in two-stage reactions where the analyte is incubated on the carousel with one reagent and the product is then treated with another reagent to form a chromogen. It is also important in two-point kinetic measurements of enzymes, because the reaction then takes place on the carousel rather than in the flow cell. Despite their disadvantages, two-point kinetic measurements are necessary if the enzyme reaction becomes non-linear at low enzyme activity; reaction-rate measurements actually in the flow cell would reduce sample productivity to 5—10 h^{-1}. With the two-point kinetic method, sample throughput is 150—180 h^{-1}; quality of the data can be maintained by running enzyme check standards every 10—20 samples.

Obviously, the facilities for sample preparation must be good. Two syringe high-dilution microprocessor-controlled diluters are used here, with some dissolution equipment for solid samples.

The assays currently in use on the analyser are shown in Table 1. These were developed over a period of about 18 months; a typical workload for the analyser is 1000—3000 samples per week. The savings in labour and reagents in the cost/benefit analysis were not fully realised because the availability of better assay facilities automatically increased the demand. However, most assays are available on a daily basis to avoid delays within the research and production functions.

The inaccuracy and imprecision tests for the optical, volumetric and diluter systems are applied on a weekly basis, and contribute to maintaining consistent data quality. Detailed procedures for these tests are available from the author on request.

REFERENCES

1 J. K. Foreman and P. B. Stockwell (Eds.), Topics in Automatic Chemical Analysis, Vol. 1, Wiley, New York, 1979.
2 M. Hjelm (Ed.), IUPAC Commission on Automation and Clinical Chemical Techniques Recommendations, Pure Appl. Chem., 55 (1983) 1041.
3 J. Buttner, J. Borth, J. Boutwell, P. M. G. Broughton and R. C. Bowyer, Clin. Chim. Acta, 98 (1979) 145F.
4 J. Buttner, J. Boutwell, P. M. G. Broughton and R. C. Bowyer, Clin. Chim. Acta, 83 (1978) 191F.
5 M. Hjelm and T. D. Geary, J. Automatic Chem., 2 (1980) 26.
6 F. L. Mitchell, J. Automatic Chem., 2 (1980) 23.

Analytica Chimica Acta, 163 (1984) 263—267
Elsevier Science Publishers B.V., Amsterdam — Printed in The Netherlands

Short Communication

REFLECTOMETRY IN KINETIC STUDIES OF IMMUNOLOGICAL AND ENZYMATIC REACTIONS ON SOLID SURFACES

STEFAN WELIN*, HANS ELWING, HANS ARWIN and INGEMAR LUNDSTRÖM

Laboratory of Applied Physics, Department of Physics and Measurement Technology, Linköping University, S-581 83 Linköping (Sweden)

MAUDE WIKSTRÖM

Department of Oral Microbiology, University of Gothenburg, S-413 46 Göteborg (Sweden)

(Received 3rd April 1984)

Summary. An optical method is described, by means of which immunological and enzymatic reactions can be followed at a primary level on a solid surface, without labelling procedures. When plane-polarized light is reflected at a solid surface, there is a minimum in reflectance at a certain angle of incidence, the pseudo-Brewster angle. For example, a layer of protein adsorbed on a silicon surface increases the reflectance with increasing amount of adsorbed material. High sensitivity is obtained because of the large difference in refractive index between silicon and organic material; about 0.1 $\mu g\ cm^{-2}$ adsorbed protein can be detected. In a model system of human IgG and anti-human IgG, the primary adsorption of IgG on a hydrophobic surface is first measured, and on this IgG-coated surface the binding kinetics of anti-IgG could be measured. The kinetics of proteolytic degradation of IgG-coated surfaces by trypsin was also investigated.

Most methods for quantification of binding reactions on solid surfaces, e.g., radioimmunoassay (r.i.a.) or enzyme-linked immunosorbent assay (e.l.i.s.a.) [1], do not permit continuous measurement of binding reactions. Some methods, however, can follow the kinetics in such biochemical reactions. One example is ellipsometry [2,3] which is based on oblique reflection of polarized light at surfaces; its use is limited because of high cost and difficult handling. Some special optical properties of light reflection at solid surfaces can be utilized to construct a simple instrument, without moving parts, for continuous measurement of binding reactions, such as antibody binding on solid surfaces. The new instrument, a reflectometer, is briefly described below, and some biochemical applications are given. More detailed information will be given in a later paper.

The reflectance of plane-polarized light from a solid surface has a minimum at the so-called pseudo-Brewster angle. For a material with a high refractive index, the reflectance minimum is very pronounced. The angle is around 71° for a water/silicon interface at a wavelength of 632.8 nm (Fig. 1). At this angle, any substance adsorbed at the silicon/water interface which has a

0003-2670/84/$03.00

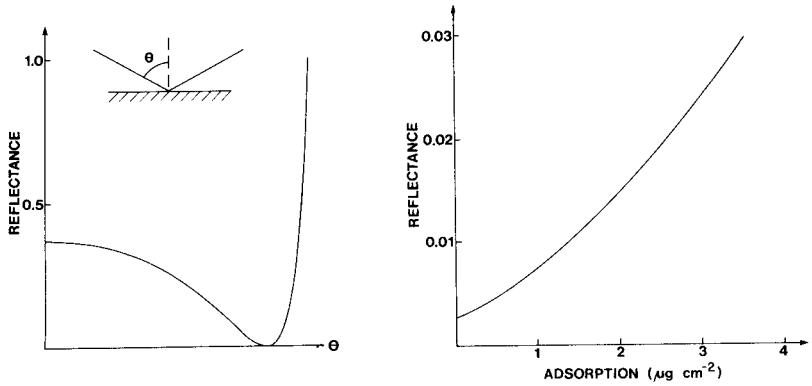

Fig. 1. Dependence of reflectance from a clean silicon surface on the angle of incidence, θ.

Fig. 2. Relation between amount of protein adsorbed and reflectance at a silicon/water interface, calculated theoretically with a slightly improved McCrackin/Fortran program [4] for a silicon dioxide layer of 30 nm (refractive index 1.40) on top of the silicon. Assumed refractive indices for the solution and the adsorbed protein film were 1.3338 and 1.4600, respectively.

refractive index different from the two media will change the reflectance. A protein layer adsorbed at the interface will give increased reflectance with increased amounts of adsorbed protein (Fig. 2). This is the basis for the technique described.

Experimental

Materials. Human immunoglobulin, IgG (16.5%), was from KabiVitrum, Stockholm. Bovine pancreas trypsin and gelatin were from Sigma Chemical Company. The anti-human IgG was gamma-chain specific, produced in swine (Orion Diagnostica, Finland; lot no. IE 38). All reagents were dissolved in 0.15 M sodium chloride (pro analysi, Merck) to give the desired concentrations. The helium–neon laser was a Hughes 3221H-PC. The silicon wafers (Wacker Chemie, German Federal Republic) were washed carefully, as recommended in semiconductor technology, and oxidized to give a 30-nm silica film. This makes the sensitivity greater and the relation between reflectance and mass/area as nearly linear as possible. The oxidized wafers were washed and immersed in dichlorodimethylsilane (Merck), dissolved in trichloroethylene (1 + 9) for 10 min. After this silanization, the wafers were washed with ethanol, rinsed in trichloroethylene, and stored in ethanol until used.

Instrument design. A laser giving a plane-polarized light beam was used as light source. The light beam entered a 100-μl two-sided cuvette made of soda glass. This was pressed onto the piece of silicon of which an area of 25 mm^2 was exposed to the liquid added to the cuvette. The arrangement is shown in Fig. 3(a); the cuvette is shown in Fig. 3(b). The intensity of the reflected light was measured with a photodiode and converted to a voltage. The voltage, which was proportional to intensity, was displayed on a recorder.

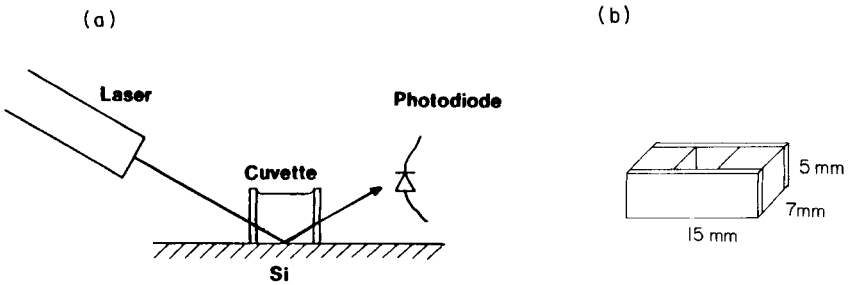

Fig. 3. (a) Diagram of the essential components of the reflectometer; (b) the cuvette.

Results

Primary adsorption on a hydrophobic silicon surface. Immunoglobulin (IgG) was added to the cuvette at room temperature (21° C), and the adsorption kinetics was recorded (Fig. 4). Typical adsorption curves with an initially rapid, and later, a slow adsorption were obtained. For higher protein concentrations, the initial signal was frequently unstable probably because of refractive index variations in the solution. The technique allowed the detection of as little as ca. 1 mg l^{-1} protein.

Antibody binding to an antigen-covered surface. A typical stepwise experiment with antigen—antibody binding is shown in Fig. 5. The IgG was first adsorbed on a silicon surface causing an increase in reflected light intensity. Incubation with gelatin caused a further increase indicating the presence of uncovered binding sites on the surface. Specific binding of anti-IgG was investigated at three dilutions. Binding from (1 + 999) dilution was at the detection limit; (1 + 99) dilution showed a slow rise in signal over 10 min. The signal for the (1 + 9) dilution was significantly lowered because of the increase of refractive index in the solution as a result of the high protein concentration (5 g l^{-1}). This effect has been roughly compensated for in Fig. 6.

Tryptic digestion of IgG-covered surfaces. IgG (0.5 g l^{-1} was adsorbed on a silicon slide for 10 min at 37° C. Trypsin (1 g l^{-1}) was added to the cuvette and digestion of the protein layer was observed as a decrease in signal output (Fig. 7). After rinsing with buffer, a slight desorption could be detected followed by a stable signal slightly higher than the initial value.

Discussion

The reflectometer described seems to have approximately the same sensitivity as that achieved by ellipsometry for quantification of the mass of organic layers on solid/liquid interfaces. In contrast to ellipsometry, the reflectometer is simple and inexpensive and has no moving parts. These attractive features greatly simplify quantitative investigations of binding reactions at solid/liquid interfaces and should expand interest in such reactions.

One interesting application is to use the reflectometry principle in connection with small-volume flow cuvettes and surfaces prepared for adsorption of,

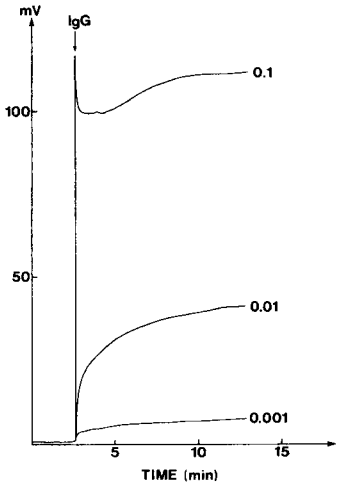

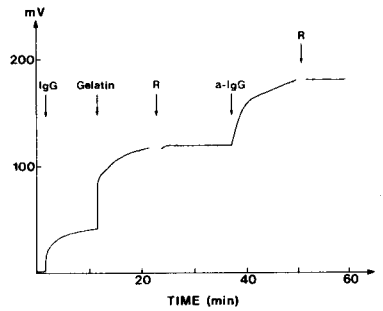

Fig. 4. Primary adsorption of IgG at the concentrations (g l^{-1}) indicated on the curves, as measured by the light intensity in mV.

Fig. 5. Stepwise experiment showing an antigen—antibody binding reaction. Arrows indicate addition of reagents: 0.01 g l^{-1} IgG, 1 g l^{-1} gelatin and (1 + 99) anti-IgG; R indicates rinsing 5 times with 75 μl of 0.15 M NaCl.

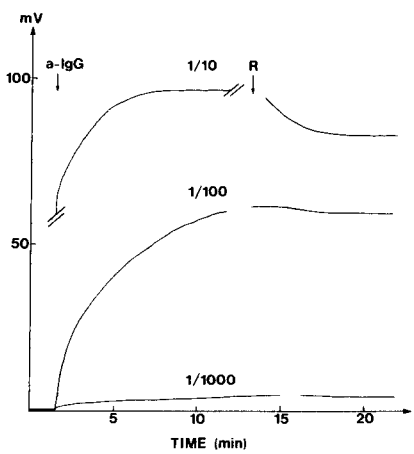

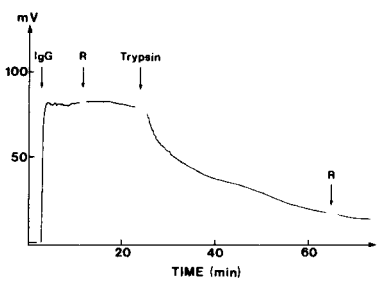

Fig. 6. Binding of anti-IgG to a silicon surface coated with IgG and gelatin. Adsorption from control serum without anti-IgG was not significant (R as in Fig. 5).

Fig. 7. Tryptic digestion of IgG adsorbed on a silicon surface. Arrows indicate addition of reagents (R as in Fig. 5).

for example, different proteins. Such flow cells may be used in a number of applications such as group-specific detection of protein in liquid chromatography or rapid detection of antibodies or proteolytic enzymes in solutions [5, 6].

We thank Agneta Askendal for technical assistance. This work was supported by grants from the National Swedish Board for Technical Development.

REFERENCES

1 E. Engvall and A. J. Pesce, Scand. J. Immunol., 8(7) (1978).
2 H. J. Trurnit, Arch. Biochem. Biophys., 47 (1953) 251.
3 R. M. A. Azzam, P. G. Rigby and J. A. Kreuger, Phys. Med. Biol., 22(3) (1977) 422.
4 F. L. McCrackin, A FORTRAN program for analysis of ellipsometer measurements, National Bureau of Standard, Technical Note 479, Washington, DC, 1969.
5 M. Wikström, H. Elwing and Å. J. R. Möller, Enzyme Microb. Technol., 4 (1982) 265.
6 A. Rothen, Physiol. Chem. Phys., 5 (1973) 243.

Analytica Chimica Acta, 163 (1984) 269—273
Elsevier Science Publishers B.V., Amsterdam — Printed in The Netherlands

Short Communication

FERMENTATION CONTROL WITH PERSONAL COMPUTERS

W. HAMPEL* and M. ROEHR

Institute of Biochemical Technology and Microbiology, Technical University Vienna, Getreidemarkt 9, A-1060 Vienna (Austria)

(Received 4th April 1984)

Summary. A cheap but efficient computer network system for advanced fermentation control is described. Two Commodore C-64 computers are connected to a single-drive floppy disk; possible bus conflicts are avoided by software programming. The first computer is dedicated to data acquisition and process control with conventional parameters whereas the second computer unit utilizes previously stored parameter values for on-line high-resolution color graphics and for the evaluation of derived process variables such as growth rate and productivity. These variables can then be used for more refined process control.

The benefits of using computers for on-line parameter monitoring and process control in fermentation industry and research has been emphasized by many authors [1—14]. Barriers to the more extensive use of computers in research laboratories have been the high cost/benefit ratio and the lack of appropriate software and trained personnel. These disadvantages have dissipated considerably with the widespread introduction of personal computers, which make a wide range of capabilities available cheaply with interactive possibilities. This communication describes the application of personal computers for data acquisition of several process parameters and the monitoring and control of small laboratory bioreactors by means of a configuration of two personal computers.

Description and system configuration

Figure 1 is a schematic diagram of the configuration of the system. Commodore 64 microcomputers were chosen because of their cheapness, adequate RAM and ROM capacity, ancillaries (high-resolution graphics, sound synthesizer, matrix printer), and interfacing possibilities. Program and data storage is done by a single-drive floppy disk (VC-1541). One disadvantage of cheap computers is the lack of interrupt structures, so that some of the capabilities mentioned cannot be used simultaneously. Therefore, two microcomputers were connected to the same single disk drive by standard cables, forming a computer network. By means of appropriate software, it can be arranged that either microcomputer can load or store a program or data from disk without interfering with the other one. The network can be crashed if one of the computers is turned off.

0003-2670/84/$03.00

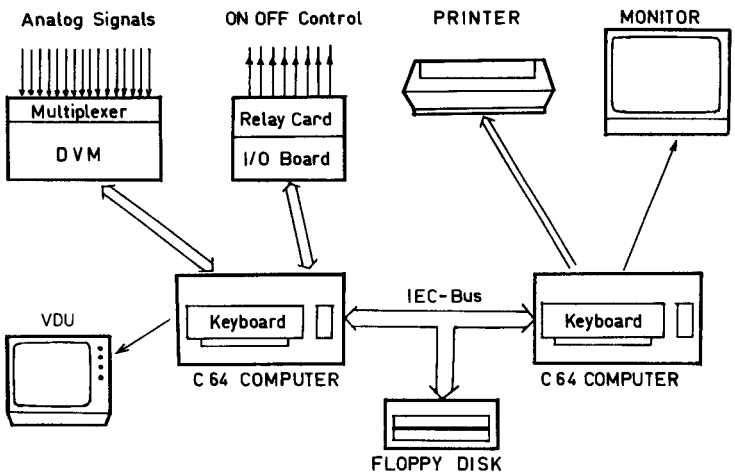

Fig. 1. Hardware configuration with Commodore 64 computers.

Data and programs are made visible with a color CRT (Commodore video monitor 1701). Displaying graphics calls for a large memory and complex software. High-resolution graphic display (199 X 319 pixel) was achieved [15] either by appropriate software programming (Graphic Aid Program) or by inserting a specific ROM module (C64-plus, R. Köhler GmbH, Vienna, Austria). Displayed programs or graphics were documented by a color matrix printer with graphic capabilities (GP-700 A; Seikosha Co., Tokyo, Japan).

The interfaces allow data transfer from and to devices connected to a bioreactor. Analog signals generated by various sensors (e.g., resistance thermometer, pH probe, infrared detectors) are multiplexed and digitized by a digital voltmeter. A simple single-board device [16] is used. The device multiplexes 16 different signals (channels) and converts voltages in the range of −99 to 999 mV to a digital signal with 0.1% resolution on 9 I/O lines, which can be connected to the user port of the microcomputer. Current signals (0—20 mA) and higher voltages are adjusted to the measuring range by appropriate resistor circuitry. One scan takes 2 s. On-line process control is achieved by eight on/off control loops. A relay card is connected to the data bus of the computer by an I/O expansion board.

The system configuration is dedicated mainly to controlling single laboratory fermentation units. Thus, the complex software organization used for controlling several pilot or production units [17—19] can be reduced to the essential sequences. In the initialization sequence, the operator must specify pertinent information about the experiment interactively, selecting the sensors (channels) to be used, entering calibration functions for defined variables, fixing periods and intervals of scanning sequences, and scheduling time or setpoint sequences for process control. The computer creates the relative data file on disk. After the fermentation process has been started,

two program sequences (data acquisition and process control) are activated, depending on the schedule and the requirements. At fixed intervals, the data-acquisition routine initiates the scanning of sensors. The values of the mean and the variance of each signal are calculated, and data outside the defined limits are rejected. The data from all the sensors involved are stored, with the actual fermentation time, on one record of fixed length. In the first record, the total number of data-acquisition sequences already done is stored. For process monitoring, the actual data are displayed on the video screen. The process-control sequence is activated according to the requirements for relay switching in time sequences; but if an increased frequency is necessary in the DDC loops (e.g., for the addition of acid or alkali to maintain constant pH value), the time interval can be reduced to a minimum of 10 s.

In the computer network, the second microcomputer is dedicated to data analysis of parameter values stored in the records of relevant files. The programs loaded must be modified to prevent disk conflicts and to maintain control so that no disk-load command is entered in the immediate mode. To prevent bus conflicts, each program must execute a program statement immediately before trying to load a program or to store data. This causes the computer to cycle until the bus is accessible.

Aims of the computer network

The successful interfacing of different microcomputers for simple data acquisition and process control has been demonstrated by several authors. Parameters controlled or monitored are limited to directly accessible process variables (e.g., temperature, pH, dissolved oxygen concentration, aeration rate, exhaust air composition, etc.) and to several easily calculated process indicators such as oxygen and carbon dioxide transfer rate, respiration quotient and heat evolved [20—23]. For documentation and off-line data analysis, these values may be stored on low-speed tape cassettes. Evaluation of derived or complex parameters (e.g., metabolic rates, growth rate and productivity) provides greater insight into the actual biological situation and the state of the process. Continuous utilization of these parameters requires numerous calculations with smoothing routines because of the scattering of measured values. In on-line systems, this is usually feasible by incorporating computers with large memories and interrupt structures (minicomputer). The alternative possibility described here offers very favorable cost/performance ratios, by coupling two cheap microcomputers: one computer is dedicated to conventional data acquisition and process control, while the other is assigned to data analysis. The system can be used for on-line presentation of experimental values, previous and current process data being displayed as high-resolution color graphics. Floppy disks provide adequate data exchange between the two computers, because of the short access time to a particular address or storage location. For example, within 10 s, data of 100 records stored in an equal number of scanning sequences can be loaded to the second computer for data analysis. During such an interval, the data-

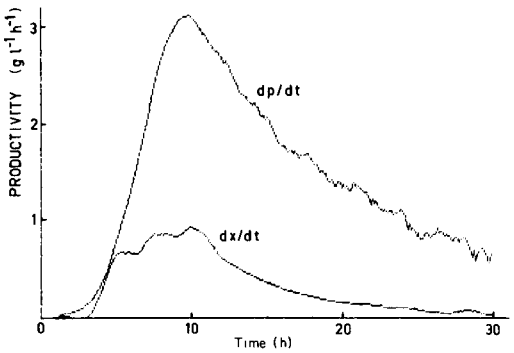

Fig. 2. On-line evaluation of biomass (dx/dt) and ethanol (dp/dt) productivity in a batch yeast fermentation.

storage function of the first computer is interrupted; this period of interruption represents the lower limit of data-acquisition and process-control frequency, which is a fairly good limit for fermentation work.

Example of application

In order to test the computer network system, it was applied for continuous monitoring of a yeast fermentation yielding ethanol. Product concentration was measured by a gas sensor described earlier [24]; yeast biomass was estimated by absorbance measurements. After conversion to conventional units (g l^{-1}) by calibration functions, data were smoothed by cubic polynomials [25] and used for the (on-line) calculation of derived parameters (i.e., productivities, $\dot{x}$, $\dot{p}$, which can be used for more refined process control.) A typical output is shown in Fig. 2.

Grants from the Hochschuljubiläumsstiftung der Stadt Wien are gratefully acknowledged.

REFERENCES

1 L. K. Nyiri, in T. K. Ghose, A. Fiechter and N. Blakebrough (Eds.), Advances in Biochemical Engineering, Vol. 2, Springer, New York, 1972, p. 49.
2 D. D. Dobry and J. L. Jost, in G. T. Tsao (Ed.), Annual Reports on Fermentation Processes, Vol. 1, Academic Press, New York, 1977, p. 95.
3 W. A. Weigand, in G. T. Tsao (Ed.), Annual Reports on Fermentation Processes, Vol. 2, Academic Press, New York, 1978, p. 43.
4 W. B. Arminger and A. E. Humphrey, in H. J. Peppler (Ed.), Microbial Technology, Vol. 2, Academic Press, New York, 1979, p. 376.
5 W. A. Hampel, in T. K. Ghose, A. Fiechter and N. Blakebrough (Eds.), Advances in Biochemical Engineering, Vol. 13, Springer, New York, 1979, p. 1.
6 A. Veres, L. Nyeste, I. Kurucz, L. Kirchknopf, L. Szigeti and J. Hollo, Biotechnol. Bioeng., 23 (1981) 405.
7 W. A. Knorre, R. Gutke and F. Bergter, in V. Krumphanzl, B. Sikyta and Z. Vanek Eds.), Overproduction of Microbial Products, Academic Press, New York, 1982, p. 623.

8 M. J. Rolf, P. J. Henningan, R. D. Mohler, W. A. Weigand and H. C. Lim, Biotechnol. Bioeng., 24 (1982) 1191.
9 R. Oinas, Process Biochem., 17 (1982) 6, 10.
10 W. Hampel, W. Woehrer, H. P. Bach and M. Roehr, Acta Biotechnol., 2 (1982) 331.
11 M. J. Rolf and H. C. Lim, Enzyme Microb. Technol., 4 (1982) 370.
12 R. T. Hatch, in G. T. Tsao (Ed.), Annual Reports on Fermentation Processes, Vol. 5, Academic Press, New York, 1982, p. 291.
13 W. Beyeler, S. Strub and W. Kappel, in H. Dellweg (Ed.), 5th Symp. Technische Mikrobiologie, Energie durch Biotechnologie, Versuch- u. Lehranstalt f. Spiritusfabrikation, Berlin, 1982, p. 252.
14 A. Bernard, M. Cordonnier and J. M. Lebeault, Process Biochem., 18 (1983) 3, 2.
15 M. Angerhausen, R. Brückmann, L. Englisch and K. Gerits, 64 Intern, Data Becker GmbH, Düsseldorf, 1983, p. 58.
16 A. Lenk, Microcomputer, (1982) 4, 34.
17 R. P. Jefferies III, Process Biochem., 10 (1975) 4, 15.
18 M. Meiners and W. Rapmundt, Biotechnol. Bioeng., 25 (1983) 809.
19 L. Bowski, C. R. Perley and J. M. West, Biotechnol. Bioeng., 25 (1983) 1237.
20 P. Whaite, S. Aborhey, E. Hong and P. L. Rogers, Biotechnol. Bioeng., 20 (1978) 1459.
21 E. H. Forrest, N. B. Jansen, M. C. Flickinger and G. T. Tsao, Biotechnol. Bioeng., 23 (1981) 455.
22 K. Bayer and F. Fuehrer, Process Biochem., 17 (1982) 4, 42.
23 B. H. A. van Kleef, Antonie van Leeuwenhoek; J. Microbiol. Serol., 48 (1982) 521.
24 H. P. Bach, W. Woehrer and M. Roehr, Biotechnol. Bioeng., 20 (1978) 799.
25 A. Savitzky and M. J. E. Golay, Anal. Chem., 36 (1964) 1627.

Analytica Chimica Acta, 163 (1984) 275—280
Elsevier Science Publishers B.V., Amsterdam — Printed in The Netherlands

Short Communication

COMPUTER MONITORING OF SUGARS, ACIDS AND VOLATILE COMPOUNDS IN FERMENTATIONS

J. C. MOTTE*, X. MONSEUR, M. TERMONIA, M. HOFMAN, G. ALAERTS, A. DE MEYER, P. DOURTE and J. WALRAVENS

Institut de Recherches Chimiques, Ministère de l'Agriculture, Museumlaan 5, B-1980 Tervuren (Belgium)

(Received 17th April 1984)

Summary. Head-space gas chromatography coupled to computer-assisted mass spectrometry is used to follow the formation kinetics of ethanol in fermentations. High-performance liquid chromatography, coupled to a computerized integrator, is used to follow the kinetics of disappearance of sugars and the formation of acids during the fermentation process. Flow injection analysis is used to monitor feed streams of low sugar content during downstream processing and recovery of the lactic acid. The kinetics pattern of volatile and nonvolatile products can be used in order to control fermentation parameters.

In many European countries, sour whey is available in excessive amounts. Usually, the whey is ultrafiltered and the lyophilized proteins are used for cattle feed. The water, rejected to waste, contains up to 5% sugars and low-molecular-weight proteins. This solution is an excellent growth medium for bacteria in yeast fermentation. The fermentation of sugars to alcohols or acids is well known and very reliable but in this study, instead of a high sugar concentration, the lactose is only present at a level of 4—5%. Accordingly, the conversion must lead to products with the highest possible yields. The products must be easily isolated with a high added value and have a high marketing potential. In order to meet those different needs, both alcohol and acid fermentations have been studied here.

The products that can be obtained are so numerous and diverse that different chromatographic methods are needed to quantify them. The analytical methods, selected according to the nature of the products to be quantified, are flow injection analysis (f.i.a.), head-space gas chromatography (h.s.g.c.) and high-performance liquid chromatography (h.p.l.c.). The results obtained from those methods, reduced by the integrator, are sent to a host computer in order to monitor the fermentation process.

Experimental

For head-space gas chromatography, a Hewlett-Packard 5700 gas chromatograph equipped with flame ionization detection and two sampling valves,

0003-2670/84/$03.00

is used. The heated valves (150°C) are electrically actuated from the keyboard of the Hewlett-Packard 3385 integrator or automatically via the time-event program provided by the integrator. The first valve selects one of the three fermentors by routing the head-space gases of the chosen fermentor to a second valve equipped with a 1-ml sample loop, which acts as the injection system. The temperature of the valves and of the sampling lines is maintained at 150°C. The glass column (1.83 m, 0.635 cm o.d., 0.3 cm i.d.) used is provided with Carbopak A impregnated with 0.2% (w/w) SP-1000.

For components of higher boiling point than ethanol, listed in Table 1, 10 l of head-space gases is preconcentrated; the gases are pumped through a 25-mg charcoal filter, at a pumping rate of 100 l h^{-1}. After this enrichment, the analytes are eluted from the charcoal cartridge by 50 μl of carbon disulfide, and 1 μl of the carbon disulfide solution is used for g.c./m.s. (Finnigan-Mat 4500 with INCOS data system). Those substances are subsequently determined twice a day during the course of an ethanol fermentation.

The modular high-performance liquid chromatographic system used is equipped with a 6000A pump, a WISP automatic injector and a R401 refractometer, all from Waters Associates. The results are collected on a Hewlett-Packard computing integrator or a Hewlett-Packard 3390A. The column used is a BioRad HP-X87-H cation-exchanger heated at 75°C and protected with a column microguard. The mobile phase is 5×10^{-3} M sulfuric acid made with twice-distilled water filtered on a 0.45-μm filter and continuously degassed with helium. The flow rate is set at 0.7 ml min^{-1}. The injected sample (5 μl) comes from an ultracentrifuged aliquot of the fermentor brew which is diluted two-fold with water spiked with an internal standard (ribose).

The flow-injection system for the determination of reducing sugars is set up from Skalar BV modules; for lactic acid monitoring, a custom-built electrode and a digital Knick pH monitor were added. The procedure used for

TABLE 1

Relative concentration of volatile compounds produced during ethanol fermentation of whey

Compound	Abundance[a]	Compound	Abundance[a]
1-Methylbutylpropanoate	100	Ethylbutanoic acid	37
2-Heptanone	10	Butylbutyrate	500
Ethylbutanoate	4	2-Methylpropanol	500
Ethylhexanoate	25	Butanol	25
3-Methyl-1-butanol acetate	75	Isoundecane	15
3-Methylbutanol	500	Propylacetate	7
3-Ethylpentane	1000	Nonanol	25
Butylpentanoate	750	Propylpentanoate	5
Butylhexanoate	11		

[a]Relative abundance at point of maximum production.

reducing sugars is that described by Bittner and McCleary [1]. For lactic acid quantification, the oxidative conversion to acetaldehyde proposed originally by Barker and Summerson [2] is used. The samples from the fermentor are ultracentrifuged just before injection.

Data acquisition and processing. The analytical channels are serviced by individual data stations, to allow for independent operation during set-up and calibration procedures. Data transmission is over serial links under the EIA-RS-232-C protocol. The host computer extracts selected data from the data station reports. Primary data are reduced. Data are logged only when significant deviations are detected. Preliminary information on the system used is available [3]; more detailed information is to be published.

Results and discussion

The first bioconversion studied was the alcohol fermentation. Very easy, rapid and almost quantitative, this bioconversion was ideal to study the different parameters of the process. In order to follow the kinetics of ethanol fermentation of the lactoserum, h.s.g.c. was used to examine the off-gases from the broth. Both static, equilibrium and dynamic head-space methods were used for the determination of volatile alcohols in the percentage concentration range and for less concentrated organic compounds such as flavors. Off-line h.s.g.c. has been reported [4, 5], but the present work offers a technique for removing the fermentation gas continuously for automated h.s.g.c., which obviates the need for head-space vials. A typical gas chromatogram is shown in Fig. 1. An external standard method was used to quantify ethanol by standard addition of the analyte to a fermentor containing the substrate only.

Dynamic head-space analysis, with preconcentration of the volatiles, was used to monitor the presence of higher boiling components. This procedure is based on a method described by Grob and Grob [6] for the determination of C_6—C_{20} compounds in air. The substances listed in Table 1 were determined twice a day during the course of an ethanol fermentation lasting 10 days. Figure 2 shows the relative concentration of the measured components plotted against the elapsed fermentation time, in order to follow their formation and disappearance. The reliability of h.s.g.c. has been demonstrated and is currently used where volatile organics can serve as parameters for fermentation monitoring.

Because of the difficulties encountered in concentrating the ethanol, it was rapidly obvious that the ethanol fermentation was not the best choice. In practice, starting with 4—5% sugars, 2.5% alcohol was the best obtainable yield; thus the concentration process is too expensive to have a chance of becoming competitive on a big scale. For this reason, acid fermentations were studied in order to produce organic acids with high commercial value, which are easy to isolate to usable concentrations. The chosen acid was lactic acid.

Analysis for organic acids is possible by gas chromatography [7] but the

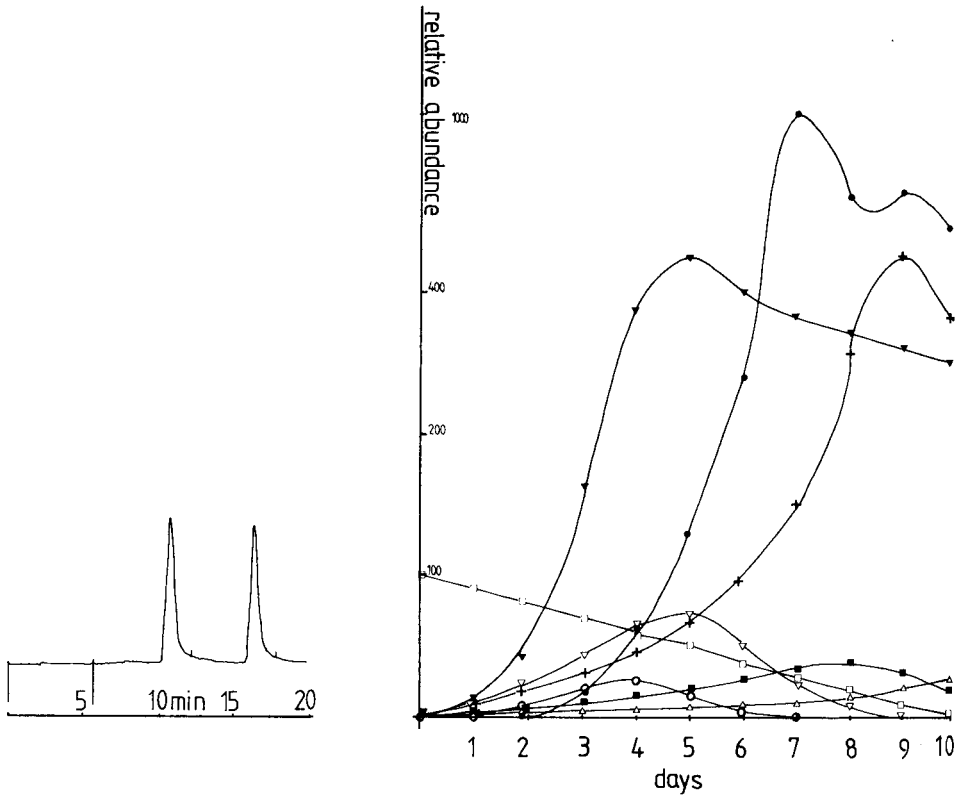

Fig. 1. Typical head-space gas chromatogram from fermentation of whey. Two injections are made in the same run to improve reliability. Both peaks correspond to ethanol.

Fig. 2. Relative abundance of the detected volatile compounds as a function of the elapsed time of the ethanol fermentation process. (□) 1-Methylbutylpropanoate; (○) ethylhexanoate; (▽) 3-methyl-1-butanol acetate; (▼) 3-methylbutanol; (●) 3-ethylpentane; (■) ethylheptanoic acid; (+) butylbutyrate; (△) nonanol.

acids must be esterified before injection to avoid adsorption problems. To reduce the sample preparation time, another method was developed. Methods for the determination of acids by h.p.l.c. have been reviewed by Schwarzenbach [8]. Of the available procedures, cation-exchange methods have the advantages that, with minor modifications, acids, sugars and alcohols can be detected in the same run, and that no derivatization is needed. The method was modified by heating the column to 75°C to improve the resolution of the eluting peaks. A chromatogram of the standard compounds is presented in Fig. 3(a); Fig. 3(b) is a typical chromatogram obtained for a sample collected during the fermentation. These results show that the h.p.l.c. method allows monitoring of the fermentation, via the disappearance of the initial sugars and the formation of the lactic acid.

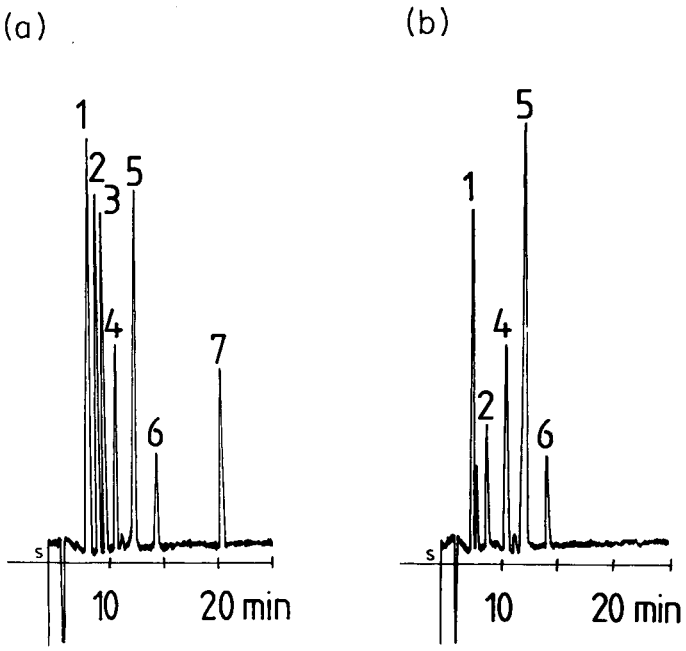

Fig. 3. (a) Chromatogram of the standards. (b) Typical chromatogram obtained during the lactic acid fermentation process. Peaks: (1) lactose; (2) glucose; (3) galactose; (4) ribose; (5) lactic acid; (6) acetic acid; (7) ethanol. Ribose is the internal standard.

As an alternative to h.p.l.c., flow-injection systems were tested for monitoring lactic acid and reducing sugars in the fermentation brew and the downstream effluents. To monitor the reducing sugars by the spectrophotometric method of Bittner and McCleary, reaction conditions (temperature, heating time, pH and reagent concentrations) were optimized. The method is useful for monitoring glucose down to 1.25 μg ml^{-1}, particularly if a fed-batch yeast culture is to be maintained at low available sugar concentrations. For studies of the evolution of sugar concentrations at higher levels, the method is less valuable because the colour intensities developed by equimolar solutions of various reducing sugars differ greatly.

The method used for lactic acid was based on the oxidative conversion to acetaldehyde [2], which is widely used. The original method has often been modified and refined. The well-known condensation reaction between hydroxylamine and acetaldehyde [9] was preferred here. However, under any of the conditions studied, acetaldehyde was generated from substances such as ethanol and sugars and so interfered with the lactic acid determination. These experiments will be discussed in detail elsewhere.

In conclusion, the flow-injection system is of limited use for direct monitoring of lactic acid in fermentation broths unless corrections for the other components present can be introduced at the central processor level. This

method proves valuable, however, for monitoring feed streams of low sugar content during downstream processing and recovery of the lactic acid. While head-space gas chromatography is limited to monitoring readily volatile substances, h.p.l.c. seems to be the method of choice for monitoring the lactic acid fermentation process. This method is still off-line because of the ultrafiltration or ultracentrifugation step needed for sample preparation. A true on-line method is under development.

REFERENCES

1 D. L. Bittner and M. L. McCleary, Am. J. Clin. Pathol., 40 (1963) 423.
2 S. A. Barker and P. Summerson, J. Biol. Chem., 126 (1983) 413.
3 M. Hofman, Advances in Fermentation, Wheatland Journals Ltd., London, 1983.
4 M. Termonia, A. De Meyer, M. Wybauw and H. Jacobs, HRC & CC, 5 (1981) 277.
5 B. Kolb (Ed.), in Applied Headspace Gas Chromatography, Heyden, London, 1980.
6 K. Grob and G. Grob, J. Chromatogr., 62 (1971) 1.
7 X. Monseur, J. Walravens, P. Dourte and M. Termonia, HRC & CC, 4 (1981) 49.
8 R. Schwarzenbach, J. Chromatogr., 251 (1982) 339.
9 E. H. Rodd (Ed.), Chemistry of Carbon Compounds, Vol. 1, Elsevier, Amsterdam, 1951, p. 496.

Analytica Chimica Acta, 163 (1984) 281—285
Elsevier Science Publishers B.V., Amsterdam — Printed in The Netherlands

Short Communication

MONITORING GLUCOSE CONSUMPTION IN AN *ESCHERICHIA COLI* CULTIVATION WITH AN ENZYME ELECTRODE

NEIL CLELAND and SVEN-OLOF ENFORS*

Department of Biochemistry and Biotechnology, Royal Institute of Technology, S-100 44 Stockholm (Sweden)

(Received 10th April 1984)

Summary. An autoclavable enzyme electrode, the externally buffered glucose oxidase electrode, is used to monitor the glucose consumption during batch cultivations of *E. coli*. The electrode signal showed good correlation with data from a conventional procedure and was independent of the dissolved oxygen concentration in the fermentation broth.

Glucose is of such biological importance that much work has been done on developing methods for its detection and determination. Glucose electrodes based on enzymatic oxidation of glucose have been constructed, especially for clinical purposes [1—5]. In the field of fermentation processes, however, few reports have appeared [6—8]. When an enzyme electrode is used in a fermentation process, serious difficulties arise. Sterility must be maintained (which means that the electrode must be autoclavable). In aerobic fermentation, the dissolved oxygen concentration in the broth may change from saturation to zero in a few hours and the composition and ionic strength of the broth may undergo substantial changes. In anaerobic fermentations, the dissolved oxygen concentration is zero at all times.

There are two basic types of enzymatic analyzers. One is the enzyme reactor, in which sample is withdrawn from the sampling site of analysis, sometimes dialyzed, and pumped to an enzymatic sensor situated elsewhere. The other is the enzyme electrode which is self-contained and is placed directly in the sample. Each has inherent advantages and disadvantages. The present work involves the latter principle. The different sorts of electrode are shown schematically in Fig. 1. Type A is an enzyme electrode with an immobilized enzyme preparation. It is based on glucose oxidase (which is oxygen-dependent) and the solubility of oxygen lies around or below the K_m of the enzyme. Therefore, the oxygen stabilization principle was developed, as used in the type B electrode. In response to decreasing output from the oxygen electrode, more oxygen is generated at the platinum net to keep the oxygen content of the enzyme preparation constant. The current required for this is a measure of the glucose concentration [7]. Because this electrode had a linear measuring range only up to ca. 4 g l^{-1} glucose, a flow

0003-2670/84/$03.00

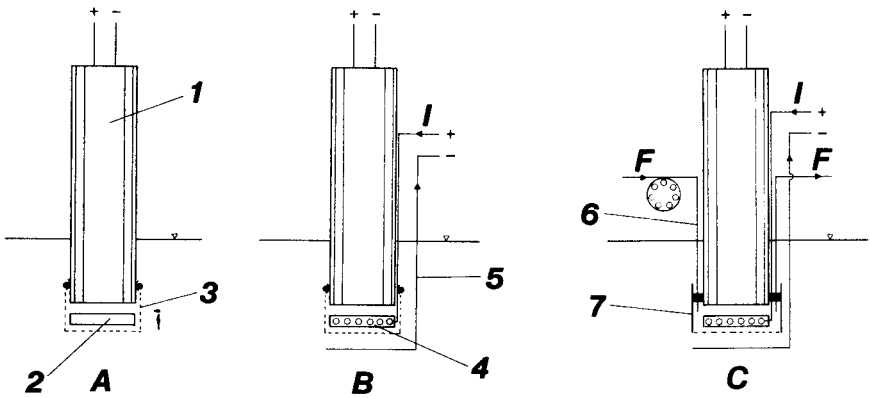

Fig. 1. Schematic views of different types of enzyme electrode. A: (1) oxygen electrode; (2) immobilized enzyme; (3) dialysis membrane. B: (4) Pt gauze with immobilized enzyme; (5) Pt wire cathode. C: (6) tubing; (7) enzyme chamber; (I) electrolysis current; (F) buffer flow.

of buffer was introduced into the enzyme chamber (type C electrode). The linear range was dependent on the buffer flow rate.

In fermentation applications, two different modes of operation are needed for a glucose electrode, either for monitoring glucose concentration during a batch fermentation or for control of glucose concentration at a certain (low) level in a fed-batch fermentation. Fed-batch fermentation using a type B electrode has been described elsewhere [8]. In this study, a modified version of a type C electrode was used to monitor an *E. coli* batch cultivation.

Experimental

Equipment. The glucose electrode system as installed in the fermentor is outlined in Fig. 2. The incoming buffer first passes through a dialysis chamber contained in a sterilizable glass housing, after which it passes into the enzyme electrode (type C, Fig. 1). The enzyme electrode is contained in an autoclavable polycarbonate housing, and is introduced after autoclaving. Both the dialyzer and electrode units are held in the fermentor lid by means of standard connections. The electrolysis cathode consists of a platinum wire (2 mm diameter) and enters the fermentor through a membrane. The electronic instrumentation for the electrode and its mode of operation have been described previously [7, 8].

An LKB Multiperpex peristaltic pump was used to pump the buffer through the system. Tygon tubing (1.6 mm i.d.) was used except between the dialyzer and the enzyme electrode, where teflon tubing (1 mm i.d.) was used. The fermentor was a Chemoferm 3l equipped with automatic pH control, and with a working volume of 2 l.

Solutions and reagents. Sodium hydroxide (4 M) was used for pH control. The glucose stock solution was 220 g l^{-1}. The buffer in the enzyme electrode was 0.025 M phosphate buffer, pH 7.0.

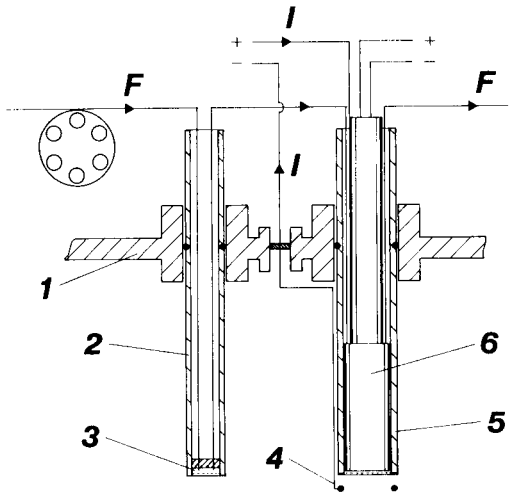

Fig. 2. Main components of autoclavable enzyme electrode used in this study: (1) fermentor lid; (2) dialyzer housing; (3) dialyzing chamber; (4) Pt wire cathode; (5) enzyme electrode outer housing; (6) enzyme electrode as shown in Fig. 1C; (I) electrolysis current; (F) buffer flow.

The mineral salts medium used for bacterial cultivation had the following composition (g l^{-1}): $(NH_4)_2SO_4$, 10; KH_2PO_4, 1.6; $Na_2HPO_4 \cdot 2H_2O$, 6.6; ammonium hydrogen citrate, 0.5; $MgSO_4$, 0.2. The trace elements added were (mg l^{-1}): $CaCl_2 \cdot 2H_2O$, 0.5; $FeCl_3 \cdot 6H_2O$, 16.7; $ZnSO_4 \cdot 7H_2O$, 0.18; $CuSO_4 \cdot 5H_2O$, 0.16; $MnSO_4 \cdot 4H_2O$, 0.15; $CaCl_2 \cdot 6H_2O$, 0.18; Na_4EDTA, 20.1. The pH was adjusted to 7.0 with 2.5 M H_2SO_4.

Glutaraldehyde (25% w/v) was used for inner electrode sterilization and enzyme immobilization after dilution to 2.5% with distilled water. All chemicals were of analytical grade. The enzymes, and immobilization procedure were as described previously [7]. *Escherichia coli* ATCC 15224 was kept on nutrient agar slopes at 37°C. The organism was grown in shaken flasks (2 × 100 ml) at 37°C and pH 7.0 overnight, centrifuged at 4°C, suspended in 100 ml of fresh medium and used as an inoculum in the fermentor.

Procedure for glucose. Glucose was determined by means of the enzymatic GLOX method (Kabi AB, Sweden). Measurements were made at 450 nm.

Monitoring procedure. The enzyme electrode was placed in a thermostatted beaker containing phosphate buffer, where it could also be tested for response to glucose. Prior to inoculation, the fermentor, containing the medium and the outer electrode housing, were autoclaved at 120°C for 1 h. When the fermentor had cooled, the enzyme electrode inner unit was dipped into 2.5% glutaraldehyde solution and introduced into its housing and the flow of buffer was started. The buffer stock solution had previously been autoclaved and the entire flow system including the enzyme chamber was

sterilized by pumping 2.5% glutaraldehyde for 10 min. The fermentor agitation was set at 700 rpm and aeration at 2.0 l min^{-1}, and the glucose electrode was allowed to equilibrate. Aliquots of glucose were added to give the desired concentrations to establish a calibration curve.

Results and discussion

Characteristics of the glucose electrode. The present electrode (Fig. 2) differs slightly from type C in Fig. 1. The main difference in behaviour is that the present system is insensitive to variations in dissolved oxygen concentration. This was shown by flushing a previously fully aerated fermentor with nitrogen, an operation which did not affect the output signal from the electrode. In contrast, the previous electrode showed a small, linear dependence on dissolved oxygen concentration [8—10], which could be compensated for by using the signal from an auxiliary oxygen electrode.

The glucose concentrations used in the present investigation were rather high, thus the buffer flow rates were correspondingly high to prevent excess glucose from entering the enzyme chamber. This means that there is little loss of oxygen from the dialyzer and enzyme chamber by diffusion. For work at lower glucose concentrations, the flow must be lowered in order to increase sensitivity; some sensitivity to dissolved oxygen concentration might then be expected, which could be compensated for as mentioned above. The response time to glucose additions is 5—10 min. Response to a decrease in glucose is often slightly faster. The linear response range depends on the buffer flow rate [10], it exceeded 30 g l^{-1} glucose in this study.

When exposed to an invariant glucose concentration (20 g l^{-1}) in 0.025 M phosphate buffer, pH 6.0, the electrode was stable to within 5% for at least 24 h.

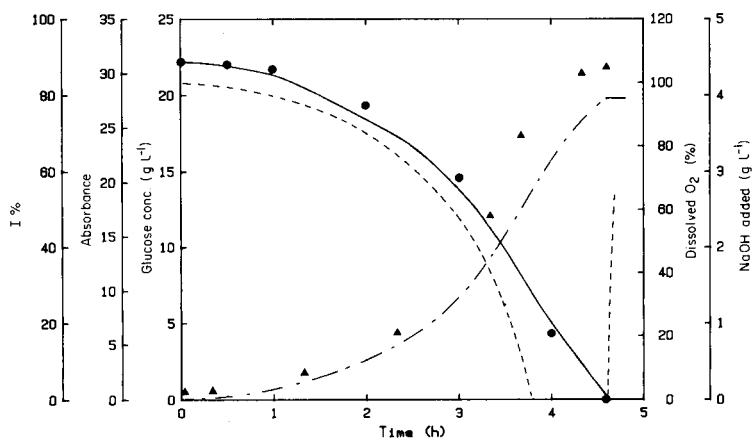

Fig. 3. Time course of a batch cultivation of *E. coli* in a mineral salts medium. (•) Glucose concentration; (▲) absorbance at 580 nm; (—) electrolysis current (I) as % of the initial value 165 μA; (---) dissolved oxygen pressure as % of air saturation; (···) NaOH added (g l^{-1}) (buffer flow rate 1.15 ml min^{-1}).

Monitoring of glucose concentration during an E. coli *batch cultivation.* The progress of a batch cultivation of *E. coli* is shown in Fig. 3. Cultivation was started at 22.2 g l^{-1} glucose, and the glucose electrode was used to monitor the glucose concentration, which reached zero after 4.6 h. After 3.8 h, the dissolved oxygen concentration became zero, and the previously logarithmic microbial growth rate became approximately linear. The sodium hydroxide additions needed to keep the pH constant were recorded by means of a dose monitor [11]. The rate of alkali additions decreased slowly when the dissolved oxygen concentration reached zero, and the additions ceased when the glucose was exhausted. At this point, the oxygen signal rose steeply. The electrode output (electrolysis current) showed a good linear correlation (r = 0.9986) with the data from the check analysis over the course of the cultivation. Thus it can be concluded that the enzyme electrode described here is useful for monitoring glucose consumption in fermentation processes.

REFERENCES

1 L. C. Clark, Jr, and C. Lyons, Ann. N.Y. Acad. Sci., 102 (1962) 29.
2 G. G. Guilbault, Enz. Microb. Technol., 2 (1980) 258.
3 A. S. Barker and P. J. Somers, in A. Wiseman (Ed.), Topics in Enzyme and Fermentation Biotechnology, Wiley, Vol. 2, 1978, pp. 120—151.
4 J.-L. Romette, B. Froment and D. Thomas, Clin. Chim. Acta, 95 (1979) 249.
5 K. Berterman, P. Elze, F. Scheller, D. Pfeiffer and M. Janchen, Anal. Lett., 15 (1982) 397.
6 C. F. Mandenius, B. Danielsson and B. Mattiasson, Biotechnol. Lett., 3 (1981) 629.
7 S.-O. Enfors, Enz. Microb. Technol., 3 (1981) 29.
8 N. Cleland and S.-O. Enfors, Eur. J. Appl. Microbiol. Biotechnol., 18 (1983) 141.
9 S.-O. Enfors and N. Cleland, in T. Sciyama (Ed.), Chemical Sensors; Proceedings of the International Meeting, Fukuoka, Japan, September 19—22, 1983, Elsevier, Amsterdam, 1983, p. 672.
10 N. Cleland and S.-O. Enfors, Anal. Chem., (1984), in press.
11 S.-O. Enfors and M. Dostalek, Proc. Biochem., 10 (1975) 13.

Analytica Chimica Acta, 163 (1984) 287—291
Elsevier Science Publishers B.V., Amsterdam — Printed in The Netherlands

Short Communication

SEMICONDUCTOR GAS SENSORS IN BIOREACTOR CONTROL

KLAUS-DIETER VORLOP*, JÜRGEN WERNER BECKE, JÜRGEN STOCK and JOACHIM KLEIN

Institut für Technische Chemie, TU Braunschweig, Hans-Sommer-Str. 10, D-3300 Braunschweig (Federal Republic of Germany)

(Received 12th April 1984)

Summary. A simple semiconductor gas sensor (TGS 812) is used for the on-line measurement and control of indole during the production of L-tryptophan from indole and L-serine with immobilized *E. coli* cells. Indole is estimated in the reactor gas space. In combination with an automatic indole supply system, a feed-batch process became possible. The indole concentration was monitored and kept within the optimal range (300—600 mg l^{-1}). A simple gas-sensing electrode dipped in the reaction medium provides direct measurement of organic solvents and gases in the liquid. Such a system is suitable for on-line determination of ethanol (10—70 g l^{-1}) during continuous production of ethanol with immobilized yeast cells.

On-line monitoring and control of process parameters during fermentation is vital for optimal process design. Several methods for the measurement of volatile organic compounds (e.g., ethanol, methanol, alkanes) during fermentation have been described. The concentration in the liquid has been determined by measuring the concentration in the exhaust gas with a flame ionization detector, mass spectrometer or a simple semiconductor gas sensor. The semiconductor sensor was first used for on-line monitoring of ethanol produced during yeast cultivation [1] but the measurement of ethanol in the exhaust gas was affected by air flow rate, CO_2 formation and stirring speed. To prevent these effects, a combination of the gas sensor and the "tubing method" [2] was applied [3]; ethanol diffused into a silicone rubber tube placed in the culture broth, and was transferred by a continuous air stream at constant flow rate to the thermostated gas sensor. Similar systems with continuous dilution of liquid or gas flow streams were recently applied [4]. A teflon membrane can replace the silicone rubber tube [5]. To avoid extra thermostating of the gas sensor, a device was developed [6] in which the silicone rubber tube and sensor were placed directly in the fermentor, but clean carrier gas at a precise flow rate was still necessary.

A gas-sensing electrode that can be dipped in solutions and does not need extra thermostating or a carrier gas are not necessary was developed recently [7]. This communication outlines its applicability for the direct measurement of ethanol in culture broths during continuous fermentation with

0003-2670/84/$03.00

immobilized cells. In another example, the utility of the gas sensor placed in the fermentor gas space, for on-line monitoring and control of indole during the production of L-tryptophan is demonstrated.

Experimental

Gas-sensing system for ethanol. The gas-sensing electrode was described previously [7]. The sensor is dipped directly in the fermentation medium, so that it is thermostated by the medium. Ethanol in the medium permeates the silicone rubber tube and the ethanol content in the gas quickly attains equilibrium with the ethanol in the fermentation liquid. Depending on the ethanol concentration the sensor changes its resistance, which is converted to a voltage output and transmitted to a recorder. The gas sensor used for measurements of ethanol was the model TGS 813 (Figaro, Minoo City, Osaka 562, Japan).

Ethanol production. Continuous ethanol fermentation with immobilized yeast cells was done in a 3-stage cascade at 32°C. Each cone-shaped glass reactor had a total volume of 33 ml with an initial calcium alginate biocatalyst content of 3.3 g [7]. A substrate solution containing 15% (w/v) D-glucose [7] was fed from the bottom of each reactor and the rate was regulated by a membrane pump. The ethanol concentration was monitored continuously behind the last reactor with the gas-sensing electrode. Ethanol was also quantified by gas chromatography.

L-Tryptophan production. The continuous and discontinuous production of L-tryptophan with free or immobilized *E. coli* cells has been described [8—11]. The most effective way to produce L-tryptophan from indole and L-serine is the feed-batch process [12]. The kinetic behaviour of this reaction makes it necessary to maintain the indole concentration at the optimal level of 300—600 mg l^{-1}; at higher indole concentrations, the reaction is inhibited. By using the gas sensor (TGS 812), placed in the reactor gas space, the indole concentration could be monitored and controlled.

Figure 1 shows the experimental set-up for the production of L-tryptophan with free or immobilized *E. coli* cells. The feed-batch reaction was done

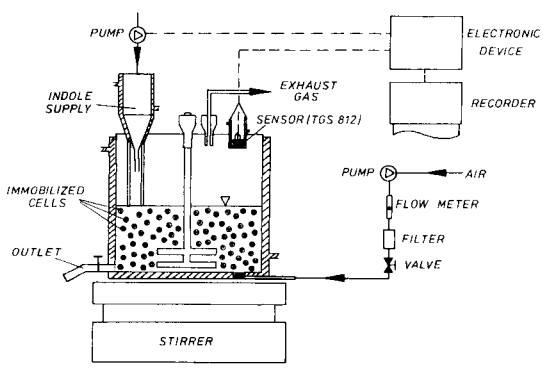

Fig. 1. Set-up for L-tryptophan production with on-line control of indole.

in a stirred tank reactor with a total volume of 280 ml. To prevent condensation, the gas sensor was fixed in a glass tube fitted with a circulation jacket (70°C) and inserted in the lid of the reactor. The stirrer was kept at 400 rpm at an aeration rate of 1.8 l h^{-1}. The temperature was maintained at 37°C. The composition of the medium was as follows: 975 mg of L-serine, 100 mg of indole, 1 mg of pyridoxal-5-phosphate in 100 ml of buffer (0.08 M K_2HPO_4, 0.2% NaCl, pH 7.8 adjusted with phosphoric acid), 20 g of the chitosan/polyphosphate biocatalyst (diameter ≈1 mm, cell loading 42%, specific activity 40 mg of L-tryptophan/g of wet catalyst/h). Molten indole (875 mg) was added dropwise to the reaction solution, so that a concentration of 300—600 mg l^{-1} was maintained. This was monitored and controlled by the combination of gas sensor and electronics (Fig. 1). The indole concentration was also checked by high-performance liquid chromatography (h.p.l.c.). When the indole was totally converted to L-tryptophan, the solution was drained off; the biocatalyst beads were retained by a nylon net. A new reaction solution was then added and L-tryptophan production was restarted.

Results and discussion

On-line ethanol monitoring with the gas sensor. The response time for ethanol of the sensor with a 0.5-mm thick silicone rubber membrane was 10 min for the final response. This suffices for control of biochemical processes. The relationship between voltage drop and ethanol concentration at different temperatures is shown in Fig. 2. It was possible to monitor the ethanol concentration for at least 50 days during the alcohol production with immobilized yeast cells in the three-stage cascade without apparent degradation of the performance of the sensor. The ethanol concentrations

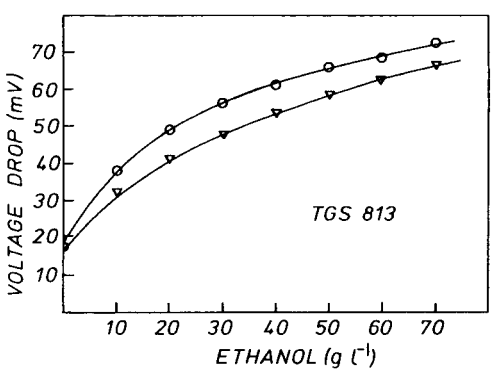

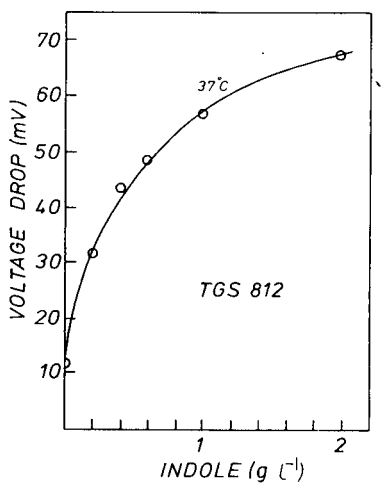

Fig. 2. Calibration curves for ethanol in the range 10—70 g l^{-1} with the TGS 813 sensor: (○) at 30°C; (▽) at 20°C.

Fig. 3. Calibration curve for indole at 37°C with the TGS 812 sensor.

estimated in this way were in good agreement with those measured by g.c. (±3%). This sensor was used earlier to observe directly oscillations in ethanol concentrations during a fermentation process at high glucose concentrations (20% w/v) [7]. In conclusion, this gas sensor placed in the fermentation medium is well suited for on-line monitoring of ethanol during a continuous process. The system is simple and should be useful for other reaction systems.

Indole monitoring during L-tryptophan production. The response time for indole in the reaction system shown in Fig. 1 was about 10 min, mainly because of the time needed to attain equilibrium between the liquid and gas phases. The gas sensor itself has a response time of about 1 min. This short response time was sufficient for monitoring and control of the indole concentration during L-tryptophan production with free or immobilized *E. coli* cells. Figure 3 shows the relationship between the voltage drop of the gas sensor and the indole concentration in solution. No drift in the voltage drop of the calibration graph was observed over 3—4 weeks. The calibration was significantly affected by a change of the air flow rate, because of variable dilution of indole by the gas stream; a constant air flow rate (1.8 l h^{-1}) was therefore essential. In other experiments, the gas sensor was dipped in the reaction solution for the measurement of indole, in the same way as for ethanol. The main problem was to find a suitable membrane. Good results were obtained with polyethylene and porous teflon membranes, but the time required was about 60 min for a stable response. This system was suitable only for the control of indole during continuous L-tryptophan production in a continuously stirred tank reactor.

In one experiment, the indole concentration was controlled during a batch process (500-ml reaction solution, 1.8 g of wet cells, 1 g of L-serine, 1 g of indole, 5 mg of pyridoxal-5-phosphate, 37°C, pH 8). The voltage drop of the

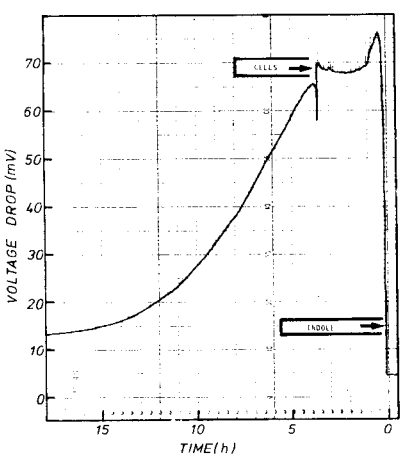

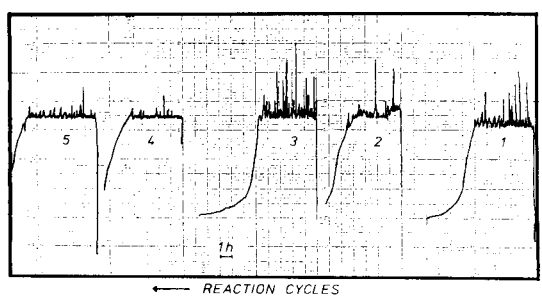

Fig. 4. Indole control during batchwise production of L-tryptophan.

Fig. 5. Indole control for the production of L-tryptophan in repeated feed-batch runs with immobilized cells.

gas sensor with time is shown in Fig. 4; the conversion of indole is clearly seen. The initial activity calculated from the gas-sensor values was 183 mg of L-tryptophan/g of wet cells/h; an activity of 203 mg of L-tryptophan/g of wet cells/h was calculated from the indole values obtained by h.p.l.c. Thus there is reasonably good agreement between the indole concentrations measured on-line with the simple gas sensor system and off-line by h.p.l.c.

In further experiments, the gas sensor system was used to control L-tryptophan production in the more efficient feed-batch process, which required the indole concentration to be maintained in the range 300—600 mg l^{-1}. This was done by connecting the gas sensor and the electronics controlling the indole supply. Graphs of the voltage drop of the gas sensor are shown in Fig. 5 for the first 5 feed-batch cycles. The indole concentration in each cycle was kept constant for about 4 h, then the indole supply was stopped and the total conversion of indole was observed by the gas-sensor system. It was thus possible to produce highly concentrated L-tryptophan solutions.

These two examples, the measurement of ethanol and indole with the simple gas-sensor systems, clearly demonstrate the applicability of this cheap method for bioreactor control.

REFERENCES

1 H. P. Bach, W. Woehrer and M. Roehr, Biotechnol. Bioeng., 20 (1978) 799.
2 D. H. Phillips and M. J. Johnson, J. Biotechnol. Microbiol. Technol. Eng., 3 (1961) 261.
3 E. Puhar, L. H. Guerra, I. Lorencez and A. Fiechter, Eur. J. Appl. Microbiol. Biotechnol., 9 (1980) 227.
4 C. F. Mandenius and B. Mattiasson, Eur. J. Appl. Microbiol. Biotechnol., 18 (1983) 197.
5 J. H. Lee, J. C. Woodard, R. J. Pagan and P. L. Rogers, Biotechnol. Lett., 3 (1981) 251.
6 Vogelbusch, European Patent (1981) 890199.
7 K. D. Vorlop, J. W. Becke and J. Klein, Biotechnol. Lett., 5 (1983) 509.
8 W. G. Bang, S. Lang, H. Sahm and F. Wagner, Prepr.-Eur. Congr. Biotechnol. 1st, 1 (1978) 186.
9 K. D. Vorlop and J. Klein, Biotechnol. Lett., 3 (1981) 9.
10 F. Wagner, S. Lang, W. G. Bang, K. D. Vorlop and J. Klein, Enzyme Eng., 6 (1982) 251.
11 W. G. Bang, U. Behrendt, S. Lang and F. Wagner, Biotechnol. Bioeng., 25 (1983) 1013.
12 K. D. Vorlop, Dissertation, TU Braunschweig, 1984.

Analytica Chimica Acta, 163 (1984) 293—297
Elsevier Science Publishers B.V., Amsterdam — Printed in The Netherlands

Short Communication

RAPID DETERMINATION OF SULFIDE IN WASTE WATERS BY CONTINUOUS FLOW ANALYSIS AND GAS DIFFUSION AND A POTENTIOMETRIC DETECTOR

K. BRUNT

Analytical Department, Potato Processing Research Institute TNO, 27 Rouaanstraat, 9723 CC Groningen (The Netherlands)

(Received 30th March 1984)

Summary. The continuous-flow system is based on a flow-through gas diffusion unit and a potentiometric detection with sulfide-selective electrode. The sampling rate is about 15 h^{-1}. In the 0.5—600 mg l^{-1} sulfide range, the mean slope of the response is 30.2 ± 0.3 mV per decade. The percentage transference of H_2S across the teflon membrane is 48 ± 1%. Up to sample concentrations of 50 mg l^{-1} sulfide, results agree well with those obtained by a distillation method. Sample storage is discussed.

Many industrial waste waters contain inorganic sulphur compounds such as sulfate and sulfite which are reduced to sulfide during anaerobic waste-water purification. It is well known that when the sulfide concentration in the waste water exceeds certain levels, methane formation in the anaerobic purification process is inhibited. It can be time-consuming to determine the sulfide concentrations in waste waters at the different stages of this process because of the rather high COD values (up to 15 000 mg l^{-1}) of the influent [1]. Although many methods are available for quantifying sulfide (e.g., [2, 3]), most methods require an elaborate sample clean-up procedure for removing interfering compounds and/or avoiding contamination problems. As will be shown below, the sulfide concentration in anaerobic waste water samples decreases very easily by volatilization and/or air oxidation during sampling, storage and clean-up of the sample. Time-consuming and complex procedures must therefore be avoided.

The continuous-flow (c.f.) system described here for the determination of sulfide in waste water is based on a gas-diffusion flow-through cell and a sulfide-selective electrode. Apart from the removal of undissolved particles, no sample pretreatment is required. The principle of gas diffusion has been applied for years in Auto-Analyzer systems. Nygaard [4] used gas diffusion in his discontinuous determination of sulfide and sulfite by pneumato-amperometry. Recently, gas-permeable membranes have also been applied in flow injection analysis [5—7]. Van der Linden [5] derived a general expression for the membrane transport in a flow-through cell and van Son et al. [6] applied the gas-diffusion cell for the determination of total ammoniacal

0003-2670/84/$03.00

nitrogen in (surface) water. Marshall and Midgley [7] determined sulfite with a gas-diffusion unit in combination with an ion-selective electrode.

Because of the relatively slow response of the sulfide-selective electrode, the method described below was based on continuous-flow instead of flow-injection techniques. The results obtained by the proposed system were compared with the data obtained by a distillation method. The serious problem of a sample preservation is also addressed.

Experimental

Reagents. All chemicals used were of analytical-reagent grade and were used as received.

A 1.5 M acetic acid buffer solution, adjusted to pH 4.0 with sodium hydroxide was used to acidify the sample stream. The alkaline sulfide antioxidant buffer (SAOB) solution was prepared more or less as recommended by Orion for the sulfide-selective electrode; it contained 30 g of ascorbic acid and 60 g of disodium-EDTA per liter, adjusted to pH 10 with sodium hydroxide. A stock solution of about 10^{-3} M sodium sulfide was used to prepare working solutions for calibration. The stock solution was standardized by iodimetric titration [8].

Apparatus. The manifold of the continuous-flow system is shown in Fig. 1. The sample and acetate buffer streams are both pumped by a multichannel peristaltic pump (Technicon) at a flow rate of 0.23 ml min^{-1}. The mixing coil is 80 cm of teflon tubing (i.d. 0.8 mm) in 26 coils. The acidified sample flows through the home-made gas diffusion cell. The sulfide-absorbing SAOB solution is pumped at 0.44 ml min^{-1} along the other side of the gas-permeable teflon membrane (teflon tape, 0.05 mm thick) through the gas-diffusion cell, which was kept at 30° C in a waterbath. The alkaline stream is connected by teflon tubing (25 cm, 0.5 mm i.d.) to a home-made flow-through cell [9]. An Orion sulfide-selective electrode (model 94-16) was used in a wall-jet mode. A saturated calomel electrode was used as reference. The potentials were monitored by an Orion 701A pH-mV meter connected to a Kipp recorder (model BD-40). The gas diffusion cell is composed of two equal perspex halves, each with a groove of 8 cm length, 1.2 mm width and 0.8 mm depth,

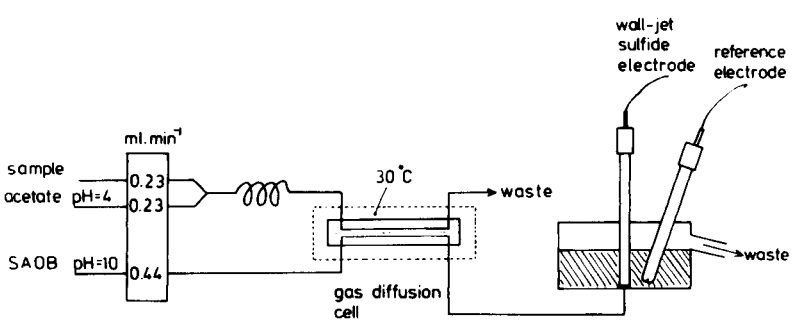

Fig. 1. Manifold for the continuous-flow system.

between which the teflon membrane is placed, as described by van der Linden [5].

Sulfide determination by the distillation method. A three-necked 500-ml distillation flask was equipped with a refluxing condenser, a dropping funnel and a nitrogen inlet. The condenser was connected to two Drechsel bottles in series, each filled with 15 ml of SAOB solution, made 1 M in sodium hydroxide instead of being at pH 10. The dropping funnel was filled with 20 ml of concentrated sulfuric acid and the distillation flask contained 1 ml of 2 M zinc acetate. Sample solution (50.0 ml) was transferred to the flask and homogenized; after 5 min 1 ml of 1 M sodium carbonate was added and mixed in well. Then 50 ml of water was added and purging with nitrogen was started. After a few minutes, the sulfuric acid was added carefully, and the solution was heated gently without boiling. The evolving H_2S was swept by the nitrogen to the absorbers. After 15 min of purging, the contents of the Drechsel bottles were quantitatively transferred to a 100-ml volumetric flask containing 20 ml of the strongly alkaline SAOB solution and diluted to the mark with water. The sulfide content was measured in this solution with the sulfide-selective electrode, using an appropriate calibration graph.

Results and discussion

Continuous flow method. As stated by the manufacturer, the response of the sulfide-selective electrode is strongly affected by the pH of the sample. Therefore samples must be buffered to a constant (and high) pH and ionic strength. In a simple continuous-flow system, this can be done on-line with the potentiometric measurement of the sulfide content. In the proposed system, the (waste water) sample is acidified to pH 4.5 by the acetate buffer, so that all the sulfide present is converted to the H_2S form. In the gas diffusion cell, the H_2S diffuses through the gas-permeable membrane into the alkaline SAOB solution. In the potentiometric detector, the sulfide concentration in this solution is monitored with the sulfide-selective electrode. This procedure enables sulfide to be transferred from samples of various composition, pH and ionic strength to a solution with a well defined pH and ionic strength in which potentiometric measurements are very reproducible. Figure 2 shows a recorder trace of a set of responses obtained during the daily calibration of the system. Sampling rates of 15 h^{-1} are usual.

The response of the continuous-flow system was Nernstian over the range 1.5×10^{-2}—1.5×10^{-5} M. The data from many calibrations were fitted to the conventional equation $E = E^* - k \log [S^{2-}]$, in which E^* is the formal standard potential for the conditions concerned and k is the slope (i.e., RT/zF). The numerical values of E^* and k were calculated by a logarithmic curve-fitting procedure. Although E^* was affected by the exact composition of the SAOB solution (especially by pH), the slope k was virtually independent of the exact SAOB composition. The average value of k with standard deviation from the average, was 30.2 ± 0.3 mV (theoretically, 29.6 mV at 25°C), calculated from 19 different calibration graphs measured on 19 different days.

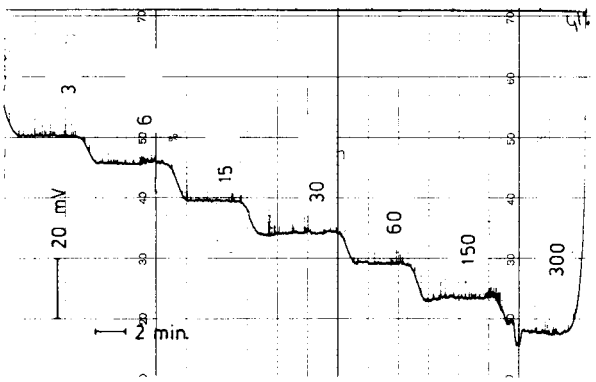

Fig. 2. Response of the detection system. The numbers on the plateau are mg l^{-1} sulfide.

The sulfide levels measured in anaerobic waste-water samples by the proposed flow method were compared with the levels measured at the same time in the same samples by the distillation method. Provided that the sulfide content was determined immediately after sampling and that only centrifuged samples were examined, the results obtained by both methods agreed very well (Table 1). However, at high sulfide concentrations (>100 mg l^{-1}), deviations occurred; these may have been caused by incorrect sample preservation (see below). When the samples were not centrifuged, the distillation method gave higher sulfide values than were found with the continuous-flow method, indicating that the latter method is useful only for quantifying dissolved sulfide. With the distillation method, any sulfide adsorbed on the sludge and some metal sulfides will also contribute to the result.

The percentage transference of H_2S across the teflon membrane in the gas-diffusion cell at 30°C was measured over the concentration range 1—300 mg l^{-1}. This was done by preparing sulfide standard solutions in exactly the same SAOB as used in the flow system. The responses of the sulfide electrode to these standard samples were measured first in the continuous-flow system specified in Fig. 1, and then in the same system after removal of the gas-diffusion cell and the donor stream, the standard samples replacing the SAOB stream. The average percentage transfer across the membrane was 48 ± 1%, calculated from seven different sulfide standards.

Sample preservation. The reliability of the results of any analytical method depends strongly on how the samples were collected and preserved. Sulfide concentrations in anaerobic waste-water samples decrease rapidly by volatilization and/or air oxidation if no special precautions are taken. Usually sulfide samples are pretreated with zinc acetate; the zinc sulfide precipitated is quite resistant to oxidation [10]. However the proposed flow method is suitable only for dissolved sulfide. Therefore, other methods were sought to make storage of samples possible for several days. Preliminary experiments indicate that good results can be obtained by storing samples in completely filled,

TABLE 1

Single determinations of sulfide concentrations measured immediately after sampling in centrifuged anaerobic waste water by the distillation method and by the flow method

Sample	Sulfide found (mg l^{-1})		Sample	Sulfide found (mg l^{-1})	
	Flow	Distillation		Flow	Distillation
1	18	17	5	51	49
2	20	21	6[a]	119	169
3	25	25	7[a]	142	169
4	50	51			

[a]Samples not centrifuged.

tightly closed glass bottles at 4°C. The anaerobic character of the samples is thus maintained and the microbiological activity of the sludge is stopped by cooling. Obviously, prolonged investigations are necessary to check these aspects of sampling and storage of anaerobic waste-water samples.

REFERENCES

1 D. J. Wijbenga, J. B. M. Meiberg and K. Brunt, in E. C. Houwink and R. R. van der Meer (Eds.), Innovations in Biotechnology, Progress in Industrial Microbiology, Elsevier, Amsterdam, 1984, p. 121.
2 L. Szekeres, Talanta, 21 (1974) 1.
3 W. J. Williams, Handbook of Anion Determination, Butterworth, London, 1979, Ch. 4.
4 D. D. Nygaard, Anal. Chim. Acta, 127 (1981) 257.
5 W. E. van der Linden, Anal. Chim. Acta, 151 (1983) 359.
6 M. van Son, R. C. Schothorst and G. den Boef, Anal. Chim. Acta, 153 (1983) 271.
7 G. B. Marshall and D. Midgley, Analyst (London), 108 (1983) 701.
8 A. I. Vogel, Quantitative Inorganic Analysis, Longmans, London, 3rd edn., 1975, p. 370.
9 K. Brunt, Analyst (London), 107 (1982) 1261.
10 R. Pomeroy, Anal. Chem., 26 (1954) 571.

Analytica Chimica Acta, 163 (1984) 299—303
Elsevier Science Publishers B.V., Amsterdam — Printed in The Netherlands

Short Communication

DETERMINATION OF THE SUBSTRATES OF DEHYDROGENASES IN BIOLOGICAL MATERIAL IN FLOW-INJECTION SYSTEMS WITH ELECTROCATALYTIC NADH OXIDATION

A. SCHELTER-GRAF, H.-L. SCHMIDT* and H. HUCK

Lehrstuhl für Allgemeine Chemie und Biochemie der Technischen Universität München, 8050 Freising-Weihenstephan (Federal Republic of Germany)

(Received 11th April 1984)

Summary. Flow-injection systems for the sensitive determination of dehydrogenase substrates are constructed by combining small columns of Eupergit-bound dehydrogenases with mediator-impregnated graphite electrodes as NADH sensors. Examples of applications given are the determination of D- and L-lactate in butter, L-glutamate in beef cubes, ethanol in beer, and the control of the enzymatic hydrolysis of *N*-acetyl-D,L-leucine by aminoacylase.

The applications of flow injection analysis (f.i.a.) based on immobilized enzymes are developing rapidly [1, 2]. Such a procedure has been used to determine ethanol in beer by oxidation catalyzed by immobilized alcohol oxidase, with amperometric oxygen monitoring [3]. By using amperometric NADH oxidation, substrates of dehydrogenases can also be quantified [4, 5]. However, the direct oxidation of NADH on platinum or graphite electrodes demands high electrode potentials (0.5—0.8 V vs. SCE), which causes high background currents because of oxidation of impurities present in the biological liquids.

Recently, electrocatalytic NADH oxidation was shown to be possible at low electrode potentials (ca. 100 mV vs. SCE) [6]. By coupling this sensitive NADH detection method to substrate dehydrogenation in small enzyme reactors with Eupergit-bound dehydrogenases, highly sensitive and stable flow-injection systems for the determination of dehydrogenase substrates were obtained. As well as the general advantages of f.i.a. (versatility and automatic control of sensitivity and baseline) [7, 8], these dehydrogenase systems have additional advantages; for example, in many cases the slope of the calibration curves can be predicted, as will be derived theoretically in a later paper. In the present communication, some practical applications in food analysis and process control are demonstrated.

Experimental

Enzyme and reagents. L-Lactate dehydrogenase from rabbit muscle (EC 1.1.1.27) and D-lactate dehydrogenase from *Lactobacillus Leichmannii*

0003-2670/84/$03.00

(EC 1.1.1.28) were from Sigma Chemical Company. L-Malate dehydrogenase from porcine heart (EC 1.1.1.37), L-glutamate dehydrogenase from beef liver (EC 1.4.1.3), alcohol dehydrogenase from yeast (EC 1.1.1.1), L-alanine dehydrogenase from *Bacillus subtilis* (EC 1.4.1.1), isocitrate dehydrogenase from porcine heart (NAD^+-dependent, EC 1.1.1.42) and NAD^+ (grade II) were from Boehringer-Mannheim. L-Leucine dehydrogenase from *Bacillus sphaericus* (EC 1.4.1.9), aminoacylase from fungi (EC 3.5.1.14), and *N*-acetyl-D,L-leucine were a kind gift from Prof. C. Wandrey, Institut für Biotechnologie, Kernforschungsanlage Jülich. β-D-Glucose dehydrogenase (EC 1.1.1.47) and all other chemicals were from Merck and Serva Feinbiochemica. Eupergit was from Röhm Pharma (Weiterstadt, F.R.G.).

Enzyme immobilization. Dehydrogenases were covalently bound to Eupergit (epoxyacryl resin beads) as described by the manufacturer. Dehydrogenases purchased as suspensions in ammonium sulphate solution were dialyzed before immobilization.

Flow-injection system. The system (Fig. 1) consists of a peristaltic pump (P-1, Pharmacia, Uppsala, Sweden), an injector (Reichelt Chemie, Heidelberg, F.R.G.), an enzyme reactor with the immobilized enzyme, and the electrocatalytic flow-through sensor. The three-electrode arrangement comprises a potentiostat (Minipotentiostat MP 75, Bank Elektronik, Göttingen, F.R.G.) with a Kipp and Zonen recorder (Delft, Netherlands), a saturated calomel electrode, a platinum counter electrode and the measuring electrode for NADH oxidation, which was a graphite electrode impregnated with the catalyst 3-β-naphthoyl-Nile Blue [9]. The enzyme reactor is a glass tube (i.d. 3.8 mm, variable length), containing 50 mg (dry weight) of Eupergit with the immobilized dehydrogenase. The substrate solution (0.01—10 mM in 0.2 M phosphate buffer, pH 8.0) is pumped through the system at 0.5 ml min^{-1}; 50-μl portions of a 10 mM NAD^+ solution are injected every 4—6 min.

This method is economical on coenzyme and the results are not affected by oxidizable impurities in the substrate solution. The peak current is used for the substrate determination, using log—log calibration graphs. Calibration graphs can also be obtained by injections of the substrate solution into a buffer containing NAD^+.

Sample preparation. A known amount of butter was extracted several times with hot water (60° C). The filtered aqueous extract was made up to 100 ml. A (1 + 9) dilution with buffer was injected into the flow-injection systems with immobilized L- or D-lactate dehydrogenase, with peaks produced by NAD^+ injection. Correspondingly beef cubes were extracted and analyzed for L-glutamate. For the ethanol determination in non-alcoholic beer, 1-ml samples were diluted with 9 ml (diet beer 99 ml) of buffer, pH 8.0, and NAD^+ was injected as before. The incubation medium for L-leucine formation from *N*-acetyl-D,L-leucine was 0.5 ml of a 5 mM substrate solution in 0.2 M phosphate buffer, pH 8.0. The reaction was started by addition of 0.2 mg of aminoacylase. From the medium incubated at 25°C, a sample of

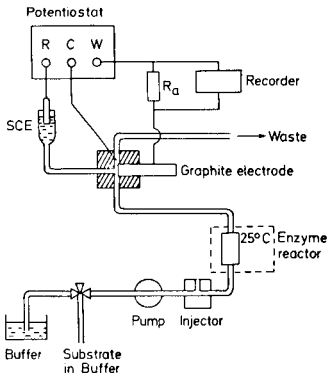

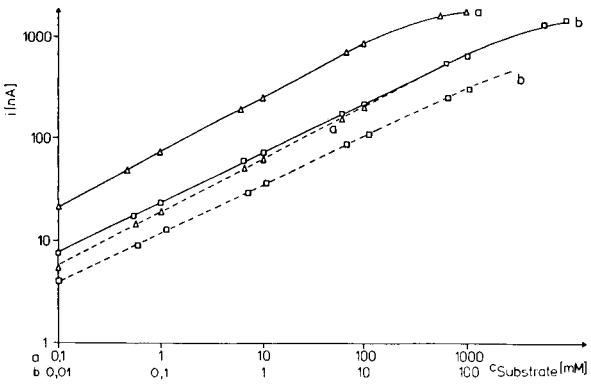

Fig. 1. Flow-injection system for the determination of dehydrogenase substrates (enzyme reactor and three-electrode device on enlarged scale). The enzyme reactor is a glass tube (i.d. 3.8 mm, variable length); the three-electrode sensor is a 3-cm long plexiglass cube. R reference, C counter, W working electrode, R_a external resistance.

Fig. 2. Calibration graph: (—) L-lactate; (- - -) D-lactate. Injected solution: (△) 50 µl of substrate solution into 1 mM NAD^+ in buffer (range a); (□) 50 µl of 10 mM NAD^+ into 0.01—500 mM substrate in buffer (range b).

50 µl was injected every 6 min into a flow of 1 mM NAD^+ in buffer passing through a L-leucine dehydrogenase reactor. All reference analyses were done by standard spectrophotometric methods.

Results and discussion

Figure 2 presents two typical log—log calibration graphs for D- and L-lactate. Depending on the injected material (NAD^+ or substrate), different concentration ranges could be covered; in general, more sensitive ranges were obtained with NAD^+ injection. The graphs were linear over at least one concentration decade, and their slopes are determined by the reaction order of the particular reverse dehydrogenase reaction. As will be shown in a later paper, the slopes for substrates of reversible bimolecular reactions with small equilibrium constants are theoretically 26.7°; for substrates with large equilibrium constants and for irreversible reactions the slopes are 45°. As shown in Table 1 these calculated slopes are observed in most cases, which indicates the excellent reliability of the enzyme reactors. The response times (time elapsed between injection and maximum response) are between 0.5 and 1 min.

These calibration graphs were used in quantifying L- and D-lactate in butter, L-glutamate in beef cubes, and ethanol in beer (Table 2). There is good agreement between the results obtained by the bioelectrochemical method and the spectrophotometric procedure. For L-lactate, the relative standard deviation for 9 results was 1.2%, and the correlation coefficient

TABLE 1

Calibration and stability of flow-injection systems with Eupergit-immobilized dehydrogenases (50-mg reactor; flow rate 0.5 ml min^{-1})

Immobilized dehydrogenase	Substrate injection		NAD^+ injection		Half-life stability[a] (days)
	Slope [°]	Linear range [mM]	Slope [°]	Linear range [mM]	
L-Lactate	27.2	0.1—150	26.0	0.01—10	>150
D-Lactate	27.2	0.1—150	26.5	0.01—10	>150
L-Isocitrate	45.0	0.1—1	45.0	0.01—10	n.d.[b]
Alcohol	28.5	1—1000	26.5	0.01—10	55
L-Malate	28.0	1—500	26.0	0.1—100	60
Formate	45.0	1—100	45.0	10—100	50
β-D-Glucose	45.0	0.1—10	45.0	0.01—1	n.d.[b]
L-Alanine	45.0	0.1—1	45.0	0.01—0.1	60
L-Glutamate	45.0	0.1—10	45.0	0.01—1	73
L-Leucine	45.0	0.1—1	45.0	0.01—0.1	>150

[a]Defined as the time for the sensitivity of the system (maximum current for a given substrate concentration) to decrease to half of its initial value under the working conditions. [b]n.d. = not determined.

TABLE 2

Dehydrogenase substrates in food determined by the electro-enzymatic flow-injection system (f.i.a.) and by spectrophotometry (spect.)

L-Lactate in butter (mg l^{-1})		D-Lactate in butter (mg l^{-1})		L-Glutamate in beef cubes (g l^{-1})		Ethanol in beer (g l^{-1})	
F.i.a.	Spect.[a]	F.i.a.	Spect.[a]	F.i.a.	Spect.[a]	F.i.a.	Spect.[a]
66.9	66.3	28.5	28.7	0.470	0.466	0.218[b]	0.212
69.6	69.9	27.1	27.8	0.433	0.433	0.222[b]	0.219
72.9	72.4	32.8	32.3	0.444	0.446	4.09[c]	4.08
81.2	82.0	30.8	30.2	0.465	0.466	4.11[c]	4.09
87.7	88.9	0.68	0.65	0.449	0.449		
73.8	71.9	1.00	1.10	0.454	0.459		
87.5	85.2	30.6	30.2	0.441	0.439		
77.0	78.7	1.06	1.00	0.468	0.466		
75.4	74.9	0.86	0.97	0.446	0.449		
82.3	84.6			0.438	0.439		
59.1	58.7			0.471	0.459		
				0.449	0.446		

[a]Determination in other laboratories; Profs. Drawert and Klostermeyer are thanked for their kind support. [b]Non-alcoholic beer. [c]Diet beer.

(r) between the results of the two methods was 0.999. For L-glutamate in beef cubes, r = 0.989. Thus the reliability of the proposed method is well established. Its sensitivity is 10—50 fold higher than that of the spectrophotometric procedure. Therefore, f.i.a. with bioelectrochemical detection

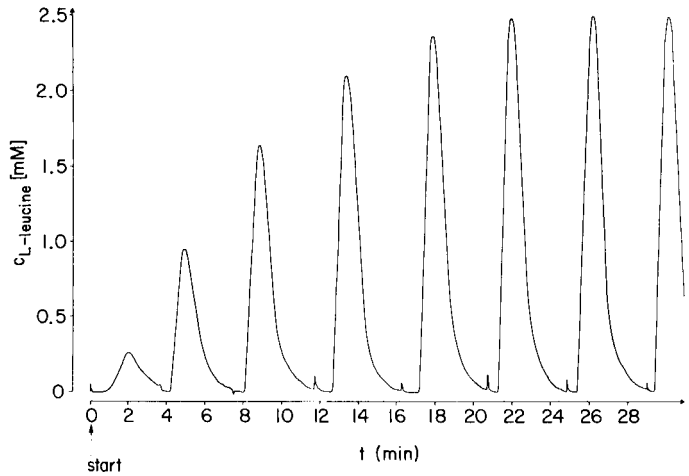

Fig. 3. Application of a flow-injection system for monitoring an enzymatic process. Formation of L-leucine during incubation of *N*-acetyl-D,L-leucine with aminoacylase. The concentration as a function of time is monitored by the injection of 50-μl samples of the medium (5 mM *N*-acetyl-D,L-leucine and 0.4 mg ml^{-1} aminoacylase) into a system containing L-leucine dehydrogenase, while 1 mM NAD^+ is pumped at 1 ml min^{-1}.

of dehydrogenase substrates should be very well suited to automated analysis for process control.

Figure 3 demonstrates such an application. The industrial production of L-amino acids is often based on the enzymatic hydrolysis of the L-isomer in the racemate of the *N*-acetyl derivatives [10]. This procedure was simulated for the production of L-leucine, and the monitoring was done by a flow-injection system based on L-leucine dehydrogenase. The increase in the peak heights reflects directly the rate of L-leucine formation. The final value attained after 25 min exactly corresponds to the total hydrolysis of the L-isomer.

We thank Mr. J. Danzer for skillful experimental help. This work was supported by a grant of the Bundesministerium für Forschung und Technologie, Projektträger Biotechnologie.

REFERENCES

1 B. Olsson and L. Ögren, Anal. Chim. Acta, 145 (1983) 87.
2 P. J. Worsfold, Anal. Chim. Acta, 145 (1983) 117.
3 A. Schelter-Graf, H. Huck and H.-L. Schmidt, Z. Lebensm. Unters. Forsch., 177 (1983) 356.
4 T. Yao, Y. Kobayashi and S. Musha, Anal. Chim. Acta, 139 (1982) 363.
5 T. Yao, Y. Kobayashi and S. Musha, Anal. Chim. Acta, 138 (1982) 81.
6 H. Huck, A. Schelter-Graf, J. Danzer, P. Kirch and H.-L. Schmidt, Analyst (London), 109 (1984) 147.
7 J. Růžička and E. Hansen, Anal. Chim. Acta, 78 (1975) 145.
8 K. K. Stewart, Anal. Chem., 55 (1983) 931.
9 H. Huck, Fresenius Z. Anal. Chem., 313 (1982) 548.
10 Y. Izumi, J. Chibata and T. Itoh, Angew. Chem., 90 (1978) 187.

Analytica Chimica Acta, 163 (1984) 305—308
Elsevier Science Publishers B.V., Amsterdam — Printed in The Netherlands

Short Communication

CONDUCTIMETRIC MEASUREMENTS OF ENZYME ACTIVITIES

C. BALLOT, B. SAIZONOU-MANIKA, C. MEALET, G. FAVRE-BONVIN and J. M. WALLACH*

Laboratoire de Biochimie Analytique, Université Lyon I, 69622 Villeurbanne Cedex (France)

(Received 2nd April 1984)

Summary. Some new developments of conductimetry are described for measurements of enzyme activities. For pancreatic elastase, conductance measurements in the microgram range are sensitive and reproducible and give a good picture of elastolytic activity within 30 min. For lipases, conductimetry can be used with either triacetin or triolein as the substrate. Lipase assays are possible in duodenal fluid or serum. Improvements in apparatus allow urea assay in the nanomolar range.

Conductimetry was little applied in enzyme kinetics before 1971, when the hydrolysis of urea by urease was studied [1]. Since then, it has been shown that other enzymatic reactions are accompanied by conductivity changes, allowing measurements of both metabolite concentrations and enzymatic activities, especially of hydrolases [2—6]. The principle of such measurements is simple: when the enzyme is added to the conductimetric cell, if the enzymatic reaction occurs with changes in charge distribution, then conductivity changes can be correlated with enzymatic reaction rate. Such measurements can be done with either a high-precision bridge or a conductimeter, provided with alternating current to avoid electrode polarization.

In recent years, this technique has been improved to increase its sensitivity. The present communication describes the most recent results concerning elastase, lipase and urease.

Experimental

Equipment. Conductivity is measured in a 4-ml thermostatted cell, the design of which provides increased sensitivity and liquid circulation [6]; it is now commercially available (Solea-Tacussel, Villeurbanne, France). The cell is connected to a CD-810 conductimeter (Solea-Tacussel) and conductance changes are recorded with a Kipp and Zonen BD40 recorder. Temperature is 30 ± 0.1°C, variations being kept under 0.02°C during a complete kinetic recording with a Lauda thermostat S-15/22 with a PTR-Regler R-20/2.

Procedure. In a typical experiment, the conductivity cell is filled with 4 ml of substrate solution. After thermal equilibrium, a small volume of enzyme is added from a concentrated stock solution. The enzyme activity

0003-2670/84/$03.00

can be calculated from the total conductance variation if the reaction is complete. If the reaction rate is too low, the curve may be standardized, as previously described [4]. Whichever way is used, the changes of conductance with time dG/dt can be correlated with the enzymatic reaction rate.

Chemicals. Pancreatic elastase (E.C. 3.4.21.11) was type II, chromatographically purified and lyophilized (95 U mg^{-1}; Sigma). Lipase was from *Pseudomonas* (E.C. 3.1.1.34; Amano, Japan). Both gave a single band when subjected to SDS polyacrylamid gel electrophoresis at pH 8.8, as described by Hardison and Chalkley [7]. Urease (E.C. 3.5.1.5) was from jack beans (Type VI; Sigma). Enzyme solutions were prepared in the buffer corresponding to their assay. Stock solutions were kept frozen at −20°C.

All other products (substrates, salts, buffers) were of analytical grade and were prepared according to the cited papers. Turbidimetric assay of lipase was done with a standard kit (Boehringer).

Results and discussion

Elastase activity. Well-known methods based on synthetic substrates such as *N*-succinyl-tri(alanine)-*p*-nitranilide [8] are accurate, but do not measure proteolytic activity. Elastase assays in the nanogram range need labelled-elastin [9]. The earlier conductimetric method for elastase activity measurements was useful in the 8—50-μg range, when native insoluble elastin was used [4]. The above-mentioned technical improvements allow measurements in the 0—2-μg range. The relationship between initial rate and elastase is linear; the relevant equation is v (10^{-5} H^+ l^{-1} min^{-1}) = 0.097 x (μg) + 0.015 (with r = 0.995 for n = 10). A reproducibility test with 1 μg of elastase in the cell gave a relative standard deviation of 7.5% (n = 5).

The most important advantage of this method is that it is done within 30 min, corresponding to the initial rate of elastolysis; indeed, because of longer incubation times, some other assays based on elastin as substrate give artificially high values, as non-specific proteolysis may occur after the initial steps of elastolysis [10]. This is particularly important when crude extracts are assayed.

Lipase activity. Lipase assays are usually done by nephelometry (or turbidimetry) [11] or by potentiometry (pH-stat) [12]. The conductimetric method avoids some of the drawbacks of these techniques and was used previously with triacetin as the substrate [6].

When a clear triolein solution prepared as described by Peled and Krenz [13] was used, similar results were obtained. The initial conductivity change, measured within 1 min, could be converted in terms of hydrolysis rate. Figure 1 shows the results obtained with three different bacterial lipases. Measurements in the unit range of enzyme activity are thus possible. This method was recently applied for lipase assay in duodenal fluid [14]. Improvements were needed to permit serum lipase assay. When a reconstituted substrate (Boehringer) was used, lipase activities of less than 0.1 U could be measured. When the results obtained for a control serum (520 U l^{-1}) were

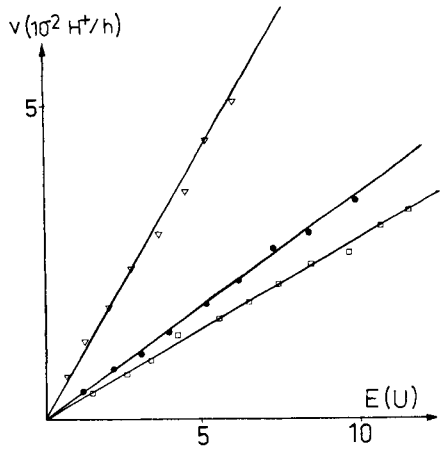

Fig. 1. Initial rate of triolein hydrolysis by three bacterial lipases using conductimetry: (▽) *Pseudomonas* lipase; (•) *Chromobacterium viscosum* lipase; (□) *Candida cylindracea* lipase. Triolein (2.6 mM) was prepared [13] in Tris—HCl buffer (5 mM, pH 8.0); T = 30°C.

compared with those by the classical turbidimetric method (Table 1), there was good correlation between both methods, the equation being Y(turb.) = 2.73 X(cond.) + 0.42 with r = 0.975. It can therefore be concluded that a conductimetric assay of serum lipase is viable.

Urease activity. The urea-urease reaction was the first enzymatic reaction to be studied fully by conductimetry [1], allowing a serum urea assay. An automatic device based on this principle is available (Beckman-BUN apparatus). The modified device outlined above makes lower urea concentrations measurable. Table 2 lists the overall conductance changes obtained for amounts of urea ranging from 0 to 0.5 nmol in the conductimetric cell. These values give a linear relationship: G (nS) = 37.8 X (nmol) + 0.05 with r = 0.998.

The K_m value for urea is relatively high under the experimental conditions used (about 10 mM): thus, if urea is added in excess, low urease activities can be measured. This method should therefore be of interest, for example, in the measurement of urease activities in soils and sands [15].

TABLE 1

Comparison of conductimetric (μS h^{-1}) and turbidimetric methods (10^{-3} absorbance min^{-1}), for different amounts of lipase units present in the cell[a]

Lipase present (10^{-3} U)	23	28	38	47	56	65	75	85
Conductimetry (μS h^{-1})	3.2	5.1	5.9	6.4	8.5	9.7	10.6	12.8
Turbidimetry (10^{-3} A min^{-1})	9.3	12.2	16.0	18.3	28.1	26.0	29.8	33.8

[a]Commercial triolein solution (0.3 mM; Boehringer) was hydrolysed by 0—0.2 units of a standard pancreatic lipase solution (940 U l^{-1}) prepared in Tris—HCl buffer (5 mM, pH 8.0).

TABLE 2

Overall conductivity changes for different amounts of urea in the conductivity cell[a]

Urea (nmol)	0.125	0.25	0.375	0.50
ΔG (nS)	5.0	9.0	14.6	18.9

[a]For each experiment, 6.25 U of urease was added to the 4-ml cell (0.1 mM Tris buffer, pH 7.5; T = 30°C). The four dilutions of urea were prepared in concentrated solutions, 10 μl being added for each dilution.

To conclude, conductimetry appears to be a competitive alternative technique because of its sensitivity and because it can be used even when solutions are turbid or coloured, which limits conventional spectrophotometry. The only drawback of the method is that a specific procedure is required for each assay (very frequently different from more classical techniques, especially in terms of physicochemical conditions). Furthermore, the method is restricted to low ionic strength media, because the sensitivity is defined by the experimental $\Delta G/G$ ratio. The higher the conductance, the higher will be the detectable ΔG variation. To solve this problem, further technical improvements are necessary to decrease $\Delta G/G$, and to improve the thermostatting to increase the signal-to-noise ratio.

REFERENCES

1 M. Hanss and A. Rey, Biochim. Biophys. Acta, 227 (1971) 630.
2 M. Hanss and A. Rey, Biochim. Biophys. Acta, 227 (1971) 618.
3 A. J. Lawrence and G. R. Moores, Eur. J. Biochem., 24 (1972) 538.
4 H. Bakala, J. Wallach and M. Hanss, Biochimie, 60 (1978) 1205.
5 C. R. Hill and G. Tomalin, Anal. Biochem., 120 (1982) 165.
6 C. Ballot, G. Favre-Bonvin and J. M. Wallach, Anal. Lett., 15 (1982) 1119.
7 R. Hardison and R. Chalkley, in G. Stein (Ed.), Methods in Cell Biology, Vol. XVII, Academic Press, New York, 1978, p. 235.
8 J. Bieth, B. Spiess and G. C. Wermuth, Biochem. Med., 11 (1974) 350.
9 S. Takahashi, S. Seifter and F. C. Yang, Biochim. Biophys. Acta, 327 (1973) 138.
10 G. Gnosspelius, Anal. Biochem., 81 (1977) B15.
11 L. Zinterhofer, S. Wardlaw, P. Jatlow and D. Seligson, Clin. Chim. Acta, 44 (1973) 173.
12 P. Desnuelle, M. J. Constantin and J. Baldy, Bull. Soc. Chim. Biol., 37 (1955) 285.
13 N. Peled and M. C. Krenz, Anal. Biochem., 112 (1981) 219.
14 C. Ballot, G. Favre-Bonvin and J. M. Wallach, Clin. Chim. Acta, (1984) in press.
15 U. Skiba and M. Wainwright, Enzyme Microb. Technol., 4 (1982) 310.

Analytica Chimica Acta, 163 (1984) 309—313
Elsevier Science Publishers B.V., Amsterdam — Printed in The Netherlands

Short Communication

OXYGEN ELECTRODE-BASED ENZYME IMMUNOASSAY FOR THE AMPEROMETRIC DETERMINATION OF HEPATITIS B SURFACE ANTIGEN

JEAN-LOUIS BOITIEUX and DANIEL THOMAS*

Laboratoire de Technologie Enzymatique, Université de Technologie de Compiegne B.P. 233, 60206 Compiegne Cedex (France)

GÉRARD DESMET

Laboratoire d'Hormonologie, Centre Hospitalier Sud, B.P. 3009, 80030 Amiens Cedex (France)

(Received 29th March 1984)

Summary. Specific antibodies labelled with glucose oxidase are immobilized onto a gelatin membrane, which is fixed over an oxygen electrode. The sensor is immersed in a standard glucose solution and a signal is obtained by measuring the consumption of oxygen by the enzyme catalyzed reaction. The response increases linearly with increasing antigen concentration over the range 0.1—100 $\mu g\ l^{-1}$. A microcomputer is used for data acquisition and processing.

Numerous methods are available for the accurate determination of traces of antigens and haptens in biological fluids. Radioimmunoassay and enzyme immunoassay (e.i.a.) are the most sensitive. Since the introduction of immunosorbents, many solid-phase techniques aimed at obtaining optimum results with enzyme-linked immunosorbent assays (e.l.i.s.a.) have been extensively described [1, 2]. Recently, however, protein membranes have been used for the immobilization of enzymes [3]. The binding of immunoglobulins onto gelatin membranes has been described [4] and an enzyme immunoassay technique has been introduced for the determination of hepatitis B surface antigen (HB_sA_g) in biological fluids [5].

In this communication, the use of glucose oxidase as the enzyme label is reported; the labelled antibody is bound to a protein membrane. The advantages of the glucose oxidase label have recently been demonstrated [6]. The purpose of this work is to study the possibilities of automation of this type of antigen estimation by using a semi-continuous flow mode, and processing the signals with the aid of a microcomputer. The active membrane is fixed over a modified oxygen electrode, designed in this laboratory. The oxygen consumption of the enzyme catalyzed reaction is measured when the electrode is in contact with a standard glucose solution. The signal from the electrode is directly proportional to the oxygen consumption and to the antigen concentration.

0003-2670/84/$03.00

Experimental

Chemicals. Glucose oxidase (E.C.1.1.3.4.; Type II, 18400 U g^{-1}; Sigma) and pig skin gelatin (Rousselot Laboratory, 60400 Ribécourt, France) were used. Glutaraldehyde and other chemicals used were of analytical grade (Merck).

For the determination of HB_sA_g, a panel of the reference center for virus hepatitis at the Institute of Hygiene, Göttingen University, was used by courtesy of Dr. Gerlich.

Hepatitis B surface antigen (HB_sA_g) was isolated and purified from human positive sera by a simple method described elsewhere [7]. Anti-HB_sA_g antibodies were prepared and purified by preparative electrophoresis followed by chromatography on DEAE cellulose [5].

Equipment. Amperometric measurements were done with an oxygen analyzer. The microcomputer was an Apple II+ computer with 48K of main memory. The interface card cage was constructed in the Electronics Department, University of Technology of Compiegne.

The measurement cell (Fig. 1) was designed in this laboratory. The internal peripheral bus of the computer enabled a variety of peripheral units to be added. A disc controller card and parallel interface cards (Apple) were added for the printer and interface card cage. The interface card cage was mounted on the computer through a ribbon cable and contained circuit boards for signal conditioning and buffering, and analog-to-digital card based upon the Datel ADC (EK-12B) an oxygen analyzer and a 4-bit logic system.

The flow system used for the measurements is shown in Fig. 2.

Preparation of the glucose oxidase—antibody conjugate. Glucose oxidase (ex. *Aspergillus niger*) was conjugated to specific antibodies by use of glutaraldehyde [8]. Further fractionation on Sephadex G200 equilibrated with 0.01 mol l^{-1} phosphate buffer, pH 6.8, was used to eliminate the free enzyme. The fractions of the first peak were pooled and distributed in sterile 0.2-ml aliquots. This solution could be stored at 4°C for several months without significant loss in activity.

Immobilization of antibodies on pig skin gelatin. The general procedure used to prepare an active membrane and to fix the specific antibodies has

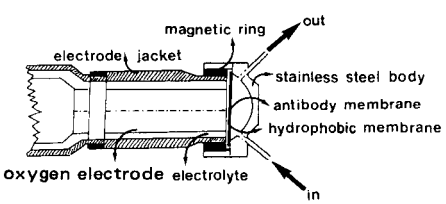

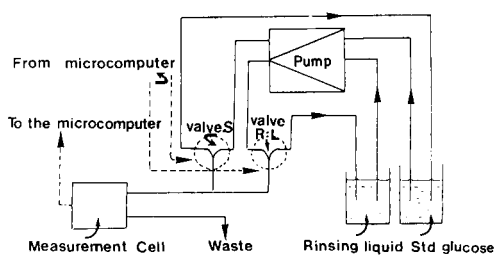

Fig. 1. Cross-section of the immunosensor electrode and measuring cell.

Fig. 2. Flow system used for the antigen determination.

been described previously [4]. Antibodies were immobilized on discs (10 mm diameter, ≈0.2 mm thick) cut from the activated membranes. The discs were immersed in a 30 g l^{-1} bovine serum albumin solution for 1 h and thoroughly washed in distilled water. These antibody-coated discs could be stored at −4° C in 0.02 mol l^{-1} phosphate buffer, pH 6.8, or in the presence of 1 g l^{-1} of gentamicin solution at 4° C.

Procedure for the determination of HB_sA_g. The gelatin membrane was immersed for 30 min in 0.5 ml of diluted (1:1000) HB_sA_g positive serum, immobilized antibodies G being in excess with respect to the antigen. The membrane was then thoroughly washed. The active membrane was incubated for 1 h in 1 ml of a solution of conjugate (1:200 in 0.01 mol l^{-1} phosphate buffer, pH 6.8) as in the "sandwich" method [9]. The membrane was washed with 0.01 mol l^{-1} sodium phosphate buffer pH 6.8 and fixed on the hydrophobic selective gas membrane of an oxygen sensor by a magnetic device, as shown in Fig. 1. The measuring cell was filled with standard glucose solution. Consumption of oxygen was measured by the oxygen sensor. It was proportional to the enzyme activity retained on the membrane and therefore to the HB_sA_g concentration.

Signal processing. In the direct measurement mode, the program starts by asking for a time interval for the collection or sampling of data. Next, it runs an accuracy test before plotting the data points. This test is done on the 20 data points (N = 20, Fig. 3). If $S(t_i)$ (with i = 0, . . ., N) are the measured values, the accuracy test is operated through $S(t_i) - S(t_0) = P_i$ for each sampled point. It checks that $P_i = P_i - 1$. The program calculates the value D which is the concentration to be determined, i.e., $D = P_i$ for $i = N$ (when $P_i = P_i - 1$); t_i (the interval between two data points) is obviously an important parameter.

A machine language subroutine was written for data acquisition from the ADC. The rest of the software was implemented in Basic in the usual way.

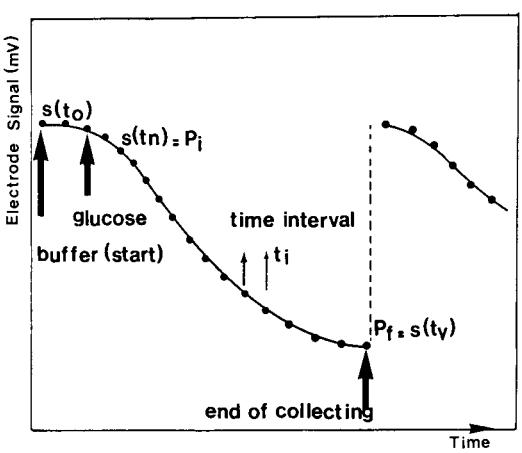

Fig. 3. Outline of data acquisition.

Results and discussion

The effects of experimental conditions on the detection of glucose oxidase activity were first established. A preliminary report [10] has shown that the coupling of glucose oxidase with antibodies does not affect significantly the Michaelis constant. The stability of glucose oxidase after coupling to the antibodies allowed a good reproducibility of the HB_sA_g measurement to be achieved. The stoichiometry of the enzyme reaction has been studied, using the computerized enzyme electrode system for glucose determination in blood and serum [11, 12]. The binding capacity and selectivity of the membrane were also considered. A pig-skin gelatin membrane was chosen for linking the antibodies. Previous work based on electron microscopy studies of artificial protein membranes [4] showed the homogeneity of the pig-skin gelatin membrane, which has a uniform thickness, a glossy surface and a regular network.

The calibration graph of signal vs. log HB_sA_g concentration was linear over the range 0.1—100 $\mu g\ l^{-1}$. The precision at various concentrations are shown in Table 1. The between-assay relative standard deviation was 7--12%. The average recovery of known amounts of HB_sA_g added to a serum pool was 95%. An unknown sample of HB_sA_g positive serum was analyzed by the present procedure and by radio-immunoassay with good agreement. These results are encouraging because the limit of detection of a classical enzyme immunoassay is about 2.4 $\mu g\ l^{-1}$ [13], and radio-immunoassay has a limit of 3—4 $\mu g\ l^{-1}$ [14].

The enzyme immunosensor depends on the immunochemical reaction for its selectivity, because an antibody binds to its corresponding antigen. Accordingly, the antibodies used are highly selective for HB_sA_g but are not completely specific.

This computerized enzyme immunosensor allowed 30 sample measurements per hour including the washing step between samples, sampling and oxygen measurement. The volume of the sample for each measurement was ca. 50 μl. The stability of the active membrane when stored at 4° C is very good (not more than 20% loss of initial activity after six months) so that the calibration graph can be reproduced easily with the original membrane.

TABLE 1

Precision of the method (10 measurements with the same membrane)

HB_sA_g taken ($\mu g\ l^{-1}$)	1.00	10.0	100
Mean found ($\mu g\ l^{-1}$)	1.01	9.6	94
S.d.[a]	0.04	0.2	3
R.s.d.	4	2	3

[a]Standard deviation ($\mu g\ l^{-1}$) and relative standard deviation (%).

In conclusion, the computerized continuous flow system described for HB_sA_g measurements can be used for quantitative immunological reactions. This technology has also been tested for the estimation of the hormone 17-β-oestradiol; a competitive enzyme-linked immunoassay was used. The first tests with standard oestradiol solutions gave satisfactory results at levels of a few pmol l^{-1} and above.

REFERENCES

1 E. Engvall and P. Perlmann, Immunochem., 8 (1971) 871.
2 A. H. W. M. Schuurs and B. K. van Weemen, Clin. Chim. Acta, 81 (1977) 1.
3 D. Thomas, in D. Thomas and J. P. Kernevez (Eds.), Analysis and Control of Immobilized Enzyme Systems, Elsevier North-Holland, 1976, p. 115.
4 J. L. Boitieux, G. Desmet and D. Thomas, FEBS Lett., 93 (1978) 133.
5 J. L. Boitieux, G. Desmet and D. Thomas, Clin. Chim. Acta, 88 (1978) 329.
6 R. B. Johnson, R. M. Libby and R. M. Nakamura, J. Immunoassay, 1 (1980) 27.
7 G. Desmet and J. L. Boitieux, Clin. Chim. Acta, 74 (1977) 59.
8 S. Avrameas and T. Ternynck, Immunochemistry, 8 (1971) 1175.
9 L. Wide, Acta Endocrinol., 142 (1970) 207.
10 J. L. Boitieux, J. L. Rometle, N. Aubry and D. Thomas, Clin. Chim. Acta, 136 (1984) 19.
11 J. L. Rommette, B. Froment and D. Thomas, Clin. Chim. Acta, 95 (1979) 249.
12 J. P. Kernevez, L. Konate and J. L. Romette, Biotechnol. Bioeng., (1982) in press.
13 G. Walters, L. Kuijpens, J. Kaccki and A. Schuurs, J. Clin. Pathol., 28 (1976) 873.
14 W. Gerlich, B. Stamm and R. Thomssen, J. Biol. Stand., 4 (1976) 189.

Analytica Chimica Acta, 163 (1984) 315—322
Elsevier Science Publishers B.V., Amsterdam — Printed in The Netherlands

Short Communication

USE OF NUCLEAR MAGNETIC RESONANCE AND GAS—LIQUID CHROMATOGRAPHY FOR THE STUDY OF MICROBIAL NITRILE-HYDRATASES AND AMIDASES

K. BUI, H. FRADET, A. THIÉRY, M. MAESTRACCI, A. ARNAUD* and P. GALZY

Chaire de Génétique et Microbiologie, Ecole Nationale Supérieure Agronomique, 9, Place Viala, 34060 Montpellier Cédex (France)

(Received 29th March 1984)

Summary. Some microbial strains can hydrolyse many nitriles to the corresponding organic acids by means of two enzymes: a nitrile-hydratase which hydrates the nitrile to the corresponding amide, and an amidase which hydrolyses the amide to the corresponding acid. Two methods are proposed for the assay of the enzymatic activities: proton magnetic resonance spectrometry (n.m.r.) and gas—liquid chromatography (g.l.c.). For the assay of these enzymatic activities (nitrile-hydratase and amidase), g.l.c. was better, because it was more precise and much more sensitive than the n.m.r. method. The examples of acetonitrile and acetamide are described in detail.

Some bacterial strains can hydrolyse different nitriles to the corresponding acids by the successive action of two enzymes: a nitrile-hydratase which hydrates the nitrile to the corresponding amide, and an amidase which hydrolyses this amide to the corresponding acid [1—3]. Studies of these reactions have been difficult because of the lack of simple methods for monitoring the disappearance of the substrates or the appearance of the reaction products. The detection of these activities has been based mainly on the assay of evolved ammonia [4—10]. Most methods used to monitor the hydrolysis of nitriles and amides are delicate and discontinuous [4—13], and interferences by proteins sometimes exclude the use of unpurified acellular bacterial preparations. Simple methods for the continuous assay of nitriles and amides based on g.l.c. and n.m.r. techniques were therefore needed.

Digeronimo and Antoine [14] have studied a *Nocardia* and Mimura et al. [15] have studied a *Corynebacterium* by using a g.l.c. procedure to monitor the metabolism of acetonitrile and propionitrile. Gas chromatography has also been used as a discontinuous method in two particular studies: the hydrolysis of naphthyl acetate by an esterase from beef liver [16] and the reduction of acetylene to ethylene by a nitrogenase from different organisms [17, 18]. Nuclear magnetic resonance has often been used for the investigation of biological systems, in particular for the observation of intermediary compounds in biochemical reactions [19, 20]. The technique has been used for the study of only a few enzyme reactions: deuteration of α-aminoacids

0003-2670/84/$03.00

by glutamine pyruvate transaminase [21], formation of α-lipoate or lipoamide from dihydrolipoate or dihydrolipoamide in the presence of rhodanese [22], conversion of DL-histidine to histamine by a histidine decarboxylase [23], hydrolysis of tetrasaccharides by lysozyme [24] and hydrolysis of the t-butyl ester of L-phenylalanine by chymotrypsin [25]. The great advantage of the g.l.c. and n.m.r. methods over other usual techniques is that the appearance or disappearance of chemical compounds can be monitored almost continuously during the reaction.

The present communication describes the application of these techniques in the study of biological hydrolysis of nitriles and amides by demonstrating the reactions qualitatively and by evaluating the corresponding reaction kinetics.

Experimental

Biological material and culture. The wild type *Brevibacterium* sp. R-312 and its mutant strain A4 were used. These strains both possess the nitrile-hydratase activity, but only the R-312 strain shows amidase activity for a wide spectrum of substrates [26].

The two strains were grown on a minimum medium, the composition of which was described previously [27]. Ammonium sulfate (5 g l^{-1}) and glucose (10 g l^{-1}) were added to this minimum medium. The wide spectrum amidase of the wild strain being inducible, acetamide (5 g l^{-1}) was used as inducer and nitrogen source. The strains were maintained on YMPG agar slants, the composition of which was given by Jallageas et al. [28]. The cultures were done in Erlenmeyer flasks, filled to 10% of their volume. The flasks were incubated at 28° C and shaken (80 oscillations/min; amplitude 8 cm). The culture medium was inoculated with a preculture on the same medium.

Enzyme extraction. Cells were ground and enzymes were extracted as previously described [28]. The K_m value was determined by using the S_2 supernatant liquid resulting from centrifugation of ground cells at 180 000 *g* for 90 min.

Gas chromatography. For g.l.c., an Intersmat IGC-121-DFL apparatus was used with a flame-ionization detector. The peak areas were calculated by an Intersmat ICR-1B integrator/calculator. The nickel column used (50 cm long, 3 mm i.d.) was filled with Porapak Q (80—100 mesh). The gas flows were: air 400 ml min^{-1}, hydrogen 25 ml min^{-1}, nitrogen 30 ml min^{-1} (0.6 bar). The temperature conditions were: injector 250° C, detector 300° C, oven 150—240° C depending on the compound to be examined.

Nuclear magnetic resonance. Most compounds were detected with a Varian EM-360 spectrometer (probe temperature 30° C). Methacrylonitrile, acrylonitrile and their hydrolysis products were detected with a Varian HA-100 spectrometer. The external reference used for the determination of chemical shifts was a hexamethyldisiloxane (HMDS) solution.

Results and discussion

Detection of nitriles, amides and acids by n.m.r. and g.l.c. The determination of the nitrilase and amidase activities by n.m.r. was possible only when the chemical shifts of some protons of the substrates (nitriles or amides) were sufficiently different in order to give distinct peaks. The commonest water-soluble nitriles and their corresponding amide and acid mixtures were first examined by n.m.r. Table 1 indicates the values for the chemical shifts

TABLE 1

Chemical shifts for different nitriles, amides and acids[a]

Compound	Protons examined	δ (Hz)		
		Nitrile (X = CN)	Amide (X = $CONH_2$)	Acid (X = COOH)
CH_3-X	CH_3	72.5(s)[b]	70(s)	67.5(s)
CH_3-CH_2-X	CH_3	46.5(t)	42.5(t)	41.0(t)
$(CH_3)_2CH-X$	CH_3	48.5(d)	46.5(d)	44.5(d)
$(CH_3)_3C-X$	CH_3	51.5(s)	46.0(s)	43.5(s)
$CH_2=CH-X$	=CH—	6.10(q)	6.12(q)	5.88(q)
$CH_2=C(CH_3)-X$	CH_3	2.30(d)	2.21(s)	2.20(s)
	CH_2	6.24(d)	6.10(s)	6.08(s)
$CH_2(X)OH$	CH_2	144.0(s)	136.0(s)	131.5(s)
$CH_3-CH(X)OH$	CH_3	56.0(d)	54.0(d)	52.0(d)
$CH_3-C(CH_3)(X)OH$	CH_3	59.5(s)	53.0(s)	51.0(s)
$CH_2(X)NH_2$	CH_2	119.5(s)	122.0(s)	118.0(s)
$CH_3-CH(X)NH_2$	CH_3	53.5(d)	55.5(d)	55.5(d)
$CH_3-CH(X)NH-CHO$	CH_3	57.0(d)	55.5(d)	53.5(d)
$CH_3-CH(X)NH-CH_3$	CH_3-C	55.5(d)	52.75(d)	65.0(d)
$CH_3-C(CH_3)(X)NH_2$	CH_3	55.5(s)	59.0(s)	52.0(s)

[a]Aqueous solutions at pH 7.0; HMDS as external standard. [b]s, singlet; d, doublet; t, triplet; q, quadruplet.

of protons for the compounds, in an aqueous solution at pH 7.0, which could be differentiated by this technique. It can be seen that only a few nitriles and their hydrolysis products would be differentiated by n.m.r. However, these compounds belong to different chemical classes: aliphatic, α-ethylene, α-hydroxy, α-amino and *N*-substituted α-amino compounds. This could be used for the demonstration of nitrilase and amidase activities with a large range of substrates.

The g.l.c. technique was first used to test the commonest nitriles and their corresponding hydrolysis products. The organic acids could only be detected from acidic solutions, and different operational precautions were needed to avoid "ghost" peaks during identification and determinations of these acids [29]. The following compounds were detected by g.l.c. under the conditions described: acetonitrile, propionitrile, butyronitrile, isobutyronitrile, valeronitrile, isovaleronitrile, pivalonitrile, acrylonitrile, methacrylonitrile, crotononitrile, allyl cyanide, and their corresponding amides and acids. Other compounds would also be detected by the g.l.c. method: cyanamide, formamide, benzonitrile, *o*-, *m*-, *p*-tolunitriles, malonitrile, succinonitrile, adiponitrile, nicotinonitrile and isonicotinonitrile. Mixtures of nitriles and corresponding amides and acids were analyzed by g.l.c. In contrast to the n.m.r. method, it appeared that no nitrile interfered with the detection of its corresponding amide, and no amide interfered with the detection of its acid product. However, a nitrile and its corresponding acid often had very similar retention times.

Application of the two techniques to the study of the enzymatic hydrolysis of nitriles and amides. Except for propionitrile and acrylonitrile, and their corresponding amides, for which the peaks appeared as complex multiplets, the enzymatic hydrolyses of the nitriles and amides listed in Table 1 could be monitored continuously by the n.m.r. technique. The reaction was started by the addition of the enzyme extract (0.1 ml) to a mixture of 0.1 ml of nitrile solution (0.5 M) and 0.3 ml of buffer. The buffered nitrile solution in the n.m.r. tube was pre-incubated at 30°C. The reaction kinetics was monitored by recording the n.m.r. spectra at regular intervals. Examples of kinetics monitored with a Varian EM-360 apparatus are given in Fig. 1; shown are the hydrolyses of acetonitrile to acetamide, of acetamide to acetic acid, and of acetonitrile to acetamide and acetic acid by enzyme extracts of strain A4, R-312 and R-312, respectively. The peaks corresponding to the reaction products increased regularly with time. These spectra show that differentiation between substrate and reaction product would be obtained only for changes in chemical shifts of at least 2 Hz. One measurement every minute was viable. The percentage hydrolysis could be calculated from the ratios $h_b/(h_a + h_c)$, $h_c/(h_b + h_a)$ or $(h_b + h_c)/(h_a + h_b + h_c)$, depending on the reactions involved; h represents peak height and subscripts a, b and c refer to acetonitrile, acetamide and acetic acid, respectively (Fig. 1). Comparable results were obtained for the other nitriles and amides mentioned above.

The hydrolysis of nitriles results in basic or acidic compounds that are protonated as a function of pH. In consequence, the chemical shift of the

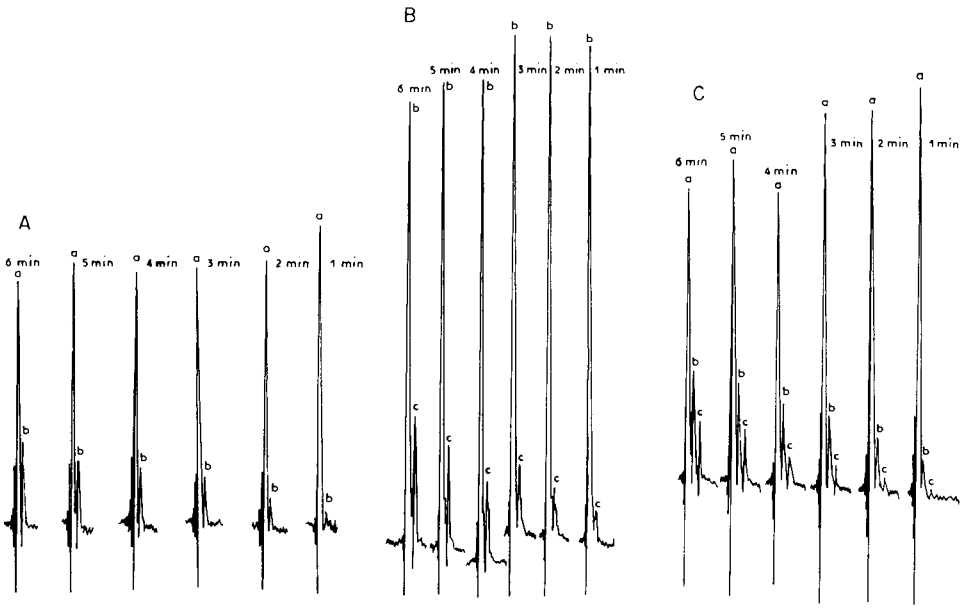

Fig. 1. Kinetics of hydrolysis of acetonitrile and acetamide monitored by n.m.r. (A) Acetonitrile to acetamide by strain A4; (B) acetamide to acetic acid by strain R-312; (C) acetonitrile to acetamide and acetic acid by strain R-312. Conditions: 30°C and pH 7.0 (phosphate buffer 0.1 M). Methyl peaks of acetonitrile (a), acetamide (b) and acetic acid (c) are marked. The reaction was monitored continuously by recording a spectrum every minute (1—6).

proton bordering amide and acid functions varies with pH and the resonance peaks of protons overlap at certain pH values. This is the case for methyl doublets of α-alanine and α-aminopropionamide at pH 7.5 and 8.0 and also for methyl singlets of acetamide and acetic acid at pH 3.0 and 4.0. In such cases, the reaction can be done in a buffered medium in a thermostated vessel from which samples are withdrawn every minute. The reaction is stopped by adding one drop of concentrated hydrochloric acid and the sample is subjected to n.m.r. after adjustment to the appropriate pH. Because the products may be formed in relatively high concentrations (0.1 M), the pH of the medium may vary, particularly for the hydrolysis of α-aminonitriles yielding α-aminoamides, α-amino acids and ammonia. Therefore, it is necessary to ensure that the ionic strength of the buffer used is sufficient to prevent variations in pH.

For monitoring by g.l.c., the enzyme reaction proceeded in a thermostated test tube containing the buffer and substrate mixture which was pre-incubated for 2—3 min. The reaction was started by the addition of the appropriately diluted enzyme extract. Aliquot portions of the reaction mixture were taken at regular intervals with a syringe and injected directly into the chromatograph. The hydrolysis percentage was calculated from the peak areas. Figure 2

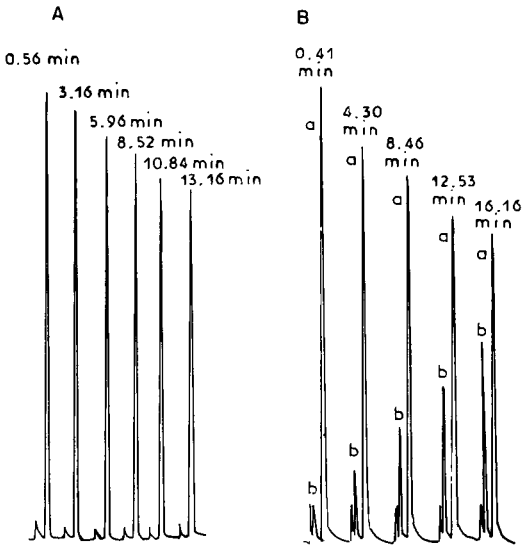

Fig. 2. Kinetics of hydrolysis monitored by g.l.c.: (A) acetonitrile; (B) acetamide. Conditions: 1.6 ml of 0.1 M phosphate buffer (pH 7.0), 0.4 ml of 0.01 M acetonitrile or acetamide, 0.5 ml of enzyme extract from *Brevibacterium* sp. A4 or R-312, respectively; 25°C; volume injected 2 μl. In B: (a) acetamide peak; (b) acetic acid peak.

shows chromatograms obtained during hydration of acetonitrile by an enzyme extract from strain A4 and during hydrolysis of acetamide by an enzyme extract from strain R-312. The hydrolysis rates of the nitriles and amides previously cited were readily measured by this method, and the K_m and V_{max} values of the nitrile-hydratase and the amidase of the *Brevibacterium* sp. were determined for different substrates [30, 31]. For these determinations, different concentrations of nitrile and amide substrates were hydrolysed with the same amount of enzyme extract. It was thus possible to calculate the rate of hydrolysis versus the initial substrate concentration and to evaluate the Michaelis constants (K_m) in the usual way.

The results obtained by the n.m.r. and g.l.c. methods for the hydrolysis of different substrate concentrations using the same enzyme extract were compared. Figure 3 shows, for acetonitrile, that the correlation between the n.m.r. and g.l.c. techniques is good.

In conclusion, these experiments showed that the n.m.r. and g.l.c. techniques can be used to demonstrate quickly the presence of nitrilase and amidase activity and to monitor the reaction kinetics. The n.m.r. technique can be applied in an almost continuous mode, and the enzymatic reactions can be checked at different temperatures by using an n.m.r. spectrometer equipped with a thermostat accessory. The g.l.c. measurements are discontinuous, and would be improved by using an automatic sampling and injection system and an appropriate internal standard. The n.m.r. technique could be

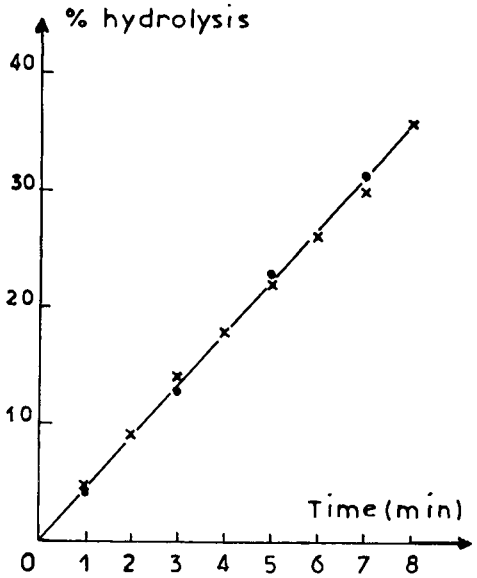

Fig. 3. Comparison of kinetics of enzymatic hydrolysis of acetonitrile as monitored by n.m.r. (×) and g.l.c. (•).

used only for a limited number of nitriles and amides, and the concentrations used were relatively high compared to those usually required for classical enzymatic analysis. The K_m values of nitrilases and amidases could not be determined by this method. Only the more sensitive g.l.c. could be used in quantitative studies of the nitrilase and amidase activities of the *Brevibacterium* sp. strains.

REFERENCES

1 A. Arnaud, P. Galzy and J. C. Jallageas, C.R. Acad. Sci. Ser. D., 287 (1976) 571.
2 A. Arnaud, P. Galzy and J. C. Jallageas, Rev. Ferment. Ind. Aliment., 31 (1976) 39.
3 A. Arnaud, P. Galzy and J. C. Jallageas, Folia Microbiol., 21 (1976) 178.
4 K. S. Thimann and S. Mahadevan, Arch. Biochem. Biophys., 105 (1964) 133.
5 W. G. Robinson and R. H. Hook, J. Biol. Chem., 239 (1964) 4257.
6 D. B. Harper, Biochem. J., 167 (1977) 685.
7 D. B. Harper, Biochem. J., 165 (1977) 309.
8 J. D. Findlater and B. A. Orsi, Anal. Chem., 58 (1974) 294.
9 Y. Z. Huang, Anal. Chem., 61 (1974) 464.
10 H. C. van Anken and M. E. Schiphorst, Clin. Chim. Acta, 56 (1974) 151.
11 A. Szewczuk, Chem. Anal., 4 (1959) 971.
12 R. B. Bruce, J. W. Howard and R. F. Hanzal, Anal. Chem., 27 (1955) 1346.
13 M. W. Scoggins and J. W. Miller, Anal. Chem., 47 (1975) 152.
14 M. J. Digeronimo and A. D. Antoine, Appl. Environ. Microbiol., 31 (1976) 900.
15 A. Mimura, T. Kawano and Y. Yamada, J. Ferment. Technol., 47 (1969) 631.
16 J. M. Navarro and E. S. Cornwell, J. Chromatogr., 138 (1977) 423.
17 R. H. Burris, Methods Enzymol., 24 (1972) 415.

18 W. D. P. Stewart, G. P. Fritzgerald and R. H. Burris, Proc. Nat. Acad. Sci. U.S., 58 (1967) 2071.
19 A. Kowalski and M. Cohn, Annu. Rev. Biochem., 33 (1964) 481.
20 J. Grimaldi, J. Baldo, C. MacMurray and B. D. Sykes, J. Am. Chem. Soc., 94 (1972) 7641.
21 U. M. Babu and R. B. Johnston, J. Biochem., 15 (1976) 5671.
22 U. M. Babu, R. B. Johnston and L. C. MacNeff, Anal. Biochem., 63 (1975) 208.
23 M. Silver, O. W. Howarth and D. P. Kelly, J. Gen. Microbiol., 97 (1976) 285.
24 H. L. Johnson, D. W. Thomas, M. Ellis, L. Carry and J. I. De Graw, J. Pharm. Sci., 66 (1977) 1660.
25 S. L. Patt, D. Dolphin and B. D. Sykes, Ann. N.Y. Acad. Sci., 222 (1973) 211.
26 J. C. Jallageas, A. Arnaud and P. Galzy, C.R. Acad. Sci. Paris. Ser. D., 288 (1979) 655.
27 M. P. Kiény-L'Homme, A. Arnaud and P. Galzy, J. Gen. Appl. Microbiol., 27 (1981) 307.
28 J. C. Jallageas, A. Arnaud and P. Galzy, J. Gen. Appl. Microbiol., 24 (1978) 103.
29 J. C. Du Preez and P. M. Lategan, J. Chromatogr., 124 (1976) 63.
30 K. Bui, H. Fradet, A. Arnaud and P. Galzy, J. Gen. Microbiol., 130 (1984) 89.
31 M. Maestracci, A. Thiéry, K. Bui, A. Arnaud and P. Galzy, Arch. Microbiol., 138 (1984) 315.

ANALYTICA CHIMICA ACTA, VOL. 163 (1984)

AUTHOR INDEX

Alaerts, G., see Motte, J. C. 275
Andersen, H. D., see Dinesen, B. 119
Arnaud, A., see Bui, K. 315
Arwin, H., see Welin, S. 263
Aston, W. J., see Turner, A. P. F. 161

Ballot, C.
—, Saizonou-Manika, B., Mealet, C., Favre-Bonvin, G. and Wallach, J. M.
Conductimetric measurements of enzyme activities 305
Becke, J. W., see Vorlop, K.-D. 287
Bell, J. M., see Turner, A. P. F. 161
Bellgardt, K.-H., see Schmidt, W. J. 101
Boitieux, J. L.
—, Thomas, D. and Desmet, G.
Oxygen electrode-based enzyme immunoassay for the amperometric determination of hepatitis B surface antigen 309
Boon, J. J.
—, Tom, A., Brandt, B., Eijkel, G. B., Kistemaker, P. G., Notten, F. J. W. and Mikx, F. H. M.
Mass spectrometric and factor discriminant analysis of complex organic matter from the bacterial culture environment of *Bacteroides gingivalis* 193
Bourne, J. R., see Heinzle, E. 219
Brakenhoff, G. J.
—, van der Voort, H. T. M. and Nanninga, N.
High-resolution confocal scanning light microscopy in biology 231
Brandt, B., see Boon, J. J. 193
Brink, L. E. S.
—, Tramper, J., Van't Riet, K. and Luyben, K. Ch. A. M.
Automation of an experimental system for the microbial epoxidation of propene and 1-butene 207
Bruins, A. P.
— and Pras, N.
Isolation of 3,4-dihydroxyphenylacetic acid produced from *p*-hydroxyphenylacetic acid by immobilized plant cells of *Mucuna pruriens* and its identification by liquid chromatography/mass spectrometry 91
Brunt, K.
Rapid determination of sulfide in waste waters by continuous flow analysis and gas diffusion and a potentiometric detector 293
Bui, K.
—, Fradet, H., Thiéry, A., Maestracci, M., Arnaud, A. and Galzy, P.
Use of nuclear magnetic resonance and gas–liquid chromatography for the study of microbial nitrile-hydratases and amidases 315

Cleland, N.
— and Enfors, S.-O.
Monitoring glucose consumption in *Escherichia coli* cultivation with an enzyme electrode 281
Colby, J., see Turner, A. P. F. 161

Danielsson, B., see Mandenius, C. F. 135
Danielsson, B., see Winquist, F. 143
Davis, G., see Turner, A. P. F. 161
Decristoforo, G.
— and Knauseder, F.
Rapid determination of cephalosporins with an immobilized enzyme reactor and sequential subtractive spectrophotometric detection in an automated flow-injection system 73
Decristoforo, G.
High-performance liquid chromatography of carbapenem antibiotics in complex biological samples with column switching and simultaneous multichannel ultraviolet monitoring 25
De Meyer, A., see Motte, J. C. 275
Desmet, G., see Boitieux, J. L. 309
Dinesen, B.
— and Andersen, H. D.
Monitoring the production of biosynthetic human growth hormone by micro enzyme-linked immunosorbent assay 119
Dissing, U.
—, Ling, T. G. I. and Mattiasson, B.
Monitoring of methanogenic processes

with an immobilized mixed culture in combination with a gas-flow meter 127
Dourte, P., see Motte, J. C. 275
Dunn, I. J., see Heinzle, E. 219
Dussap, C. G.
— and Gros, J. B.
Interpretation of static and dynamic responses of a dissolved oxygen electrode in viscous broths 151

Eijkel, G. B., see Boon, J. J. 193
Elwing, H., see Welin, S. 263
Enfors, S.-O., see Cleland, N. 281

Favre-Bonvin, G., see Ballot, C. 305
Fleischmann, Th., see Leidner, H. A. 35
Fradet, H., see Bui, K. 315

Galzy, P., see Bui, K. 315
Gebauer, A., see Scheper, T. 111
Gelleri, B.
— and Sernetz, M.
Fractal structure of gel porosity 17
Gibson, M.
—, Soper, C. J. and Parfitt, R. T.
Application of ^{13}C-n.m.r. spectroscopy to study the mechanism of *N*-demethylation of [*N*—Me—^{13}C] codeine by cell-free extracts of *Cunninghamella bainieri* 175
Gottschalk, D., see Körner, H. U. 55
Griot, M., see Heinzle, E. 219
Groneman, A. F.
—, Posthumus, M. A., Tuinstra, L. G. M. Th. and Tragg, W. A.
Identification and determination of metabolites in plant cell biotechnology by gas chromatography and gas chromatography/mass spectrometry. Application to nonpolar products of *Chrysanthemum cinerariaefolium* and *Tagetes* species 43
Gros, J. B., see Dussap, C. G. 151

Hamer, G., see Leidner, H. A. 35
Hampel, W.
— and Roehr, M.
Fermentation control with personal computers 269
Heinzle, E.
—, Moes, J., Griot, M., Kramer, H., Dunn, I. J. and Bourne, J. R.
On-line mass spectrometry in fermentation 219
Henshaw, B. G.
Application of a clinical analyser in biotechnology 257
Higgins, I. J., see Turner, A. P. F. 161
Hill, H. A. O., see Turner, A. P. F. 161
Hofman, M., see Motte, J. C. 275
Hofmann, J.
— and Sernetz, M.
Immobilized enzyme kinetics analyzed by flow-through microfluorimetry. Resorufin-β-D-galactopyranoside as a new fluorogenic substrate for β-galactosidase 67
Huck, H., see Schelter-Graf, A. 299

Kistemaker, P. G., see Boon, J. J. 193
Klein, J., see Vorlop, K.-D. 287
Knauseder, F., see Decristoforo, G. 73
Körner, H. U.
—, Gottschalk, D., Wiegel, J. and Puls, J.
The degradation pattern of oligomers and polymers from lignocelluloses 55
Kramer, H., see Heinzle, E. 219
Kroner, K. H.
— and Kula, M.-R.
On-line measurement of extracellular enzymes during fermentation by using membrane techniques 3
Kuhlmann, W., see Schmidt, W. J. 101
Kula, M.-R., see Kroner, K. H. 3

Lai, P.-H.
Technical improvements in protein microsequencing 243
Leidner, H. A.
—, Fleischmann, Th. and Hamer, G.
Molecular weight fractionation for the study of complex biodegradation processes 35
Ling, T. G. I., see Dissing, U. 127
Lundström, I., see Welin, S. 263
Lundström, I., see Winquist, F. 143
Luyben, K. Ch. A. M., see Brink, L. E. S. 207

Maestracci, M., see Bui, K. 315
Mandenius, C. F.
—, Danielsson, B. and Mattiasson, B.
Evaluation of a dialysis probe for continuous sampling in fermentors and in complex media 135
Mattiasson, B., see Dissing, U. 127
Mattiasson, B., see Mandenius, C. F. 135
Mealet, C., see Ballot, C. 305

Mechsner, Kl.
An automated nephelometric system for evaluation of the growth of bacterial cultures 85
Meyer, A. De., see Motte, J. C. 275
Meyer, H.-D., see Schmidt, W. J. 101
Mikx, F. H. M., see Boon, J. J. 193
Moes, J., see Heinzle, E. 219
Monseur, X., see Motte, J. C. 275
Motte, J. C.
—, Monseur, X., Termonia, M., Hofman, M., Alaerts, G., De Meyer, A., Dourte, P. and Walravens, J.
Computer monitoring of sugars, acids and volatile compounds in fermentations 275

Nanninga, N., see Brakenhoff, G. J. 231
Niehoff, A., see Scheper, T. 111
Notten, F. J. W., see Boon, J. J. 193
Nyeste, L., see Pungor Jr., E. 185

Parfitt, R. T., see Gibson, M. 175
Parfitt, R. T., see Sewell, G. J. 237
Pecs, M., see Pungor Jr., E. 185
Posthumus, M. A., see Groneman, A. F. 43
Pras, N., see Bruins, A. P. 91
Puls, J., see Körner, H. U. 55
Pungor Jr., E.
—, Pecs, M., Szigeti, L., Nyeste, L. and Szilagyi, J.
Mass spectrometric monitoring of 2-oxoglutaric acid in fermentation broth 185

Reuter, B. W., see Schneckenburger, H. 249
Riet, Van't, K., see Brink, L. E. S. 207
Roehr, M., see Hampel, W. 269

Saizonou-Manika, B., see Ballot, C. 305
Sauerbrei, A., see Scheper, T. 111
Schelter-Graf, A.
—, Schmidt, H.-L. and Huck, H.
Determination of the substrates of dehydrogenases in biological material in flow-injection systems with electrocatalytic NADH oxidation 299
Scheper, T.
—, Gebauer, A., Sauerbrei, A., Niehoff, A. and Schügerl, K.
Measurement of biological parameters during fermentation processes 111
Schmidt, H.-L., see Schelter-Graf, A. 299
Schmidt, W. J.
—, Meyer, H.-D., Schügerl, K., Kuhlmann, W. and Bellgardt, K.-H.
On-line analysis of fermentation media 101
Schneckenburger, H.
—, Reuter, B. W. and Schoberth, S. M.
Time-resolved fluorescence microscopy for measuring specific coenzymes in methanogenic bacteria 249
Schoberth, S. M., see Schneckenburger, H. 249
Schügerl, K., see Scheper, T. 111
Schügerl, K., see Schmidt, W. J. 101
Sernetz, M., see Gelleri, B. 17
Sernetz, M., see Hofmann, J. 67
Sewell, G. J.
—, Soper, C. J. and Parfitt, R. T.
Extraction and gas—liquid chromatography of microbial *N*-dealkylation systems 237
Soper, C. J., see Gibson, M. 175
Soper, C. J., see Sewell, G. J. 237
Spetz, A., see Winquist, F. 143
Stock, J., see Vorlop, K.-D. 287
Szigeti, L., see Pungor Jr., E. 185
Szilagyi, J., see Pungor Jr., E. 185

Termonia, M., see Motte, J. C. 275
Thiéry, A., see Bui, K. 315
Thomas, D., see Boitieux, J. L. 309
Tom, A., see Boon, J. J. 193
Tragg, W. A., see Groneman, A. F. 43
Tramper, J., see Brink, L. E. S. 207
Tuinstra, L. G. M. Th., see Groneman, A. F. 43
Turner, A. P. F.
—, Aston, W. J., Higgins, I. J., Bell, J. M., Colby, J., Davis, G. and Hill, H. A. O.
Carbon monoxide: acceptor oxidoreductase from *Pseudomonas thermocarboxydovorans* strain C2 and its use in a carbon monoxide sensor 161

Van der Voort, H. T. M., see Brakenhoff, G. J. 231
Van't Riet, K., see Brink, L. E. S. 207
Voort, van der, H. T. M., see Brakenhoff, G. J. 231
Vorlop, K.-D.
—, Becke, J. W., Stock, J. and Klein, J.
Semiconductor gas sensors in bioreactor control 287

Wallach, J. M., see Ballot, C. 305
Walravens, J., see Motte, J. C. 275
Weigel, J., see Körner, H. U. 55
Welin, S.
—, Elwing, H., Arwin, H., Lundström, I. and Wikström, M.
Reflectometry in kinetic studies of immunological and enzymatic reactions on solid surfaces 263
Wikström, M., see Welin, S. 263
Winquist, F.
—, Spetz, A., Lundström, I. and Danielsson, B.
Determination of urea with an ammonia gas-sensitive semiconductor device in combination with urease 143

(Continued from outside back cover)

Mass spectrometric monitoring of 2-oxoglutaric acid in fermentation broth
E. Pungor Jr., M. Pecs, L. Szigeti, L. Nyeste (Budapest, Hungary), and J. Szilagyi (Debrecen, Hungary) . . 185
Mass spectrometric and factor discriminant analysis of complex organic matter from the bacterial culture environment of *Bacteroides gingivalis*
J. J. Boon, A. Tom, B. Brandt, G. B. Eijkel, P. G. Kistemaker (Amsterdam, The Netherlands), F. J. W. Notten and F. H. M. Mikx (Nijmegen, The Netherlands) 193
Automation of an experimental system for the microbial epoxidation of propene and 1-butene
L. E. S. Brink, J. Tramper, K. Van 't Riet (Wageningen, The Netherlands) and K. Ch. A. M. Luyben (Delft, The Netherlands) 207
On-line mass spectrometry in fermentation
E. Heinzle, J. Moes, M. Griot, H. Kramer, I. J. Dunn and J. R. Bourne (Zurich, Switzerland) . . . 219

Short Communications

High-resolution confocal scanning light microscopy in biology
G. J. Brakenhoff, H. T. M. van der Voort and N. Nanninga (Amsterdam, The Netherlands) 231
Extraction and gas—liquid chromatography of microbial *N*-dealkylation systems
G. J. Sewell, C. J. Soper and R. T. Parfitt (Bath, Great Britain) 237
Technical improvements in protein microsequencing
P.-H. Lai (Thousand Oaks, CA, U.S.A.) 243
Time-resolved fluorescence microscopy for measuring specific coenzymes in methanogenic bacteria
H. Schneckenburger, B. W. Reuter (Neuherberg, West Germany) and S. M. Schoberth (Jülich, West Germany) 249
Application of a clinical analyser in biotechnology
B. G. Henshaw (Selby, Great Britain) 257
Reflectometry in kinetic studies of immunological and enzymatic reactions on solid surfaces
S. Welin, H. Elwing, H. Arwin, I. Lundström (Linköping, Sweden) and M. Wikström (Göteberg, Sweden). 263
Fermentation control with personal computers
W. Hampel and M. Roehr (Vienna, Austria) 269
Computer monitoring of sugars, acids and volatile compounds in fermentations
J. C. Motte, X. Monseur, M. Termonia, M. Hofman, G. Alaerts, A. De Meyer, P. Dourte and J. Walravens (Tervuren, Belgium) 275
Monitoring glucose consumption in *Escherichia coli* cultivation with an enzyme electrode
N. Cleland and S.-O. Enfors (Stockholm, Sweden) 281
Semiconductor gas sensors in bioreactor control
K.-D. Vorlop, J. W. Becke, J. Stock and J. Klein (Braunschweig, West Germany) 287
Rapid determination of sulfide in waste waters by continuous flow analysis and gas diffusion and a potentiometric detector
K. Brunt (Groningen, The Netherlands) 293
Determination of the substrates of dehydrogenases in biological material in flow-injection systems with electrocatalytic NADH oxidation
A. Schelter-Graf, H.-L. Schmidt and H. Huck (Freising-Weihenstephan, West Germany) 299
Conductimetric measurements of enzyme activities
C. Ballot, B. Saizonou-Manika, C. Mealet, G. Favre-Bonvin and J. M. Wallach (Villeurbanne, France) . . 305
Oxygen electrode-based enzyme immunoassay for the amperometric determination of hepatitis B surface antigen
J. L. Boitieux, D. Thomas (Compiegne, France) and G. Desmet (Amiens, France) 309
Use of nuclear magnetic resonance and gas—liquid chromatography for the study of microbial nitrile-hydratases and amidases
K. Bui, H. Fradet, A Thiéry, M. Maestracci, A. Arnaud and P. Galzy (Montpellier, France) 315

Author Index 323

VOL. 163 ANALYTICA CHIMICA ACTA SEPTEMBER 1984

CONTENTS

(Abstracted, Indexed in: Anal. Abstr.; Biol. Abstr.; Chem. Abstr.; Curr. Contents Phys. Chem. Earth Sci.; Life Sci.; Index Med.; Mass Spectrom. Bull.; Sci. Citation Index; Excerpta Med.)

ANABIOTEC '84 — Proceedings of the International Symposium on Analytical Methods and Problems in Biotechnology, April 17–19, 1984

On-line measurement of extracellular enzymes during fermentation by using membrane techniques
K. H. Kroner and M.-R. Kula (Braunschweig, West Germany) . . . 3

Fractal structure of gel porosity
B. Gelleri and M. Sernetz (Giessen, West Germany) . . . 17

High-performance liquid chromatography of carbapenem antibiotics in complex biological samples with column switching and simultaneous multichannel ultraviolet monitoring
G. Decristoforo (Kundl, Austria) . . . 25

Molecular weight fractionation for the study of complex biodegradation processes
H. A. Leidner, Th. Fleischmann and G. Hamer (Dübendorf, Switzerland) . . . 35

Identification and determination of metabolites in plant cell biotechnology by gas chromatography and gas chromatography/mass spectrometry. Application to nonpolar products of *Chrysanthemum cinerariaefolium* and *Tagetes* species
A. F. Groneman, M. A. Posthumus, L. G. M. Th. Tuinstra and W. A. Tragg (Wageningen, The Netherlands) . . . 43

The degradation pattern of oligomers and polymers from lignocelluloses
H. U. Körner, D. Gottschalk, J. Wiegel and J. Puls (Hamburg, West Germany) . . . 55

Immobilized enzyme kinetics analyzed by flow-through microfluorimetry. Resorufin-β-D-galactopyranoside as a new fluorogenic substrate for β-galactosidase
J. Hofmann and M. Sernetz (Giessen, West Germany) . . . 67

Rapid determination of cephalosporins with an immobilized enzyme reactor and sequential subtractive spectrophotometric detection in an automated flow-injection system
G. Decristoforo and F. Knauseder (Kundl, Austria) . . . 73

An automated nephelometric system for evaluation of the growth of bacterial cultures
Kl. Mechsner (Dübendorf, Switzerland) . . . 85

Isolation of 3,4-dihydroxyphenylacetic acid produced from *p*-hydroxyphenylacetic acid by immobilized plant cells of *Mucuna pruriens* and its identification by liquid chromatography/mass spectrometry
A. P. Bruins and N. Pras (Groningen, The Netherlands) . . . 91

On-line analysis of fermentation media
W. J. Schmidt, H.-D. Meyer, K. Schügerl (Hannover, West Germany), W. Kuhlmann (Melsungen, West Germany) and K.-H. Bellgardt (Braunschweig, West Germany) . . . 101

Measurement of biological parameters during fermentation processes
T. Scheper, A. Gebauer, A. Sauerbrei, A. Niehoff and K. Schügerl (Hannover, West Germany) . . . 111

Monitoring the production of biosynthetic human growth hormone by micro enzyme-linked immunosorbent assay
B. Dinesen and H. D. Andersen (Gentofte, Denmark) . . . 119

Monitoring of methanogenic processes with an immobilized mixed culture in combination with a gas-flow meter
U. Dissing, T. G. I. Ling and B. Mattiasson (Lund, Sweden) . . . 127

Evaluation of a dialysis probe for continuous sampling in fermentors and in complex media
C. F. Mandenius, B. Danielsson and B. Mattiasson (Lund, Sweden) . . . 135

Determination of urea with an ammonia gas-sensitive semiconductor device in combination with urease
F. Winquist, A. Spetz, I. Lundström (Linköping, Sweden) and B. Danielsson (Lund, Sweden) . . . 143

Interpretation of static and dynamic responses of a dissolved oxygen electrode in viscous broths
C. G. Dussap and J. B. Gros (Aubière, France) . . . 151

Carbon monoxide: acceptor oxidoreductase from *Pseudomonas thermocarboxydovorans* strain C2 and its use in a carbon monoxide sensor
A. P. F. Turner, W. J. Aston, I. J. Higgins (Cranfield, Great Britain), J. M. Bell, J. Colby (Sunderland, Great Britain), G. Davis and H. A. O. Hill (Oxford, Great Britain) . . . 161

Application of ^{13}C-n.m.r. spectroscopy to study the mechanism of *N*-demethylation of [*N*—Me—^{13}C] codeine by cell-free extracts of *Cunninghamella bainieri*
M. Gibson, C. J. Soper and R. T. Parfitt (Bath, Great Britain) . . . 175

(Continued on inside back cover)